BIOCHEMICAL PHARMACOLOGY 77 (2009) 238–247

available at www.sciencedirect.com

ScienceDirect

journal homepage: www.elsevier.com/locate/biochempharm

Human carboxylesterases HCE1 and HCE2: Ontogenic expression, inter-individual variability and differential hydrolysis of oseltamivir, aspirin, deltamethrin and permethrin☆

Dongfang Yang[a], *Robin E. Pearce*[b], *Xiliang Wang*[a], *Roger Gaedigk*[b], *Yu-Jui Yvonne Wan*[c], *Bingfang Yan*[a,*]

[a] *Department of Biomedical and Pharmaceutical Sciences, Center for Pharmacogenomics and Molecular Therapy, University of Rhode Island Kingston, Kingston, RI 02881, United States*

[b] *Section of Developmental Pharmacology and Experimental Therapeutics, Division of Pediatric Pharmacology and Medical Toxicology, Children's Mercy Hospital and Clinics, 2401 Gillham Road, Kansas City, MO 64108, United States*

[c] *Department of Pharmacology, Toxicology and Therapeutics, University of Kansas Medical Center, Kansas City, KS 66160, United States*

ARTICLE INFO

Article history:
Received 7 September 2008
Accepted 6 October 2008

ABSTRACT

Carboxylesterases hydrolyze chemicals containing such functional groups as a carboxylic acid ester, amide and thioester. The liver contains the highest carboxylesterase activity and expresses two major carboxylesterases: HCE1 and HCE2. In this study, we analyzed 104 individual liver samples for the expression patterns of both carboxylesterases. These samples were divided into three age groups: adults (≥ 18 years of age), children (0 days–10 years) and fetuses (82–224 gestation days). In general, the adult group expressed significantly higher HCE1 and HCE2 than the child group, which expressed significantly higher than the fetal group. The age-related expression was confirmed by RT-qPCR and Western immunoblotting. To determine whether the expression patterns reflected the hydrolytic activity, liver microsomes were pooled from each group and tested for the hydrolysis of drugs such as oseltamivir and insecticides such as deltamethrin. Consistent with the expression patterns, adult microsomes were ~4 times as active as child microsomes and 10 times as active as fetal microsomes in hydrolyzing these chemicals. Within the same age group, particularly in the fetal and child groups, a large inter-individual variability was detected in mRNA (430-fold), protein (100-fold) and hydrolytic activity (127-fold). Carboxylesterases are recognized to play critical roles in drug metabolism and insecticide detoxication. The findings on the large variability among different age groups or even within the same age group have important pharmacological and toxicological implications, particularly in relation to pharmacokinetic alterations of ester drugs in children and vulnerability of fetuses and children to pyrethroid insecticides.

☆ This work was supported by NIH grants R01ES07965 and R01GM61988 (BY) and R01CA053596 (YJW).

* *Corresponding author.* Tel.: +1 401 874 5032; fax: +1 401 874-5048.
E-mail address: byan@uri.edu (B. Yan).

Abbreviations: GAPDH, glyceradehyde-3-phosphate dehydrogenase; HCE, human carboxylesterase; HPLC, high-performance liquid chromatography; PBS, phosphate buffered saline; RT-qPCR, reverse transcription-quantitative polymerase chain reaction.

0006-2952/$ – see front matter © 2008 Elsevier Inc. All rights reserved.
doi:10.1016/j.bcp.2008.10.005

1. Introduction

Carboxylesterases constitute a class of enzymes that hydrolyze chemicals containing such functional groups as a carboxylic acid ester, amide and thioester [1]. These enzymes are known to play important roles in drug metabolism and insecticide detoxication. Two major human carboxylesterases (HCE1 and HCE2) are abundantly expressed in the liver, whereas HCE2 is predominately expressed in the gastrointestinal tract [1,2]. In addition to the difference in tissue distribution, these two enzymes differ markedly in the hydrolysis of certain drugs. For example, HCE1, but not HCE2, rapidly hydrolyzes the anti-influenza viral agent oseltamivir [3,4]. In contrast, HCE2, but not HCE1, rapidly hydrolyzes the anticancer agent irinotecan [5]. In addition to hydrolyzing numerous compounds, carboxylesterases catalyze transesterification. In the presence of ethyl alcohol, HCE1 effectively converts the anti-platelet agent clopidogrel (a methyl ester) into ethyl clopidogrel [4].

The expression of carboxylesterase is altered by xenobiotics and pathological conditions. In human primary hepatocytes, therapeutic agents such as dexamethasone and phenobarbital cause a slight or moderate induction of HCE1 and HCE2 [6]. Dexamethasone and phenobarbital also alter the expression of rat carboxylesterases [7]. However, the pattern of the alteration is different. Phenobarbital moderately induces rat carboxylesterases (hydrolase A and hydrolase B), whereas dexamethasone profoundly suppresses the expression of these enzymes [7]. Suppression also occurs in human primary hepatocytes treated with the pro-inflammatory cytokine interleukin-6 (IL-6), and the suppression is achieved by transcriptional repression [8]. More importantly, the IL-6 mediated suppression strongly alters cellular responsiveness to therapeutic agents such as clopidogrel, irinotecan, and oseltamivir [8]. Hydrolysis of clopidogrel represents inactivation. In contrast, hydrolysis of irinotecan and oseltamivir leads to the formation of therapeutically active metabolites thus represents activation [5,9].

The expression of carboxylesterases is regulated in a developmental manner, and it seems likely that these enzymes are developmentally regulated in humans as well. One to two week old rats express no hydrolase A or B based on immunoblotting analysis [7]. Consistent with the low level expression of carboxylesterases, the intrinsic clearance of the pyrethroid deltamethrin through hydrolysis in 10-day-old rats is only ~3% of adult rats [10]. Even in 4-week-old rats, the intrinsic clearance is less than half of that of adult rats [10]. In addition, young animals are generally much more sensitive to pesticides such as organophosphates and pyrethroids [11–13]. Carboxylesterases are known to protect against these chemicals by hydrolysis in the case of pyrethroids or scavenging mechanism in the case of organophoaphates. The developmental regulation of human carboxylesterases remains to be established. A previous report by Pope et. al. [14] observed that infants differ from adults in the expression and hydrolytic activity of carboxylesterases, but the difference was statistically insignificant [14]. The Pope's study, however, used a small number of samples and had only five samples for each group.

In the current study, we analyzed a total of 104 individual liver samples for the expression patterns of HCE1 and HCE2. These samples were grouped according to age: adults (>18 years old), children (0–10) and fetuses. Multiple experimental approaches were used including RT-qPCR, Western analysis and enzymatic assays. The fetuses expressed lower carboxylesterases than the children, and the children expressed lower carboxylesterases than the adults. Overall, the expression of both HCE1 and HCE2 showed a large inter-individual variability with the largest variability in the fetal group.

2. Materials and methods

2.1. Chemicals and supplies

Acetaminophen, aspirin, naproxen, and salicylic acid were purchased from Sigma (St. Louis, MO). Clopidogrel and clopidogrel carboxylate were from ChemPacific (Baltimore, MD). Oseltamivir and oseltamivir carboxylate were from Toronto Research Chemicals (Canada). Deltamethrin and permethrin were purchased from ChemService (West Chester, PA). Deltamethrin had a purity of 99%, and permethrin was from a batch that contained a mixture of *cis*- and *trans*-isomers at a ratio of 46% and 52%, respectively. *TaqMan* probes were from Applied Biosystems (Foster City, CA). The antibody against glyceradehyde-3-phosphate dehydrogenase (GAPDH) was from Abcam (Cambridge, MA). Unless otherwise specified, all other reagents were purchased from Fisher Scientific (Pittsburgh, PA).

2.2. Liver RNA and microsomal samples

A total of 104 RNA samples were used in this study and some of the RNA samples were matched with microsomes. Pure RNA samples were purchased from (ADMET Technologies (Durham, NC). Liver tissues were acquired from the National Disease Research Interchange (Philadelphia, PA), the Midwest Transplant Network (Westwood, KS), the University of Maryland Brain and Tissue Bank for Developmental Disorders (Baltimore, MD), and the University of Washington Central Laboratory for Human Embryology (Seattle, WA). Isolation of total RNA from the liver tissues was described previously [15,16], and the quality was determined on an Experion RNA StdSens micro fluidic chip (Bio-Rad, Hercules, CA) or by electrophoresis. Microsomes of child and fetal livers were prepared by differential centrifugation as described previously [17]. Adult liver microsomes (individual samples) were from CellzDirect (Pittsboro, NC) and described previously [4]. The demographics of the RNA samples in each group are summarized in Table 1. The use of the human samples was approved by the Institutional Review Board.

Table 1 – Demographic data for RNA samples.

Group	n	M/F	CA	AA	H	Others	Unk
Fetus	48	26/22	19	17	1	5	6
Child	34	15/19	21	8	3	2	
Adult	22	14/8	19	2			

Abbreviations: M/F: male/female; CA: Caucasian-American; AA: African American; H: Hispanic; Unk: unknown.

2.3. *Reverse transcription-quantitative polymerase chain reaction (RT-qPCR)*

Total RNA (0.1 μg) was subjected to the synthesis of the first strand cDNA in a total volume of 25 μl with random primers and M-MLV reverse transcriptase. The reactions were conducted at 25 °C for 10 min, 42 °C for 50 min and 70 °C for 10 min. The cDNAs were then diluted 6-fold and quantitative PCR was performed with *TaqMan* Gene Expression Assay (Applied Biosystems, Foster City, CA). The *TaqMan* assay identification numbers were: HCE1, Hs00275607_m1 (NM_001266); HCE2, Hs00187279_m1 (NM_198061); and polymerase (RNA) II, Hs01108291_m1 (NM_000937). It should be noted that the HCE1 probe could detect both HCE1A1 and HCE1A2 transcripts. The PCR amplification was conducted in a total volume of 20 μl containing universal PCR master mixture (10 μl), gene-specific *TaqMan* assay mixture (1 μl), and cDNA template (3 μl). The cycling profile was 50 °C for 2 min, 95 °C for 10 min, followed by 40 cycles of 15 s at 95 °C and 1 min at 60 °C, as recommended by the manufacturer. Amplification and quantification were done with the Applied Biosystems 7900HT Real-Time PCR System. All samples were analyzed in triplicate and the signals were normalized to polymerase (RNA) II [18] and then expressed as relative levels of mRNA among all samples.

2.4. *Western analysis*

Microsomal proteins (1.5 μg) were resolved by 7.5% SDS-PAGE in a mini-gel apparatus and transferred electrophoretically to nitrocellulose membranes. After non-specific binding sites were blocked with 5% non-fat milk, the blots were incubated with an antibody against HCE1, HCE2 and GAPDH, respectively. The preparation of the antibodies against HCE1 and HCE2 was described elsewhere [6]. The primary antibodies were subsequently localized with goat anti-rabbit IgG conjugated with horseradish peroxidase, and horseradish peroxidase activity was detected with a chemiluminescent kit (SuperSignal West Pico). The chemiluminescent signals were captured by a KODAK Image Station 2000 and the relative intensities were quantified by the KODAK 1D Image Analysis Software.

2.5. *Enzymatic assays*

All enzymatic assays were carried out at 37 °C in a total volume of 100 μl. Pilot studies were performed to determine conditions (e.g., protein concentrations) to maintain the metabolism in the linear range. Generally, microsomes (20–80 μg protein) were prepared in 50 μl incubation buffer (phosphate buffer, 100 mM, pH 7.4; or Tris–HCl, 50 mM, pH 7.4) and then mixed with an equal volume of substrate solution (the same buffer). Hydrolysis of aspirin was performed in phosphate buffer, whereas hydrolysis of oseltamivir, deltamethrin and permethrin was carried out in Tris–HCl buffer. Aspirin was assayed at 1 mM, oseltamivir at 200 μM, both deltamethrin and permethrin at 100 μM. The incubations lasted for 10–60 min depending on a substrate, and the reactions were terminated with 150 μl of acetonitrile containing an internal standard (IS): acetaminophen (750 ng/ml) for aspirin, clopidogrel carboxylate (50 ng/ml) for oseltamivir, napronex (4 μg/ml) for deltamethrin and clopidogrel (33 μg/ml) for permethrin. The reaction mixtures were subjected to centrifugation for 15 min at 4 °C (15,000 *g*). Hydrolysis of aspirin and oseltamivir was previously reported [3,4]. It should be noted that various controls were performed such as 0 min incubation and incubation without microsomes.

2.6. *Monitoring of hydrolysis by HPLC or LC–MS/MS*

The hydrolysis of aspirin or pyrethroids was separated by high-performance liquid chromatography (HPLC) (Hitachi LaChrom Elite-300) with a Chromolith SpeedROD column RP-18e (Merck, Germany). The supernatants (10–30 μl) of the reaction mixtures were injected and separated by an isocratic for aspirin or gradient mobile phase for deltamethrin and permethrin. The isocratic mobile phase consisted of 12% methanol and 0.25% acetate acid at pH 3.9 [4]. The gradient mobile phase consisted of acetonitrile and 0.01% formic acid. The gradient was run at 20–50% acetonitrile (v/v) for 6 min, 50–80% for 3 min followed by 80–20% for 6 min. Both mobile phases were run at a flow rate of 2 ml/min. For aspirin, the formation of hydrolytic metabolite was monitored, whereas for deltamethrin and permethrin the disappearance of parent compounds was monitored by a diode array detector at 230 nm. All quantifications were performed using peak area ratios and calibration curves generated from the internal control. The calibration curve ranged from 2 to 300 μg/mL with good linearity for salicylic acid, 0.8–160 μg/mL for deltamethrin, and 0.6–120 μg/mL for permethrin.

The hydrolysis of oseltamivir was monitored by LC–MS/MS system (API 3200) as described previously [3]. Briefly, the supernatants of the incubation mixtures were separated isocratically using a mobile phase composition of 70:30% (v/v) acetonitrile: 0.05% (v/v) formic acid in deionized water maintained at a flow rate of 0.25 ml/min with a total run time of 6.0 min. Detection of the analytes was performed in positive ion mode using the mass transitions of *m/z*: 313.3 → 166.1 for oseltamivir, *m/z*: 285.2 → 138.0 for oseltamivir carboxylate and *m/z*: 308.2 → 152.0 for IS. Flow injection analysis was performed at a flow rate of 20 μl/min to obtain optimum source parameters. The following compound parameters were used for oseltamivir, oseltamivir carboxylate and IS, respectively. Declustering potential: +5, +5 and +30 V, focusing potential: +360 V each, entrance potential: +8 V each, collision cell entrance potential: +20 V each, collision energy: +25, +25 and +30 V and collision cell exit potential: +7 V each. The optimum source parameters that gave the highest oseltamivir intensity were Curtain gas: 10 psi, collision gas: 4 psi, ion spray voltage: +5500 V, temperature: 450 °C, ion source gas1: 25 psi and ion source gas2: 85 psi. Integration of the peaks was performed by manual baseline adjustment using the ANALYST SP version 1.2 software (Applied Biosystems). All quantifications were performed using peak area ratios and calibration curves consisted of oseltamivir or oseltamivir carboxylate to clopidogrel carboxylic acid concentration ratios plotted against the oseltamivir or oseltamivir carboxylate to clopidogrel carboxylic acid peak area ratios. The calibration curve ranged from 1 to 250 ng/mL with good linearity for oseltamivir and 4 to 1000 ng/mL for oseltamivir carboxylate.

The calibration curves were constructed with $1/x^2$ weighting and the regression coefficients were greater than 0.99.

2.7. Other analyses

Protein concentrations were determined with BCA assay (Pierce) based on bovine serum albumin standard. Data are presented as mean ± S.D. All enzymatic assays were repeated three times with the same microsomal preparation. Statistical tests were performed to compare means (Student's t-test) or correlations (Spearman). In all cases, significant differences were assumed when p-values were less than 0.05.

3. Results

3.1. Ontogenic expression of human carboxylesterases HCE1 and HCE2 by RT-qPCR

In this study, we first evaluated the expression patterns of human carboxylesterases HCE1 and HCE2 in various age groups. A total of 104 RNA samples were analyzed including 48 samples from fetuses (82–224 gestation days), 34 from children (0 days–10 years of age) and 22 from adults (≥18). The levels of HCE1 and HCE2 mRNA were determined with RT-qPCR, and the results are summarized in Fig. 1 and Table 2. Overall, the adult group had the highest levels of HCE1 and HCE2 mRNA, and the fetal group had the lowest levels for both enzymes. Based on the values of the means, the adult group expressed HCE1 at levels 319-fold higher than the fetal group, and ~50% higher than the child group (Fig. 1 and Table 2). Likewise, the adult group expressed HCE2 at levels 55-fold higher than the fetal group and ~40% higher than the child group. In all cases, the differences among various age groups were statistically significant (Fig. 1). It should be noted that two different sets of Y axial values were used in Fig. 1 to accommodate the large difference in the mRNA levels between the fetal and the other two groups.

In addition to the large difference among various age groups (inter-group), a large inter-individual variability was detected within a group. The fetal group, for example, showed a 431-fold difference (ratio between the maximum and the minimum) in HCE1 mRNA with a coefficient of variation (CV) of as high as 172% (Table 2). The child and adult groups, on the other hand, varied less in HCE1 mRNA with a 218- and 12-fold difference, respectively (Table 2). Similarly, the levels of HCE2 mRNA varied in all age groups, however, the overall variability was much less than HCE1 mRNA. The variation in HCE2 mRNA

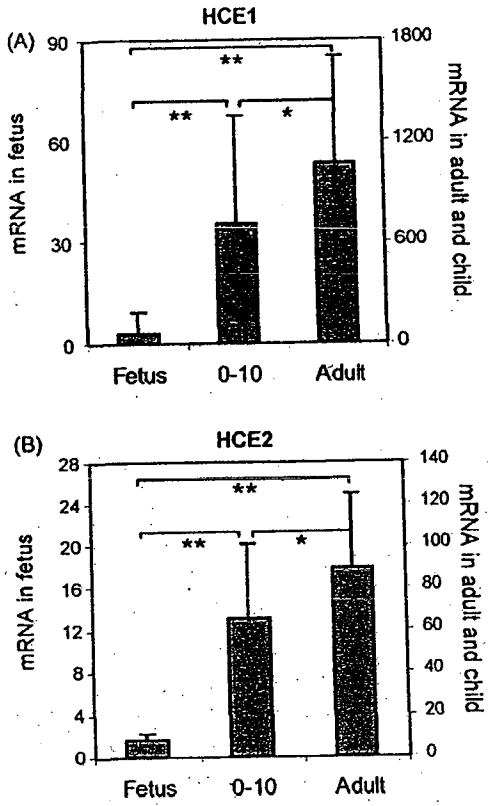

Fig. 1 – Levels of HCE1 and HCE 2 mRNA in the adult, child and fetal groups. Total RNAs were subjected to RT-qPCR analysis for the level of HCE1 mRNA (A) and HCE2 mRNA (B) by *Taqman* probes as described in Section 2. The adult group contained 22 samples, the child group contained 34 samples and the fetal group contained 48 samples. The signals from each target were normalized based on the signal from PolII and expressed as relative levels among all samples. The data are presented as mean ± S.D. (*) Statistical significance at $p < 0.05$, (**) statistical significance at $p < 0.001$.

was the same in the fetal and child groups and higher than that in the adult group (21- versus 4-fold) (Table 2).

We next examined whether the expression of carboxylesterases is age-related within a group. The levels of mRNA were plotted against age or gestation days, and the correlation coefficients were computed. The adult group showed no clear correlation for either HCE1 or HCE2 (data not shown). In the fetal samples, the level of HCE2 but not HCE1 mRNA was

Table 2 – Relative mRNA levels of carboxylesterases HCE1 and HCE2 in fetuses, children (0–10 years old) and adults (≥18).

Group	n	Minimum	Maximum	Variability	Mean	S.D.	CV (%)
Fetus-HCE1	48	0.07	30.15	431 (fold)	3.32	5.70	172
Child-HCE1	34	12.18	2657.77	218	711.47	638.51	90
Adult-HCE1	22	225.50	2659.61	12	1059.59	644.92	61
Fetus-HCE2	48	0.20	4.28	21	1.63	1.36	91
Child-HCE2	34	7.00	148.78	21	65.82	34.90	53
Adult-HCE2	22	39.89	168.66	4	89.87	34.83	39

Abbreviations: S.D.: standard deviation; CV: coefficient of variation.

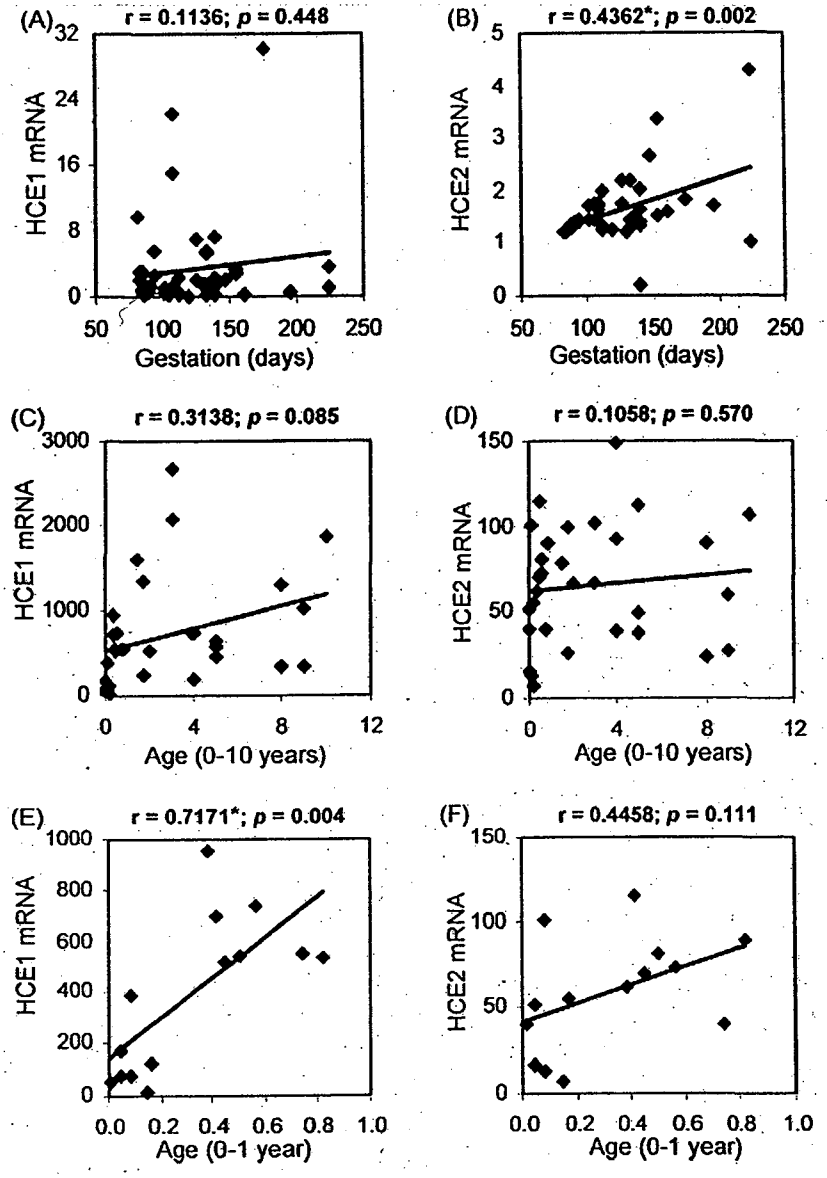

Fig. 2 – Age-related expression of HCE1 and HCE2. The data from Fig. 1 were plotted against age with SPSS version 16. (A) Correlation of HCE1 mRNA with gestation days. (B) Correlation of HCE2 mRNA with gestation days. (C) Correlation of HCE1 mRNA with age in the child group (0–10 years old). (D) Correlation of HCE2 mRNA with age in the child group (0–10 years old). (E) Correlation of HCE1 mRNA with age in the sub-child group (0–1-year-old). (F) Correlation of HCE2 mRNA with age in the sub-child group (0–1-year-old), (*) statistical significance ($p < 0.05$).

significantly correlated with age (Fig. 2A and B). In contrast, the child group showed better correlation with age on HCE1 than HCE2 mRNA, although neither correlation reached the level of statistical significance (Fig. 2C and D). To gain additional information on age-related expression, correlation analysis was performed on the samples from donors under one year old (0–1 year). In this sub-group, much improved correlation was observed on both HCE1 and HCE2 with a p-value of 0.004 and 0.111, respectively (Fig. 2E and F).

3.2. *Inter-individual variability in carboxylesterase proteins and oseltamivir hydrolysis in the child group*

We next examined whether the levels of carboxylesterase mRNA reflected the levels of corresponding proteins. RNA-microsome matched samples from 11 available pediatric-aged subjects were evaluated. Fetal matched samples were not tested because of low mRNA expression and low activities towards marker substrates (described below). No RNA-microsome matched samples were available for the adult group. The microsomal samples were first analyzed by Western immunoblotting with antibody against HCE1 or HCE2, and the immunostaining intensities were quantified by the KODAK 1D Image Analysis Software. As shown in Fig. 3A, all samples contained HCE1 and HCE2 proteins, but the relative abundance varied markedly. In particular, one donor (lane 6) showed extremely low levels of both carboxylesterases (Fig. 3A). Based on the immunostaining intensities, HCE1 protein varied by ~100-fold, and HCE2 protein varied by ~20-fold. The inter-individual variability, however, was decreased

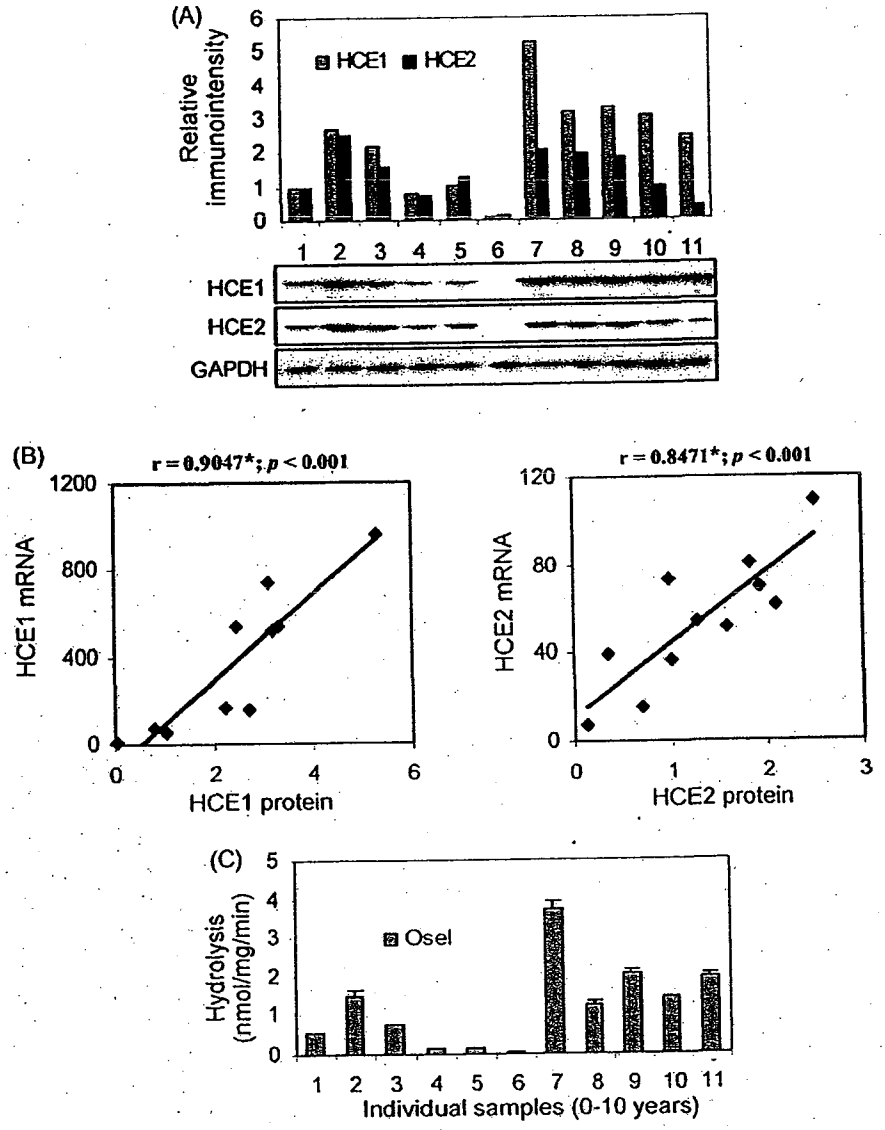

Fig. 3 – Individual variation of HCE1 and HCE2 proteins and oseltamivir hydrolysis in the child group. (A) *Western analyses.* Microsomes (1.5 μg) were resolved by 7.5% SDS-PAGE and transferred electrophoretically to nitrocellulose membranes. The blots were incubated with an antibody against HCE1, HCE2 or GAPDH and chemiluminescent substrate. The signal was captured by a KODAK Image Station 2000 and the relative intensities were quantified by the KODAK 1D Image Analysis Software. (B) *Correlation analyses.* The immunointensities of HCE1 and HCE2 were plotted against the levels of respective mRNA. The correlation coefficients and evaluations on statistical significance were performed with SPSS version 16. (*) Statistical significant ($p < 0.001$). (C) *Oseltamivir hydrolysis by individual liver samples of the child group.* Microsomes (20 μg) were incubated with oseltamivir (200 μM) at 37 °C for 10 min, and the formation of oseltamivir carboxylate was detected by LC–MS/MS. Data were assembled from three independent experiments with two injections of each experiment.

to ~8-fold for both carboxylesterases when the data-point (lane 6) was eliminated. For both HCE1 and HCE2, the mRNA levels were correlated significantly with the levels of respective proteins ($p < 0.001$) (Fig. 3B). The HCE1 matched samples had a correlation coefficient of 0.9047, and the HCE2 matched samples had a slightly lower correlation coefficient (0.8471) (Fig. 3B).

The large individual variability in carboxylesterase protein pointed to the possibility of marked differences in the metabolism of therapeutic agents and other xenobiotics. To directly test this possibility, the anti-influenza viral agent oseltamivir (an ester prodrug) was incubated with individual donor samples (Fig. 3A), and the hydrolysis was monitored. As shown in Fig. 3C, all samples hydrolyzed this anti-viral agent, and the overall hydrolysis varied by 127-fold. Such a large inter-individual variability was in agreement with the variation in the abundance of HCE1 (Fig. 3A), which has been shown to catalyze the hydrolysis of oseltamivir (3). As expected, sample 6 (lane 6) contained the lowest HCE1 protein and showed the lowest hydrolytic activity toward oseltamivir. Conversely, sample 7 (lane 7) contained the highest level of HCE1 protein and was the most active toward this anti-viral

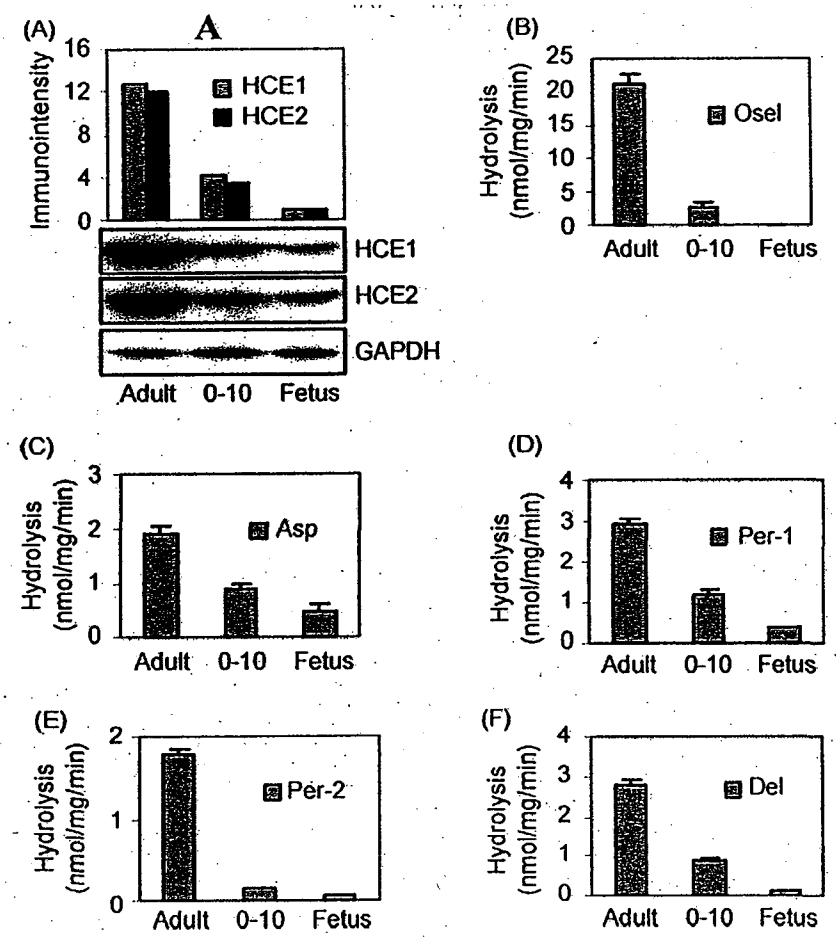

Fig. 4 – Hydrolysis of oseltamivir, aspirin, deltamethrin and permethrin. (A) *Western analysis of pooled samples for various groups.* Microsomes (1.5 μg) pooled from the adult, child and fetal group were analyzed by Western blotting and the immunostaining intensities were quantified by the KODAK 1D Image Analysis Software. (B) *Hydrolysis of oseltamivir by pooled microsomes.* Microsomes (20 μg) from various age groups were incubated with oseltamivir (200 μM) at 37 °C for 10 min, and the formation of oseltamivir carboxylate was detected by LC–MS/MS. (C) *Hydrolysis of aspirin by pooled microsomes.* Microsomes (80 μg) from various age groups were incubated with aspirin (1 mM) at 37 °C for 60 min, and the formation of salicylic acid was detected by HPLC. (D and E) *Hydrolysis of permethrin by pooled microsomes.* Microsomes (50 μg) from various age groups were incubated with permethrin (100 μM) at 37 °C for 60 min, and the disappearance of the parent compounds was detected by HPLC. Permethrin contained a mixture of *cis*- and *trans*-isomers at a ratio of 46 and 52%, respectively with the *cis*-form having a retention time of 10.41 and the *trans*-form of 10.18. (F) *Hydrolysis of deltamethrin by pooled microsomes.* Microsomes (50 μg) from various age groups were incubated with deltamethrin (100 μM) at 37 °C for 60 min, and the disappearance of the parent compound was detected by HPLC. Data were assembled from three independent experiments with each experiment having two injections.

agent (Fig. 3A and C). The hydrolysis of oseltamivir among these individual samples was highly correlated with the protein level of HCE1 with a correlation coefficient of 0.9373, although samples 8 and 10 exhibited relatively lower hydrolysis compared with their relatively HCE1 contents (Fig. 3A and C).

3.3. *Hydrolysis of drugs and insecticides by liver microsomes of fetuses, children and adults*

We next extended the metabolism study to include the anti-inflammatory agent aspirin, and insecticides permethrin (*cis*- and *trans*-) and deltamethrin. In addition to their pharmacological and toxicological implication, these chemicals were chosen because they are hydrolyzed in an isoform-specific manner. Oseltamivir and deltamethrin are predominately hydrolyzed by HCE1 [3,19,20], whereas aspirin is predominately hydrolyzed by HCE2 [4]. The cis-form of permethrin is favorably hydrolyzed by HCE2, whereas the *trans*-form is comparably hydrolyzed by both forms. The extended metabolism study was performed with microsomes pooled from various age groups, and the microsomes were so pooled by mixing equal amount from all individuals in an age group. The pooled samples enabled comparison to be made on the overall hydrolysis of these chemicals among different age groups.

We first determined the levels of HCE1 and HCE2 in the pooled samples by Western immunoblotting. Based on the immunostaining intensities, the child group expressed ~25%

of carboxylesterases (both HCE1 and HCE2) of the adult group and the fetal group expressed less than 10% of the adult group (Fig. 4A). Overall, the magnitude of hydrolysis of these chemicals was correlated well with the relative levels of carboxylesterases in these samples (Fig. 4B–F). The adult pooled sample showed the highest activity toward all chemicals and the fetal pooled samples showed the lowest activity. Hydrolysis of aspirin and *trans*-permethrin (Per-1) by the samples pooled from the fetuses and children was slightly higher than that predicted according to their relative abundance of carboxylesterases. For example, the fetal sample contained less than 10% of carboxylesterases of the adult sample but showed 25% of aspirin hydrolysis (Fig. 4A and C). Conversely, the hydrolysis of oseltamivir, cis-permethrin and deltamethrin by the fetal group was less than 10% of the adult group. The precise mechanism on these discrepancies remains to be determined. On the other hand, the higher-than predicted hydrolysis, in the case of aspirin, was likely due to hydrolysis by other enzymes (highly expressed in the fetal liver) or due to polymorphic variants. In support of these possibilities, butyrylcholinesterase has been shown to hydrolyze aspirin [21], and certain polymorphic variants of HCE2 were found to differ from the wild-type enzyme in hydrolyzing this anti-platelet agent [4]. In addition, the liver expresses a third carboxylesterase [22], but it remains to be determined whether this carboxylesterase hydrolyzes these compounds (i.e., aspirin and *trans*-permethrin) and whether the expression of this carboxylesterase is developmentally regulated.

4. Discussion

Carboxylesterases constitute a class of hydrolytic enzymes that play important roles in the metabolism of therapeutic agents and detoxication of insecticides [1]. In this study, we analyzed a large number of individual liver samples for the expression patterns of HCE1 and HCE2, two human carboxylesterases predominately expressed in the liver. Overall, the adult group expressed significantly higher HCE1 and HCE2 than the child group or the fetal group. The age-related expression was confirmed on the levels of both mRNA and protein. In agreement with the expression patterns, the adult microsomes were approximately 4 times as active as the child microsomes and more than 10 times as active as the fetal microsomes in hydrolyzing a group of therapeutic agents and insecticides. Even within the same age group, a large inter-individual variability was detected in mRNA and protein levels as well as hydrolytic activity.

Although both HCE1 and HCE2 exhibited a similar expression pattern among the various age groups, there were several major differences. First, HCE1 exhibited much greater inter-group and inter-individual variability than HCE2. For example, based on the values of the means, the adult group displayed a 319-fold higher level in HCE1 mRNA compared with the fetal group. In contrast, these two groups showed only a 55-fold difference in the level of HCE2 mRNA (Fig. 1 and Table 2). Likewise, the adult group showed a 430-fold inter-individual variability in HCE1 mRNA (ratio between maximum over minimum), in contrast, only a 21-fold difference in HCE2 mRNA was detected in the same group (Table 2). Second, HCE1 displayed better age-related expression than HCE2 in the child group with correlation coefficients of 0.3138 and 0.1058, respectively (Fig. 2C and D). In contrast, HCE2 displayed better correlation in the fetal group with correlation coefficients of 0.4362 and 0.1136, respectively (Fig. 2A and B).

The large inter-individual variability, particularly in the fetal and children groups, was likely an outcome coordinated by multiple mechanisms. In this study, we have shown that the adult group expressed the highest levels of HCE1 and HCE2 followed by the child group, and the fetal group expressed the lowest levels of both enzymes (Fig. 1 and Table 2). Such age-related expression patterns were confirmed by RT-qPCR and Western analyses (Figs. 1, 3 and 4) and established that developmental regulation is involved in the expression of HCE1 and HCE2. However, the correlation with age in many cases was only moderate at the most and did not reach the levels of statistical significance (Fig. 2C and F). Although the precise mechanisms remain to be determined, the lack of strong correlation with age in these groups was likely due to complicated factors such as the administration of therapeutic agents and disease conditions. We have previously reported that pathological condition and therapeutic agents markedly altered the expression of HCE1 and HCE2 [6,8]. Interleukin-6, a cytokine usually elevated during inflammation, profoundly suppressed the expression of both HCE1 and HCE2 (8). Consistent with the suppression of carboxylesterases by cytokines, patients with elevated cytokine conditions such as liver cirrhosis had much lower capacity of hydrolyzing ester drugs such as perindopril, a non-sulphydryl angiotensin converting enzyme inhibitor [23,24].

The significantly lower level of HCE1 in the child group, compared with the adult group, provides a molecular explanation to the large pharmacokinetic difference in oseltamivir between these two groups. In this study, the sample pooled from the children was only ~15% as active as the sample pooled from the adults in hydrolyzing oseltamivir (Fig. 4C). Consistent with the in vitro metabolism, children under 12 years old reportedly produced only approximately half of the hydrolytic metabolite produced by adults [25]. Apparently the low level production of oseltamivir carboxylate in children was likely due to ineffective hydrolysis of the parent drug and higher clearance of the metabolite. Furthermore, we have shown that individual samples in the child group varied by as many as 127-fold in oseltamivir hydrolysis (Fig. 4A). Pharmacokinetic studies in children, however, did not detect such a large inter-individual variation in the production of hydrolytic metabolite of oseltamivir [25,26]. One explanation is that the frequency with an extremely low expression level of HCE1 is rare in the general population, and the pharmacokinetic studies were performed in 24 or fewer children [25,26]. Indeed, there was a reported rare case that an adult patient with diabetes mellitus had only 1–2% capacity of normal people in hydrolyzing clopidogrel based on the values of the means and standard deviations [27]. Like oseltamivir, clopidogrel is a substrate of HCE1 [3]. Ineffective hydrolysis of oseltamivir, on the other hand, likely leads to increased concentration in the brain. Some patients taking oseltamivir reportedly developed neurobehavioral changes [28], although a direct link remains to be established between the developed neurotoxiciy and the use of oseltamivir.

In contrast to oseltamivir, pyrethroids have long been recognized to exert neurotoxicity [29]. As a class of the most used insecticides in the world, both the general population and workers have a high risk to be exposed to these insecticides. Epidemiological studies have shown that the exposure level, in some cases, can be high [30,31]. Pyrethroid insecticides are generally considered safe to mammals, because they are rapidly eliminated by carboxylesterases. In this study, we have shown that the fetuses and children hydrolyzed pyrethroids at a rate of only ~20% or lower of the adults (Fig. 4D–F), suggesting their vulnerability to pyrethroids-induced toxicity. In support of this notion, neonatal rats were reportedly 17 times as sensitive as adult rats to cypermethrin [12]. Neurotoxicity induced by pyrethroids appears to cause irreversible damage. Prenatal exposure to deltamethrin, for example, led to a deficit in locomotor activity of offspring post-natally at 9 weeks [32]. In humans, micromolar concentrations were reported in the meconium [33]. This is particularly of relevance as fetuses have only limited capacity of hydrolytic detoxication as described in this report.

In summary, our work points to several important conclusions. First, the expression of both HCE1 and HCE2 increases with age, establishing that their expression is developmentally regulated and that fetuses and children generally have lower capacity of hydrolytic metabolism than adults. Second, there is a large inter-individual variability in the expression of these enzymes, particularly in the fetal and child groups. It is likely that the expression of HCE1 and HCE2 in these age groups is subjected to non-developmental regulation with high sensitivity (e.g., xenobiotic regulation). Carboxylesterases are recognized to play important roles in drug metabolism and insecticide detoxication. The findings on the large variability among different age groups or even within the same age group have important pharmacological and toxicological implications, particularly in relation to altered pharmacokinetics of ester drugs in children and vulnerability of fetuses and children to insecticides such as pyrethroids.

REFERENCES

[1] Satoh T, Hosokawa M. Structure, function and regulation of carboxylesterases. Chem Biol Interact 2006;162:195–211.

[2] Schwer H, Langmann T, Daig R, Becker A, Aslanidis C, Schmitz G. Molecular cloning and characterization of a novel putative carboxylesterase, present in human intestine and liver. Biochem Biophys Res Commun 1997;233:117–20.

[3] Shi D, Yang J, Yang D, LeCluyse EL, Black C, You L, et al. Anti-influenza prodrug oseltamivir is activated by carboxylesterase human carboxylesterase 1, and the activation is inhibited by antiplatelet agent clopidogrel. J Pharmacol Exp Ther 2006;319:1477–84.

[4] Tang M, Mukundan M, Yang J, Charpentier N, LeCluyse EL, Black C, et al. Antiplatelet agents aspirin and clopidogrel are hydrolyzed by distinct carboxylesterases, and clopidogrel is transesterificated in the presence of ethyl alcohol. J Pharmacol Exp Ther 2006;319:1467–76.

[5] Wu MH, Yan B, Humerickhouse R, Dolan ME. Irinotecan activation by human carboxylesterases in colorectal adenocarcinoma cells. Clin Cancer Res 2002;8:2696–700.

[6] Zhu W, Song L, Zhang H, Matoney L, LeCluyse E, Yan B. Dexamethasone differentially regulates expression of carboxylesterase genes in humans and rats. Drug Metab Dispos 2000;28:186–91.

[7] Morgan EW, Yan B, Greenway D, Parkinson A. Regulation of two rat liver microsomal carboxylesterase isozymes: species differences, tissue distribution and the effects of age, sex and xenobiotic treatment of rats. Arch Biochem Biophys 1994;315:514–26.

[8] Yang J, Shi D, Yang D, Song X, Yan B. Interleukin-6 suppresses the expression of carboxylesterases HCE1 and HCE2 through transcriptional repression. Mol Pharmacol 2007;72:686–94.

[9] Oxford JS, Mann A, Lambkin R. A designer drug against influenza: the NA inhibitor oseltamivir (Tamiflu). Expert Rev Anti Infect Ther 2003;1:337–42.

[10] Anand SS, Kim KB, Padilla S, Muralidhara S, Kim HJ, Fisher JW, et al. Ontogeny of hepatic and plasma metabolism of deltamethrin in vitro: role in age-dependent acute neurotoxicity. Drug Metab Dispos 2006;34:389–97.

[11] Pope CN, Chakraborti TK, Chapman ML, Farrar JD, Arthun D. Comparison of in vivo cholinesterase inhibition in neonatal and adult rats by three organophosphorothioate insecticides. Toxicology 1991;68:51–61.

[12] Cantalamessa F. Acute toxicity of two pyrethroids, permethrin, and cypermethrin in neonatal and adult rats. Arch Toxicol 1993;67:510–3.

[13] Sheets LP, Doherty JD, Law MW, Reiter LW, Crofton KM. Age-dependent differences in the susceptibility of rats to deltamethrin. Toxicol Appl Pharmacol 1994;126:186–90.

[14] Pope CN, Karanth S, Liu J, Yan B. Comparative carboxylesterase activities in infant and adult liver and their in vitro sensitivity to chlorpyrifos oxon. Regul Toxicol Pharm 2005;42:62–9.

[15] Vyhlidal CA, Gaedigk R, Leeder JS. Nuclear receptor expression in fetal and pediatric liver: correlation with CYP3A expression. Drug Metab Dispos 2006;34:131–7.

[16] Wortham M, Czerwinski M, He L, Parkinson A, Wan YJ. Expression of constitutive androstane receptor, hepatic nuclear factor 4 alpha, and P450 oxidoreductase genes determines interindividual variability in basal expression and activity of a broad scope of xenobiotic metabolism genes in the human liver. Drug Metab Dispos 2007;35:1700–10.

[17] Leeder JS, Gaedigk R, Marcucci KA, Gaedigk A, Vyhlidal CA, Schindel BP, et al. Variability of CYP3A7 expression in human fetal liver. J Pharmacol Exp Ther 2005;314:626–35.

[18] Radonić A, Thulke S, Mackay IM, Landt O, Siegert W, Nitsche A. Guideline to reference gene selection for quantitative real-time PCR. Biochem Biophys Res Commun 2004;313:856–62.

[19] Godin SJ, Scollon EJ, Hughes MF, Potter PM, DeVito MJ, Ross MK. Species differences in the in vitro metabolism of deltamethrin and esfenvalerate: differential oxidative and hydrolytic metabolism by humans and rats. Drug Metab Dispos 2006;34:1764–71.

[20] Nishi K, Huang H, Kamita SG, Kim IH, Morisseau C. Hammock BD Characterization of pyrethroid hydrolysis by the human liver carboxylesterases hCE-1 and hCE-2. Arch Biochem Biophys 2006;445:115–23.

[21] Kolarich D, Weber A, Pabst M, Stadlmann J, Teschner W, Ehrlich H, et al. Glycoproteomic characterization of butyrylcholinesterase from human plasma. Proteomics 2008;8:254–63.

[22] Sanghani SP, Quinney SK, Fredenburg TB, Davis WI, Murry DJ, Bosron WF. Hydrolysis of irinotecan and its oxidative metabolites, 7-ethyl-10-[4-N-(5-aminopentanoic acid)-1-piperidino] carbonyloxycamptothecin and 7-ethyl-10-[4-(1-piperidino)-1-amino]-carbonyloxycamptothecin, by human

carboxylesterases CES1A1, CES2, and a newly expressed carboxylesterase isoenzyme, CES3. Drug Metab Dispos 2004;32:505–11.
[23] Thiollet M, Funck-Brentano C, Grange JD, Midavaine M, Resplandy G, Jaillon P. The pharmacokinetics of perindopril in patients with liver cirrhosis. Br J Clin Pharmacol 1992;33:326–8.
[24] Eriksson AS, Gretzer C, Wallerstedt S. Elevation of cytokines in peritoneal fluid and blood in patients with liver cirrhosis. Hepatogastroenterology 2004;51:505–9.
[25] Oo C, Barrett J, Hill G, Mann J, Dorr A, Dutkowski R, et al. Pharmacokinetics and dosage recommendations for an oseltamivir oral suspension for the treatment of influenza in children. Paediatr Drugs 2001;3:229–36.
[26] Oo C, Hill G, Dorr A, Liu B, Boellner S, Ward P. Pharmacokinetics of anti-influenza prodrug oseltamivir in children aged 1-5 years. Eur J Clin Pharmacol 2003;59:411–5.
[27] Heestermans AA, van Werkum JW, Schömig E, ten Berg JM, Taubert D. Clopidogrel resistance caused by a failure to metabolize clopidogrel into its metabolites. J Thromb Haemost 2006;4:1143–5.
[28] FDA Patient Safety News (2007) Caution on Neuropsychiatric Events with Tamiflu: Show #59:http://www.accessdata.fda.gov/psn/printer.cfm?id=486.
[29] Ray DE, Fry JR. A reassessment of the neurotoxicity of pyrethroid insecticides. Pharmacol Ther 2006;111:174–93.
[30] Leng G, Kühn KH, Idel H. Biological monitoring of pyrethroids in blood and pyrethroid metabolites in urine: applications and limitations. Sci Total Environ 1997;199:173–81.
[31] Heudorf U, Angerer J. Metabolites of pyrethroid insecticides in urine specimens: current exposure in an urban population in Germany. Environ Health Perspect 2001;109:213–7.
[32] Johri A, Yadav S, Singh RL, Dhawan A, Ali M, Parmar D. Long lasting effects of prenatal exposure to deltamethrin on cerebral and hepatic cytochrome P450 s and behavioral activity in rat offspring. Eur J Pharmacol 2006;544:58–68.
[33] Ostrea Jr EM, Bielawski DM, Posecion Jr NC, Corrion M, Villanueva-Uy E, Jin Y, et al. A comparison of infant hair, cord blood and meconium analysis to detect fetal exposure to environmental pesticides. Environ Res 2008;106:277–83.

A-05 異常行動モデルとしての薬物誘発ジャンピング行動に対するタミフルの影響とその防御法に関する研究

○小野信文、牛島逸子、木村公彦
福岡大・薬・医薬品情報学

【背景と目的】タミフルを代表とする抗インフルエンザウイルス剤服用者が、異常行動の結果、事故死を起こしたことが報告され、緊急安全性情報が出された。その後この因果関係に関しては国家的研究班が組織され、調査研究が行われているが、詳細は未だ明らかでない。しかし、世界的に見れば新たなインフルエンザウイルスの出現もあり、それらの対処は急がねばならない状況と思われる。このような状況を踏まえ、我々は新たな視点から抗インフルエンザウイルス薬の欠点を補う可能性を検討した。

【実験方法】ジャンピング行動は、直径 32 cm の正八角形、高さ 35 cm の台に置いたマウスが薬物投与後 40 分間に下の床に飛び降りる行動とし、飛び降りるまでの時間と回数を（飛び降りた動物は台に戻し）測定した。尚、マウスは測定までこの測定台へ置かれたことはない。薬物の投与スケジュールは、haloperidol 0.5 mg/kg (ip) 5 分後に clonidine 10mg/kg (ip)投与し、測定台へ移し測定を開始した。タミフル 0.1%CMC 懸濁液は haloperidol 15 分前に経口投与し、前処置薬はタミフルのさらに 10 分前に ip 投与した。

【結果並びに考察】タミフル 150mg/kg、haloperidol、clonidine それぞれ単独投与では測定時間内にジャンピング行動は全く起こさなかった。haloperidol と clonidine の併用では、0.63 回/匹のジャンピング行動が見られた。この haloperidol-clonidine 誘発行動は、タミフル 150mg/kg の併用により 22.6 回/匹と有意に増強された。このタミフルによる増強作用は、acetazolamide 20 mg/kg 前処置により 0.50 回/匹と有意に抑制し、150 mg/kg 前処置ではジャンピング行動を完全に消失させた。さらに、diazepam 0.5、1 mg/kg、valprorate 40 mg/kg、fluoxetine 5 mg/kg 前処置により、タミフルによる薬物誘発ジャンピング行動は消失した。したがって、このようなジャンピング行動は、異常行動の一つの指標として有用と考えられる。現時点ではこれらの行動の発現機序は不明であるが、各種中枢神経伝達物質系の不均衡が関与し、抑制作用はその是正によることが示唆される。

A-06 Morphine 誘発精神依存形成における L 型高電位開口性カルシウムチャネル (HVCCs) 機能亢進に対する PI 3-kinase の関与

○芝崎真裕、黒川和宏、桂 昌司、大熊誠太郎
川崎医大・薬理学

【目的】我々は既に、精神依存の評価法である条件づけ場所嗜好性試験において、L 型 HVCC 拮抗薬である nifedipine により、morphine 誘発報酬効果が有意に抑制されることを報告した。一方、PI 3-kinase class III である Vps34 は trafficking に深く関与することが報告されていることから、morphine による L 型 HVCC の発現増加に関与している可能性が考えられる。そこで本研究では、morphine による精神依存形成過程における L 型 HVCC の発現増加を伴った機能亢進機序を、精神依存マウスおよび依存性薬物を連続曝露した初代培養大脳皮質神経細胞（神経細胞）を用いて、行動薬理学的および神経科学的観点から検討した。

【方法】Morphine による報酬効果は条件づけ場所嗜好性試験により行った。神経細胞への morphine の連続曝露は、Hanks 液で希釈したものを直接培養液中に添加した。[$^{45}Ca^{2+}$]流入は 2 分間の 30 mM KCl 刺激により神経細胞内へ取り込まれた放射活性を測定した。蛋白発現量は Western blot 法により解析した。

【結果および考察】Morphine による報酬効果は、L 型 HVCC 阻害薬 (nifedipine) の前処置により完全に消失した。この時点での側坐核を含む領域および大脳皮質画分における L 型 HVCC α 1c および α 2/δ subunit ならびに Vps34 蛋白の発現量に有意な増加が認められた。同様に、神経細胞に morphine を連続曝露した場合に観察される 30 mM KCl 誘発[$^{45}Ca^{2+}$]流入の増加は、L 型 HVCC 阻害薬の併用により完全に阻害された。また、morphine の連続曝露により L 型 HVCC α 1c および α 2/δ subunit ならびに Vps34 蛋白量の有意な増加が認められた。この α 1c subunit 蛋白量の増加は、PI 3-kinase 阻害薬 (LY294002) の併用処置により有意に減少した。以上の成績より、morphine による L 型 HVCC α 1c subunit 蛋白発現増加機構に、Vps34 が一部関与することが明らかとなった。

日本薬理学会近畿部会，第１１３回（２００８．０６．２０，岡山）

平成21年6月16日安全対策調査会
資料2－3

平成２１年２月６日 タミフル基礎WG
参考資料1

リン酸オセルタミビルの基礎的調査検討に関連するその他の文献等

○中枢作用

○低体温

○中枢移行性

現代化学 2008 年 2 月号 ・・・p43

・Low Penetration of Oseltamivir and Its Carboxylate into Cerebrospinal Fluid in Healthy Japanese and Caucasian Volunteers

Jhee et al., (Roche) Antimicrobial Agents and Chemotherapy, Oct. 2008, 3687-3693・・・p45

○ シアリダーゼ関係

・Limited Inhibitory Effects of Oseltamivir and Zanamivir on Human Sialidases

Hata et al., (宮城がんセンター) Antimicrobial Agents and Chemotherapy, Oct. 2008, 3484-3491 ・・・p53

○ その他

・Biodistribution and metabolism of the anti-influenza drug[11C]oseltamivir and its active metabolite [11C]Ro 64-0802 in mice

Akiko Hatori et al,Nuclear Medicine and Biology 36(2009)47-55 ・・・p61

・Synaptic and behavioral interactions of oseltamivir (Tamiflu) with neurostimulants

Y Izumi et al, Human &Experimental Toxicology(2008)27:911-917 ・・・p70

(基礎 WG において調査検討した後に公表されたため追加するもの)

Neuroscience Letters 438 (2008) 67–69

Contents lists available at ScienceDirect

Neuroscience Letters

journal homepage: www.elsevier.com/locate/neulet

Oseltamivir (Tamiflu®) increases dopamine levels in the rat medial prefrontal cortex

Tatsuki Yoshino[a,b,*], Koichi Nisijima[b], Katsutoshi Shioda[b], Kunio Yui[c], Satoshi Kato[b]

[a] Department of Hospital Pharmacy, Jichi Medical University, 3311 Yakushiji, Shimotsuke-shi, Tochigi 329-0498, Japan
[b] Department of Psychiatry, Jichi Medical University, Tochigi 329-0498, Japan
[c] Research Institute of Asperger Disorder, Ashiya University Graduate School of Clinical Education, Ashiya 659-8511, Japan

ARTICLE INFO

Article history:
Received 19 November 2007
Received in revised form 2 April 2008
Accepted 3 April 2008

Keywords:
Oseltamivir
Dopamine
Medial prefrontal cortex
Rat
Abnormal behaviors

ABSTRACT

Oseltamivir (Tamiflu®), a neuraminidase inhibitor, is effective for treating both seasonal flu and H5N1 influenza A virus infection. Oseltamivir is generally well tolerated, and its most common adverse effects are nausea and vomiting. However, neuropsychiatric behaviors including jumping and falling from balconies by young patients being treated by oseltamivir have been reported from Japan; this has led to warnings against its prescribing by many authorities. The pharmacological mechanism of the neuropsychiatric effects of oseltamivir remains unclear. Many studies reported that changes in neurotransmission and abnormal behaviors are closely related. We investigated the changes in dopamine and serotonin metabolism after systemic administration of oseltamivir in the medial prefrontal cortex (mPFC) of rats by using microdialysis. After systemic administration of oseltamivir (25 mg/kg or 100 mg/kg; intraperitoneally (i.p.)), extracellular dopamine in the mPFC was significantly increased as compared to the control values; 3,4-dihydroxyphenylacetic acid and homovanillic acid, the metabolites of dopamine, had also increased significantly. Serotonin was unchanged after the administration of oseltamivir. These findings suggest that oseltamivir increased dopamine release in the mPFC; further, they suggest that the increase in dopamine during oseltamivir treatment may have caused abnormal behaviors in young patients. In cases where oseltamivir is prescribed to children, close observation is required.

Influenza virus infection is a significant public health concern. Vaccination and antiviral drugs are effective in providing protection against the influenza virus. Oseltamivir (Tamiflu®) and zanamivir are neuraminidase inhibitors that prevent influenza virus replication [1,9]. Oseltamivir is the prodrug of Ro 64-0802, which is a known influenza virus neuraminidase inhibitor, and oseltamivir is effective when administered orally [5]. Many clinical studies have reported the efficacy of oseltamivir as treatment for influenza [2,12]. Moreover, since oseltamivir is expected to be effective for the clinical management of the highly pathogenic H5N1 influenza A viruses, several countries are stockpiling oseltamivir [6,7]. Oseltamivir is generally well tolerated; the most common adverse effects observed in clinical studies were nausea and vomiting [5,12]. However, abnormal behaviors such as jumping or falling from balconies by adolescents during oseltamivir treatment were reported from Japan, following which the Japanese authorities advised against prescribing oseltamivir to adolescents aged between 10 and 19 years. The U.S. Food and Drug Administration (FDA) also require that patients be closely monitored for signs of abnormal behavior throughout the treatment period. The pharmacological mechanism of the neuropsychiatric effects of oseltamivir remains unclear. However, the abnormal behaviors observed during oseltamivir administration resemble those induced by psychoactive drugs [3,8] such as amphetamines that influence monoamine metabolism in the brain. However, no change in monoamine metabolism in the brain during oseltamivir administration has been revealed thus far. Therefore, in the present study, we evaluated the effect of oseltamivir on dopamine (DA) and serotonin (5-HT) metabolism in the medial prefrontal cortex (mPFC) of rat by using microdialysis.

Male Wistar rats (Clea Japan Inc., Japan) weighing 200–250 g were used in this study. The rats were housed at a constant room temperature (23 ± 1 °C) and maintained on rat chow and tap water ad libitum. All animal procedures were approved by the Animal Investigation Committee of Jichi Medical University and were in strict accordance with the National Institute for Health (NIH) Guide for the Care and Use of Laboratory Animals. In vivo microdialysis was performed as previously described [16,17]. In brief,

* Corresponding author at: Department of Hospital Pharmacy, Jichi Medical University, 3311 Yakushiji, Shimotsuke-shi, Tochigi 329-0498, Japan.
Tel.: +81 285 58 7188; fax: +81 285 44 8243.
E-mail address: yoshino@jichi.ac.jp (T. Yoshino).

0304-3940/$ – see front matter © 2008 Elsevier Ireland Ltd. All rights reserved.
doi:10.1016/j.neulet.2008.04.011

the rats were anesthetized with sodium pentobarbital (50 mg/kg; intraperitoneally (i.p.)) and placed in a stereotaxic frame (David Kopf Instruments; nose bar positioned 3.5 mm below inter-aural zero). The skull was exposed during surgery, and a burr hole was drilled to accommodate the plantation. Straight-type cellulose dialysis tubing (length, 1.0 mm; internal diameter, 0.16 mm; molecular weight cutoff, 50,000; Eicom Co. Ltd., Kyoto, Japan) was steadily and carefully inserted into the right mPFC (AP, 3.2 mm; ML, 0.6 mm; DV, −5.2 mm from the Bregma) after reference to a brain atlas and fixed with acrylic dental cement and three skull screws. Two days after the surgery, the probe was connected to a microinfusion pump and perfused with Ringer's solution (NaCl, 147 mM; KCl, 4 mM; $CaCl_2$, 1.9 mM) at a flow rate of 2 μl/min. The rats were allowed to move freely during this period. The outflow from the mPFC was automatically collected every 30 min for an additional 240 min and directly injected into a high-performance liquid chromatography (HPLC) unit using an automatic injector (Eicom AS-100, Eicom, Kyoto, Japan). A reverse-phase column (Eicompack CA-5ODS, 150 mm × 2.1 mm, Eicom, Japan) was used for DA and 5-HT separation and another reverse-phase column (Eicompack SC-5ODS, 150 mm × 3.0 mm, Eicom, Japan) was used for 3,4-dihydroxyphenylacetic acid (DOPAC), homovanillic acid (HVA), and 5-hydroxyindoleacetic acid (5-HIAA) separation; the results were immediately analyzed. The DA, DOPAC, HVA, 5-HT, and 5-HIAA concentrations in the samples were determined by an electrochemical detector (Eicom ECD-300, Eicom, Kyoto, Japan). The column and detector were kept in a temperature controller at 25 °C. The composition of the mobile phase used for the DA and 5-HT analyses were 0.1 M phosphate buffer (pH 6.0), 18% methanol, 0.6 g/l sodium 1-octane-sulfonate, and 50 mg/l Na_2EDTA; the flow rate was set at 0.23 ml/min. The mobile phase used in the DOPAC, HVA, and 5-HIAA analyses was 0.1 M acetate–citrate buffer (pH 3.5), 17% methanol, 0.19 g/l sodium 1-octane-sulfonate, and 5 mg/l Na_2EDTA; the flow rate was set at 0.5 ml/min. After a 3-h stabilization period, three consecutive dialysate samples were collected and the baseline DA levels were measured. Capsules containing 75 mg oseltamivir (Tamiflu®) were purchased from Chugai Pharmaceutical Co. (Japan). The capsule ingredients were dissolved in distilled deionized water. Either 25 mg/kg or 100 mg/kg of the drug was administered i.p. to the rats. Following the microdialysis experiments, the brains were removed and frozen at −80 °C. In each case, the position of the dialysis probe was macroscopically verified on 150-μm-thick serial coronal slices. When a bloody region was found around the probe site, the data were excluded. The average of 3 fractions prior to drug administration was defined as 100% (control), and the subsequent perfusate levels were expressed as percentages of the control. Statistical analyses were conducted by two-way ANOVA and one-way ANOVA followed by Dunnett's test. The Windows-compatible software Dr. SPSS2 (SPSS Japan Inc., Tokyo, Japan), was used.

The mean basal extracellular DA, 5-HT, DOPAC, HVA, and 5-HIAA values per 60 μl dialysate for each group were as follows: DA = 0.60 ± 0.08 pg, 5-HT = 3.26 ± 0.85 pg, DOPAC = 86.37 ± 19.05 pg, HVA = 194.10 ± 35.90 pg, and 5-HIAA = 1867.42 ± 289.80 pg.

When 25 and 100 mg/kg of oseltamivir were administered i.p., the DA level increased to 156% and 223% of the pre-administration level, respectively and was also significantly greater than those in the vehicle-administered rats (Fig. 1a). Ataxia was observed following systemic administration of 100 mg/kg of oseltamivir. When 25 and 100 mg/kg oseltamivir was administered i.p., the DOPAC level increased to 147% and 169% of the pre-administration level, respectively (Fig. 1b). The HVA concentration increased to 127% and 146% of the pre-administration level after 25 and 100 mg/kg oseltamivir was administered i.p. (c).

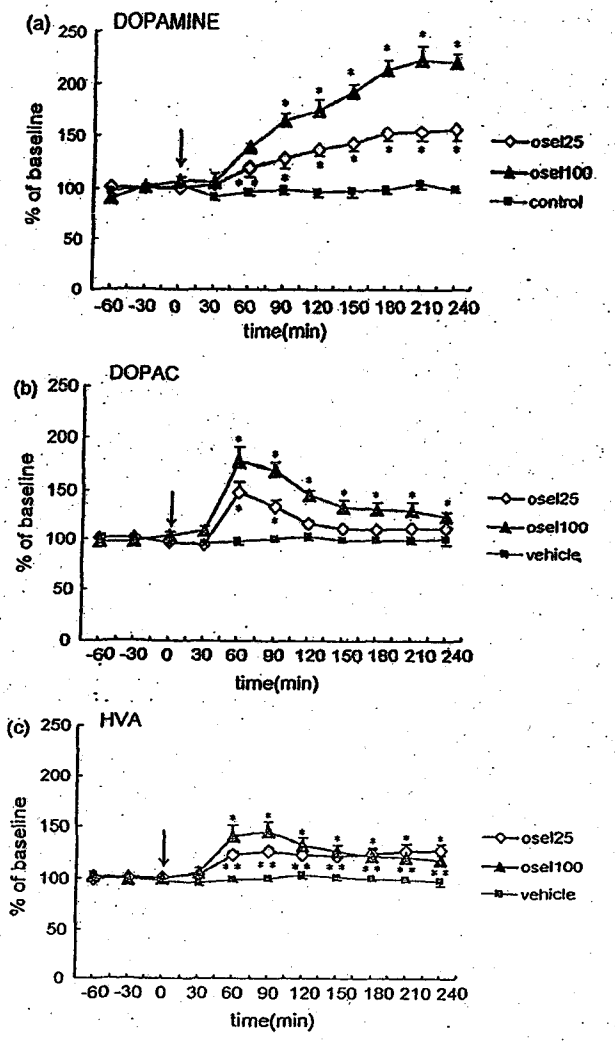

Fig. 1. Effects of oseltamivir on the extracellular DA concentration in the rat mPFC. (a) Effects of oseltamivir on the extracellular 5-HT concentration in the rat mPFC. (b) Drug injection is indicated by the arrow. Data are represented as the mean ± S.E.M. of the values obtained in five rats. $^{*}p < 0.01$, $^{**}p < 0.05$ compared with the corresponding value for vehicle (one-way ANOVA followed with Dunnett's test).

5-HT levels were unchanged after 25 and 100 mg/kg oseltamivir was administered i.p. (Fig. 2a). The 5-HIAA level showed a mild increase after 25 mg/kg oseltamivir administration i.p.; the increase was not significant (Fig. 2b). When 100 mg/kg oseltamivir was administered i.p., the 5-HIAA level showed a significant increase to 126% of the pre-administration level (b).

The present study showed that oseltamivir increased DA levels in dialysates of the rat mPFC in a dose-dependent manner. This is the first demonstration of the effects of oseltamivir on the DA system by using in vivo dialysis. Since the increase in DA levels in animal brains is closely related with abnormal behaviors [13], the abnormal behaviors of patients while being administered oseltamivir may be explained by the present findings.

The increase in extracellular DA levels is assumed to be a consequence of the DA-releasing or DA-reuptake-inhibiting effect of oseltamivir. If oseltamivir can inhibit DA reuptake, reuptake of DA in synaptic clefts should be inhibited and the oxidative deamination of DA by monoamine oxidase within presynaptic sites should be decreased, resulting in a decrease in DOPAC and HVA concentra-

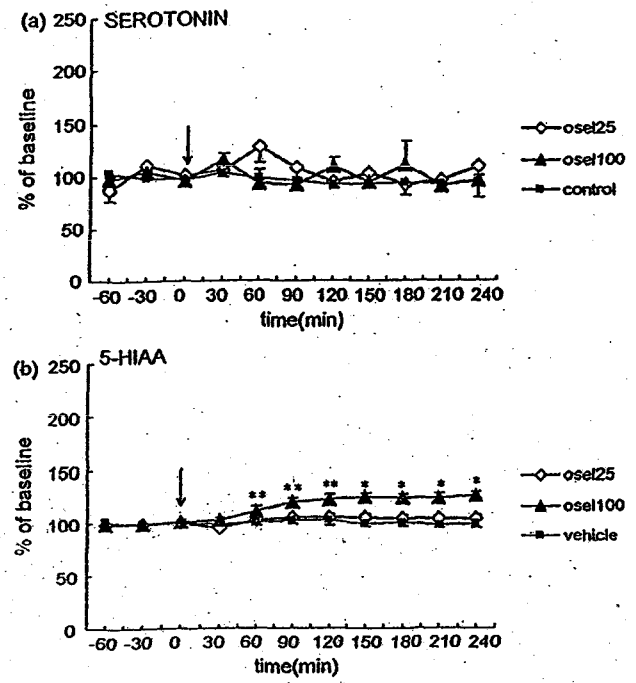

Fig. 2. Effects of oseltamivir on the extracellular DOPAC concentration in the rat mPFC. (a) Effects of oseltamivir on the extracellular HVA concentration in the rat mPFC. (b) Effects of oseltamivir on the extracellular 5-HIAA concentration in the rat mPFC. (c) Drug injection is indicated by the arrow. Data are represented as the mean ± S.E.M. of the values obtained in five rats. $^{*}p < 0.01$, $^{**}p < 0.05$ compared with the corresponding value for vehicle (one-way ANOVA followed with Dunnett's test).

tions. However, in the present study, the levels of DOPAC, HVA, DA metabolites, and DA in the rat mPFC were increased by oseltamivir administration. Therefore, oseltamivir may cause the release of DA from presynaptic sites.

The present study showed that DA increased to 156% and 223% of the pre-administration level following the intraperitoneal administration of 25 and 100 mg/kg oseltamivir, respectively. In rats, ataxia was observed within 10 min after 100 mg/kg oseltamivir was administered, and the ataxia continued for a few minutes. However, compared with the marked increase in DA levels (over 10-fold of the pre-administration level) induced by psychostimulants including phencyclidine and methamphetamine [13], the action of oseltamivir as a DA releaser is less potent. It is reported that oseltamivir does not readily cross the blood–brain barrier (BBB) [6]. Recently, Morimoto et al. [10] reported that P-glycoprotein affects the accumulation of oseltamivir in the brain. The rats used in our experiment were normal; however, if the experimental animals are infected with the influenza virus or have high fever due to infection or insufficient P-glycoprotein activity, it is possible that the BBB is impaired and oseltamivir may reach the central nervous system more easily [14]. In this case, the extracellular DA levels may markedly increase.

Because 5-HT as well as DA neurotransmission in the central nervous system influences animal behavior [4,15], we also measured the levels of 5-HT and 5-HIAA, a metabolite of 5-HT, in the rat mPFC after oseltamivir injection. Although the 5-HIAA levels were significantly increased (126% of the pre-administration level), the 5-HT levels were unchanged after oseltamivir injection. Currently, it is not clear whether 5-HT neurotransmission is closely associated with the abnormal behaviors observed during oseltamivir treatment.

Recently, Izumi et al. [6] reported that oseltamivir and oseltamivir carboxylate, the active metabolite of oseltamivir, affect the central nervous system in vitro, and that the metabolite is more active than oseltamivir. Therefore, further studies are required to investigate the effects of oseltamivir carboxylate on the DA system.

The abnormal behaviors of many patients during oseltamivir treatment may be due to influenza-associated encephalopathy [11]. However, patients showing abnormal behaviors have been observed only in Japan where 70–80% of all oseltamivir consumed and not in Western countries. This fact suggests that not all abnormal behaviors were due to influenza-associated encephalopathy and that some of the abnormal behaviors may result from the use of oseltamivir. The present study suggests that the mechanism underlying the abnormal behaviors observed during oseltamivir use may, to some extent, be due to the transmission of overactive DA.

In conclusion, systemic administration of oseltamivir increased the concentrations of DA and its metabolites in the rat mPFC in a dose-dependent manner. These findings indicate that oseltamivir treatment is related to the manifestation of abnormal behaviors.

References

[1] P.J. Drinka, T. Haupt, Emergence of rimantadine-resistant virus within 6 days of starting rimantadine prophylaxis with oseltamivir treatment of symptomatic cases, J. Am. Geriatr. Soc. 55 (2007) 923–926.
[2] N.M. Ferguson, D.A. Cummings, C. Fraser, J.C. Cajka, P.C. Cooley, D.S. Burke, Strategies for mitigating an influenza pandemic, Nature 442 (2006) 448–452.
[3] A.A. Grace, Phasic versus tonic dopamine release and the modulation of dopamine system responsivity: a hypothesis for the etiology of schizophrenia, Neuroscience 41 (1991) 1–24.
[4] S.L. Handley, J.W. McBlane, M.A. Critchley, K. Njung'e, Multiple serotonin mechanisms in animal models of anxiety: environmental, emotional and cognitive factors, Behav. Brain Res. 58 (1993) 203–210.
[5] G. He, J. Massarella, P. Ward, Clinical pharmacokinetics of the prodrug oseltamivir and its active metabolite Ro 64-0802, Clin. Pharmacokinet. 37 (1999) 471–484.
[6] Y. Izumi, K. Tokuda, K.A. O'dell, C.F. Zorumski, T. Narahashi, Neuroexcitatory actions of Tamiflu and its carboxylate metabolite, Neurosci. Lett. 426 (2007) 54–58.
[7] V.J. Lee, K.H. Phua, M.I. Chenm, A. Chow, S. Ma, K.T. Goh, Y.S. Leo, Economics of neuraminidase inhibitor stockpiling for pandemic influenza, Singapore, Emerg. Infect. Dis. 12 (2006) 95–102.
[8] C.A. Marsden, Dopamine: the rewarding years, Br. J. Pharmacol. 147 (Suppl. 1) (2006) S136–S144.
[9] A.J. McGeer, W. Lee, M. Loeb, A.E. Simor, M. McArthur, K. Green, J.H. Benjamin, C. Gardner, Adverse effects of amantadine and oseltamivir used during respiratory outbreaks in a center for developmentally disabled adults, Infect. Control Hosp. Epidemiol. 25 (2004) 955–961.
[10] K. Morimoto, M. Nakakariya, Y. Shirasaka, C. Kakinuma, T. Fujita, I. Tamai, T. Ogihara, Oseltamivir (Tamiflu) efflux transport at the blood–brain barrier via P-glycoprotein, Drug Metab. Dispos. 36 (2008) 6–9.
[11] M. Nakamura, G. Yamanaka, H. Kawashima, Y. Watanabe, H. Ioi, Y. Kashiwagi, K. Takekuma, A. Hoshika, M. Hayakawa, S. Suzuki, Clinical application of rapid assay of interleukin-6 in influenza-associated encephalopathy, Dis. Mark. 21 (2005) 199–202.
[12] K.G. Nicholson, F.Y. Aoki, A.D. Osterhaus, S. Trottier, O. Carewicz, C.H. Mercier, A. Rode, N. Kinnersley, P. Ward, Efficacy and safety of oseltamivir in treatment of acute influenza: a randomised controlled trial, Lancet 355 (2000) 1845–1850.
[13] K. Nisijima, A. Kashiwa, A. Hashimoto, H. Iwama, A. Umino, T. Nishikawa, Differential effects of phencyclidine and methamphetamine on dopamine metabolism in rat frontal cortex and striatum as revealed by in vivo dialysis, Synapse 22 (1996) 304–312.
[14] R. Noor, C.X. Wang, A. Shuaib, Hyperthermia masks the neuroprotective effects of tissue plaminogen activator, Stroke 36 (2005) 665–669.
[15] N.V. Weisstaub, M. Zhou, A. Lira, E. Lambe, J. González-Maeso, J.P. Hornung, E. Sibille, M. Underwood, S. Itohara, W.T. Dauer, M.S. Ansorge, E. Morelli, J.J. Mann, M. Toth, G. Aghajanian, S.C. Sealfon, R. Hen, J.A. Gingrich, Cortical 5-HT2A receptor signaling modulates anxiety-like behaviors in mice, Science 313 (2006) 536–540.
[16] T. Yoshino, K. Nisijima, K. Shioda, K. Yui, S. Katoh, Perospirone, a novel atypical antipsychotic drug, potentiates fluoxetine-induced increases in dopamine levels via multireceptor actions in the rat medial prefrontal cortex, Neurosci. Lett. 364 (2004) 16–21.
[17] T. Yoshino, K. Nisijima, S. Katoh, K. Yui, M. Nakamura, Tandospirone potentiates the fluoxetine-induced increases in extracellular dopamine via 5-HT (1A) receptors in the rat medial frontal cortex, Neurochem. Int. 40 (2002) 355–360.

J Pharmacol Sci 106, 659 – 662 (2008) No. 4

Journal of Pharmacological Sciences

Short Communication **D17845**

Oseltamivir Enhances Hippocampal Network Synchronization

Atsushi Usami[1], Takuya Sasaki[1], Nobuhiro Satoh[2], Takahiro Akiba[2], Satoshi Yokoshima[2], Tohru Fukuyama[2], Kenzo Yamatsugu[3], Motomu Kanai[3], Masakatsu Shibasaki[3], Norio Matsuki[1], and Yuji Ikegaya[1,4,*]

[1]*Laboratory of Chemical Pharmacology,* [2]*Laboratory of Synthetic Natural Products Chemistry,* and [3]*Laboratory of Synthetic Organic Chemistry, Graduate School of Pharmaceutical Sciences, The University of Tokyo, Tokyo 113-0033, Japan*

[4]*Precursory Research for Embryonic Science and Technology (PRESTO), Japan Science and Technology Agency, 5 Sanbancho Chiyoda-ku, Tokyo 102-00075, Japan*

Received December 4, 2007; Accepted February 4, 2008

Abstract. Oseltamivir, a widely used anti-influenza drug, inhibits virus neuraminidase. A mammalian homologue of this enzyme is expressed in the brain, yet the effect of oseltamivir on central neurons is largely unknown. Patch-clamp recordings ex vivo revealed that oseltamivir enhanced spike synchronization between hippocampal CA3 pyramidal cells. Time-lapse multineuron calcium imaging revealed that oseltamivir and its active metabolite evoked synchronized population bursts that recruited virtually all neurons in the network. This unique, so-far-unknown, event was attenuated by muscarinic receptor antagonist. Thus, oseltamivir is a useful tool for investigating a new aspect of neural circuit operation.

Supplementary Fig. and movie: available only at http://dx.doi.org/10.1254/jphs.SC0070467

Keywords: oseltamivir, functional multineuron calcium imaging, network excitability

Sialic acid is a component of glycoproteins in the cell membrane and regulates various biological functions by inhibiting cellular adhesion. In the central nervous system, sialic acid is mainly present as a chain of neural cellular adhesion molecules, which is abundant in the paleocortical dentate gyrus-CA3 region (1, 2). Neuraminidase (exo-α-sialidase) is a key regulator of the length of sialic acid chains, and the malfunction of this enzyme is associated with epileptic conditions (2). Indeed, sialylation in rat CA3 pyramidal neurons changes the action potential threshold by modulating the properties of voltage-sensitive sodium channels, resulting in an alteration in the excitability of hippocampal networks (3).

Oseltamivir was designed according to the X-ray crystal structure of sialic acid analogues bound to the active site of neuraminidase. This drug is an ethyl-ester prodrug: its active metabolite inhibits virus-type neuraminidase and thereby prevents influenza virus from emerging from infected cells. The structure of viral neuraminidase, however, is very similar to that of HsNEU2, one of four human sialidases (4). HsNEU2 contains exactly the same active site residues, thus being a possible target of oseltamivir. Consistent with this, a recent study has demonstrated that oseltamivir and its active metabolite facilitate the presynaptic function of CA1 excitatory synapses in rat hippocampal slices (5). Here we use electrophysiological recording and functional multineuron calcium imaging (fMCI) techniques to examine the effect of oseltamivir on the excitability of CA3 networks.

Hippocampal slice cultures were prepared from postnatal day 7 Wistar/ST rats (SLC, Shizuoka). Rat pups were decapitated, and the brains were cut into horizontal 300-μm-thick slices using a DTK-1500 microslicer (Dosaka, Kyoto) in aerated, ice-cold Gey's balanced salt solution (Invitrogen, Gaithersburg, MD, USA) supplemented with 25 mM glucose. Entorhinohippocampal stumps were cultivated for 7 – 14 days on Omnipore membrane filters (JHWP02500, ϕ25 mm; Millipore, Bedford, MA, USA) (6). Cultures were fed with 1 ml of 50% minimal essential medium, 25%

*Corresponding author (affiliation #1). ikegaya@mol.f.u-tokyo.ac.jp
Published online in J-STAGE on April 9, 2008 (in advance)
doi: 10.1254/jphs.SC0070467

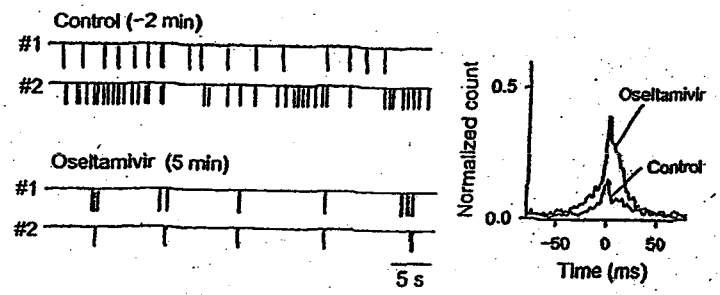

Fig. 1. Oseltamivir synchronizes action potentials between neuron pairs in hippocampal CA3 networks. Dual loose-patch-clamp recordings were performed with glass pipettes filled with ACSF to record extracellular single-unit activity from adjacent hippocampal CA3 pyramidal cell pairs. Recordings were carried out using Axopatch 700B amplifiers (Molecular Devices. Union City, CA. USA). and signals were low-pass filtered at 1 kHz. digitized at 10 kHz. and analyzed with pCLAMP 8.0 software (Molecular Devices). Bursts were defined as any series of spikes with an interval of less than 1 s. Left panels: representative traces of simultaneous loose-patch recordings from two CA3 pyramidal cells 2 min before (top) and 5 min after bath application of 100 μM oseltamivir (bottom). Right panel: crosscorrelogram of spike counts in the same neurons. Oseltamivir increased the degree of spike synchronization. Similar results were obtained in all 4 cases tested.

Hanks' balanced salt solution (Invitrogen), and 25% horse serum (Cell Culture Laboratory, Cleveland, OH, USA) in a humidified incubator at 37°C in 5% CO_2. The medium was changed every 3.5 days.

Experiments were performed in artificial cerebrospinal fluid (ACSF) consisting of 127 mM NaCl, 26 mM $NaHCO_3$, 3.3 mM KCl, 1.24 mM KH_2PO_4, 1.0 mM $MgSO_4$, 1.0 mM $CaCl_2$, and 10 mM glucose, bubbled with 95% O_2 and 5% CO_2 (7). Slices were pre-incubated in ACSF at room temperature for more than 30 min and transferred to a 36°C recording chamber perfused with ACSF at a rate of 1.5 to 2 ml/min. Oseltamivir was chemically synthesized (8 – 10). *N*-Acetyl-2,3-dehydro-2-deoxyneuraminic acid (NADNA) was purchased from Sigma-Aldrich (St. Louis, MO, USA). Both inhibitors were dissolved in ASCF and bath-applied.

For calcium imaging, slices were incubated with 0.0005% Oregon green 488 BAPTA-1AM (Invitrogen) for 1 h at 37°C and then with ACSF at room temperature for >30 min (11). They were transferred to a 36°C recording chamber. The CA3 stratum pyramidale was illuminated at 488 nm and imaged at 10 – 100 frames/s with a CSU22/CSUX1 Nipkow-disk confocal unit (Yokogawa Electric, Tokyo) and a cooled CCD camera (iXon DV887/DU860; Andor Technology, Belfast, UK). Spike-triggered Ca^{2+} signals were detected with custom-written software in Microsoft Visual Basic (Microsoft, Seattle, WA, USA) (11).

We recorded spike activity simultaneously from two CA3 pyramidal cells under control conditions for a total time of 13 min and then in the presence of oseltamivir for a total time of 11 min (n = 4 pairs) (Fig. 1). Neurons spontaneously fired a series of action potentials. Under control conditions, the timings of the action potentials were almost uncorrelated between the neuron pairs, but after bath application of 100 μM oseltamivir, the same pairs became to emit intermittent bursts of action potentials. On average, single bursts included 5.3 ± 0.2 spikes at 44.7 ± 3.4 Hz (mean ± S.E.M., n = 234 bursts). This burst frequency corresponds to the so-called "gamma frequency" range. Importantly, the bursts concurred between neuron pairs; spike-timing crosscorrelogram (Fig. 1 right) shows that oseltamivir increased the peak amplitude at a time difference of 0 ms, indicating that it enhanced spike synchronization between hippocampal CA3 neurons.

To address the effect of oseltamivir at the network level, we used functional multineuron calcium imaging (11). By taking advantage of the fact that action potentials evoke Ca^{2+} transients in the soma (Fig. 2A), this optical technique can reconstruct spike activity from hundreds of neurons in a network with single-cell resolution (Fig. 2B). Under control conditions, the activity of CA3 neurons was sparse in time and space, but after bath application of 100 μM oseltamivir, they showed a gradual increase in activity rates and abruptly started to show globally synchronized "population burst" activity after 3 – 20 min (Fig. 2C; see also supplementary Fig. 1 and movie 1: available at online version only). The same effect was produced by 100 μM NADNA, another neuraminidase inhibitor (Fig. 3A, n = 5 slices).

We sought to characterize the population burst events. The emergence of these events, that is, the percentage of slices that showed population bursts, depended on the concentration of oseltamivir in the range from 0.3 – 100 μM (Fig. 3A, n = 5 – 8 slices for each concentration). This dose-response curve shifted leftward for the active metabolite of oseltamivir (Fig. 3A). With least-square regression to a sigmoid curve, the ED_{50} value was estimated to be 10.2 μM for oseltamivir and 0.7 μM for the active form. The event frequency, that is, the number of events per min, had no relation to the oseltamivir concentration ($R = 0.20$, $P = 0.29$, Pearson's test) (Fig. 3B) nor did the event duration, that is, the mean period during which individual burst persisted, have any

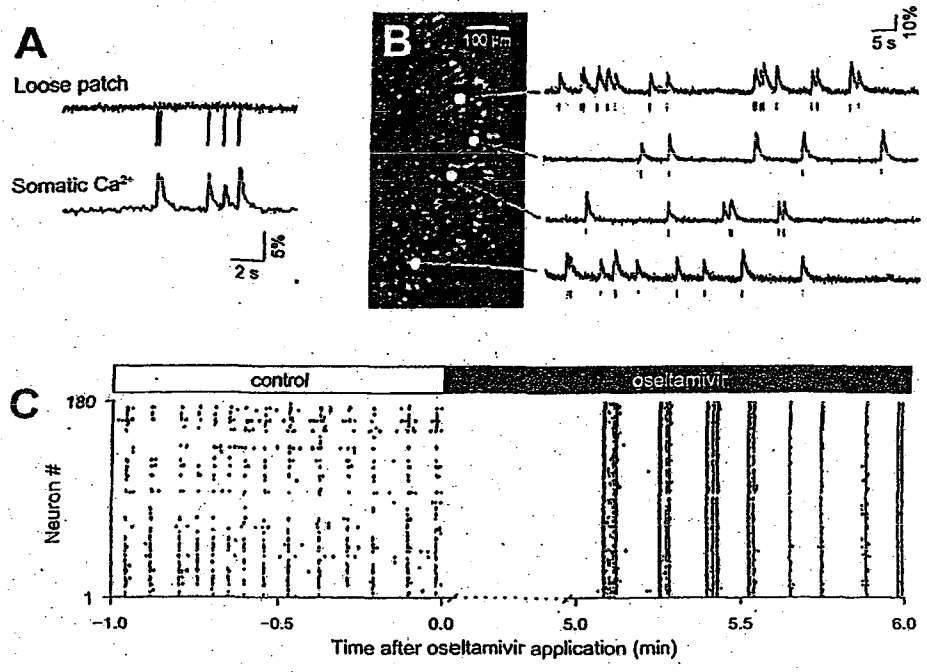

Fig. 2. Oseltamivir induces globally synchronized "population burst" activity. A: Simultaneous loose-patch-clamp recordings and time-lapse imaging of somatic Ca^{2+} signals from a CA3 pyramidal neuron loaded with Oregon green 488 BAPTA-1 reveal that action potentials are faithfully reflected as Ca^{2+} transients. B: Functional calcium imaging and reconstruction of multineuronal spike trains. Representative Ca^{2+} traces of 4 cells indicated in the confocal image of the CA3 pyramidal cell layer of a dye-loaded hippocampal slice culture. Vertical bars under each trace indicate the timings of spikes reconstructed from the raw Ca^{2+} trace. The movie was taken at 100 Hz. C: Examples of the effect of 100 μM oseltamivir on CA3 network activity. Each dot represents the onset of a single calcium transient. After 5 min of treatment with oseltamivir, spikes became synchronized in the whole network.

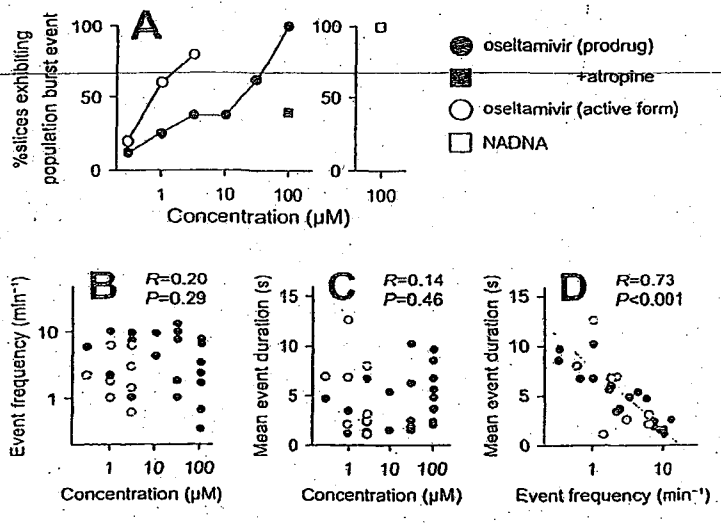

Fig. 3. Characterization of oseltamivir-induced population bursts. A: Concentration-dependent emergence of population bursts. The ordinate indicates the percentage of slices that showed population bursts in response to oseltamivir (closed circles), its hydrolyzed active metabolite (open circles), and NADNA (open square). Atropine was co-applied with 100 μM oseltamivir (closed square). n = 5–8 slices for each concentration. B and C: The frequency of population burst events per min (B) and the average duration for individual population bursts persisted (C) were plotted against the concentrations of oseltamivir and its active form. Each symbol indicates a single slice. D: Negative relationship between the frequency and the duration of population bursts. Line indicates the best linear fit with least square estimation. Significance was determined by Pearson's test.

relation to the concentration ($R = 0.14$, $P = 0.46$) (Fig. 3C). There was a negative relationship, however, between the event frequency and the event duration ($R = 0.73$, $P < 0.001$) (Fig. 3D).

As shown in the above data, oseltamivir-induced bursting had a gamma frequency rhythm. Hippocampal gamma oscillations are believed to arise from activation of muscarinic acetylcholine receptors (12). Consistent with this, we found that in the presence of 10 μM atropine, a muscarinic receptor antagonist, 3 out of 5 slices failed to generate population bursts in response to 100 μM oseltamivir, a concentration of oseltamivir that readily evoked population bursts in all 8 cases tested ($P = 0.035$, Fisher's exact test) (Fig. 3A).

We have demonstrated that oseltamivir and its active metabolite enhanced neuronal synchronization and induced population burst events of rat hippocampal CA3 networks in a concentration-dependent manner. Population bursts did not occur under normal conditions and reflected a globally synchronized state with action potentials at gamma frequency. They seemed to be mediated, at least in part, by muscarinic receptor activity.

Cholinergically induced gamma oscillations are accompanied by rhythmic activity of the inhibitory network, which shunts excitatory synaptic inputs and sharpens the window in which pyramidal neurons can fire action potentials, leading to a tighter synchrony among pyramidal neurons (12). Thus, oseltamivir-induced population bursts may be shaped by the phasic activity of inhibitory interneurons, rather than pyramidal cells. Our preliminary data indicate that even at a high concentration of 1 mM, oseltamivir does not induce either depolarization or hyperpolarization of membrane potential of hippocampal excitatory neurons in primary dispersed cultures (n = 8, data not shown). Thus, our data imply two, but not mutually exclusive, possibilities concerning the action site of oseltamivir: i) inhibitory interneurons are an action target of oseltamivir, and ii) the effect of oseltamivir requires network activity flows, rather than single neurons. Given that two structurally unrelated neuraminidase inhibitors, that is, oseltamivir and NADNA, exerted the sane effect on network activity and that sialic acid, a neuraminidase substrate, regulates neurite adhesion between hippocampal neurons (1), we speculate that oseltamivir modulates sialylation-mediated neurite connectivity and enhances network synchronicity through interneurons.

Animal experiments with rodents demonstrate that orally (30 – 300 mg/kg) or intravenously (8 μmol/h per kg) administered oseltamivir accumulates in the brain via the blood-brain barrier, the brain-to-plasma concentration ratio ranging from 0.1 – 0.7 (roughly equal to 0.1 – 5 μM in the brain) (13, 14). Safety examinations of Tamiflu™ (oseltamivir), conducted by Roche, show that in 7 – 14-day-old rats, the brain concentration reaches more than 500 times greater than that in adult animals (see basic product information of Tamiflu™), suggesting a higher risk of a side-effect in younger brains. Interestingly, a minor allele with single nucleotide polymorphism in HsNEU2, which shows a strong binding affinity to oseltamivir, is frequently observed in Asians (9.29%), but not in Europeans and African Americans (15). This Asian population may be highly susceptible to oseltamivir and thus affected by neuropsychiatric disorders. Because our current data are not linked to behavioral alternations in human and animals, investigations in vivo will be necessary to examine whether oseltamivir-induced population bursts are related to some psychologic behaviors frequently seen in influenza-infected children.

Acknowledgments

This work was supported in part by a Grants-in-Aid for Science Research (No. 18021008, 17689004) from Japan Society for the Promotion of Science.

References

1 Cremer H, Chazal G, Carleton A, Goridis C, Vincent JD, Lledo PM. Long-term but not short-term plasticity at mossy fiber synapses is impaired in neural cell adhesion molecule-deficient mice. Proc Natl Acad Sci U S A. 1998;95:13242–13247.
2 Boyso A, Ayala J, Gutiérrez R, Hernández-RJ. Neuraminidase activity in different regions of the seizing epileptic and non-epileptic brain. Brain Res. 2003;964:211–217.
3 Isaev D, Isaeva E, Shatskih T, Zhao Q, Smits NC, Shworak NW, et al. Role of extracellular sialic acid in regulation of neuronal and network excitability in the rat hippocampus. J Neurosci. 2007;27:11587–11594.
4 Chavas LM, Tringali C, Fusi P, Venerando B, Tettamanti G, Kato R, et al. Crystal structure of the human cytosolic sialidase Neu2. Evidence for the dynamic nature of substrate recognition. J Biol Chem. 2005;280:469–475.
5 Izumi Y, Tokuda K, O'Dell KA, Zorumski CF, Narahashi T. Neuroexcitatory actions of tamiflu and its carboxylate. Asymmetric membrane ganglioside sialidase activity specifies axonal fate. Neurosci Lett. 2007;426:54–58.
6 Koyama R, Muramatsu R, Sasaki T, Kimura R, Ueyama C, Tamura M, et al. A low-cost method for brain slice cultures. J Pharmacol Sci. 2007;104:191–194.
7 Sasaki T, Matsuki N, Ikegaya Y. Metastability of active CA3 networks. J Neurosci. 2007;27:517–528.
8 Satoh N, Akiba T, Yokoshima S, Fukuyama T. A practical synthesis of (–)-oseltamivir. Angew Chem Int Ed. 2007;46:5734–5736.
9 Yamatsugu K, Kamijo S, Suto Y, Kanai M, Shibasaki M. A concise synthesis of tamiflu: third generation route via the diels-alder reaction and the curtius rearrangement. Tetrahedron Lett. 2007;48:1403–1406.
10 Ishii K, Hamamoto H, Sasaki T, Ikegaya Y, Yamatsugu K, Kanai M, et al. Pharmacologic action of oseltamivir on the nervous system. Drug Discov Ther. 2008;2:24–34.
11 Takahashi N, Sasaki T, Usami A, Matsuki N, Ikegaya Y. Watching neuronal circuit dynamics through functional multineuron calcium imaging (fMCI). Neurosci Res. 2007;58:219–225.
12 Fisahn A, Yamada M, Duttaroy A, Gan JW, Deng CX, McBain CJ, et al. Muscarine induction of hippocampal gamma oscillations requires coupling of the M1 receptor to two mixed cation currents. Neuron. 2002;33:615–624.
13 Morimoto K, Nakakariya M, Shirasaka Y, Kakinuma C, Fujita T, Tamai I, et al. Oseltamivir (Tamiflu™) efflux transport at the blood-brain barrier via P-glycoprotein. Drug Metab Dispos. 2008;36:6–9.
14 Ose A, Kusuhara H, Yamatsugu K, Kanai M, Shibasaki M, Fujita T, et al. P-glycoprotein restricts the penetration of oseltamivir across the blood-brain barrier. Drug Metab Dispos. 2008;36:427–434.
15 Li CY, Yu Q, Ye Z, Sun Y, He Q, Li XM, et al. A non-synonymous SNP in human cytosolic sialidase in a small Asian population results in reduced enzyme activity: potential link with severe adverse reactions to oseltamivir. Cell Res. 2007;17:357–362.

The 81st Annual Meeting of The Japanese Pharmacological Society
日本薬理学会年会，第81回（2008．03．17－19，横浜）

G0756052

P1L-40 Higenamine is the main active substance responsible for the inhibitory effect of *Nandina domestica* Thunberg on histamine-induced contraction of guinea pig tracheal smooth muscle

Takuro Ueki[1,2], Tatsuhiro Akaishi[1], Muneo Tsukiyama[1,3], Hiroko Kikuchi[3], Yoichi Yasuda[3], Tsuneo Morioka[2], Kazuho Abe[1]

[1]Lab. Pharmacol., Fac. Pharm., Musashino Univ., 1-1-20 Shinmachi, Nishitokyo-shi, Tokyo 202-8585, Japan, [2]TOKIWA Pharmaceut, Co. Ltd., Osaka 541-0052, Japan, [3]NOEVIR, Co. Ltd., Kobe 650-8521, Japan

We have previously reported that the crude extract from *Nandina domestica* Thunberg (NDE: 0.1-1 mg/ml) inhibits histamine-induced contraction of isolated guinea pig trachea and the inhibitory effect of NDE cannot be accounted for nantenine, a major alkaloid isolated from NDE. To identify the active constituent(s) responsible for the inhibitory effect of NDE on tracheal contraction, we obtained several fractions of NDE and investigated their pharmacological effects on contractile responses in isolated guinea pig trachea. Among five fractions prepared from NDE by HP-20 column chromatography, only the 40% methanol fraction inhibited histamine-induced tracheal contraction. The 40% methanol fraction was further analyzed with the ultraviolet spectrometer and liquid chromatograph/mass spectrometer. Finally, we obtained only one fraction that inhibited histamine-induced tracheal contraction, and the mass spectrometry and nuclear magnetic resonance analysis identified higenamine as the active substance. We conclude that higenamine is the main active constituent of NDE in inhibiting tracheal contraction.

P1L-41 Effects of pressure stimulus on cell proliferation and differentiation in L6 skeletal muscle cells

Yoshiki Fujisawa[1], Kenji Iizuka[1], Noriteru Morita[2], Takuji Machida[1], Masahiko Hirafuji[1]

[1]Dept. Pharmacol., Facul. Pharm. Sci., Health Sci. Uni. of Hokkaido, 1757 Kanazawa, Ishikari-Tobetsu, Hokkaido 061-0293, Japan, [2]Dept. Wellness Planning., School of Lifelong Learning Support Systems, Hokusho Uni., 23 Bunkyodai, Ebetsu, Hokkaido 069-8511, Japan

Mechanical forces related to pressure is an important factor for cell hypertrophy and proliferation. The effects of pressure stimuli on skeletal muscles are not yet well characterized. The purpose of this study is to examine the effects of a pure pressure stimulus on skeletal muscle cells. Atmospheric pressure was applied to rat L6 myoblasts and myotubes at 160 mmHg for 3 hours. Protein and mRNA expressions were analyzed by using immunoblotting and real-time RT-PCR, respectively. Phosphorylated ERK and JNK were both increased in pressurized skeletal muscle myoblasts. Phosphorylated p38, myogenin protein and insulin-like growth factor mRNA were all decreased in pressurized skeletal muscle myoblasts. Induction of cell differentiation to myotubes resulted in an increase of phosphorylated ERK compared to myoblasts. However, pressurization to myotubes failed to induce significant change in phosphorylated ERK. These findings demonstrate that a pure mechanical pressure stimulus enhances cell proliferation and suppresses cell differentiation in skeletal muscle myoblast, and raise the possibility that elevated intramuscular pressure may have diverse effects according to the differentiative stage of skeletal muscle.

D16575

P2L-01 Oseltamivir induces spike synchronization in hippocampal networks

Atsushi Usami[1], Takuya Sasaki[1], Nobuhiro Satoh[2], Takahiro Akiba[2], Satoshi Yokoshima[2], Tohru Fukuyama[2], Kenzo Yamatsugu[3], Motomu Kanai[3], Masakatsu Shibasaki[3], Norio Matsuki[1], Yuji Ikegaya[1]

[1]Laboratory of Chemical Pharmacology, Graduate School of Pharmaceutical Sciences, Tokyo University, 7-3-1 Hongo, Bunkyo-ku, Tokyo 113-0033, Japan, [2]Laboratory of Synthetic Natural Products Chemistry, Graduate School of Pharmaceutical Sciences, Tokyo University, 7-3-1 Hongo, Bunkyo-ku, Tokyo 113-0033, Japan, [3]Laboratory of Synthetic Organic Chemistry, Graduate School of Pharmaceutical Sciences, Tokyo University, 7-3-1 Hongo, Bunkyo-ku, Tokyo 113-0033, Japan

Oseltamivir is an antiviral drug used to treat influenza. It inhibits neuraminidase, thereby preventing influenza virus from emerging from infected cells. The effect of oseltamivir on the central nervous system is largely unknown, however. We monitored the activity of neurons treated with oseltamivir in hippocampal slice cultures, by using electrophysiological recordings and functional multineuron calcium imaging. Double patch-clamp recordings revealed that oseltamivir led to spike synchronization among adjacent hippocampal CA3 neurons. To investigate how oseltamivir alters neuronal network operation, we simultaneously recorded the spike activity of hundreds of hippocampal neurons. Oseltamivir and its active form both induced global spike synchronization that recruited virtually all neurons in the network and persisted for more than several seconds. The effect was concentration-dependent. Network excitability may be regulated by extracellular sialic residues through neuraminidase.

P2L-02 Visualization of neuronal network activity: implications for a new drug-screening method in systems neuropharmacology

Naoya Takahashi, Takuya Sasaki, Norio Matsuki, Yuji Ikegaya

Lab. Chem. Pharmacol., Grad. Sch. Pharm. Sci. Univ. Tokyo, 7-3-1 Hongo, Bunkyo-ku, Tokyo 113-0033, Japan

Synchronization in cortical networks is a prevalent feature that reflects dynamic processing of sensory input and internal information. We developed high-speed functional multineuron calcium imaging (fMCI) to simultaneously record action potentials from about hundreds of neurons at up to 2000 frames/s and reconstructed the spatiotemporal pattern of hippocampal CA3 network activity in vitro. Spontaneous activity displayed the emergence and dynamics of synchronized network activity with millisecond coordination. Whole-cell recordings from synchronized neuron pairs revealed that coordinated excitatory inputs potentially contributed to precise synchronization. To elucidate the profile of network synchrony, in fMCI data sets, we estimated the statistical significance of synchronicity between all possible neuron pairs. The graphs, in which individual neurons were functionally connected based on strength of pairwise correlation, were sparse, complex and locally clustered, exhibiting small-world architectures. These findings provide a simplified strategy for evaluating network operations, which will provide a new drug screening technique in systems neuropharmacology.

28J-am06

ラット脳および培養アストロサイトにおけるTissue Inhibitor of Matrixmetalloproteinase発現に対するエンドセリンの作用

○小山 登[1]. 田中 一裕[1](1大阪大谷大薬)

【目的】Matrix Metalloproteinases(MMPs)は、細胞外マトリクス分子の分解を行う分泌型プロテアーゼファミリーで、脳病態時の脳浮腫や神経細胞死の発生に関わる。一方、内因性の MMP 阻害因子として見いだされた Tissue Inhibitor of Matrixmetalloproteinase (TIMP)も脳病態時に発現が増加する。この増加した TIMP は、過剰な MMP 活性を抑制し、傷害から脳を保護すると考えられている。エンドセリン（ET）は、神経系の病態生理反応に関わる因子である。我々は既に、ET_B 受容体アゴニストが、ラット脳内の MMP2 および MMP9 の発現を増加させることを報告している。今回、ラット脳での TIMP 発現に対する ET の作用を検討した。【方法】ラット脳室内への ET アゴニスト持続投与はミニ浸透圧ポンプを用い行なった。TIMP の mRNA およびタンパク量の測定は定量的 RT-PCR 法およびイムノブロットにより測定した。培養アストロサイトは生後 0―2 日齢の Wistar 系ラット大脳皮質より調製した。【結果】ET_B アゴニスト Ala-ET-1(500pmole/day)を 7 日間脳室内へ持続投与したラットの大脳では TIMP-1 および TIMP-3 mRNA の増加が、海馬および線条体では TIMP-1 mRNA の増加が観察された。免疫組織化学的検討は、これらの TIMP が GFAP 陽性アストロサイトで発現していることを示した。培養アストロサイトに対し ET-1 (100nM)は、TIMP-1 および TIMP-3 mRNA 発現、および細胞外へ遊離を促進した。【考察】以上の結果は、脳病態時のアストロサイトの TIMP 産生における、ET の関与を示唆する。

28J-am07

ブラジキニン(BK)による逆モードNa⁺-Ca²⁺交換機構(NCX)の活性化及びB₁受容体を介するミクログリアの遊走性・化学走性増加

○井福 正隆[1], Katrin Farber[2], 奥野 祐子[1], 山川 裕希子[1], 宮本 恭貴[1], Christiane Nolte[2], 和田 圭司[1], Helmut Kettenmann[2], 野田 百美[1](1九大院薬, 2MDC, 3国立精神・神経セ)

【目的】中枢神経系で免疫系を司るミクログリアは、様々な神経変性疾患や傷害、虚血時に活性化され、また炎症とも深く関わっていることが知られている。我々は、炎症性メディエーターであるブラジキニン(BK)の受容体がミクログリアにも発現しており、Ca^{2+}依存性の K^+電流（$I_{K(Ca)}$）を誘発することを報告してきた。$I_{K(Ca)}$ の誘発はミクログリアの遊走性増加に関与するという報告があるので、BK によるミクログリアの遊走性・化学走性への関与及びその要因について検討した。【方法】初代培養ミクログリアは生後 3 日目の Wister ラットまたは BK 受容体ノックアウト(KO) マウス、Na^{2+}/Ca^{2+}交換機構タイプ 1 （NCX1）KO マウス（ヘテロ）の大脳皮質より単離した。遊走性は、長期培養観察装置を、化学走性は Boyden chamber を用いて解析した。

【結果・考察】BK 処置により、遊走性・化学走性の増加が見られ、これらの反応は B_1 受容体の拮抗薬により抑制され、B_1-KO マウスから得られたミクログリアでは消失した。BK による遊走性・化学走性増加はプロテインキナーゼ C (PKC)・$I_{K(Ca)}$ の阻害薬、逆モード NCX1（Ca^{2+}流入モード）の特異的な拮抗薬および NCX1-KO マウスより単離したミクログリアで有意に抑制された。また *in vivo* においても、傷害部位へのミクログリアの集積は、$I_{K(Ca)}$の阻害薬及び B_1-KO マウスで有意に減少していた。以上の結果より、BK によるミクログリアの遊走性・化学走性増加および傷害部位への集積のメカニズムは B_1 受容体を介した PKC の活性化と逆モード NCX1 の活性化による細胞内への Ca^{2+}の流入、及びそれによる $I_{K(Ca)}$の誘発を介することが明らかとなった。このようなシグナリングを介したミクログリアの集積が傷害部位でどのような役割を演じているのかを検討するのが今後の課題である。

G0756444

28J-am08

ットの睡眠覚醒サイクルに対する kavain の影響

村井 隆賀[1], 四宮 一昭[1], 武田 麻宏[1], 亀井 千晃[1](1岡山大院医歯薬)

【目的】現在臨床で繁用されている benzodiazepine 系睡眠薬は，様々な副作用を有し，睡眠の質を低下させることが報告されている．従って，新規睡眠薬として，生薬抽出成分が注目されている．Kava-kava はその抽出成分が睡眠作用を有することが判明している生薬である．しかし長期服用により劇症肝炎を発症されることが知られており，国内においてその使用が制限されている．そこで今回，kava-kava 中に含まれる成分のうち，肝炎発症に関与していないとされている kavain に注目し，睡眠覚醒サイクルに対する効果を rilmazafone および diphenhydramine の効果と比較検討した．

【方法】右前頭葉皮質および頸部筋に慢性電極を挿入したラットを用い，薬物投与後の脳波および筋電図を 6 時間測定した．睡眠ステージの分類および脳波の周波数解析には，睡眠解析プログラムである SleepSign ver.2.0 を用いた．

【結果】Kavain，rilmazafone および diphenhydramine は睡眠導入潜時を有意に短縮させた．また kavain および rilmazafone では有意な覚醒時間の短縮作用および NREM 睡眠時間の延長作用が確認されたが，diphenhydramine では認められなかった．次に NREM 睡眠時間を延長した kavain および rilmazafone の睡眠の質 （delta activity）に対する影響を検討した．その結果，kavain は delta activity を有意に上昇させたが，rilmazafone は逆に有意に低下させた．

【考察】Diphenhydaramine は睡眠導入作用のみ有することが明らかとなった．一方 kavain は，rilmazafone と同様の睡眠パターンを有するが，rilmazafone とは異なり，睡眠の質をも改善する化合物である可能性が示唆された．

日本薬学会，第１２８年会
（２００８．０３．２６－２８，横浜）

28J-am09

強制水泳によって誘導されるうつ様症状に対するLeu-Ileの効果

○日比(古川) 陽子[1,2], 新田 淳美[2], 池田 武史[2], 森下 幸治[3], 山田 清文[2], 鍋島 俊隆[1](1(財)長寿科学振興財団, 2名大病院薬, 3協和発酵, 4名城大薬)

（目的）近年、多くの人々がうつ病に罹患しており、社会問題にもなりつつある。うつ病患者の脳では海馬の縮小がみとめられるなど、神経変性や神経新生の異常が起こっていることが示唆されている。一方、我々はこれまでに疎水性ジペプチド Leu-Ile が様々な神経変性精神疾患に効果を示すことを示してきた。そこで今回、Leu-Ile が抗うつ作用を示すのではないかと考え、マウスにうつ様症状を誘導するモデルを用いて Leu-Ile の効果を調べた。

（方法）雄性 ICR マウスを水を張った円筒形の容器に入れ、毎日 6 分間の強制水泳試験を 2 週間連続して行った。投入直後のマウスは水槽から逃れようと泳ぐが次第に浮いているだけの無動状態となる。この無動時間の長短はうつ様症状の指標とされており、抗うつ薬投与によって短縮する。そこで Leu-Ile を強制水泳直後に連続経口投与し、無動時間に及ぼす影響を調べた。

（結果および考察） 2 週間の強制水泳によってマウスの無動時間は著しく増大し、うつ様症状が誘導されたことが確認された。Leu-Ile を 750 μmol/kg 投与したマウス群では、投与開始 10 日前後から無動時間がコントロール群に比べて有意に短縮した。自発行動量は Leu-Ile 投与マウスとコントロールの間に差はなかった。Real time RT-PCR の結果から、Leu-Ile 連続投与によって海馬と前頭皮質において BDNF の発現量が増大することが示された。さらに、BrdU の取り込みを指標として細胞新生について検討したところ、2 週間の強制水泳によって海馬歯状回における BrdU 陽性細胞数が著しく減少したが、Leu-Ile 投与によって、この細胞数減少は抑制された。以上の結果より、Leu-Ile が BDNF シグナル伝達経路を介してストレスによる細胞増殖抑制を改善し、抗うつ作用を示す可能性が示唆された。

D16576

28J-am10

リン酸オセルタミビア(タミフル)とその生体内活性体のラット脳モノアミン神経伝達系におよぼす影響

○佐藤 かな子[1], 野中 良一[1], 小縣 昭夫[1], 中江 大[1], 上原 眞一[1](1東京都健安研)

【目的】インフルエンザ治療薬である、リン酸オセルタミビア（タミフル）服用者に、近年、飛び出し、転落等の異常行動が報告されたため、現在、厚生労働省より、「10 代の患者にはタミフルの処方を原則中止」の方針が示されている。しかし、タミフル服用と異常行動との因果関係は、いまだ明らかになっていない。タミフルはラットの血液脳関門を通過することが報告[1]されており、このことはタミフル服用時の異常行動が覚醒剤や麻薬と類似した機序で発生することを示唆する。タミフルは、プロドラッグであり、生体内で代謝され活性体（GS4071）となり作用を発揮する。そこで、本報告は、タミフル服用と異常行動との関連性の有無を明らかにすることを目的に、タミフルとGS4071 の脳モノアミン神経伝達系の前シナプス側における 3 種類の神経伝達物質（ドーパミン、セロトニン、ノルエピネフリン系）および後シナプス側におよぼす影響を試験管内試験で検索した。

【方法】ラット脳より前シナプス側および後シナプス側のシナプトソームをそれぞれ調整した。これらにタミフルまたは GS4071 を作用させた時、前シナプス側における神経伝達物質の再取り込み阻害および遊離促進作用と後シナプス側における G タンパク活性化への影響を覚醒剤および麻薬等と比較検討した。

【結果および考察】タミフルおよびGS4071 は、前シナプスにおける 3 種類の神経伝達物質の再取り込み阻害と遊離促進作用、および後シナプスでのGタンパク活性化のいずれにも影響しなかった。[2]したがって、タミフル服用時における異常行動の発生機序には、脳モノアミン神経伝達系の変化が関与しないものと示唆された。

[1] http://www.fda.gov/medwatch/SAFETY/2003/tamiflu_deardoc.pdf

[2] Satoh, K., *et al.*, *Biol. Pharm. Bull.*, 30 (9), 1816 (2007)

G0756447

28J-am11

モルヒネ誘発嘔気・嘔吐および精神依存形成に対する非定型抗精神病薬アリピプラゾール （エビリファイ®） の効果

○塩川 満[1,2], 成田 年[1], 武井 大輔[1], 鶴川 百合[1], 中邨 篤史[1], 橋本 敬輔[1], 葛巻 直子[1], 鈴木 雅美[1], 井上 忠夫[1], 鈴木 勉[1](1星薬大・薬・薬品毒性, 2聖路加国際病院薬)

モルヒネはがん疼痛緩和で有用な薬剤であるが、副作用として嘔気・嘔吐を発現させるためその予防に中枢性ドパミン受容体拮抗薬が中心に処方される。しかし中枢性ドパミン受容体拮抗薬には副作用として錐体外路症状が発現するため、より副作用の少ない非定型抗精神病薬が適している。非定型抗精神病薬アリピプラゾールは既存の抗精神病薬とは異なり、ドパミン D2 受容体部分作動性を有することからドパミン作動性神経伝達が過剰な場合には、ドパミン D2 受容体の拮抗薬として作用し、ドパミン作動性神経伝達が低下している場合には、ドパミン D2 受容体の作動薬として作用することが基礎実験で確認されている。そこで本研究ではモルヒネ誘発ドパミン関連行動に対する非定型抗精神病薬アリピプラゾールの効果を検討した。

フェレットを用いたモルヒネ誘発嘔気・嘔吐は、アリピプラゾールの前処置により、有意に抑制された。また、モルヒネ誘発ドパミン関連行動である報酬効果ならびに自発運動促進作用はアリピプラゾール処置により用量依存的かつ有意に抑制された。また、モルヒネ誘発嘔気・嘔吐を抑える用量のアリピプラゾールの処置では、錐体外路症状の指標となるカタレプシーは観察されなかった。さらに、モルヒネにより誘発される G 蛋白質活性化作用はアリピプラゾール処置により変化が認められなかったが、ドパミン誘発 G 蛋白質活性化作用は有意に抑制された。これらのことから、アリピプラゾールは μ受容体刺激には直接影響を与えず、ドパミン受容体を拮抗することにより、嘔気・嘔吐や精神依存形成などのドパミン関連行動のみを抑制し、さらには錐体外路症状がほとんど現れない非常に有用なオピオイドとの併用薬物である可能性が示唆された。

Biol. Pharm. Bull. 30(9) 1816—1818 (2007) Vol. 30, No. 9

Effects of Oseltamivir Phosphate (Tamiflu) and Its Metabolite (GS4071) on Monoamine Neurotransmission in the Rat Brain

Kanako SATOH,* Ryouichi NONAKA, Akio OGATA, Dai NAKAE, and Shin-ichi UEHARA

Department of Environmental Health and Toxicology, Tokyo Metropolitan Institute of Public Health; 3-24-1 Hyakunincho, Shinjuku-ku, Tokyo 169-0073, Japan.
Received June 19, 2007; accepted July 10, 2007; published online July 10, 2007

As abnormal behaviors such as jumping and falling from balcony were reported in patients aged 10 to 19 years who administrated oseltamivir phosphate (Tamiflu) for treatment influenza infection, the Ministry of Health, Labor and Welfare in Japan notified that, as a rule, Tamiflu should not be prescribed to patients aged 10 to 19 years. To examine the relationship between Tamiflu and abnormal behaviors, we investigated the effects of Tamiflu and its carboxylic acid metabolite, GS4071, on the central nervous system, that is, on 3 neurotransmitters (dopamine, serotonin, and norepinephrine) in presynapses (inhibition of re-uptake, promotion of release) and postsynapses (guanosine 5′-triphosphate (GTP) γS binding), using rat brain synaptosomes. Neither Tamiflu nor GS4071 influenced the re-uptake/release of the 3 monoamines or GTP binding in postsynapses.

Key words Tamiflu; oseltamivir phosphate; GS4071; dopamine; serotonin; norepinephrine

As an anti-influenza virus agent, oseltamivir phosphate (ethyl-(3*R*,4*R*,5*S*)-3-(1-ethylpropyloxy)-4-acetamido-5-amino-1-cyclohexane-1-carboxylate phosphate, Fig. 1A) (proprietary name: Tamiflu®) was developed by Roche Laboratory Inc. (Switzerland). In Japan, the Ministry of Health, Labor and Welfare approved this agent in 2000. In February 2001 and July 2002, Chugai Pharmaceutical Co., Ltd., as a Japanese agency, started the sales of 75-mg Tamiflu® capsules and 3% Tamiflu® dry syrup, respectively. The action mechanism of Tamiflu is reported as follows[1]: it suppresses viral release from the surfaces of infected cells by inhibiting neuraminidase, an enzyme essential for the proliferation of type A/B influenza virus, preventing viral infection/proliferation in other cells. This mechanism is similar to that of zanamivir hydrate (Relenza®, anti-influenza virus agent). Relenza is an inhalation agent, whereas Tamiflu is an oral preparation; therefore, the administration method is simpler, although the interval until Tamiflu reaches the infected site is prolonged. Furthermore, amantadine hydrochloride (Symmetrel®) is also administered as an oral anti-influenza virus agent. However, it is not effective for influenza infection other than type A influenza infection. Thus, Tamiflu can be simply administered to treat influenza infection, and may be useful for preventing and treating bird influenza infection. According to Roche Laboratory Inc., the sales situation of Tamiflu is as follows.[2] Japanese patients (n=34000000) account for approximately 75% of the total world Tamiflu consumption (45000000 persons, as of March 12, 2007). American patients comprise the second highest percentage (20%). The amount of Tamiflu administered to children in Japan was 13 times higher than that in the United States. The usage of Tamiflu in Japan is numerous.

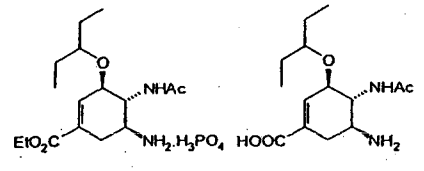

(A) Tamiflu (B) GS4071

Fig. 1. Chemical Structures
A: Tamiflu (oseltamivir phosphate), B: GS4071.

In 2007, abnormal behaviors such as jumping and falling were reported in 10- to 19-year-old patients administrated Tamiflu. Therefore, the Ministry of Health, Labor and Welfare in Japan notified that, as a rule, Tamiflu should not be prescribed to patients aged 10 to 19 years. On April 25, 2007, the Ministry of Health, Labor and Welfare published the "Reports on the Side Effects of Oseltamivir Phosphate (Tamiflu)",[3] which had been submitted between the start of sales and March 20, 2007. According to the report, abnormal behaviors were observed in 186 of 1268 patients with side effects (8 of them died). In the presence of influenza encephalopathy, abnormal behaviors similar to those after Tamiflu administration have also been reported. In Japan (1999, 2000), encephalopathy frequently develops in children aged less than 6 years (2.5/100000 persons),[4,5] and the mortality rate (10 to 30% of patients with encephalopathy) and incidence of squeal (approximately 20% of them) are high.[4,6] In children aged over 1 year, the side effects of Tamiflu are rare and slight.[7] A study indicated that there was no association between Tamiflu and mortality/encephalopathy in infants aged less than 1 year.[8] Concerning the relationship between Tamiflu and abnormal behaviors, another study reported that there was no significant difference in the incidence of abnormal behaviors between patients with and without Tamiflu (11.9% *vs.* 10.6%, respectively).[9]

To evaluate psychoactive drug activity quickly, we reported an assay system for investigating the influence on the central nervous system using synaptosomes prepared from the rat brain[10]: a system for examining the influence of various chemicals including psychoactive drugs on 3 neurotransmitters (dopamine (DA) system, serotonin (5HT) system, and norepinephrine (NE) system) in presynapses (inhibition of re-uptake, promotion of release). Many of the monoamine receptors, including DA, 5HT, and NE receptors, are considered to belong to the superfamily of guanosine 5′-triphosphate (GTP) binding protein-coupled receptors in postsynapses (GTP binding). Abnormal behaviors seen in the case of Tamiflu administration to treat influenza closely resemble those seen in the case of the acute psychoactive drugs intoxication, a pleasurable mix of stimulant-like and hallucinogen-like effects. Oral administration of Tamiflu, an ethyl ester prodrug, is converted to the active form, (3*R*,4*R*,5*S*)-3-(1-ethylpropyloxy)-4-acetamido-5-amino-1-cyclohexane-1-carboxylic acid (GS4071, Fig. 1B) *in vivo*.[1] As an animal experiment it is reported that Tamiflu passes the brain barrier,[11] we investigated the influence of Tamiflu and its metabolite GS4071, which were supplied by Prof. Shibasaki (the Uni-

* To whom correspondence should be addressed. e-mail: Kanako_Satou@member.metro.tokyo.jp

versity of Tokyo, Tokyo, Japan), on DA, 5HT, and NE as well as GTP binding using a psychoactive drug-assay system to examine the relationship between Tamiflu and abnormal behaviors.

MATERIALS AND METHODS

Reagents Tamiflu and GS4071 were a kind gift from Prof. Shibasaki. They were synthesized according to Fukuta *et al.*[12] and Mita *et al.*[13] Methamphetamine (MAP) and cocaine were purchased from Takeda Pharmaceutical Company Limited and Dainippon Sumitomo Pharma Co., Ltd., respectively. Chemicals were dissolved in dimethyl sulfoxide (DMSO, final concentration: 0.1%). ^{3}H-DA (2.20 TBq/mmol), ^{3}H-5HT (1.11 TBq/mmol), ^{3}H-NE (1.93 TBq/mmol), and [^{35}S]GTPγS (46.25 TBq/mmol) were purchased from PerkinElmer Inc. (MO, U.S.A.). Other reagents used in the study were of the highest grade commercially available.

Animals Male Sprague Dawley rats (crlj:CD (SD)) at 5 weeks old were obtained from Charles River Japan (Kanagawa, Japan). After the rats were preliminary bred for one week, they were killed under ether anesthesia and their brains were quickly removed.[10,14] All animal studies were performed in accordance with the UFAW Handbook on the Care and Management of Laboratory Animals.

Preparation of Cerebral Synaptosomes for Re-uptake and Release Assay The striatum and cerebral cortex were dissected from the rat brain. Crude synaptosomes were obtained by the methods described in our previous reports.[10,14] The crude synaptosome from the striatum was used for the assay of re-uptake and release of DA, and that from the cortex was used for the assays of 5HT and NE. For the release assay, 1 μM reserpine was added to 0.32 M sucrose and buffer. The re-uptake and release assays were started immediately after the preparation of synaptosomes. Protein concentrations were determined by the modified Lowry method using a Bio-Rad assay kit.

Preparation of Cerebral Synaptosomes for GTPγS Binding Assay The whole brain dissected on ice was homogenized. Crude synaptosomes were obtained by the modified methods described in previous[15] and our personal reports. The synaptosome was divided into aliquots and stored at −80 °C until use.

^{3}H-DA, ^{3}H-5HT, and ^{3}H-NE Re-uptake and Release Assays The re-uptake and release assays were conducted using the methods described in our previous reports.[10,14] The final concentration of 0.1% DMSO had no effect on the activity. Specific uptake or release was calculated by subtracting the non-specific uptake (DA; 260, 5HT; 500, NE; 720 dpm) or release (DA; 5210, 5HT; 4960, NE; 2200 dpm) content from the total uptake (DA; 11600, 5HT; 2960, NE; 8480 dpm) or release (DA; 10160, 5HT; 7560, NE; 6770 dpm) content. From these results, the drug concentration giving the IC_{50} or EC_{50} was obtained.

[^{35}S]GTPγS Binding Assay The GTP binding assay was determined by the methods modified in previous[16] and our personal reports. Specific monoamine- or chemical-stimulated [^{35}S]GTPγS binding values were calculated by subtracting basal binding values (obtained in monoamine or chemical absence; 900 cpm) from stimulated values (obtained in monoamine or chemical presence). The % of 5-HT maxima was determined by dividing DA-, NE-, or chemical-induced maximal binding using the 5-HT-stimulated maximal binding value (2110 cpm) as a reference compound.

Statistical Analysis IC_{50} and EC_{50} values were determined using the sigmoidal dose-response curve fitting obtained by a software, KaleidaGraph ver. 4 (Synergy Software, PA, U.S.A.). The data represented the mean values of three independent experiments (n=3).

RESULTS AND DISCUSSION

In this study, we examined that Tamiflu and GS4071 on DA, 5HT, NE-reuptake and release assays, and GTP binding assay using rat brain synaptosomes. We compared the influence of Tamiflu and GS4071 on ^{3}H-DA, ^{3}H-5HT, and ^{3}H-NE re-uptake with that of a stimulant, MAP, and a narcotic, cocaine (Figs. 2A—C). Both MAP and cocaine potently inhibited DA, 5HT, and NE re-uptake, and their IC_{50} values were similar to those previously reported.[10] However, neither Tamiflu nor GS4071 influenced re-uptake of the 3 monoamines. In release assay, MAP potently promoted DA/NE release, but cocaine did not influence the 3 monoamines. MAP's EC_{50} values and the finding of cocaine were consistent with the results of our previous study.[10] Neither Tamiflu nor GS4071 promoted the release of ^{3}H-DA, ^{3}H-5HT, and ^{3}H-NE (Figs. 2D—F). Subsequently, we studied a [^{35}S]GTP binding assay under conditions which facilitated the adequate responses of DA, 5HT, and NE. Neither MAP nor cocaine promoted G-protein binding, as previously reported. Also, neither Tamiflu nor GS4071 bound the G-protein binding of DA, 5HT, and NE receptors (Fig. 3).

In a symposium held by the Japanese Society of Pharmacological Epidemiology (JSPE) (May 20, 2007), some investigators reported that there was no association between Tamiflu administration and abnormal behaviors based on statisti-

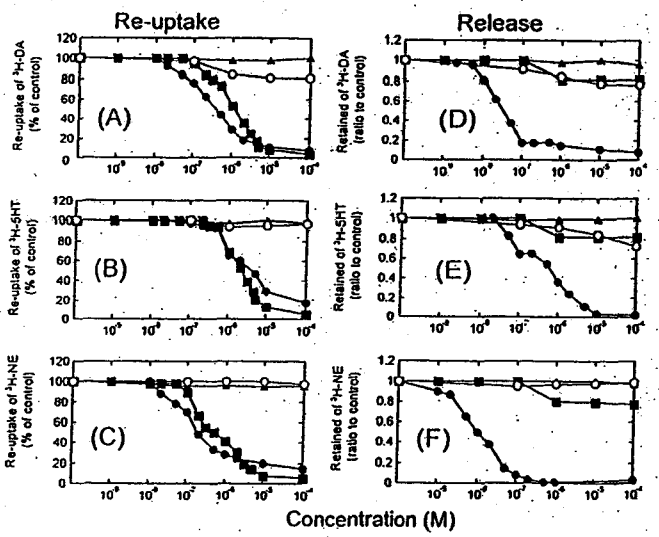

Fig. 2. Inhibition of Re-uptake and Stimulation of Release of Monoamines by Tamiflu and GS4071

The synaptsome fraction prepared from striatum was used for the assay of dopamine (A and D), and that prepared from the cortex was used for the assay of 5-HT (B and E) and norepinephrine (C and F). The S.D. values are less than 4.0%. (A), (B), and (C): re-uptake assay; (D), (E), and (F): release assay. ▲: Tamiflu; ○: GS4071; ●: methamphetamine; ■: cocaine.

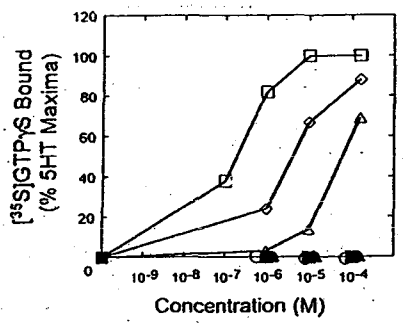

Fig. 3. Representative Concentration–Response Curves for [^{35}S]GTPγS Binding by Tamiflu and GS4071 in the Rat Whole Brain Membranes

Specific [^{35}S]GTPγS binding was measured in the presence of various concentrations of Tamiflu and GS4071 as described in Materials and Methods. The results are expressed as a percentage of the specific binding of 5HT at 10^{-4} M. The S.D. values are less than 5.0%. ▲: Tamiflu; ○: GS4071; ●: methamphetamine; ■: cocaine ; △: DA; □: 5-HT; ◇: NE.

cal data, and that Tamiflu decreased the incidence of pneumonia to 1/3. Others suggested the relationship between Tamiflu administration and abnormal behaviors. A consensus has not been reached. Concerning anti-influenza virus agents other than Tamiflu, the Ministry of Health, Labor and Welfare also announced the incidences of abnormal behaviors after administration on May 14. According to this, 10 and 6 patients with abnormal behaviors after administration of Relenza/amantadine hydrochloride (denominators unpublished) have been reported since 2000 and 1998, respectively.[2] In the package inserts of amantadine hydrochloride, side effects on the central nervous system (hallucination, delusion) are described. They may be probable, since it is described that the agent inhibited DA re-uptake while promoting its release/synthesis in an animal (rats) experiment in the new drug application. However, in the new drug application of Tamiflu (materials regarding its pharmacological effects), it is described that Tamiflu may not influence any symptoms/activities, the central/autonomic nervous systems, smooth muscle, nor immune system based on the results of general pharmacological and toxicity studies using animals, and that neither Tamiflu nor its carboxylic acid metabolite (GS4071) influenced 19 receptors involved in nausea/vomiting in an *in vitro* study regarding the central nervous system.

In the United States, 153 patients (0.21/100000 persons) aged less than 18 years died of influenza in the season between 2003 and 2004.[17] They consisted of 0.75 persons aged less than 1 years, 0.30 persons aged 1 to 4 years, and 0.11 persons aged 5 to 17 years per 100000 persons. The incidence of influenza encephalopathy in children aged less than 6 years in Japan (2.5/100000 persons)[4,5] is higher than that in the United States. This reflects differences in genetic backgrounds.[4,6] As the number of patients in whom Tamiflu was prescribed was not reported,[3] we estimated the mortality rate according to abnormal behaviors as 0.024/100000 persons from Roche's report.[2] The incidence of influenza encephalopathy is much higher than that of the abnormal behaviors occurred in those who were administered Tamiflu to treat influenza. Neither Tamiflu nor GS4071 inhibited the reuptake of 3 monoamines in presynapses, promoted their release, or influenced G-protein binding in postsynapses in our *in vitro* assay system. It is thus indicated that mechanisms underlying the abnormal behaviors due to Tamiflu are different from those underlying the effects of psychoactive drugs. It has been suggested that Tamiflu inhibits encephalopathy-related death and the onset of pneumonia in children.[18] Therefore, this agent may be useful for treating influenza infection in high-risk groups consisted of children or elderly persons.[19] We propose that the relationship between Tamiflu and abnormal behaviors should be examined quickly using influenza-infected animals, and then Tamiflu must be administered, considering its risks and benefits.

REFERENCES

1) Eisenberg E. J., Bidgood A., Cundy K. C., *Antimicrob. Agents Chemother.*, 41, 1949—1952 (1997).
2) http://www.mhlw.go.jp/shingi/2007/05/s0502-1.html/B%27&extension=html&search_lang=japanese
3) http://www.mhlw.go.jp/houdou/2007/04/h0425-1.html
4) Morishima T., *Nippon Rinsho*, 61, 2006—2012 (2003).
5) http://www.city.shinjuku.tokyo.jp/division/340700yobo/infuruenza.htm#_top
6) Kido H., Yao D., Le T. Q., Tsukane M., Chida J., *Nippon Rinsho*, 64, 1879—1886 (2006).
7) Dutkowski R., Thakrar B., Frochlich E., Suter P., Oo C., *Ward P. Drug Saf.*, 26, 787—801 (2003).
8) Okamoto S., Kamiya I., Kishida K., Shimakawa T., Fukui T., Morimoto T., *Pediatr. Inf. Disease J.*, 24, 575—576 (2005).
9) http://www.mhlw.go.jp/topics/2006/10/dl/tp1020-2.pdf
10) Nagai F., Nonaka R., Satoh K., Kamimura H., *Eur. J. Pharmacol.*, 559, 132—137 (2007)
11) http://www.fda.gov/medwatch/SAFETY/2003/tamiflu_deardoc.pdf
12) Fukuta Y., Mita T., Fukuda N., Kanai M., Shibasaki M., *J. Am. Chem. Soc.*, 128, 6312—6313 (2006).
13) Mita T., Fukuda N., Roca F. X., Kanai M., Shibasaki M., *Org. Lett.*, 9, 259—262 (2007).
14) Satoh K., Nonaka R., Tada Y., Fukumori N., Ogata A., Yamada A., Satoh T., Nagai F., *Arch. Toxicol.*, 80, 605—613 (2006).
15) Breivogel C. S., Walker J. M., Huang S. M., Roy M. B., Childers S. R., *Neuropharmacology*, 47, 81—91 (2004).
16) Moore R. J., Xiao R., Sim-Selley L. J., Childers S. R., *Neuropharmacology*, 39, 282—289 (2000).
17) Bhat N., Wright J. G., Broder K. R., Murray E. L., Greenberg M. E., Glover M. J., Likos A. M., Posey D. L., Klimov A., Lindstrom S. E., Balish A., Medina M. J., Wallis T. R., Guarner J., Paddock C. D., Shieh W. J., Zaki S. R., Sejvar J. J., Shay D. K., Harper S. A., Cox N. J., Fukuda K., Uyeki T. M., *N. Engl. J. Med.*, 353, 2559—2567 (2005).
18) Nordstrom B. L., Sung I., Suter P., Szneke P., *Curr. Med. Res. Opin.*, 21, 761—768 (2005).
19) Sugaya N., *Influenza*, 8, 31—34 (2007).

27PW-am001

シクロスポリン投与ラットにおける耐糖能異常発現と膵β細胞障害

○坂田　晃[1]，鈴木　彩人[1]，平井　正巳[1]（[1]九州保福大薬）

【目的】シクロスポリン（CsA）は、長期投与により耐糖能異常を発現することが報告されている。耐糖能異常の発現には、膵臓β細胞破壊によるインスリン分泌不全の影響が示唆されていることから、本実験では、CsA 長期投与による耐糖能異常の発現に及ぼす膵臓障害について検討した。

【方法】6 週齢の Wistar/ST 雄性ラットに、20 mg/kg および 40 mg/kg の CsA（ネオーラル®内用液）を、連日経口投与した。投与 14 日後および 28 日後に、絶食条件下で腹腔内ブドウ糖負荷試験（IPGTT）を行い、その血糖値-時間曲線下面積（AUC_G）を求めた。また、膵臓を摘出し、HE 染色法およびインスリン免疫染色法にて病理学的評価を行った。

【結果】IPGTT において、CsA の投与量や投与期間による違いは認められなかったものの、両濃度（20 mg/kg, 40 mg/kg）で有意な血糖値上昇および AUC_G の増加が確認された。また、組織標本においては、14 日間 CsA（20 mg/kg）投与群以外のラット群で膵島内分泌細胞が空胞化し、インスリン分泌不全が起きていることが観察された。

【考察】以上の結果より、CsA 長期投与による耐糖能異常は、膵臓β細胞の組織障害に先行して発現する可能性が示唆された。

27PW-am002

足むくみに対する硫酸マグネシウム含有炭酸ガス入浴の有効性

○渡邊　智[1]，石澤　太市[1]，谷野　伸吾[1]（[1]ツムラ ライフサイエンス）

＜目的＞足むくみは、日常良く実感し疲労感を伴う。足むくみの原因は立ちっ放しや座りっ放し等による血行不良や水分代謝が影響し、解消する為にマッサージや軽い運動などが行なわれている。入浴は、血流増加、水圧などにより足むくみ改善が期待されるが、入浴剤による報告はほとんどない。そこで、水分摂取が足むくみに及ぼす影響と、誘発後の入浴剤による改善について検討した。＜方法＞1．水分摂取が足むくみに及ぼす影響について、健常者 7 名を対象に脹脛周囲径の変化を指標に検討した。試験室入室後、椅子座位の姿勢を保ち、水分摂取の有無による脹脛周囲径の影響を経時的に測定した。2．硫酸マグネシウム含有炭酸ガス入浴剤使用による足むくみ改善に関して、健常者 9 名を対象に検討した。試験室入室後、足むくみを誘発し、入浴前後の脹脛周囲径、体積を測定した。3．硫酸マグネシウム含有炭酸ガス入浴剤使用による足むくみ改善に関して、健常者 6 名を対象に検討した。試験室入室後、足むくみを誘発し、入浴前後の脹脛皮膚温、血流、周囲径を測定した。＜結果＞1．水分摂取の足むくみに及ぼす影響について検討した結果、水分非摂取群と比較して、水分摂取群が有意に脹脛周囲径を増加させた。2．入浴剤群は、さら湯群と比較して、脹脛周囲径の有意な減少、体積の減少傾向がみられた。3．入浴剤群は、さら湯群と比較して、脹脛血流の有意な増加、脹脛周囲径の減少、皮膚温の上昇傾向がみられた。＜考察＞椅子座位による脹脛のむくみは、水分摂取により助長された。硫酸マグネシウム含有炭酸ガス入浴剤は、さら湯と比較して、足むくみ誘発後の脹脛周囲径増加を抑制し、作用機序として皮膚血流改善が関与しているものと考えられた。

G0756526

27PW-am003

2型糖尿病マウスの皮膚欠損傷モデルにおけるヒト血漿由来フィブロネクチンとb-FGFの併用効果

○村上　和樹[1]，平尾　豊[1]，仲野　篤史[1]，秃　英樹[1]，柏原　純一[1]，平山　文博[1]（[1]ベネシス　牧方研究所）

【目的】Fibronectin (FN)はコラーゲン、ヘパリン、フィブリン等の多くの細胞外マトリックスや細胞との結合ドメインをもつ多機能ドメイン蛋白質であり、創傷治癒過程に重要な役割を演じていることが示唆されている。今回、ヒト血漿由来 FN を精製し、II 型糖尿病マウスの皮膚欠損傷モデルにおける basic-fibroblast growth factor (b-FGF)との併用効果について検討した。

【方法】FN はヒト血漿よりクリオプレシピテートを調製後、脱フィブリノゲン処理、硫安分画、DEAE-Sephadex カラムにより精製した。薬理評価はマウスの背部皮膚に直径 18mm の円形欠損傷を作製し、薬物局所投与による創傷治癒面積を経時的に測定した。また、FN の内皮細胞に対する作用を human umbilical vein endothelial cell (HUVEC)を用いて検討した。

【結果及び考察】精製した FN は HPLC ゲルろ過および SDS-PAGE で単一な蛋白であることを確認し、最終的に 50 mg/mL に調製した。II 型糖尿病マウスはコントロールマウスと比較して明らかに創傷治癒が遅延しており、b-FGF の投与により創傷治癒が促進されることを確認した。FN (2.5 mg/site)の単独投与では有意な創傷治癒促進作用は認められなかったが、b-FGF (20 mg/site)と併用することにより著明な創傷治癒促進作用が認められた。また、in vitro における HUVEC に対する作用検討では、FN の細胞接着作用ならびに b-FGF の細胞増殖作用が確認された。以上の結果より、FN の細胞接着作用と b-FGF の細胞増殖作用が相乗的に働くことにより両者併用による創傷治癒促進作用が発揮される可能性が示唆された。

27PW-am004

D16577

培養ラット胎児へのタミフルの影響

○横山　舜[1]，秋田　正治[1]（[1]神奈川生命研）

（目的）今年もインフルエンザが猛威を振るっている。しかも、若年期において異常行動と特効薬タミフル（リン酸オセルタミビル<OTB>）との関与はいまだ不明である。我々は培養ラット胎児を用いて、胎生期の脳神経系への OTB の影響を観たので報告する。

（方法）培養ラット胎児はラット胎齢 11 日目から 48 時間の回転培養を実施した。OTB の処理濃度は、750 μg/ml 処理とし培養液内投与法で行った。

（結果）培養ラット胎児の成長・発育指標は心拍数・頂殿長・総体節数・総重量・頭長・神経管の画像解析値・外表形態で対照群と OTB 処理群とで影響を比較した。頭長において OTB 処理群は対照群に比べて 5 %、神経管の画像解析値は 11%の低下を示した。それ以外の指標は対照群と差はなかった。外表も奇形などの異常は認められなかった。

（考察）若齢のラット胎児の脳神経管の発育に影響ある点と、すでに出来上がった思春期の脳での異常が同一障害とは考え難いが、その関連性を追及していく。

G0756528

27PW-am005

卵白アルブミン感作ラットの排尿筋過活動モデルに対するFYO-750の効果

○近松　典子[1]，本　光喜[1]，栗田　直樹[1]，永田　治[1]（[1]富士薬品研究部）

【目的】下部尿路機能障害による膀胱知覚過敏に起因した頻尿にプロスタグランジンが重要な役割を担い，COX 阻害剤が夜間頻尿に有効であることが報告されている[1]．一方，基礎研究においても，シクロフォスファミドあるいは酢酸誘発膀胱炎ラットの排尿筋過活動モデルに対して，COX 阻害剤が有効であることが報告されている[2,3]．しかし，間質性膀胱炎の成因のひとつとされるアレルギーに起因した病態モデルでの COX 阻害剤の報告は無い．そこで，本試験では，卵白アルブミン（OVA）感作ラットの排尿筋過活動モデルを作製し，COX 阻害作用を有する新規化合物 FYO-750 の効果をシストメトリー法により検討した．

【方法】7 週齢の雌性 Brown Norway ラットに OVA 10 mg/rat（$Al(OH)_3$ 100 mg/rat を含む）を 6～7 日間隔で 3 回皮下投与し，更に OVA 2 mg/rat を 1 日 1 回 3 日間経尿道的に膀胱内に投与して感作した．最終感作後 11～18 日にウレタン麻酔下で膀胱瘻を作製し，生理食塩液・硫酸プロタミン液灌流後に OVA 10 mg/mL 液を滴流（0.04 mL/min）して排尿筋過活動を惹起した．FYO-750（0.03～0.3 mg/kg）を総頸静脈に留置したカニューレを介して投与し，シストメトリー法により膀胱機能を評価した．

【結果・考察】FYO-750 は，OVA 感作ラットの排尿筋過活動モデルで認められた膀胱容量の低下を有意に改善したことから，下部尿路機能障害における頻尿に対して有用であることが示唆された．

1) Araki T *et al.*, *Acta Med Okayama* 58: 45-49, 2004
2) Takagi-M H *et al.*, *J Pharmacol Sci* 95: 458-465, 2004
3) Angelico P *et al.*, *BJU Int* 97: 837-846, 2006

G0756529

27PW-am006

抗インフルエンザウイルス薬リン酸オセルタミビル(タミフル)のマウス体温低下作用：ザナミビル(リレンザ)およびジクロフェナクとの比較

○小野　秀樹[1]，永野　裕子[1]，松並　範晃[1]，杉山　慎一[1]，山本　昇平[1]，田辺　光男[1]（[1]名市大院薬）

【目的】リン酸オセルタミビル(OP)はヒト肝のカルボキシルエステラーゼ 1 (CES1)により加水分解を受け、抗インフルエンザウイルス活性を持つオセルタミビル・カルボキシレート(OC)になる。OC はノイラミニダーゼを阻害しウイルスの増殖を抑制する。OP はインフルエンザの発熱を効果的に低下させること、および OP 有害事象（因果関係を問わない）として過度の低体温が報告されていることから、本研究においては、体温への OP の影響を調べた。また、OC と同様にノイラミニダーゼを阻害するザナミビル、およびインタビューフォームに「過度の体温下降」の記載があるジクロフェナクの体温低下作用の有無を調べた。OP と同様 CES1 で加水分解され、*in vitro* で OP 加水分解を強力に阻害することが知られている抗血小板薬クロピドグレルの、OP 体温低下作用への影響も調べた。

【方法】マウスの正常直腸体温を 10 分毎に測定した。投与量は塩基として表した。

【結果】OP(30-300mg/kg, i.p.)は直腸体温を用量に依存して低下させた。300mg/kg は体温を平均 3.8℃低下させた。経口投与によっても、OP(100-1,000mg/kg)は体温を低下させ、その作用は持続した。ザナミビル(100 と 300mg/kg, i.p.)およびジクロフェナク(1-30mg/kg, i.p.)は体温を下げなかった。ジクロフェナク(30 と 60 mg/kg, s.c.)は OP(100mg/kg, i.p.)の体温低下作用に影響しなかった。クロピドグレル(100 と 300mg/kg, s.c.)は OP の体温低下作用をわずかに弱める傾向があった。

【考察】マウスにおける OP の分解は血漿中に大過剰に存在すると考えられる CES1 により生じるため、クロピドグレルは CES1 を強く競合阻害できなかったと思われる。本研究で見られたマウスにおける OP の体温低下作用は、インフルエンザ発熱時の OP の解熱作用、および OP の低体温の有害事象と関係する可能性がある。

D20548

O-25　リン酸オセルタミビル投与がEL マウスの聴覚誘発電位におよぼす影響

斉藤　賢一[1]、川上　康彦[2]、桑原　健太郎[2]、藤田　武久[2]、藤野　修[2]
[1]日本獣医生命科学大学応用生命科学部食品健康環境学教室、[2]日本医科大学医学部小児科

ヒトでは、インフルエンザの治療薬であるリン酸オセルタミビル投与による異常行動が報告されている。演者らは癲癇モデルマウス（EL mouse）にリン酸オセルタミビルを飲水による投与をし、脳波の経時的変化を記録して報告している。その結果では、投与開始 24 時間後の発作間欠期の棘波の持続時間が長くなることが記録された。しかし、投与開始 48 時間後の脳波には、これらの持続時間の長い棘波が見られなくなる興味深い結果を得た。このことから、演者らはリン酸オセルタミビルの投与 24 時間後の、マウスの聴覚誘発電位を記録し検討した。

【材料と方法】供試動物として、癲癇モデル動物である、26 週齢の EL マウス雄を対照群 3 匹および投与群 3 匹を用いた。リン酸オセルタミビルを飲水に混ぜてマウスに投与した。平均投与量はオセルタミビル 44mg/Kg/day であった。投与開始 24 時間後にケタミン麻酔処置を施し、マウス脳硬膜に傷を着けることなく後頭部の頭蓋骨に 2 カ所の穴を開けた。ここに、エポキシコーテングした銀ボール電極を配置した。クリック音はマウス用に改造したクリスタルイヤホーンを外耳道に挿入して聞かせて、聴覚誘発電位を記録した。

【結果】聴覚脳幹電位では蝸牛神経、神経核、オリーブ核、下丘の成分が記録された。この潜時を投与群と非投与群で比較した結果、投与群の下丘までの潜時が短くなることが確認された。

O-26　妊婦から回収した食事記録票の分析：妊婦は葉酸は充分に摂取しているか？

岡井　いくよ[1]、早川　ちさ[2]、下須賀　洋一[3]、近藤　厚生[4]
[1]済生会福岡第二病院、[2]明治乳業株式会社、[3]小牧市民病院、[4]津島リハビリテーション病院

【目的】厚生労働省は神経管閉鎖障害の発生リスクを低減するため、栄養バランスの取れた食事、並びに妊娠 4 週から妊娠 12 週まで葉酸サプリメント 400μg/day の内服を勧告した。妊婦が摂取する食事を栄養学的に検討した。

【方法と対象】2003 年から 2006 年の 4 年間に 336 名の妊婦から食事記録票を回収し、五訂日本食品標準成分表に基づき解析した。100 名（30%）は葉酸サプリメントを内服していた。

【調査成績】葉酸の経口摂取量は過去 4 年間ほぼ 350μg/day 前後であった。妊娠前期の摂取量は 306μg/day、中期は 372μg/day、後期は 349μg/day であり、葉酸を最も大量に必要とする前期が最低値であった。厚生労働省が期待する 400μg/day を充足していたのは、336 名中の 82 名（24%）であり、適切な食生活を過ごしている。しかし残る 254 名（76%）は、不足分を葉酸サプリメントで補充すべきである。実際に葉酸サプリメントを補充していたのは 254 名中の 69 名（21%）であり、185 名（55%）は葉酸摂取量が絶対的に不足していた。

【結論】妊婦は食事から葉酸を平均 350μg/day 摂取している。しかし葉酸の需要量が最大となる妊娠前期の摂取量は最低であった（306μg/day）。妊婦の 55%は葉酸摂取量が絶対的に不足しており、神経管閉鎖障害児を妊娠する危険性を孕んでいる。

日本先天異常学会学術集会，第４８回（２００８．０６．２８－３０，東京）

O-325　重症心身障害児（者）の喉頭ファイバーによる形態・唾液誤嚥の評価

聖隷三方原病院小児科

森　有加　池谷真苗　宮崎直樹　中島秀幸　木部哲也
大場　悟　横地健治　岡田眞人

発達期脳障害では，呼吸障害・嚥下障害が高率に認められる．これらは，咽頭・喉頭の機能障害に由来する．嚥下に対しては，嚥下造影のみならず，喉頭ファイバーによる評価も近年進歩している．しかし，発達期重度脳障害を持つ児(者)の安静時喉頭ファイバー所見は十分研究されていない．そのため，今回嚥下障害を持つ重症心身障害児（者）を対象として喉頭ファイバーを施行し，その所見を検討したので報告する．対象は，2003年から2006年までの3年間に喉頭ファイバーを施行した70例(男性41例，女性39例)である．検査は，安楽な背臥位，又は体幹後退の介助座位にて施行された．喉頭ファイバー下の外観を，喉頭狭小化・喉頭蓋の形態・披裂部の腫脹・唾液の声門からの噴き出しについて分類し検討した．さらに，喘鳴の有無と程度・食事形態・経鼻胃管の位置についても比較検討した．喉頭狭小化は0(正常)から3(喉頭蓋が咽頭後壁に付着している)に分類し，43例(61%)に喉頭狭小化を認めた．喉頭蓋の形態は正常・矩形・U型・オメガ型に分類し，42例(60%)で何らかの変形を認めた．披裂部の腫脹は，その程度を0（正常）から3（披裂部切痕が同定できない）に分類し，61例（87%）で披裂部の発赤・腫脹が認められた．唾液の噴き出しは，貯留している唾液の性状を透明及び混濁粘調に分類し，さらにその程度を持続・時々・なしに分類した．57例(82%)で唾液の声門からの噴き出しが認められ，唾液の誤嚥は高率に認められることが示唆された．また，喘鳴や披裂部の腫脹を認める例は，唾液の噴き出しを認める例が多く，唾液誤嚥との一致率が高いことが推測された．

O-326　出生予定日のMRI FLAIR法所見と就学期神経学的予後

久留米大学小児科高次脳疾患研究所[1]　ロンドン大学周生期脳研究所[2]　長野県立こども病院新生児科[3]　杏林大学小児科[4]　埼玉医科大学川越医療センター小児科[5]

岩田欧介[1,2]　岩田幸子[1,2]　中村友彦[3]　木原秀樹[3]　日詰恵里子[3]
杉浦正俊[4]　田村正徳[5]　神田　洋[1]　前野泰樹[1]　松石豊次郎[1]

背景：近年，超低出生体重児の長期フォローアップから，インタクトサバイバルを遂げたと考えられていた児が，学齢期以降に高率に学習障害を来たすことがわかってきた．予定日前後のMRIは，1歳半頃までの発達と良好な相関を見せるが，学齢期の高次脳機能との関連は明らかになっていない．目的・方法：予定日前後に撮影されたMRI白質所見と学齢期の発達指数の関係を明らかにするために，210人の早期産児のMRIと周生期の臨床情報と長期発達予後を比較した．結果：FLAIR法における白質異常輝度領域は，予定日前後の限られた週数範囲においても，撮影時の修正週数と有意な相関があり，週数が小さいほど効率に観察された．多変量解析により週数の影響を加味すると，週生期の母体発熱の既往と脳室周囲白質軟化症の発症にも，FLAIR法の異常所見と正の相関が認められた．新生時期のFLAIR法異常所見は，6歳時の総合・運動発達指数（WISC-R）と有意な相関を見せた．結論：FLAIR法を用いることで，学齢期の発達異常を新生時期に予測できる可能性が示唆された．FLAIR法上の異常所見は，周生期の病因と関連があり，微細な白質異常を見ていると考えられた．FLAIR法はほとんどの施設で撮影可能なシークエンスであり，その低輝度域は，髄液に近い長い縦緩和時間から客観的に描出されるため，画像調整の影響を受けにくいと考えられ，軽度発達異常のスクリーニング手段として将来が期待される．

O-327　多発奇形を伴う発達遅滞症例の病因診断におけるMLPA法サブテロメア解析の有用性

慶應義塾大学小児科[1]　国立成育医療センター遺伝診療科[2]
ファルコバイオシステムズバイオ事業本部[3]

小崎健次郎[1]　小崎里華[2]　東　央晋[3]　高橋孝雄[1]

[背景] 染色体末端部サブテロメア領域は構造異常の好発部位であり，通常の染色体検査（Gバンド検査）では検出できない微細なサブテロメアの構造異常が発達遅滞の重要な原因であることが明らかにされている．すでに全サブテロメアを標的とする網羅的なFISH検査が実用化されているが，検査費用が高額なために小児科診療の現場では普及していない．近年，特定の領域のゲノム領域のコピー数を計数する解析技術であるMLPA法が開発され，サブテロメア解析にも応用が可能となった．[方法] Gバンド検査の結果が正常なMCA/MR症例24例(孤発例22，同胞例2)を対象として，MLPA法によるサブテロメア解析をおこなった．[結果] 24症例中5症例(21%)にサブテロメアの構造異常が認められ，その内訳は5p欠失+10q重複，5p欠失+17q重複，5p欠失+5q重複，16p欠失，18q欠失であった．5p欠失+10q重複症例および5p欠失+17q重複症例では片親が均衡型相互転座を有し，5p欠失+5q重複の症例では片親が5番染色体腕間逆位を有していた．[考察] 診断不明のMCA/MR症例の病因確定にはMLPA法によるサブテロメア解析が有用である．サブテロメアの構造異常を認めた5症例中3症例では片親が染色体構造異常の保因者であり，次子の再罹患を考慮する必要がある．Gバンド検査が正常のMCA/MR症例の家族に遺伝カウンセリングを行う際には，サブテロメア解析を実施することが望ましい．MLPA法によるサブテロメア解析の検査コストはGバンド法と同程度であり，臨床検査として普及が期待される．

O-328　リン酸オセルタミビル経口投与によるマウス脳波の変化

日本医科大学小児科[1]　日本獣医生命科学大学[2]

川上康彦[1]　斉藤賢一[2]　小泉慎也[1]　桑原健太郎[1]　藤田武久[1]
藤野　修[1]　福永慶隆[1]

【目的】現在，経口インフルエンザ治療剤リン酸オセルタミビル（以下オ剤）の安全性が再検討されてきている．昨シーズン，重篤な副作用と推測される事例が報告され，厚労省は年長児に対する原則投与禁止を勧告した．ごく最近海外でもin vitroでオ剤が幼弱ラット神経細胞の興奮を誘発すると報告された．今回我々は供試動物にオ剤を経口投与して行動を観察すると共に，我々が開発した手法によりマウス非拘束下で長時間脳波を測定し，電気生理学的検討を行った．【材料および方法】供試動物にはてんかんモデルマウスであるElマウスの13週齢雄を用いた．マウス脳硬膜外に探査電極4個及び鼻端に基準電極1個の計5個を慢性埋め込み電極として配置した．埋め込み手術2日後に睡眠中発作間欠期脳波記録をし，これを対照脳波とした．この脳波記録以後オ剤を飲水に混ぜて投与し，投与前後で脳波を比較した．マウスは非拘束下で，脳波計を介してデジタルレコーダにて記録した．【結果】オ剤投与前のElマウスの発作間欠期脳波には，1時間に1ないし数回のsubclinical paroxysmal dischargesを認めた．オ剤投与翌日に行動は過敏・多動になったが，痙攣発作増悪は認めなかった．しかしsubclinical paroxysmal dischargesの頻度は著明に増加し，持続時間も延長した．【結語】オ剤による神経興奮性誘発作用はin vivoにおいても電気生理学的に示唆された．

Biol. Pharm. Bull. 31(4) 638—642 (2008) Vol. 31, No. 4

Oseltamivir, an Anti-influenza Virus Drug, Produces Hypothermia in Mice: Comparison Among Oseltamivir, Zanamivir and Diclofenac

Hideki ONO,* Yuko NAGANO, Noriaki MATSUNAMI, Shinichi SUGIYAMA, Shohei YAMAMOTO, and Mitsuo TANABE

Laboratory of CNS Pharmacology, Graduate School of Pharmaceutical Sciences, Nagoya City University: 3-1 Tanabe-dori, Mizuho-ku, Nagoya 467-8603, Japan.

Received December 18, 2007; accepted January 21, 2008; published online January 22, 2008

Oseltamivir phosphate (Tamiflu), an anti-influenza virus drug, is hydrolyzed by carboxylesterase to an active metabolite. The metabolite inhibits the influenza virus-specific neuraminidase. In this study, the effects of oseltamivir on normal core body temperature were studied in mice. Oseltamivir (30—300 mg/kg, intraperitoneally (i.p.) and 100—1000 mg/kg, orally (*p.o.*)) dose-dependently lowered the body temperature. The effects of oseltamivir (*p.o.*) continued longer than those of oseltamivir (i.p.), and approximately triple doses of oral oseltamivir were needed to produce the same peak effects as intraperitoneal oseltamivir. The non-steroidal anti-inflammatory drug diclofenac (1—30 mg/kg, i.p.) did not affect body temperature, and (at 30 and 60 mg/kg, s.c.) did not interact with the hypothermic effects of oseltamivir (100 mg/kg, i.p.). Zanamivir, which also inhibits neuraminidase, did not produce hypothermia at doses of 100 and 300 mg/kg, i.p. Clopidogrel (100, 300 mg/kg, i.p.), which is metabolized by the same carboxylesterase, tended to decrease the hypothermic effects of oseltamivir (100 mg/kg, i.p.). These results suggest that the hypothermic effects of oseltamivir are due to its hydrolytic metabolite, and that the hypothermia observed in mice has some relationship to the antipyretic effects and severe hypothermia (adverse event) observed in influenza patients after taking oseltamivir.

Key words oseltamivir; hypothermia; zanamivir; diclofenac; mouse

The anti-influenza drug oseltamivir (Ro64-0796) is hydrolyzed to the active metabolite oseltamivir calboxylate (Ro64-0802, OC) by human liver carboxylesterase (CES), and OC inhibits the influenza virus-specific neuraminidase.[1-4] Oral administration of the parent compound oseltamivir (OP) relieves the symptoms of influenza (cough, myalgia, nasal obstruction, sore throat, fatigue, headache, feverishness).[5] OP has strong antipyretic effects, which become apparent within 24 h after taking the drug.[6] In addition, an adverse event (unknown casual relationship)—hypothermia—after ingestion of OP has been reported. Forty-four cases of hypothermia had been reported to the MHLW (Ministry of Health, Labour and Welfare, Japan) up to March 20, 2007.[7] Data released by the Food and Drug Administration (FDA) have also described hypothermia to 34 °C in 2 cases.[8]

In the present study, we investigated the effects of OP on normal core body temperature using mice, and found relatively strong hypothermic effects. Zanamivir, which is also a neuraminidase inhibitor and an anti-influenza virus drug, was compared with the effects of OP. Absorbed OP is hydrolyzed by human liver CES1 to the active metabolite OC.[1,2] The hydrolysis is strongly inhibited by the anti-platelet drug clopidogrel, which is metabolized by the same esterase CES1.[9] Therefore, clopidogrel was used to inhibit hydrolysis of OP in an attempt to study the involvement of OP or OC in hypothermia after OP administration.

As the antipyretic diclofenac carries a warning of possible severe hypothermia in children and the elderly with high fever in the package insert and an interview form,[10,11] the effects of diclofenac on body temperature and its interaction with OP were also studied.

MATERIALS AND METHODS

Animals One hundred forty-six male mice (ddY strain, SLC Shizuoka, Japan) were kept for at least 7 d under a 12/12 h light–dark cycle before experiments with full access to water and food, except those used for oral administration of OP, which were fasted for more than 15 h.

All experimental protocols used were approved by the Animal Care and Use Committee of Nagoya City University and were conducted in accordance with the guidelines of the Japanese Pharmacological Society.

Measurement of Rectal Temperature At 5 weeks of age, the mice were used to study the effects of drugs on body temperature in an experimental room for animal behavior, which was maintained at 23—25 °C. Each mouse was placed individually in a Plexiglas cage (19×12×11 cm (depth)), then removed every 10 min, held loosely in a small cloth bag, and the core body temperature was measured using a digital thermometer with a resolution of 0.1 °C (MT-132, Mother Tool, Ueda, Japan). The thermometer probe was inserted 25 mm into the rectum.[12] After each measurement, the mouse was returned to its cage. Mice whose rectal temperature before drug administration was below 37 °C were not used for experiments. Drugs were administered after the temperature became stable.

Drugs The drugs used were oseltamivir phosphate (Tamiflu capsule, Chugai Pharmaceutical Co., Tokyo, Japan), zanamivir hydrate (Relenza, dry powder inhaler, Glaxo-SmithKline Co., Tokyo, Japan), clopidogrel sulphate (Plavix tablet, Sanofi-Aventis Co., Tokyo, Japan) and diclofenac sodium (Sigma, St. Louis, MO, U.S.A.). A Tamiflu capsule (75 mg) contains 98.5 mg of oseltamivir phosphate and 64.5 mg of additives. The soluble additive is povidone, and the insoluble additives are pregelatinized starch, croscarmellose sodium, talc and stearyl fumarate sodium. The content of the

* To whom correspondence should be addressed. e-mail: hiono@phar.nagoya-cu.ac.jp

capsule was suspended in saline. Five hundreds milligrams of oseltamivir phosphate are dissolved in 1 ml of water,[3] and the maximal concentration of OP used for oral administration (1000 mg/kg) was 100 mg/ml. Thus, insoluble substances were considered to be additives, and not OP, and the suspension was injected after shaking. A Relenza blister (5 mg) contains zanamivir hydrate and lactose, and these were completely dissolved in saline. A Plavix tablet, which contains 75 mg of clopidogrel and additives, was made into an emulsion by grinding in a mortar and pestle containing saline. Diclofenac sodium was dissolved in saline. Doses of drugs were expressed as a free base and administered intraperitoneally (i.p.), subcutaneously (s.c.) or orally (*p.o.*) at 0.1 ml volume/10 g body weight.

Statistical Analysis Mean core body temperature before drug administration was 38.2±0.03 °C (S.E.M., n=146), the range was 37—39.3 °C, and drug effects were expressed as the decrease in body temperature (Δ°C). All data were expressed as mean±S.E.M. (n=6 or 8). Multiple t-test with Bonferroni correction following ANOVA was used for multiple comparison between control and treated groups.[13] Student's t-test or Welch's procedure was also applied to the same group because multiple comparison can overslip side effects (adverse reaction) (known casual relationship) of drugs.[14] Differences at $p<0.05$ (two-tailed) were considered to be significant.

RESULTS

Effects of OP on Core Body Temperature OP (30, 100, 300 mg/kg, i.p.) dose-dependently lowered the body temperature (Fig. 1). The peak effects were observed 10, 20 and 30—40 min after administration of 30, 100 and 300 mg/kg of OP, respectively. Variations in the effects of intraperitoneal OP were smaller than those of oral OP (Fig. 2), and there were many significant time points between the saline and OP groups (multiple t-test with Bonferroni correction) (Fig. 1). $AUCs_{0-60\,min}$ of hypothermia (Δ°C×min) values were: −3.2±3.6 (n=6) (saline), −20.7±6.4 (30 mg/kg), −79.3±5.7 (100 mg/kg) and −164.1±15.9 (300 mg/kg). Significant differences in effects were observed between saline and the 100 mg ($p<0.05$) and 300 mg/kg ($p<0.01$) groups (multiple t-test with Bonferroni correction).

Oral administration of OP (100, 300, 1000 mg/kg) also lowered the core body temperature in a dose-dependent manner (Fig. 2). Saline lowered the body temperature, but significant hypothermia was observed at doses of 300 and 1000 mg/kg, *p.o.* (Fig. 2, multiple t-test with Bonferroni correction). When non-corrected Student's t-test was employed, the effect of 100 mg/kg OP was statistically significant at some time points (Fig. 2). The peak effects were observed at 30—60 min after administration, and recovery was not evident at 2 h after administration. $AUCs_{0-120\,min}$ of hypothermia (Δ°C×min) values were: −93.9±10.9 (n=8) (saline), −149.5±27.9 (100 mg/kg), −219.2±51.3 (300 mg/kg) and −300.6±39.0 (1000 mg/kg). Significant effects were observed between saline and the 300 ($p<0.05$) and 1000 mg/kg ($p<0.01$) groups (multiple t-test with Bonferroni correction). Non-corrected Student's t-test showed the same degrees of significance as those from the multiple t-test. When compared by peak effects, approximately triple doses of oral oseltamivir were needed to produce the same peak effects as intraperitoneal oseltamivir.

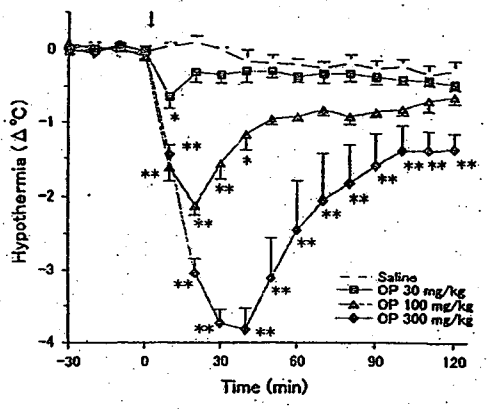

Fig. 1. Oseltamivir (30—300 mg/kg, i.p.) Decreases Core Body Temperature in a Dose-Dependent Manner in Mice

Each point represents the mean±S.E.M. of 6 mice. Ordinate: decrease in body temperature from the baseline (mean of −30—0 min). Abscissa: time in minutes after administration of the drug. Significance of differences between control and test values was determined by the two-tailed multiple t-test with Bonferroni correction following one-way analysis of variance (3 comparisons in 4 groups). $*p<0.05$ and $**p<0.01$. OP, oseltamivir.

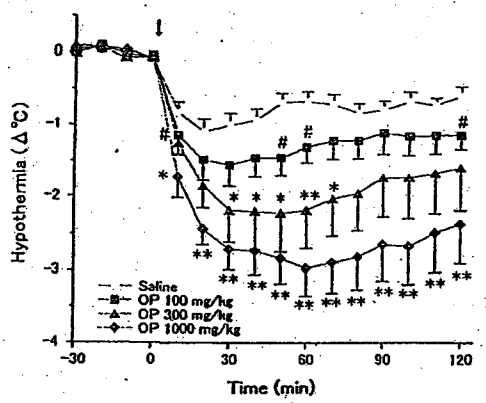

Fig. 2. Oseltamivir (100—1000 mg/kg, *p.o.*) Decreases Core Body Temperature in a Dose-Dependent Manner in Mice

Each point represents the mean±S.E.M. of 8 mice. Ordinate: decrease in body temperature from the baseline (mean of −30—0 min). Abscissa: time in minutes after administration of the drug. $*p<0.05$ and $**p<0.01$ (multiple t-test between control and test values). #$p<0.05$ (non-corrected Student's t-test was applied to those groups (see Materials and Methods). OP, oseltamivir.

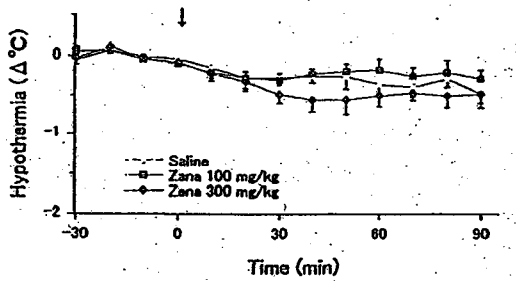

Fig. 3. Zanamivir (100, 300 mg/kg, i.p.) Does Not Alter Core Body Temperature in Mice

Each point represents the mean±S.E.M. of 6 mice. Ordinate: decrease in body temperature from the baseline (mean of −30—0 min). Abscissa: time in minutes after administration of the drug. No significant differences were seen by multiple t-test or Student's t-test. Zana, zanamivir.

Effects of Zanamivir on Core Body Temperature Zanamivir (100, 300 mg/kg, i.p.) slightly lowered the core body temperature (Fig. 3). No statistical significance was observed (multiple *t*-test with Bonferroni correction) and Student's *t*-test).

Effects of Clopidogrel on Hypothermic Effects of OP Since the hydrolysis of OP is strongly inhibited by clopidogrel,[9] clopidogrel was used to inhibit the hydrolysis of OP. Clopidogrel (300 mg/kg, s.c.), which alone slightly lowered body temperature, only tended to reduce the hypothermic effects of OP (Fig. 4).

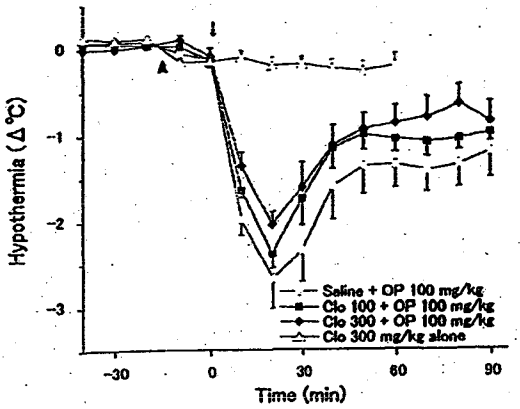

Fig. 4. Effects of Clopidogrel (100, 300 mg/kg, s.c.) on Hypothermia Induced by Oseltamivir (100 mg/kg, i.p.)

Each point represents the mean±S.E.M. of 6 mice. Ordinate: decrease in body temperature from the baseline (mean of −40–0 min). Abscissa: time in minutes after administration of the oseltamivir. Clopidogrel was administered at the point shown by the upward arrow (−15 min). No significant differences were seen by multiple *t*-test or Student's *t*-test. OP, oseltamivir, Clo, clopidogrel.

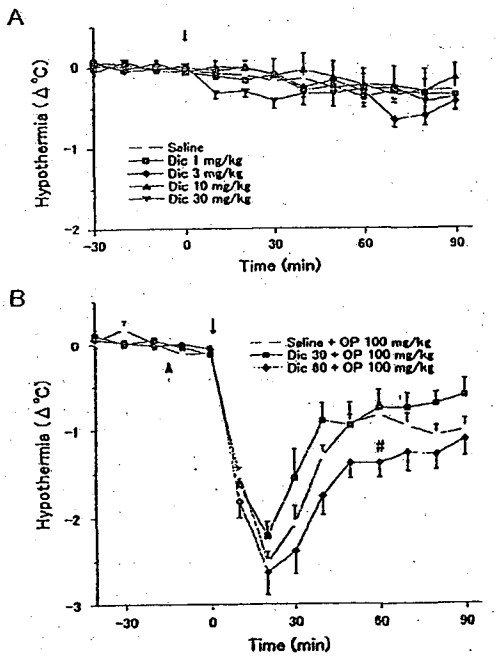

Fig. 5. Effects of Diclofenac on Core Body Temperature and the Interaction with Oseltamivir

Diclofenac (1—30 mg/kg, i.p.) does not alter core body temperature in mice (A). Diclofenac (30, 60 mg/kg, s.c.) does not affect the hypothermic effects of oseltamivir (100 mg/kg, i.p.) (B). Each point represents the mean±S.E.M. of 6 mice. Ordinates: decrease in body temperature from the baseline (mean of −30—0 min (A) and −40—0 min (B)). Abscissae: time in minutes after the administration of oseltamivir. Diclofenac was administered at the point shown by the upward arrow (−15 min). $^{*}p<0.05$ (non-corrected Student's *t*-test). Dic, diclofenac.

Effects of Diclofenac on Core Body Temperature and Its Interaction with OP Diclofenac failed to produce hypothermia at doses of 1—30 mg/kg, i.p. (Fig. 5A). Since non-steroidal anti-inflammatory drugs (NSAIDs) are sometimes prescribed with OP for influenza infection in Japan, the drug interaction between OP and the strong NSAID diclofenac was studied. Diclofenac (30, 60 mg/kg, s.c.) administered 15 min before OP did not affect the latter's hypothermic effects (100 mg/kg, i.p.) (Fig. 5B).

DISCUSSION

Tamiflu interview form and New Drug Application (NDA) data summary describe that OP at 7.6, 76.1 and 761 mg/kg, *p.o.* does not affect body temperature in adult rats,[3,15] whereas at 533 mg/kg, *p.o.* it lowered the body temperature of rats aged 7 or 14 d.[16] A recent study by Izumi *et al.*[17] has provided supplementary data indicating that OP at 50 mg/kg, i.p. significantly augmented the hypothermic effects of ethanol in 30-d-old rats. Here, we have demonstrated that OP alone generates potent hypothermic effects in mice, consistent with our preliminary study obtained using adult rats (data not shown).

Brain/plasma C_{max} ratios for OP and OC in mice administered OP at 10 mg/kg, *p.o.* were 0.42 and 0.22, respectively.[18] Thus, it is considered that both OP and OC penetrated the blood–brain barrier in the present study using a high dose of OP. Body temperature is usually regulated by opposing controls of heat production and heat loss. The preoptic anterior hypothalamus (POAH) is a thermoregulation center.[19] The organum vasculosum laminae terminalis (OVLT), part of the circumventricular organs (CVO), is located near the POAH and is the target site of endogenous pyrogens.[20] In addition, the CVO lacks the blood–brain barrier.[21,22] These circumstances suggest that OP or OC can affect body temperature regardless of whether or not the target site of either drug is located within the blood–brain barrier.

OP (30—300 mg/kg, i.p. and 100—1000 mg/kg, *p.o.*) dose-dependently lowered the normal core body temperature in mice (Figs. 1, 2). The Tamiflu NDA data summary describes very rapid hydrolysis of OP in mice,[23] and the present study indicated that the hypothermic effects of OP were relatively sustained (Figs. 1, 2). Therefore, it is suggested that the active compound that lowered body temperature was metabolized OC, and not the parent compound OP. However, a further study using OC powder will be required before a final conclusion can be reached. Tamiflu capsule contains insoluble additives. In our preliminary study, a filtrate of Tamiflu suspension lowered the body temperature (data not shown). As the soluble additive povidone is a very high-polymer compound (molecular weight several tens of thousands) and its molar dose included in a Tamiflu capsule is very low, it seems unlikely that additives other than OP or OC lowered the body temperature. Oral saline (10 ml/kg) administration unexpectedly produced hypothermia (Fig. 2). In the preliminary study ($n=6$ or 7), oral water administration to fasted

mice and oral saline administration to nonfasted mice lowered the body temperature by about 1 °C. In addition, insertion alone of an oral probe to the stomach *via* esophagus produced mild hypothermia (0.5 °C). Although pyrogenic messages *via* peripheral (largely vagal) afferent nerves activated by the cytokines induces hyperthermic response by direct afferent transmission to the POAH,[24] evidences of reflex hypothermia by mechanical vagal afferent stimuli could not be found in literatures. Nevertheless, these findings suggest that mechanical messages from esophagus and stomach *via* vagal afferents reflexly lower body temperature.

Zanamivir as well as OC inhibit the influenza virus-specific neuraminidase and also the release of virus from host cells.[25] As the hydrolyzed compound zanamivir cannot be absorbed by the gastrointestinal tract, a fine powder of zanamivir is inhaled (10 mg, twice a day) when used for treatment of humans. After inhalation of zanamivir powder, distribution of the drug is restricted to an upper respiratory tract, a target site of influenza virus. In order to elevate its plasma concentration, the same doses of zanamivir (100, 300 mg/kg) as OP were intraperitoneally administered. Zanamivir (100, 300 mg/kg, i.p.) did not produce hypothermia (Fig. 3). From these results, it is considered that hypothermia after OP administration is not due to neuraminidase inhibition at a thermoregulation center or a peripheral organ that is involved in thermoregulation.

CESs are classified into 5 subfamilies (CES1—CES5), and CES1 is subclassified into CES1A—CES1H.[26] The CESs that hydrolyze OP are suggested to be the CES1A and CES1B isozymes in human liver and mouse plasma, respectively.[4,26,27] Clopidogrel, a substrate of CES1, inhibits the hydrolysis of OP to OC *in vitro*: hydrolysis of OP (50 μM) is inhibited by 5 and 50 μM clopidogrel to 50% and 10%, respectively, in human CES1-expressing cells.[9] *In vivo*, a large proportion of clopidogrel is rapidly metabolized by CES to the non-active metabolite SR26334 in humans,[28,29] and T_{max} of the hydrolyzed metabolite SR26334 after oral administration of clopidogrel (75 mg) is 1.9 h in humans.[29,30] T_{max} of OP administered orally at a dose of 75 mg is 1 h, and T_{max} of its metabolite OC is 4 h,[3,31] suggesting that clopidogrel competitively inhibits the hydrolysis of OP to OC in humans. Clopidogrel 300 mg/kg, s.c., which alone slightly lowered body temperature and did not affect behavior of mice, tended to inhibit the hypothermic effects of OP, although not to a significant degree (Fig. 4). Conversion of OP to OC is very rapid in mouse plasma: the concentration of OC after oral OP administration in mice attains a near C_{max} value within 15 min after administration[23] and high amounts of CES are present in mouse plasma.[27] These findings support the negative non-significant interaction of clopidogrel with OP in the present *in vivo* mouse study. The tendency for clopidogrel to exert inhibitory effects on OP-induced hypothermia (Fig. 4) and the prolonged effect of OP on temperature (Figs. 1, 2) suggest that hypothermia is induced by OC, but hypothermic effects induced by OP also cannot be ruled out. In fact, it has been demonstrated that both OP and OC facilitate neuronal firing in hippocampal slices, OC being 30 times more potent than OP in this respect.[17]

Diclofenac, a strong NSAID, is used for treating high fever. Although diclofenac does not lower the normal body temperature in animals, it effectively reduces fever due to pyrogens: the ED_{50} is 0.13 mg/kg, *p.o.* in rats.[32] Voltaren package insert and interview form give a warning of severe hypothermia if used in children and the elderly with high fever.[10,11] In this study, very high doses of diclofenac (1—30 mg/kg, i.p.) did not decrease the body temperature (Fig. 5A) and at 30 and 60 mg/kg, s.c. it did not interact with the hypothermic effects of OP (100 mg/kg, i.p.) (Fig. 5B). Thus, no drug interaction between diclofenac and OP was evident, at least in terms of normal body temperature. However, as diclofenac can be used in patients with high fever, further studies using pyrexia mice are needed to investigate drug interaction between diclofenac and OP.

In the present study, intraperitoneal and oral administration of OP induced dose-dependent hypothermic effects in normal mice. However, since recent clinical studies have shown that the antipyretic effect of OP on type A influenza is stronger than that on type B influenza,[33,34] the antipyretic effect of OP is considered to be due to not only direct pharmacological effects on thermoregulation, but also anti-influenza virus activity.

Severe hypothermia as an adverse event has been reported to the MHLW from manufacturer of OP and also from medical institutions.[7] The proportion of hypothermia cases in Japanese patients below 10 years old relative to all reported cases is 40.1% (18/44 cases), and this ratio is higher than those for other adverse reactions (*i.e.* 16.7% for anaphylaxis (6/36 cases)), based on initial data made available to the public by the MHLW.[7] Since the body weight of children below 10 years old is low, it is considered that more severe hypothermia may occur in comparison with that in the elderly when heat production decreases or heat loss increases after OP ingestion. Thus, it is possible that the hypothermic effects observed in mice are related to the severe hypothermia in humans after OP ingestion. Further studies are needed to elucidate the mechanisms of hypothermia in mice and their relationship to the adverse events reported in humans.

Acknowledgement This work was supported by a Grant-in-Aid for Research at Nagoya City University.

REFERENCES AND NOTES

1) Li W., Escarpe P. A., Eisenberg E. J., Cundy K. C., Sweet C., Jakeman K. J., Merson J., Lew W., Williams M., Zhang L., Kim C. U., Bischofberger N., Chen M. S., Mendel D. B., *Antimicrob. Agents Chemother.*, 42, 647—653 (1998).
2) Sidwell R. W., Huffman J. H., Barnard D. L., Bailey K. W., Wong M. H., Morrison A., Syndergaard T., Kim C. U., *Antiviral Res.*, 37, 107—120 (1998).
3) Roche Pharma Japan Co., Interview Form (Tamiflu Capsule 75 and Dry Syrup 3%), (in Japanese) (2002).
4) Roche Pharma Japan Co., Tamiflu NDA data summary, Documents on absorption, distribution, metabolism and excretion (in Japanese). Available from WEB page of Japan Pharmacists Education Center. http://www.jpec.or.jp/contents/c01/link.html (2000).
5) Nicholson K. G., Aoki F. Y., Osterhous A. D., Trottier S., Carewicz O., Mercier C. H., Rode A., Kinnersley N., Ward P., *Lancet*, 355, 1845—1850 (2000).
6) Treanor J. J., Hayden F. G., Vrooman P. S., Barbarash R., Bettis R., Riff D., Singh S., Kinnersley N., Ward P., Mills R. G., *JAMA*, 283, 1016—1024 (2000).
7) MHLW (Ministry of Health, Labour and Welfare, Japan), Public opening data (documents 5-1-1 and 5-2) at the Meeting for Safety Measure Investigation Council, held on April 4, 2007. http://www.mhlw.go.jp/shingi/2007/04/s0404-2.html (2007).

8) FDA review: Department of Health and Human Services, Public Health Service, Food and Drug Administration, Center for Drug Evaluation and Research, One-year post pediatric exclusivity post-marketing adverse event review, Drug: oseltamivir phosphate, ODS PID# D040223, p21 and 42, http://www.fda.gov/ohrms/dockets/ac/05/briefing/2005-4180b_06_01_Tamiflu%20AE_reviewed.pdf (2005).
9) Shi D., Yang J., Yang D., LeCluyse E. L., Black C., You L., Akhlaghi F., Yan B., *J. Pharmacol. Exp. Therap.*, **319**, 1477—1484 (2006).
10) Novartis Pharma Co., Japan, Voltaren package insert (Voltaren Tablet) (in Japanese).
11) Novartis Pharma Co., Japan, Interview Form (Voltaren) (in Japanese).
12) Durcan M. J., Morgan P. F., *Eur. J. Pharmacol.*, **204**, 15—20 (1991).
13) Wallenstein S., Zucker C. L., Fleiss J. L., *Circ. Res.*, **47**, 1—9 (1980).
14) Nagata Y., Yoshida M., [Japanese title: Toukeiteki Tajuhikakuhou No Kiso, English translation: Basis of Statistical Multiple Comparison], Scientist Inc., p. 28 (in Japanese) (1997).
15) Roche Pharma Japan Co., Tamiflu NDA data summary, Document on pharmacology (in Japanese), Available from WEB page of Japan Pharmacists Education Center, http://www.jpec.or.jp/contents/c01/link.html (2000).
16) Chugai Pharmaceutical Co., Japan, Tamiflu NDA data summary, Document on toxicity (in Japanese), Available from WEB page of Pharmaceuticals and Medical Devices Agency (PMDA), http://www.info.pmda.go.jp/shinyaku/g0407.html (2004).
17) Izumi Y., Tokuda K., O'Dell K. A., Zorumski C. F., Narahashi, T., *Neurosci. Lett.*, **426**, 54—58 (2007).
18) Chugai Pharmaceutical Co., Japan, Tamiflu NDA data summary, Documents on absorption, distribution, metabolism and excretion, Table He-1-1, (in Japanese), Available from WEB page of Pharmaceuticals and Medical Devices Agency (PMDA), http://www.info.pmda.go.jp/shinyaku/g0407.html (2004).
19) Boulant J. A., *Clin. Infect. Dis.*, Suppl. 5, S157—S161 (2000).
20) Blatteis C. M., *Prog. Brain Res.*, **91**, 409—412 (1992).
21) Gross P. M., Blasberg R. G., Fenstermacher J. D., Patlak C. S., *Brain Res. Bull.*, **18**, 73—78 (1987).
22) Gross P. M., *Prog. Brain Res.*, **91**, 219—233 (1992).
23) Chugai Pharmaceutical Co., Japan, Tamiflu NDA data summary, Documents on absorption, distribution, metabolism and excretion, Figure He-1-1 (in Japanese), Available from WEB page of Pharmaceuticals and Medical Devices Agency (PMDA), http://www.info.pmda.go.jp/shinyaku/g0407.html (2004).
24) Blatteis C. M., *J. Physiol.*, **526**, 470 (2000).
25) Woods J. M., Bethell R. C., Coates J. A., Healy N., Hiscox S. A., Pearson B. A., Ryan D. M., Ticehurst J., Tilling J., Walcott S. M., Penn C. R., *Antimicrob. Agents Chemother.*, **37**, 1473—1479 (1993).
26) Satoh T., Hosokawa M., *Chem. Biol. Interact.*, **162**, 195—211 (2006).
27) Li B., Sedlacek M., Manoharan I., Boopathy R., Duysen E. G., Masson P., Lockridge O., *Biochem. Pharmacol.*, **70**, 1673—1684 (2005).
28) Coukell A. J., Markham A., *Drugs*, **54**, 745—750 (1997).
29) Sanofi Aventis Co., Japan, Interview Form (Plavix Tablet) (in Japanese).
30) Laboratory Sanofi Sante/Daiichi Pharmaceutical Co., Japan, Plavix Application Data Summary (in Japanese), Available from WEB page of Pharmaceuticals and Medical Devices Agency (PMDA), http://www.info.pmda.go.jp/shinyaku/g0601.html (2004).
31) Chugai Pharmaceutical Co., Japan, Tamiflu package insert (Tamiflu capsule 75) (in Japanese).
32) Esser R., Berry C., Du Z., Dawson J., Fox A., Fujimoto R. A., Haston W., Kimble E. F., Koehler J., Peppard J., Quadrus E., Quintavalla J., Toscano K., Urban L., van Duzr J., Zhang X., Zhou S., Marshall P. J., *Br. J. Pharmacol.*, **144**, 539—550 (2005).
33) Kawai N., Ikematsu H., Iwaki N., Maeda T., Satoh I., Hirotsu N., Kashiwagi S., *Clin. Infect. Dis.*, **43**, 439—444 (2006).
34) Sugaya N., Mitamura K., Yamazaki M., Tamura D., Ichikawa M., Kimura K., Kawakami C., Kiso M., Ito M., Hatakeyama S., Kawaoka Y., *Clin. Infect. Dis.*, **44**, 197—202 (2007).

0090-9556/08/3601-6–9$20.00
DRUG METABOLISM AND DISPOSITION
Copyright © 2008 by The American Society for Pharmacology and Experimental Therapeutics
DMD 36:6–9, 2008

Vol. 36, No. 1
17699/3287995
Printed in U.S.A.

Short Communication

D14747

Oseltamivir (Tamiflu) Efflux Transport at the Blood-Brain Barrier via P-Glycoprotein

Received July 20, 2007; accepted October 11, 2007

ABSTRACT:

Oseltamivir (Tamiflu, Roche, Nutley, NJ), an ester-type prodrug of the anti-influenza drug Ro 64–0802 (oseltamivir carboxylate), has been reported to be associated with neuropsychiatric side effects, which are likely to be caused by distribution of oseltamivir and/or its metabolite into the central nervous system. Enhanced toxicity and brain distribution of oseltamivir in unweaned rats led us to hypothesize that the low level of distribution of oseltamivir and/or Ro 64–0802 in adult brain was caused by the presence of a specific efflux transporter at the blood-brain barrier. We examined the possible role of P-glycoprotein (P-gp) as the determinant of brain distribution of oseltamivir and Ro 64–0802 both in vitro using LLC-GA5-COL150 cells, which overexpress human multidrug resistance protein 1 P-gp on the apical membrane, and in vivo using mdr1a/1b knockout mice. The permeability of oseltamivir in the basal-to-apical direction was significantly greater than that in the opposite direction. The directional transport disappeared on addition of cyclosporin A, a P-gp inhibitor. The brain distribution of oseltamivir was increased in mdr1a/1b knockout mice compared with wild-type mice. In contrast, negligible transport of Ro 64–0802 by P-gp was observed in both in vitro and in vivo studies. These results show that oseltamivir, but not Ro 64–0802, is a substrate of P-gp. Accordingly, low levels of P-gp activity or drug-drug interactions at P-gp may lead to enhanced brain accumulation of oseltamivir, and this may in turn account for the central nervous system effects of oseltamivir observed in some patients.

Oseltamivir phosphate (oseltamivir) (Fig. 1), manufactured under the trade name Tamiflu (Roche, Nutley, NJ) as an ester-type prodrug of the neuraminidase inhibitor Ro 64–0802 (oseltamivir carboxylate) (Fig. 1), has been developed for the treatment of A and B strains of the influenza virus, whereas the typical anti-influenza drug amantadine is used only for the A strain. However, the drug exhibits several adverse effects, not only in the digestive system (abdominalgia, diarrhea, and nausea) but also in the central nervous system (CNS); the latter include headache, vertigo, somnolence, insomnia, numbness, and behavioral excitement (basic product information of Tamiflu from Roche). Recently, there has been concern that the drug may be associated with suicidal or abnormal behavior especially in younger patients (http://www.fda.gov/cder/drug/infopage/tamiflu/QA20051117.htm and http://www.mhlw.go.jp/english/index.html). At present, the U.S. label of the drug specifies that the drug is not to be administrated to patients less than 1 year of age, whereas the label in Japan only mentions that the safety in the patients is not confirmed and includes the caution that administration to patients older than 10 years of age is possibly at risk to develop neurological side effect.

In general, CNS effects are caused by distribution of a drug and/or its metabolite(s) into the CNS through the blood-brain barrier (BBB). When oseltamivir was administered to rats at the high dose of 1000 mg/kg in safety examinations, the brain concentrations of the unchanged drug in 7-, 14-, and 24-day-old rats were 1540, 650, and 2 times greater than that in 48-day-old ones, whereas the brain concentration of the active metabolite Ro 64–0802 was lower than the plasma concentration in all the groups. In addition, brain unchanged drug concentration-dependent toxicity was observed (basic product information of Tamiflu from Roche). Those reports suggested that oseltamivir causes CNS side effects in younger animals in which the BBB is immature (Johanson, 1980), although it is not clear which compound is responsible to cause the CNS side effect. Drug concentration in the brain may be determined not only by passive diffusion but also by active transport and/or specific accumulation. Accordingly, BBB function is partially maintained by efflux transporters such as P-glycoprotein (P-gp), which is expressed at the luminal membrane in brain capillaries. Several P-gp substrates are known to exhibit low apparent permeability from the blood to the brain. Permeation of these P-gp substrates into the brain is increased in animals in which P-gp activity is reduced or abrogated, e.g., as a result of drug-drug interaction, mdr1a/1b deficiency (mdr1a/1b$^{-/-}$ mice), or immature BBB function (Tsuji, 1998; Demeule et al., 2002; Ebinger and Uhr, 2006). In the present study, we examined whether oseltamivir and its active metabolite Ro 64–0802 are substrates of P-gp, using P-gp-overexpressing cells and mdr1a/1b knockout mice, to clarify the possible involvement of P-gp in controlling their brain distribution.

Article, publication date, and citation information can be found at http://dmd.aspetjournals.org.
doi:10.1124/dmd.107.017699.

Materials and Methods

Chemicals and Animals. Oseltamivir phosphate was purchased from Sequoia Research Products (Pangbourne, UK). Ro 64–0802 was biologically synthesized from oseltamivir using porcine liver esterase (Sigma, St. Louis, MO). All the other chemicals and solvents were commercial products of analytical, high-performance liquid chromatography (HPLC), or liquid chromatography/mass spectrometry grade. The LLC-PK1 (wild-type) and P-gp-overexpressing LLC-GA5-COL150 cells were obtained from Japan Health

ABBREVIATIONS: CNS, central nervous system; BBB, blood-brain barrier; P-gp, P-glycoprotein; HPLC, high-performance liquid chromatography.

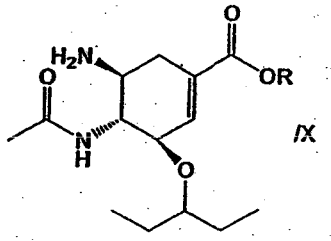

	R	X
Oseltamivir phosphate	C_2H_5	H_3PO_4
Ro 64-0802	H	—

FIG. 1. Chemical structures of oseltamivir phosphate and its active metabolite Ro 64–0802.

Science Research Resources Bank (Osaka, Japan) and Riken Gene Bank (Tsukuba, Japan), respectively (Tanigawara et al., 1992; Ueda et al., 1992). The animal study was performed according to the Guidelines for the Care and Use of Laboratory Animals at the Takasaki University of Health and Welfare and approved by the Committee of Ethics of Animal Experimentation of the university. Male FVB wild-type mice and mdr1a/1b knockout mice were purchased from Taconic Farms (Germantown, NY) and used at 8 to 9 weeks of age.

Cell Culture and Transport Experiments. LLC-PK1 and LLC-GA5-COL150 cells were cultured, passaged, and grown as described previously (Ishiguro et al., 2004). Cells were cultured at 37°C in a 5% CO_2 atmosphere. For transport studies, cells were seeded onto Transwell filter membrane inserts (Costar, Bedford, MA) at a density of 2.5×10^5 cells/cm^2. Medium 199 supplemented with 10% fetal bovine serum, 14.3 mM $NaHCO_3$, and 2 mM L-glutamine (additionally, 150 ng/ml colchicine for LLC-GA5-COL150 cells) was used as culture medium. The culture medium was replaced with fresh medium after 2 days, and cell monolayers cultured for 5 days were used for transport studies. The cell monolayers were preincubated in transport medium (Hanks' balanced salt solution; 0.952 mM $CaCl_2$, 5.36 mM KCl, 0.441 mM KH_2PO_4, 0.812 mM $MgSO_4$, 136.7 mM NaCl, 0.385 mM Na_2HPO_4, 25 mM D-glucose, and 10 mM HEPES, pH 7.4) for 10 min at 37°C. After preincubation, transport was initiated by adding the test drug to the donor side and transport medium to the receiver side. Drug transport was observed in two directions [apical (A) to basal (B) and B to A] over 150 min at 37°C. The permeability (P_{app}, cm/s) of the compounds across cell monolayers was evaluated by dividing the slope of the time course of the transport from A to B or from B to A by concentration at the donor side as $P_{app(AB)}$ or $P_{app(BA)}$, respectively. The permeability ratio was obtained by dividing $P_{app(BA)}$ by $P_{app(AB)}$. Kinetic parameters, V_{max}, and apparent K_m for P-gp-mediated drug transport were calculated by nonlinear least-squares analysis (MULTI program) using the following equation, assuming that A to B flux (V_{AB}) can be expressed as the difference between passive (V_{PD}) and P-gp-mediated flux ($V_{P\text{-}gp}$) (Yamaoka et al., 1981; Shirasaka et al., 2007).

$$V_{AB} = V_{PD} - V_{P\text{-}gp} = P_{app,PD} \cdot S \cdot C_a - \frac{V_{max} \cdot C_a}{K_m + C_a} \quad (1)$$

where $P_{app,PD}$ is the membrane permeability by passive diffusion [$P_{app,PD}$ of the test compounds in monolayers can be evaluated by using potent P-gp inhibitor, cyclosporin A (10 μM)], and C_a is the drug concentration in the apical solution. K_m value represents the apical concentration of the drug at which the decreased permeability by P-gp-mediated efflux became half of its maximal value.

Brain Distribution of Oseltamivir. Oseltamivir was dissolved in water and administered to FVB mice and mdr1a/1b knockout mice at single oral doses of 30, 100, and 300 mg/10 ml/kg (each $n = 3$). At 1 h after dosing (corresponding to T_{max}) (Li et al., 1998), blood was withdrawn from the heart with heparinized syringes. Subsequently, residual systemic blood was washed out by 3 ml of saline that was injected from the heart and discharged by cutting abdominal vein, and then the brain was removed. Blood was centrifuged (1700g) for 15 min at 4°C to obtain plasma. Quantitation of oseltamivir and Ro 64–0802 in plasma and brain tissues was performed using reported methods (Wiltshire et al., 2000) with some modifications. Briefly, aliquots of brain tissues (100 mg) were homogenized with 1 ml of 5 mM ammonium acetate buffer, followed by centrifugation at 1700g, and 0.9 ml of the supernatant was subjected to solid-phase extraction (Empore Mixed Phase Cation, 7 mm/3 ml, 3M Bioanalytical Technologies, St. Paul, MN). The methods used for the extraction of plasma and brain homogenate were identical.

Analytical Methods. Aliquots (20 μl) of oseltamivir and Ro 64–0802 samples were injected into an HPLC system (LC-20A system, Shimadzu, Kyoto, Japan) equipped with Inertsil CN-3 column (4.6 × 100 mm, 5 mm, GL Sciences Inc., Tokyo, Japan) using isocratic elution at 0.5 ml/min with 80 mM formic acid. Analytes were detected using a quadrupole mass spectrometer (LCMS-2010EV, Shimadzu) fitted with an electrospray ionization source. Analytes were detected in the positive mode, and protonated molecular ions monitored were $m/z = 313$ for oseltamivir and $m/z = 285$ for Ro 64–0802. Some oseltamivir samples were analyzed with an HPLC system (Alliance System, Waters, Milford, MA) consisting of the 2690 separation module with an analytical column, 250 × 4.6-mm i.d. Mightysil RP-18 Aqua column (Kanto Chemical, Tokyo, Japan), and mobile phases consisting of a mixture of 10 mM phosphate buffer, pH 6.0, and methanol in ratios of 40 and 60%, at a flow rate of 1 ml/min and at 40°C. Detection was done at the wavelength of 230 nm with a 2487 dual-wavelength absorption detector (Waters). Samples for calibration were prepared in a similar manner to that described above for the preparation of analytical samples. Statistical analysis of kinetic parameters was performed by means of Student's t test. A difference between means was considered to be significant when the P value was less than 0.05.

Results and Discussion

In the present study, we examined the transport of oseltamivir and its active metabolite Ro 64–0802 via P-gp using P-gp-overexpressing cells and mdr1a/1b gene-knockout mice to evaluate the factors that affect the BBB distribution of these compounds. The permeability of oseltamivir in the basal-to-apical direction in LLC-GA5-COL150 cells was significantly higher than that in the opposite direction, whereas the permeability in wild-type cells was comparable in the two directions, with the permeability ratios of approximately 7.8 and 1.2 in LLC-GA5-COL150 and wild-type cells, respectively (Table 1). In the presence of cyclosporin A, the permeability ratio in LLC-GA5-COL150 cells became approximately unity. These in vitro results indicate that oseltamivir is a substrate of P-gp, and its overall permeability is significantly affected by the efflux transporter. When oseltamivir was administered at various doses to mdr1a/1b knockout mice, an increase in the accumulation of oseltamivir in the brain was observed compared with that in wild-type mice (Table 2). Therefore, it is likely that brain distribution of oseltamivir is controlled by P-gp. Basal-to-apical transport of oseltamivir in P-gp-overexpressing cells was saturable with the K_m and V_{max} values of 1.3 mM and 0.203 nmol/min/cm^2, respectively. Because the K_m value is much higher than the free plasma concentration of oseltamivir in the clinical situation (about 50 nM; basic product information of Tamiflu from Roche), it is reasonable to consider that P-gp is not saturated by usual clinical doses of oseltamivir, and the brain accumulation of oseltamivir should be affected by P-gp in humans. These results suggest that variation in P-gp activity in the brain resulting from genetic differences or coadministered drugs may affect the brain distribution of oseltamivir, leading to CNS side effects.

As shown in Table 2, a dose-dependent increase in the $K_{p,app}$ value of oseltamivir was observed in both mdr1a/1b knockout and wild-type mice, in the range from 30 mg/kg to the highest dose of 300 mg/kg. The $K_{p,app}$ ratio ($K_{p,app}$ value in knockout mice/$K_{p,app}$ value in wild-type mice) of oseltamivir was also increased in a dose-dependent manner. The dose-dependent increase of $K_{p,app}$ value of oseltamivir in wild-type mice may be explained by the saturation of P-gp. However,

TABLE 1

Apparent permeability and permeability ratio of oseltamivir and Ro 64–0802 in LLCPK1-GA5-COL150 and LLC-PK1 cells (wild-type)

Condition	Cell Line	P_{app} cm/s ($\times 10^{-6}$)		Permeability Ratio
		Apical to Basal	Basal to Apical	
		mean. ± *S.E.*	*mean* ± *S.E.*	
Oseltamivir	LLCPK1-GA5-COL150	2.47 ± 2.47	19.2 ± 1.40	7.77
	Wild-type	6.10 ± 0.18	7.24 ± 0.40	1.19
With 10 μM CysA	LLCPK1-GA5-COL150	6.06 ± 0.10	7.06 ± 0.60	1.17
Ro 64–0802	LLCPK1-GA5-COL150	1.55 ± 0.14	1.72 ± 0.14	1.11
With 10 μM CysA	LLCPK1-GA5-COL150	1.73 ± 0.06	1.49 ± 0.07	0.86

Permeability ratio = (P_{app} B to A)/(P_{app} A to B); CysA, cyclosporin A.
The initial concentrations of test compounds were 100 μM.
Data are expressed as mean or mean ± S.E. of three experiments.

TABLE 2

$K_{p,app}$ (plasma-brain concentration ratio) of oseltamivir and Ro 64–0802 between mdr1a/1b knockout and wild-type mice

Dose	N	Oseltamivir			Ro 64–0802		
		Mdr1a/1b KO	Wild-type	Ratio	Mdr1a/1b KO	Wild-type	Ratio
mg/kg		*mean* ± *S.E.*	*mean* ± *S.E.*	*KO/wild*	*mean* ± *S.E.*	*mean* ± *S.E.*	*KO/wild*
30	3	0.647 ± 0.059**	0.137 ± 0.016	4.7	0.003 ± 0.005	0.005 ± 0.005	0.5
100	3	0.847 ± 0.176*	0.171 ± 0.056	4.9	0.007 ± 0.001	0.016 ± 0.013	0.4
300	3	6.505 ± 2.843	0.689 ± 0.250	9.6	0.017 ± 0.002	0.022 ± 0.003	0.5

KO, knockout.
$K_{p,app,brain}$ were measured at 1 h (T_{max}) after p.o. administration to mdr1a/1b KO and wild-type mice.
Each value represents the mean ± S.E. of three animals.
* $P < 0.05$; ** $P < 0.01$, by Student's t test.

$K_{p,app}$ value of oseltamivir in mdr1a/1b knockout mice also increased dose-dependently. Because this observation cannot be explained by P-gp, other transporters may be involved in the transport of oseltamivir across the BBB (Hill et al., 2002). Another possibility is that free fraction of oseltamivir, which would affect the brain penetration, was increased because of the saturation of its plasma protein binding. However, because plasma protein binding of oseltamivir administered orally at 30 and 300 mg/kg (corresponding to plasma concentration of 0.5 and 5 mg/ml, respectively) was found to be 36.3 and 32.0%, respectively (data not shown), it is reasonable to consider that plasma protein binding of oseltamivir is not saturated in this dosing range. On the other hand, plasma concentrations of oseltamivir were comparable in mdr1a/1b knockout mice and wild-type mice after oral administration of oseltamivir; those at a dose of 30, 100, and 300 mg/kg were 1.05 ± 0.21, 3.80 ± 1.89, and 2.82 ± 0.67 μg/ml for wild-type mice and 0.95 ± 0.09, 4.02 ± 0.47, and 2.27 ± 0.61 μg/ml for mdr1a/1b knockout mice, respectively. This may be because the elimination of oseltamivir occurs mainly via hydrolysis by esterase in blood and liver, and intestinal P-gp may have relatively little effect than BBB (Li et al., 1998; Ogihara et al., 2006).

In the case of the active metabolite Ro 64–0802, the permeability in LLC-GA5-COL150 cells was comparable in both directions. The permeability ratio of Ro 64–0802 was approximately unity in both the presence and absence of cyclosporin A, suggesting that the active metabolite is not a substrate of P-gp (Table 1). These results are consistent with the finding that brain accumulation of Ro 64–0802 in mdr1a/1b knockout mice was very limited and comparable with that in wild-type mice. These findings suggested that brain distribution of this active metabolite is unlikely to be affected by P-gp in humans.

In conclusion, our in vivo and in vitro results indicate that oseltamivir, but not its active metabolite Ro 64–0802, is a substrate of P-gp and that the brain distribution of oseltamivir is significantly affected by P-gp. Accordingly, interindividual variation of P-gp activity may be an important factor determining susceptibility to the CNS side effects of this drug, in addition to the genetic polymorphisms of carboxylesterase 1 (Shi et al., 2006) and sialidase (Li et al., 2007). Various factors, such as genetic polymorphisms of P-gp, drug-drug interactions at P-gp, and altered expression by inflammatory cytokines, could influence apparent P-gp activity and therefore might play a role in increasing the accumulation of oseltamivir in the brain, thereby contributing to the occurrence of CNS side effects of oseltamivir in humans.

Faculty of Pharmacy, Takasaki University of Health and Welfare, Takasaki, Gunma, Japan (K.M., C.K., T.O.);
Faculty of Pharmaceutical Sciences, Tokyo University of Science, Noda, Chiba, Japan (M.N., Y.S., I.T., T.O.); and
College of Information Science and Engineering, Ritsumeikan University, Kusatsu, Shiga, Japan (T.F.)

KAORI MORIMOTO
MASANORI NAKAKARIYA
YOSHIYUKI SHIRASAKA
CHIHAYA KAKINUMA
TAKUYA FUJITA
IKUMI TAMAI
TAKUO OGIHARA

References

Demeule M, Régina A, Jodoin J, Laplante A, Dagenais C, Berthelet F, Moghrabi A, and Béliveau R (2002) Drug transport to the brain: key roles for the efflux pump P-glycoprotein in the blood-brain barrier. *Vascul Pharmacol* 38:339–348.
Ebinger M and Uhr M (2006) ABC drug transporter at the blood-brain barrier: effects on drug metabolism and drug response. *Eur Arch Psychiatry Clin Neurosci* 256:294–298.
Hill G, Cihlar T, Oo C, Ho ES, Prior K, Wiltshire H, Barrett J, Liu B, and Ward P (2002) The anti-influenza drug oseltamivir exhibits low potential to induce pharmacokinetic drug interactions via renal secretion-correlation of in vivo and in vitro studies. *Drug Metab Dispos* 30:13–19.
Ishiguro N, Nozawa T, Tsujihata A, Saito A, Kishimoto W, Yokoyama K, Yotsumoto T, Sakai K, Igarashi T, and Tamai I (2004) Influx and efflux transport of H1-antagonist epinastine across the blood-brain barrier. *Drug Metab Dispos* 32:519–524.
Johanson CE (1980) Permeability and vascularity of the developing brain: cerebellum vs cerebral cortex. *Brain Res* 190:3–16.
Li C, Yu Q, Ye Z, Sun Y, He Q, Li Z, Zhang W, Luo J, Gu X, Zheng X, et al. (2007) A nonsynonymous SNP in human cytosolic sialidase in a small Asian population results in

reduced enzyme activity: potential link with severe adverse reactions to oseltamivir. *Cell Res* 17:357–362.

Li W, Escarpe PA, Eisenberg EJ, Cundy KC, Sweet C, Jakeman KJ, Merson J, Lew W, Williams M, Zhang L, et al. (1998) Identification of GS 4104 as an orally bioavailable prodrug of the influenza virus neuraminidase inhibitor GS 4071 *Antimicrob Agents Chemother* 42:647–653.

Ogihara T, Kamiya M, Ozawa M, Fujita T, Yamamoto A, Yamashita S, Ohnishi S, and Isomura Y (2006) What kinds of substrates show P-glycoprotein-dependent intestinal absorption? Comparison of verapamil with vinblastine. *Drug Metab Pharmacokinet* 21:238–244.

Shi D, Yang J, Yang D, LeCluyse EL, LeCluyse CB, Black C, You L, Akhlaghi F, and Yan B (2006) Anti-influenza prodrug oseltamivir is activated by carboxyesterase human 1, and the activation is inhibited by antiplatelet agent clopidgrel. *J Pharmacol Exp Ther* 319:1477–1484.

Shirasaka Y, Sakane T, and Yamashita S (2007) Effect of P-glycoprotein expression levels on the concentration-dependent permeability of drugs to the cell membrane. *J Pharm Sci*, in press.

Tanigawara Y, Okamura N, Hirai M, Yasuhara M, Ueda K, Kioka N, Komano T, and Hori R (1992) Transport of digoxin by human P-glycoprotein expressed in a porcine kidney epithelial cell line (LLC-PK1). *J Pharmacol Exp Ther* 263:840–845.

Tsuji A (1998) P-glycoprotein-mediated efflux transport of anticancer drugs at the blood-brain barrier. *Ther Drug Monit* 20:588–590.

Ueda K, Okamura N, Hirai M, Tanigawara Y, Saeki T, Kioka N, Komano T, and Hori R (1992) Human P-glycoprotein transports cortisol, aldosterone, and dexamethasone, but not progesterone. *J Biol Chem* 267:24248–24252.

Wiltshire H, Wiltshire B, Citron A, Clarke T, Scrpe C, Gray D, and Herron W (2000) Development of a high-performance liquid chromatographic-mass spectrometric assay for the specific and sensitive quantification of Ro 64–0802, an anti-influenza drug, and its pro-drug, oseltamivir, in human and animal plasma and urine. J Chromatogr B Biomed Sci Appl 745:373–388.

Yamaoka K, Tanigawara Y, Nakagawa T, and Uno T (1981) A pharmacokinetic analysis program (multi) for microcomputer. *J Pharmacobiodyn* 4:879–885.

Address correspondence to: Takuo Ogihara, Laboratory of Biopharmaceutics, Department of Pharmacology, Faculty of Pharmacy, Takasaki University of Health and Welfare, Takasaki, Gunma 370-0033, Japan. E-mail: togihara@takasaki-u.ac.jp

P-115 抗インフルエンザ薬オセルタミビルのP糖タンパク質による中枢移行性制御

Controlled brain exposure of oseltamivir by P-glycoprotein

○荻原 琢男[1]，森本 かおり[1]，柿沼 千早[1]，白坂 善之[2]，榎本 茂樹[3]，榎内 光[3]，玉井 郁巳[2]

[1]高崎健康福祉大学薬学部，[2]金沢大学大学院自然科学研究科，[3]株式会社ジェノメンブレン

○ Takuo OGIHARA[1], Kaori MORIMOTO[1], Chihaya KAKINUMA[1], Yoshiyuki SHIRASAKA[2], Shigeki ENOMOTO[3], Hikaru YABUUCHI[2], Ikumi TAMAI[2]

[1]Faculty of Pharmacy, Takasaki University of Health and Weelfare, [2]Graduate School of Natural Science and Technology, Kanazawa University, [3]Geno Membrane, Inc

【目的】中枢性副作用が懸念される医薬品の中枢移行調節機構を明確にすることは、医薬品の適正使用上重要である。本研究では、抗インフルエンザウィルス薬オセルタミビル(タミフル™)およびその活性代謝物(Ro64-0802)の血液脳関門(BBB)透過性に対するトランスポーターの影響について、P-gpを中心に検討を行った。[1] 【方法】P-gpを強制発現させたSf9細胞(MDR1-Sf9)ベシクルを用いてATPase活性を測定し、また、P-gpを強制発現させたLLC-PK1細胞(LLC-GA5-COL150細胞)を用いて輸送活性を評価した。さらに、P-gpノックアウトマウスおよびラットを用い、オセルタミビル経口投与後のオセルタミビルおよびRo64-0802の中枢移行性とP-gp発現量を比較検討した。【結果・考察】MDR1-Sf9ベシクルを用いた検討において、オセルタミビルは濃度依存的にATPase活性を上昇させた。またLLC-GA5-COL150細胞を用いた検討では、オセルタミビルはP-gpの基質として認識されたものの、Ro64-0802は認識されなかった。また、P-gpに対するオセルタミビルのKm値は1．3 mMであることが示されたが、実際の血漿中濃度(50 nM)に比べ顕著に高かったことからP-gpがオセルタミビルの体内動態に効率的に機能していることが示唆された。さらに、ノックアウトマウスにおけるオセルタミビルの脳内移行性は野生型と比較して約4～10倍と有意に高くなった。また、P-gpの発現量の乏しい幼若ラットでは、オセルタミビルの脳内移行性が成獣に比べて上昇していた。以上より、BBBに発現するP-gpがオセルタミビルの中枢移行性調節因子の一つである可能性が推察された。

1)Morimoto K et. al., Drug Metab. Dispos., 36, 1-4 (2008).

P-116 メトホルミンの乳酸アシドーシス惹起能に関するフェンホルミンとの差別化検討

The potential of metformin compared to the potential of phenformin on biguanide-induced lactic acidosis

○坂東 清子[1]，落合 尚子[2]，赤山 茂樹[3]，国松 武史[1]，出口 二郎[1]，木村 亘紀[1]，船橋 斉[1]，関 高樹[1]

[1]大日本住友製薬株式会社 安全性研究所，[2]大日本住友製薬株式会社 薬物動態研究所，[3]株式会社 イナリサーチ

○ Kiyoko BANDO[1], Shoko OCHIAI[2], Shigeki YONEYAMA[3], Takeshi KUNIMATSU[1], Jiro DEGUCHI[1], Juki KIMURA[1], Hitoshi FUNABASHI[1], Takaki SEKI[1]

[1]Safety Research Laboratories, Dainippon Sumitomo Pharma Co., Ltd., [2]Pharmacokinetics Research Laboratories, Dainippon Sumitomo Pharma Co., Ltd., [3]Ina Research Inc.

【目的】メトホルミンはビグアナイド系経口血糖降下薬であり、現在、1951年以降、世界100ヵ国以上で使用されている。近年、メトホルミンの多様な作用機序による血糖効果作用が明らかとなり、臨床現場における有用性が見直されている。ビグアナイド系の薬剤の最も危惧すべき副作用は乳酸アシドーシスであり、それによりこれまで本邦のメトホルミンの投与量は欧米の1/3程度に制限されてきた。しかしながら、臨床使用を反映した乳酸アシドーシス惹起のポテンシャルを評価した非臨床データはほとんどない。今回、過去に乳酸アシドーシス多発のため米国で販売中止となった薬剤(フェンホルミン)とメトホルミンの乳酸アシドーシス惹起能を比較することを目的として、両剤のヒトにおける曝露量をラットで再現し、血中乳酸値上昇作用を比較した。
【方法】雌雄のF344/Jclラットに、メトホルミン塩酸塩(50、100、200 mg/kg/日)およびフェンホルミン塩酸塩(100、200、400 mg/kg/日)を反復経口投与後、経時的に血漿中未変化体薬物濃度および血中乳酸値を測定し、欧米におけるヒト臨床用量(2250 mg/kg/man)での曝露量に匹敵する投与量における血中乳酸値変動を検討した。
【結果・考察】メトホルミンではヒト曝露相当の投与量で反復投与によってもほとんど影響は認められなかった。一方、フェンホルミンではヒト曝露量相当量又はヒト曝露量相当量を下回る用量において、投与後持続的に乳酸値の高値が認められ、また反復投与によって乳酸値の上昇作用がより増強する傾向が認められた。また、両剤のヒト曝露量相当量における乳酸値を比較すると、フェンホルミンの方がより強い乳酸値上昇作用を持つと考えられた。従って、メトホルミンの乳酸アシドーシス惹起能はフェンホルミンに比較して弱く、臨床現場で適正使用される限り、乳酸アシドーシスが発現する可能性は低いと考えられた。

日本トキシコロジー学会学術年会，第３５回（２００８．０６．２７－２８，東京）

0090-9556/08/3602-427–434$20.00
DRUG METABOLISM AND DISPOSITION

DMD 36:427–434, 2008

D15187

Vol. 36, No. 2
18556/3302931
Printed in U.S.A.

P-glycoprotein Restricts the Penetration of Oseltamivir Across the Blood-Brain Barrier

Atsushi Ose, Hiroyuki Kusuhara, Kenzo Yamatsugu, Motomu Kanai, Masakatsu Shibasaki, Takuya Fujita, Akira Yamamoto, and Yuichi Sugiyama

The Graduate School of Pharmaceutical Sciences, the University of Tokyo, Bunkyo-ku, Tokyo, Japan (A.O., H.K., K.Y., M.K., M.S., Y.S.); Ritsumeikan University, Kusatsu, Shiga, Japan (T.F.); and Kyoto Pharmaceutical University, Yamashina-ku, Kyoto, Japan (A.Y.)

Received August 27, 2007; accepted November 20, 2007

ABSTRACT:

Oseltamivir is an ethyl ester prodrug of [3*R*,4*R*,5*S*]-4-acetamido-5-amino-3-(1-ethylpropoxy)-1-cyclohexene-1-carboxylate phosphate (Ro 64-0802), the anti-influenza drug. Abnormal behavior has been suspected to be associated with oseltamivir medication in Japan. The purpose of the present study is to examine the involvement of transporters in the brain distribution of oseltamivir and its active form Ro 64-0802 across the blood-brain barrier (BBB). The brain-to-plasma concentration ratio ($K_{p,brain}$) of oseltamivir after i.v. infusion of oseltamivir in FVB mice was increased by pretreatment with *N*-(4-[2-(1,2,3,4-tetrahydro-6,7-dimethoxy-2-isoquinolinyl)ethyl]-phenyl)-9,10-dihydro-5-methoxy-9-oxo-4-acridine carboxamide (GF120918), a dual inhibitor for P-glycoprotein (P-gp) and breast cancer resistance protein (Bcrp), whereas that of Ro 64-0802 was only slightly increased. Furthermore, the distribution volume of Ro 64-0802 following i.v. administration of Ro 64-0802 in the brain was similar to the capillary volume, suggesting its minimal distribution. The $K_{p,brain}$ value of oseltamivir in multidrug-resistant (Mdr) 1a/1b P-gp knockout mice was 5.5-fold higher than that in wild-type mice and comparable with that obtained by pretreatment with GF120918, whereas it was unchanged in Bcrp knockout mice. The $K_{p,brain}$ value of oseltamivir was significantly higher in newborn rats, which is in good agreement with the ontogenetic expression profile of P-gp. Intracellular accumulation of oseltamivir was lower in human and mouse P-gp–expressing cells, which was reversed by P-gp inhibitor valspodar (PSC833). These results suggest that P-gp limits the brain uptake of oseltamivir at the BBB and that Ro 64-0802 itself barely crosses the BBB. However, it may be possible that Ro 64-0802 is formed in the brain from the oseltamivir, considering the presence of carboxylesterase in the brain endothelial cells.

Oseltamivir (Fig. 1) is an ester prodrug of Ro 64-0802, a potent and selective inhibitor of neuraminidase, resulting in an inhibition of release of influenza virus from the host cells and growth of influenza virus. Oseltamivir is used in the treatment and prophylaxis of both Influenzavirus A and Influenzavirus B (Bardsley-Elliot and Noble, 1999). The number of prescribed oseltamivir has reached approximately 10 million in Japan, which accounted for 75% of the world total in 2006. Recently, abnormal behavior has been reported in influenza patients prescribed oseltamivir (http://www.fda.gov/cder/drug/infopage/tamiflu/QA20051117.htm; Fuyuno, 2007). According to a report by the Ministry of Health, Labor, and Welfare, the number of people who behaved abnormally following oseltamivir treatment has increased to 211 (0.002% of all patients), approximately 80% of whom are teenagers or younger. The relationship between abnormal behavior and oseltamivir medication remains an open question and has not yet been elucidated. The Ministry of Health, Labor, and Welfare has published a caution for oseltamivir medication to teenagers or younger people. Recently, it was shown that oseltamivir and Ro 64-0802 affects neuronal excitability in rat hippocampal slices, and Ro 64-0802 exhibits 30 times more potent than oseltamivir (Izumi et al., 2007). Based on this background, there is growing interest in the penetration of oseltamivir and its active form Ro 64-0802 into the brain.

The purpose of the present study was to characterize the transport of oseltamivir and Ro 64-0802 across the blood-brain barrier (BBB). Oseltamivir is rapidly hydrolyzed to its active form, Ro 64-0802, by human carboxylesterase 1 (hCES1) in the liver (Shi et al., 2006) and then exclusively excreted into the urine by glomerular filtration and active tubular secretion via organic anion transporter 1 (OAT1) with-

This study was supported by Grants-in-Aid for Scientific Research (A) from the Japan Society for the Promotion of Science (JSPS) (KAKENHI 17209005).

Article, publication date, and citation information can be found at http://dmd.aspetjournals.org.

doi:10.1124/dmd.107.018556.

ABBREVIATIONS: Ro 64-0802, [3*R*,4*R*,5*S*]-4-acetamido-5-amino-3-(1-ethylpropoxy)-1-cyclohexene-1-carboxylate phosphate; BBB, blood-brain barrier; hCES1, human carboxylesterase 1; OAT, organic anion transporter; P-gp, P-glycoprotein; Bcrp, breast cancer resistance protein; GF120918, *N*-(4-[2-(1,2,3,4-tetrahydro-6,7-dimethoxy-2-isoquinolinyl)ethyl]-phenyl)-9,10-dihydro-5-methoxy-9-oxo-4-acridine carboxamide; MDR, multidrug-resistant; PSC833, valspodar; mMdr1a-LLC-PK1, mouse Mdr1a-expressed LLC-PK1; MDCKII, Madin-Darby canine kidney II; hMDR1-MDCKII, human MDR1-expressed MDCKII; gapdh, glyceraldehyde-3-phosphate dehydrogenase; PCR, polymerase chain reaction; PBS, phosphate-buffered saline; TBST, Tris-buffered saline/Tween 20; ECL, enhanced chemiluminescence; LC/MS, liquid chromatography/mass spectrometry; $K_{p,brain}$, brain-to-plasma concentration ratio; CES, carboxylesterase; SNP, single nucleotide polymorphism.

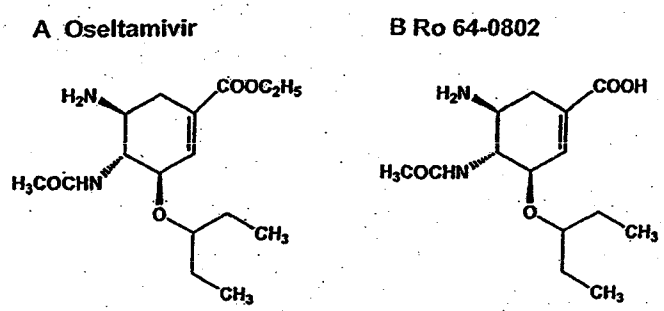

FIG. 1. Chemical structures of oseltamivir (A) and Ro 64-0802 (B).

out further metabolism (He et al., 1999). In healthy volunteers, both oseltamivir and Ro 64-0802 were detected in the blood circulation, although the C_{max} of oseltamivir was 6-fold smaller than that of Ro 64-0802 (He et al., 1999). The penetration of drugs into the brain is limited by the BBB formed by the brain capillary endothelial cells. Because of highly developed tight junctions between adjacent cells, as well as a paucity of fenestra and pinocytotic vesicles, the penetration across the paracellular route is very limited, and thus transcellular transport across the endothelial cells is the major pathway. Therefore, there is a good correlation between BBB permeability and lipophilicity. Because oseltamivir is an ester-type prodrug, it should exhibit higher BBB permeability than Ro 64-0802. hCES1 is also expressed in the brain at mRNA level (Satoh et al., 2002) and may convert oseltamivir to Ro 64-0802 in the brain, leading to an accumulation of Ro 64-0802 in the brain once oseltamivir penetrates the brain across the BBB in addition to the direct penetration of Ro 64-0802 from the systemic circulation. In addition to the physiological characteristics of the BBB, it has been accepted that active efflux across the BBB also provides a barrier function to the BBB. P-glycoprotein (P-gp), a 170-kDa membrane protein, is a well known gatekeeper protein in the BBB that plays a pivotal role in limiting the brain penetration of a range of xenobiotic compounds (Schinkel et al., 1994; Tamai and Tsuji, 2000; Kusuhara and Sugiyama, 2001). In addition to P-gp, recently it was found that breast cancer resistance protein (BCRP/ABCG2) also acts as active efflux pump in the BBB, and functional impairment of Bcrp results in a significant increase in the brain concentrations of imatinib (Breedveld et al., 2005) and phytoestrogens (Enokizono et al., 2007). These transporters may limit the exposure of the brain to oseltamivir and/or Ro 64-0802.

In the present study, the effect of GF120918 on the brain distribution of oseltamivir and Ro 64-0802 was examined in wild-type mice to suggest transporters involved in the efflux transport across the BBB. To support this in vivo inhibition study, the brain-to-plasma concentration ratios were determined in both multidrug-resistant (Mdr) 1a/1b P-gp and Bcrp knockout mice.

Materials and Methods

Reagents and Animals. Oseltamivir phosphate and its active metabolite Ro 64-0802 were synthesized (Kim et al., 1997; Yamatsugu et al., 2007). GF120918 (Elacridar) was a gift from GlaxoSmithKline (Ware, UK). PSC833 was supplied by Novartis Pharma AG (Basel; Switzerland). Mouse Mdr1a-expressed LLC-PK1 (mMdr1a-LLC-PK1) cells (Schinkel et al., 1995) were a gift from Dr. Alfred H. Schinkel (The Netherlands Cancer Institute, Amsterdam, The Netherlands), and human MDR1-expressed Madin-Darby canine kidney II (MDCKII) (hMDR1-MDCKII) cells (Evers et al., 2000) were provided by Dr. Piet Borst (The Netherlands Cancer Institute, Amsterdam, The Netherlands). All the other chemicals used in the experiments were of analytical grade.

Male FVB mice, Mdr1a/1b P-gp knockout mice, and Bcrp knockout mice were obtained from Taconic Farms (Germantown, NY) and maintained in Shimizu Laboratory Supplies (Kyoto, Japan). Male Wistar rats were supplied by Charles River (Kanagawa, Japan). All the mice (10–18 weeks) and rats (3–42 days) were maintained under standard conditions with a reverse dark-light cycle. Food and water were available ad libitum. All the experiments using animals in this study were carried out according to the guidelines provided by the institutional Animal Care Committee (Graduate School of Pharmaceutical Sciences, The University of Tokyo, Tokyo, Japan).

In Vivo Infusion Study in Mice and Rats. Male FVB mice, Mdr1a/1b P-gp knockout mice, and Bcrp knockout mice (10–18 weeks) weighing approximately 25 to 35 g and male Wistar rats weighing approximately 10 g (3 days), 13 g (6 days), 26 g (11 days), 48 g (21 days), and 200 g (42 days), respectively, were used for these experiments. Under pentobarbital anesthesia (30 mg/kg), the jugular vein was cannulated with a polyethylene-10 catheter for the injection of oseltamivir and Ro 64-0802. GF120918 (10 mg/3.3 ml/kg, dissolved in a 3:2 mixture of propylene glycol/water) was injected i.v. to male FVB mice 15 min before the i.v. infusion of oseltamivir and Ro 64-0802. The mice and rats then received a constant i.v. infusion of oseltamivir and Ro 64-0802 at a dose of 8 and 5 μmol/h/kg, respectively. Blood samples were collected from the jugular vein at 60, 90, and 120 min in mice and 20, 40, and 60 min in rats. Plasma was prepared by centrifugation of the blood samples (10,000*g*). Esterase inhibitor, dichlorvos (200 μg/ml), was used to prevent ex vivo hydrolysis of oseltamivir to Ro 64-0802 in the blood and plasma (Wiltshire et al., 2000; Lindegardh et al., 2006). The mice and rats were sacrificed after 120 and 60 min, respectively, and the brain was excised immediately. The tissues were weighed and stored at −80°C until used.

Quantification of Mdr1a mRNA Expression in Rat Cerebral Cortex. The mRNA levels of Mdr1a and glyceraldehyde-3-phosphate dehydrogenase (gapdh) were quantified by the real-time polymerase chain reaction (PCR) method. Total RNA was isolated from rat cerebral cortex pooled from one to four rats using ISOGEN (Wako Pure Chemicals, Osaka, Japan). Real-time PCR was performed with a QuantiTect SYBR Green PCR Kit (QIAGEN, Valencia, CA) and a LightCycler system (Roche Diagnostics, Mannheim, Germany). The following primers were designed: Mdr1a forward AACTTAGTCTATGGG GGAGG, reverse ACCACACCTTTCTGCTTACA; gapdh forward AGCCCAGAACATCATCCCTG, reverse CACCACCTTCTTGATGTCATC. An external standard curve was generated by dilution of the target PCR product, which was purified by agarose gel electrophoresis. The absolute concentration of the external standard was measured with PicoGreen double-stranded DNA Quantification Reagent (Molecular Probes, Eugene, OR).

Western Blot Analysis. Crude membranes from rat cerebral cortex were prepared as follows. After the addition of cold phosphate-buffered saline (PBS) at a ratio of 1 g of cerebral cortex/4 ml, the cerebral cortex pooled from one to four rats was homogenized using a Polytron homogenizer. The homogenate was centrifuged at 4°C for 15 min at 2000*g*, and the supernatant was collected and centrifuged at 4°C for 15 min at 100,000*g*. The resultant pellet was resuspended in PBS containing 0.1% protease inhibitor mixture (Sigma-Aldrich, St. Louis, MO) and stored at −80°C until used. The protein concentration was measured by the Lowry method. The specimens were loaded onto an 8.5% SDS-polyacrylamide gel electrophoresis with a 3.75% stacking gel. Proteins were electroblotted onto a polyvinylidene difluoride membrane (Pall, Port Washington, NY). The membrane was blocked with Tris-buffered saline containing 0.05% Tween 20 (TBST) and 2.5% enhanced chemiluminescence (ECL) Advance Blocking Agent (GE Healthcare, Little Chalfont, Buckinghamshire, UK) for 1 h at room temperature. After washing with TBST, the membrane was incubated with monoclonal anti-P-gp C219 antibody (Signet Laboratories, Dedham, MA) (1:100 in TBST containing 2.5% ECL Advance Blocking Agent) overnight at 4°C. Detection was carried out by binding a horseradish peroxidase-labeled anti-mouse IgG antibody (GE Healthcare) (1:5000 in TBST containing 2.5% ECL Advance Blocking Agent). Immunoreactivity was detected with an ECL Advance Western Blotting Detection Kit (GE Healthcare). The intensity of the band was quantified by Multi Gauge software version 2.0 (Fujifilm, Tokyo, Japan). Stripping of membranes was performed with Restore Western Blot Stripping buffer (Pierce, Rockford, IL) for 30 min at 37°C. After washing with TBST, the membrane was blocked with TBST containing 5% skim milk for 1 h at room temperature. After washing with TBST, the membrane was incubated with monoclonal anti-actin antibody (Chemicon International, Temecula, CA) (1:1000 in TBST containing 0.1% bovine serum albumin) for 1 h at room temperature. Detection was carried out

by binding a horseradish peroxidase-labeled anti-mouse IgG antibody (GE Healthcare) (1:5000 in TBST containing 0.1% bovine serum albumin).

Rat Liver S9 Fraction Preparation. Male Wistar rats (11 and 42 days) were anesthetized with ether, and their livers were quickly removed and washed in cold PBS. The livers were blotted dry and weighed. After the addition of cold PBS at a ratio of 1 g of liver/2 ml, the livers were homogenized using a glass homogenizer with a Teflon (DuPont, Wilmington, DE) pestle. The homogenized liver was then centrifuged at 4°C for 30 min at 9000*g*. Aliquots of the resulting supernatant were placed in several polypropylene tubes and stored at −80°C until used. The protein concentration was measured by the Lowry method.

Ro 64-0802 Formation in Rat Plasma and Liver S9 Specimens. A 0.5-ml incubation mixture contained 2.5 mg of protein of rat plasma or liver S9 in PBS. After temperature equilibration (37°C, 5 min), the incubation was started by adding 5 μl of oseltamivir (final 1.5 μM) and performed for various time periods up to 30 and 180 min for plasma and liver S9, respectively. After the reaction was terminated by ethanol, the concentrations of oseltamivir and Ro 64-0802 were determined with liquid chromatography/mass spectrometry (LC/MS) analysis.

Ro 64-0802 formation rates in the plasma protein or liver S9 protein were extrapolated to the in vivo value by taking the plasma protein content (50 mg of plasma protein/ml) or liver S9 protein content (96.1 mg of S9 protein/g liver) (Izumi et al., 1997) per milliliter plasma or gram liver, respectively, into consideration. Furthermore, Ro 64-0802 formation rates expressed per milliliter plasma or gram liver were expressed per kilogram body weight by taking the plasma content (38.5 ml of plasma/kg weight) or liver weight (40 g of liver/kg weight) per kilogram body weight into consideration.

Cellular Accumulation Studies. mMdr1a-LLC-PK1 cells and hMDR1-MDCKII cells were maintained as described with minor modifications. Uptake was initiated by adding the compounds to the incubating buffer in either the presence or the absence of 5 μM PSC833 after cells had been washed twice and preincubated with Krebs-Henseleit buffer at 37°C for 15 min. The Krebs-Henseleit buffer consisted of 142 mM NaCl, 23.8 mM $NaHCO_3$, 4.83 mM KCl, 0.96 mM KH_2PO_4, 1.20 mM $MgSO_4$, 12.5 mM HEPES, 5 mM glucose, and 1.53 mM $CaCl_2$ adjusted to pH 7.4. The uptake was terminated at designated times by adding ice-cold Krebs-Henseleit buffer, and the cells were washed twice. After the cells were suspended in water, the concentration of the compounds was determined with LC/MS analysis. The protein concentration was measured using the Lowry method. Cellular uptake is given as the cell-to-medium concentration ratio determined as the amount of compound associated with cells divided by the medium concentration.

Quantification of Oseltamivir and Ro 64-0802 in Plasma and Brain. *Sample preparation.* The brain was homogenized with a 4-fold volume of PBS to obtain a 20% brain homogenate. The plasma samples (10 μl) were mixed with 40 μl of ethanol, and the brain homogenates (100 μl) were mixed with 400 μl of ethanol. All these mixed solutions were centrifuged at 15,000*g* for 10 min. The supernatants of brain sample (350 μl) were evaporated, and the pellets were reconstituted with 50 μl of 20% ethanol. The reconstituted samples were centrifuged at 15,000*g* for 10 min to remove particles, and an aliquot of the supernatant was subjected to LC/MS analysis. The supernatants of plasma sample were mixed with an equal volume of water and subjected to LC/MS analysis.

LC/MS analysis. An LC/MS-2010 EV equipped with a Prominence LC system (Shimadzu, Kyoto, Japan) was used for the analysis. Samples were separated on a CAPCELL PAK C18 MGII column (3 μm, 2 × 50 mm) (Shiseido, Tokyo, Japan) in binary gradient mode with flow rate at 1 ml/min. For the mobile phase, 0.05% formic acid and acetonitrile were used. The acetonitrile concentration was initially 10% and then linearly increased up to 40% over 2 min. Finally, the column was re-equilibrated at an acetonitrile concentration of 10% for 3 min. The total run time was 5 min. Oseltamivir and Ro 64-0802 were eluted at 2.5 and 3.5 min, respectively. In the mass analysis, oseltamivir and Ro 64-0802 were detected at a mass-to-charge ratio of 313.20 and 285.15 under positive electron spray ionization conditions, respectively. The interface voltage was −3.5 kV, and the nebulizer gas (N_2) flow was 1.5 l/min. The heat block and curved desolvation line temperatures were 200 and 150°C, respectively.

Pharmacokinetic Analysis. The apparent brain-to-plasma concentration ratio ($K_{p,brain}$) was calculated using the following equation: $K_{p,brain} = C_{brain}/C_p$, where C_{brain} and C_p represent brain concentration at 120 min in mice and 60 min in rats (nmol/g brain) and plasma concentration at 120 min in mice and 60 min in rats (μM), respectively.

Statistical Analysis. Data are presented as the mean ± S.E. for three to seven animals unless specified otherwise. Student's two-tailed unpaired *t* test and one-way analysis of variance followed by Tukey's multiple comparison test or Dunnett's multiple comparison test were used to identify significant differences between groups when appropriate. Statistical significance was set at $P < 0.05$.

Results

Effect of Pretreatment with GF120918 on the Brain Distribution of Oseltamivir and Ro 64-0802. FVB mice were pretreated with GF120918 (10 mg/kg, i.v. administration), a dual inhibitor for P-gp and Bcrp (Allen et al., 1999), 15 min before i.v. infusion of oseltamivir. The plasma concentrations of oseltamivir and Ro 64-0802 were increased by GF120918 (Fig. 2A). Furthermore, the brain-to-plasma concentration ratio ($K_{p,brain}$) of oseltamivir was 4.8-fold increased in the GF120918-treated group compared with the control group (Fig. 2B). The $K_{p,brain}$ of Ro 64-0802 was slightly increased by GF120918 (0.007 ± 0.001 versus 0.011 ± 0.002 ml/g brain) (Fig. 2B) without any statistical significance. The $K_{p,brain}$ of Ro 64-0802 after dosing with Ro 64-0802 was also found to be unchanged between GF120918-treated and control groups (data not shown).

Effect of P-gp and Bcrp on the Brain Distribution of Oseltamivir and Ro 64-0802. The plasma concentrations and $K_{p,brain}$ of oseltamivir and Ro 64-0802 were determined after dosing with oseltamivir in Mdr1a/1b P-gp knockout mice and Bcrp knockout mice. The plasma concentrations of oseltamivir were unchanged between wild-type and Mdr1a/1b P-gp knockout mice, whereas the $K_{p,brain}$ of oseltamivir was 5.5-fold greater in Mdr1a/1b P-gp knockout mice than that in wild-type mice (Fig. 3). The $K_{p,brain}$ of oseltamivir was unchanged in Bcrp knockout mice (Fig. 3B). The $K_{p,brain}$ of Ro 64-0802 following oseltamivir administration in Mdr1a/1b P-gp knockout mice and Bcrp knockout mice was not significantly different from that in wild-type mice (Fig. 3B).

Brain Distribution of Oseltamivir in Newborn Rats and Adult Rats. The plasma concentrations, brain concentrations, and $K_{p,brain}$ of oseltamivir were determined after dosing with oseltamivir in newborn and adult rats on postnatal day (P) 3, 6, 11, 21, and 42, respectively. The plasma and brain concentrations of oseltamivir in newborn rats were significantly higher than those in adult rats (Fig. 4). Ro 64-0802 was found to be below the limit of quantification in the brain of the newborn rats.

mRNA and Protein Expression of Mdr1a in the Cerebral Cortex from Newborn Rats and Adult Rats. The mRNA expression levels of Mdr1a in the cerebral cortex from P3 through P42 rats were determined using real-time quantitative PCR. The mRNA levels in the cerebral cortex from newborn rats (P3–11) were significantly lower as compared with those from adult rats (P42) (Fig. 5). The protein expression of P-gp in the crude membrane fraction of rat cerebral cortex from P3 through P42 was also examined by Western blot analysis. Two bands were observed around 175 kDa by anti-P-gp monoclonal antibody (Fig. 6). Because the lower signal is likely (but not shown) to be nonglycosylated P-gp (Maines et al., 2005), the densitometric analysis was performed for the upper signals as specific signals of matured P-gp. It was shown that the expression levels of P-gp protein in the cerebral cortex form newborn rats were significantly lower than those from adult rats (Fig. 6).

Formation Rate of Ro 64-0802 from the Oseltamivir in the Plasma and Liver S9 from Newborn Rats and Adult Rats. The enzymatic activities of hydrolytic reaction of oseltamivir to Ro 64-0802 were compared in newborn and adult rats using plasma and liver

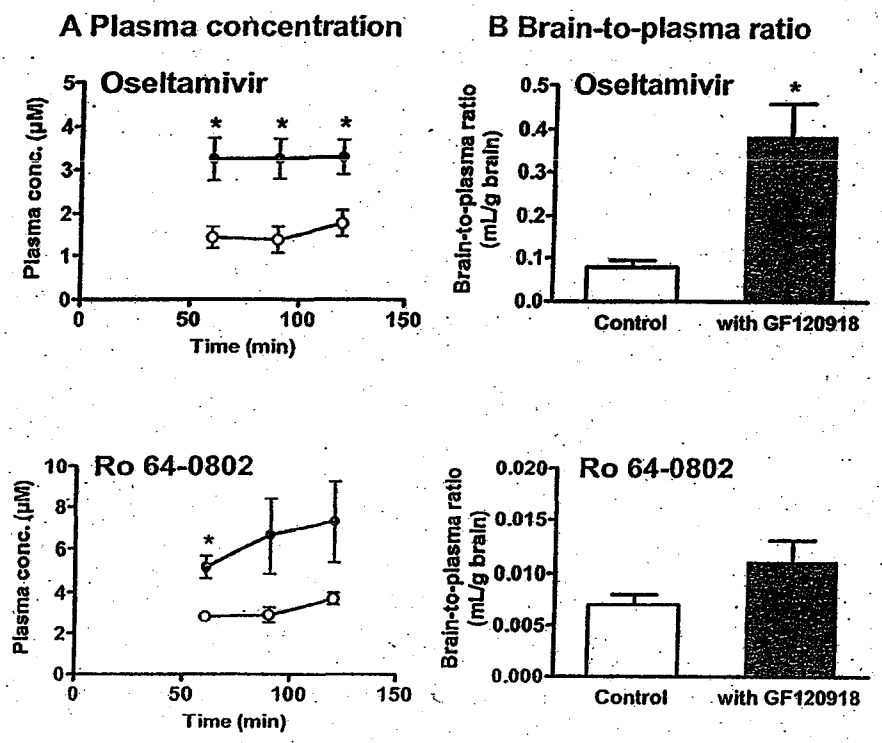

FIG. 2. Plasma concentration time profile (A) and brain-to-plasma concentration ratio ($K_{p,\ brain}$) (B) of oseltamivir and Ro 64-0802 following constant i.v. infusion of oseltamivir with and without GF120918 in FVB mice. Mice received a constant i.v. infusion of oseltamivir at a dose of 8 μmol/h/kg. GF120918 (10 mg/kg) was injected i.v. to mice 15 min before the i.v. infusion of oseltamivir. The plasma concentrations of oseltamivir and Ro 64-0802 were determined at designated times in control and GF120918-treated group (open and closed circles, respectively). The brain concentrations were determined at 120 min. Each point represents the mean ± S.E. (n = 3). Asterisks represent statistically significant differences between control and GF120918-pretreated mice; *, $P < 0.05$.

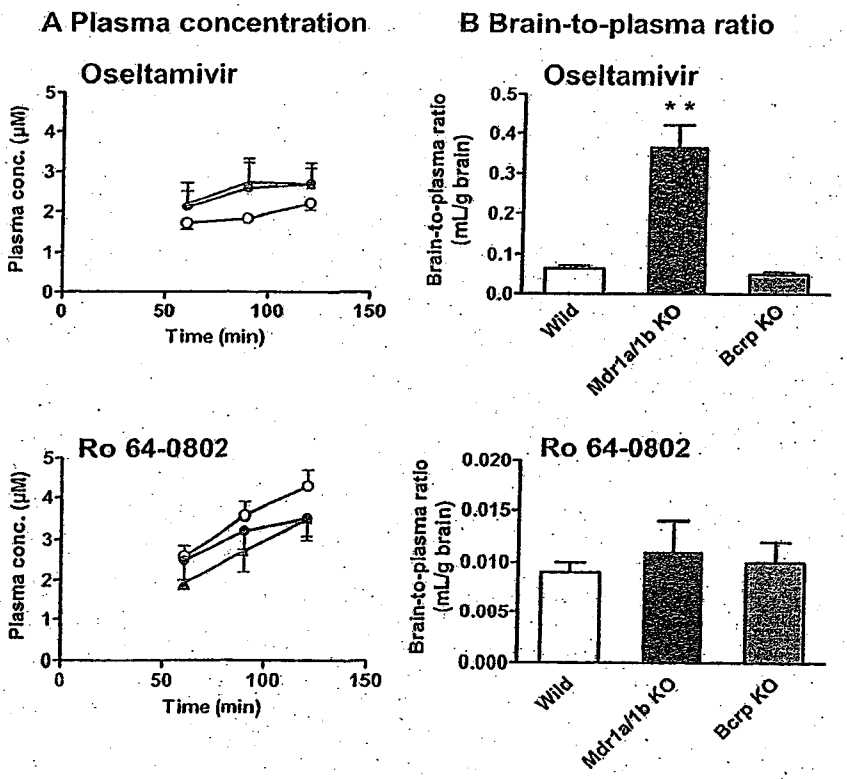

FIG. 3. Plasma concentration time profile (A) and brain-to-plasma concentration ratio ($K_{p,\ brain}$) (B) of oseltamivir and Ro 64-0802 following constant i.v. infusion of oseltamivir in Mdr1a/1b P-gp knockout, Bcrp knockout, and wild-type mice. Mice received a constant i.v. infusion of oseltamivir at a rate of 8 μmol/h/kg. The plasma concentrations of oseltamivir and Ro 64-0802 were determined at designated times in wild-type, Mdr1a/1b P-gp, and Bcrp knockout mice. The data for wild-type mice are shown by open circles, those for Mdr1a/1b P-gp knockout mice by closed squares, and those for Bcrp knockout mice by closed triangles. The brain concentrations were determined at 120 min. Each point represents the mean ± S.E. (n = 4–9). Asterisks represent statistically significant differences between wild-type and knockout mice; **, $P < 0.01$.

S9 specimens. Oseltamivir was more stable in both plasma and liver S9 from newborn rats than in those from adult rats (Fig. 7). The formation rates of Ro 64-0802 from oseltamivir in the plasma and liver S9 specimens are shown in Table 1. The formation rates of Ro 64-0802 in the plasma and liver S9 specimens of newborn rats were 16 and 35% of the adult rats, respectively (Table 1). Taking the scaling factors into consideration, the formation rate of Ro 64-0802 in plasma expressed per kilogram body weight was approximately 10- and 20-fold higher than that in liver S9 in both newborn and adult rats (Table 1).

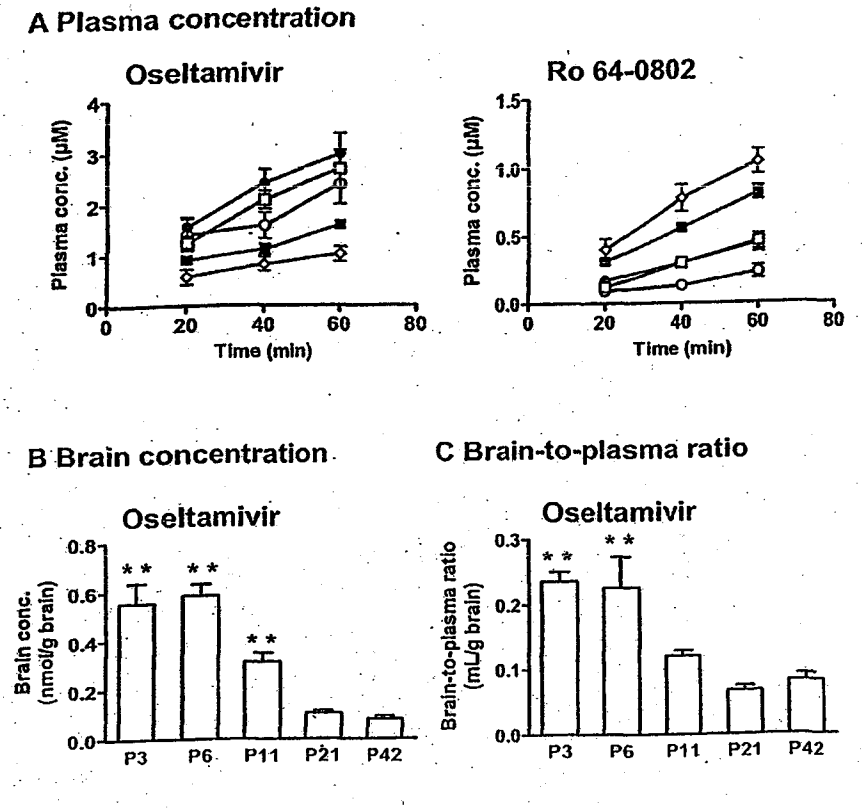

FIG. 4. Plasma concentration time profile (A), brain concentration (B), and brain-to-plasma concentration ratio ($K_{p,brain}$) (C) of oseltamivir and Ro 64-0802 following constant i.v. infusion of oseltamivir in P3 through P42 rats. Rats received a constant i.v. infusion of oseltamivir at a rate of 8 μmol/h/kg. The plasma concentrations of oseltamivir and Ro 64-0802 were determined at designated time in P3 (○), P6 (●), P11 (□), P21 (▨), and P42 (◇) rats. The brain concentrations were determined at 60 min. Each point represents the mean ± S.E. (n = 4–6). Asterisks represent statistically significant differences toward P42 rats; **, $P < 0.01$.

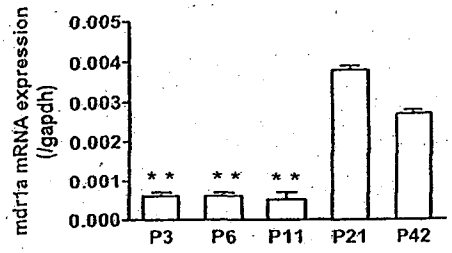

FIG. 5. The mRNA expression of Mdr1a in the cerebral cortex from P3 to P42 rats. Total RNA was isolated from the cerebral cortex pooled from one to four rats and then subjected to reverse transcription. The expression of mdr1a and gapdh mRNA in the cerebral cortex of P3 through P42 rats was determined using real-time quantitative PCR. Each bar represents the mean ± S.E. of the ratio of the mRNA expression of mdr1a and gapdh. The quantification was repeated three times using three cDNAs independently prepared from one to four rats. Asterisks represent statistically significant differences toward P42 rats; **, $P < 0.01$.

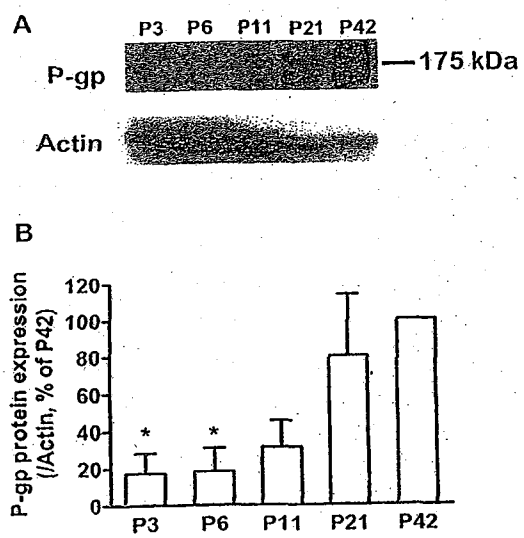

FIG. 6. Ontogenetic expression of P-gp protein in the crude membrane fractions of cerebral cortex from P3 through 42 rats. A, crude membrane fractions were prepared from the cerebral cortex from P3 to 42 rats. Each sample (50 μg protein/lane) was subjected to SDS-polyacrylamide gel electrophoresis (8.5% separating gel). P-gp and actin proteins were detected by monoclonal anti-P-gp C219 antibody and monoclonal antiactin antibody, respectively. A typical immunoblot is shown in A. B, the intensities of the bands of P-gp and actin were quantified by densitometric analysis. For P-gp, the intensity of the upper band was used for the calculation. The bar represents the ratio of the band densities of P-gp and actin relative to that in P42 rats. Each bar represents the mean ± S.E. of three determinations using three crude membrane fractions of the cerebral cortex prepared independently from one to four rats. Asterisks represent statistically significant differences toward P42 rats; *, $P < 0.05$.

Cellular Accumulation of Oseltamivir in mMdr1a-LLC-PK1 Cells and hMDR1-MDCKII Cells. To determine whether oseltamivir is a possible substrate for human and mouse P-gp, cellular accumulation studies were conducted using mMdr1a-LLC-PK1 and hMDR1-MDCKII cells. Oseltamivir exhibited less accumulation in mMdr1a-LLC-PK1 and hMDR1-MDCKII cells than in each parent cell, and PSC833 increased oseltamivir accumulation in both mMdr1a-LLC-PK1 and hMDR1-MDCKII cells (Fig. 8).

Discussion

In the present study, we investigated the transport of oseltamivir and Ro 64-0802 across the BBB using Mdr1a/1b and Bcrp knockout mice and showed that P-gp extrudes oseltamivir into the circulating blood. The plasma and brain concentrations of oseltamivir were determined in wild-type mice following i.v. infusion of oseltamivir. The

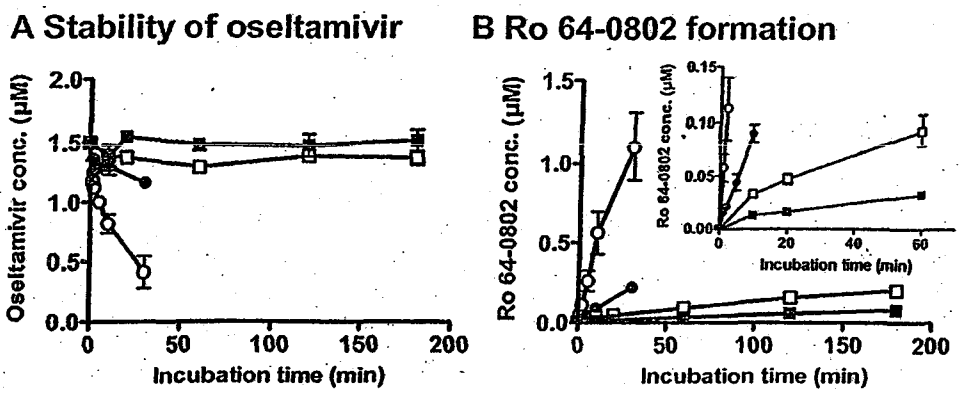

FIG. 7. The stability of oseltamivir (A) and the formation of Ro 64-0802 (B) in plasma and liver S9 from newborn and adult rats. Oseltamivir (1.5 μM) was incubated with rat plasma (circles) and liver S9 (squares) specimens (5 mg of protein/ml) for various time periods. The data for adult (P42) rats are shown by open symbols and for newborn (P11) rats by closed symbols. Data represent mean ± S.E. of three determinations using three plasma and liver S9 specimens prepared independently from three rats.

TABLE 1

Ro 64-0802 formation rate from oseltamivir in plasma and liver S9 from newborn and adult rats

Oseltamivir (1.5 μM) was incubated with rat plasma for 5 min and rat liver S9 fraction for 60 min at 37°C.

Source		Ro 64-0802 Formation Rate[a]		
		pmol/min/mg protein	*pmol/min/ml or g liver*[b]	*nmol/min/kg b.wt.*[c]
Plasma	P11	1.75 ± 0.32	87.7 ± 15.9	3.38 ± 0.61
	P42	10.6 ± 2.6	529 ± 129	20.4 ± 5.0*
Liver S9	P11	0.11 ± 0.00	10.6 ± 0.3	0.42 ± 0.01
	P42	0.31 ± 0.05	29.7 ± 4.5	1.19 ± 0.18#

* $P < 0.05$ statistical differences in Ro 64-0802 formation rate (nmol/min/kg) in plasma between newborn and adult rats.

# $P < 0.05$ statistical differences in Ro 64-0802 formation rate (nmol/min/kg) in liver S9 between newborn and adult rats.

[a] Data represent means ± S.E. of three determinations using three plasma and liver S9 prepared independently from three rats.

[b] Obtained by multiplying the value (pmol/min/mg protein) by 50.0 and 96.1 for plasma and liver S9, respectively.

[c] Obtained by multiplying the value (pmol/min/ml plasma or g liver) by 38.5 and 40.0 for plasma and liver S9, respectively.

distribution volume of oseltamivir in the brain was greater than the capillary volume (Takasato et al., 1984; Rousselle et al., 1998), indicating that oseltamivir crosses the BBB. Pretreatment with GF120918, a dual inhibitor for P-gp and Bcrp (Allen et al., 1999), caused a significant increase in the brain concentration of oseltamivir. This is partly a result of greater plasma concentrations of oseltamivir in GF120918-treated group, presumably because of an inhibition of esterase activity by GF120918 as oseltamivir is predominantly converted to Ro 64-0802 in mice, and the biliary and urinary excretion account for a limited part of the systemic elimination, at most 0.3 and 19%, respectively (data not shown). However, a significant increase in the $K_{p,brain}$ of oseltamivir by GF120918 indicates that inhibition of active efflux mediated by P-gp and/or Bcrp is another underlying mechanism (Fig. 2B). Unlike oseltamivir, the distribution volume of Ro 64-0802 was close to the capillary volume, and $K_{p,brain}$ of Ro 64-0802 following oseltamivir or Ro 64-0802 administration was slightly increased by the administration of GF120918, but the difference was not statistically significant. This would be reasonable considering the low lipophilicity of Ro 64-0802 that will exhibit low BBB permeability without the aid of uptake transporters.

To support the effect of GF120918, in vivo studies using Mdr1a/1b and Bcrp knockout mice were performed. The $K_{p,brain}$ of oseltamivir was significantly increased in Mdr1a/1b P-gp knockout mice but not in Bcrp knockout mice (Fig. 3B). The increase in the $K_{p,brain}$ of Mdr1a/1b P-gp knockout mice was comparable with that obtained by GF120918 (Figs. 2B and 3B). Therefore, P-gp, but not Bcrp, limits the brain penetration of oseltamivir across the BBB. In accordance with the in vivo results, cellular accumulation study elucidated that both mouse Mdr1a P-gp and human P-gp accept oseltamivir as substrate because the cellular accumulation of oseltamivir was lower in a cell line expressing mouse P-gp and human P-gp, which was increased by PSC833 treatment (Fig. 8).

The present study elucidated that the activity of P-gp is an important factor for the brain concentration of oseltamivir in mice. Because abnormal behavior following oseltamivir medication is more frequently observed in younger generations than in adults, postnatal ontogeny of P-gp is an important issue. Mdr1a mRNA and P-gp protein levels were significantly lower in newborn rats than adult rats (Figs. 5 and 6). This result is in good agreement with previous reports, in which it has been shown that adults had higher brain expression of Mdr1a mRNA (3-fold) and a corresponding 5-fold increase in immunodetectable P-gp (Matsuoka et al., 1999; Goralski et al., 2006). Consistent with this ontogenic profile, the brain accumulation of cyclosporin A was 80% lower in adult mice than in 1-day-old mice (Goralski et al., 2006). NDA documents reported that the $K_{p,brain}$ of oseltamivir, obtained by comparison of the area under the curve of the plasma and brain concentration time profiles, was dramatically greater in newborn rats than that in adult rats at very high doses of oseltamivir (1000 mg/kg, p.o.). The brain concentrations of oseltamivir in newborn rats were significantly higher than those in adult rats (Fig. 4B). This is partly because of greater plasma concentrations of oseltamivir in newborn rats than in adult rats (Fig. 4A); however, a significant increase in the $K_{p,brain}$ of oseltamivir in newborn rats suggests that the smaller efflux clearance across the BBB is part of the underlying mechanism. This is in good agreement with the postnatal ontogenic profile of P-gp (Matsuoka et al., 1999; Goralski et al., 2006).

Newborn rats exhibited greater plasma concentrations of oseltamivir, suggesting a smaller systemic elimination rate in newborn rats. This was confirmed by comparing the conversion activities [carboxylesterase (CES) activity] in the plasma and liver S9 specimens between newborn (P11) and adult (P42) rats. Compared with adult rats, the conversion activities (CES activity) were lower in both the plasma and the liver S9 specimens from newborn rats (Fig. 7; Table 1). Lower conversion activity of oseltamivir to Ro 64-0802, particularly in the plasma, will account for the delay in the systemic elimination of oseltamivir in newborn rats.

Recent clinical studies support that P-gp acts as a gatekeeper protein in human BBB (Sadeque et al., 2000; Sasongko et al., 2005). P-gp will also be one of the determinant factors for the brain concentrations of oseltamivir. Single nucleotide polymorphisms (SNPs) are the genetic factor for interindividual differences in drug response. A number of SNPs have been described in the human MDR1 gene (Fromm, 2002; Kim, 2002). Of these, linkage disequilibrium has been shown between SNPs in exons 26 (C3435T), 21 (G2677T), and 12 (C1236T), and the TTT haplotype correlates with low P-gp activity in

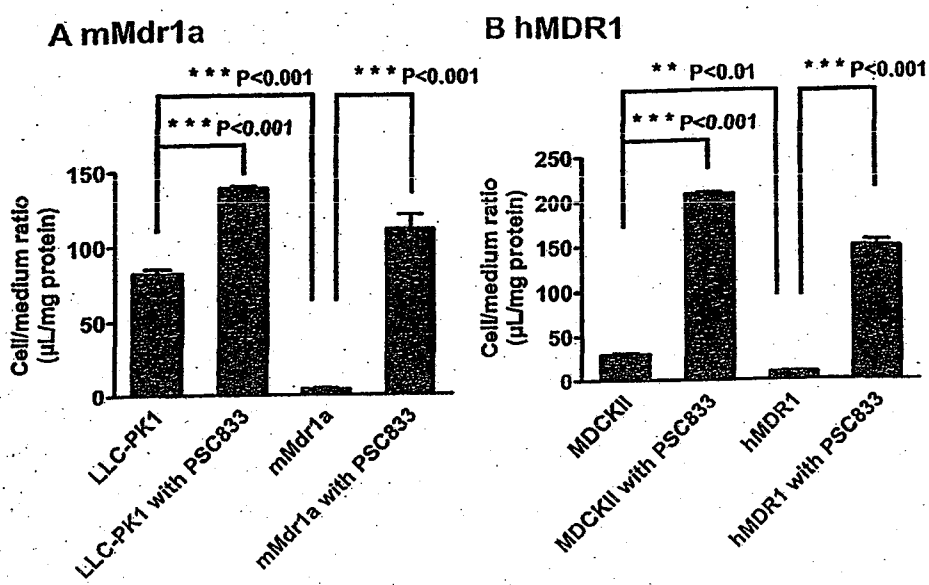

FIG. 8. Cellular accumulation of oseltamivir in; mMdr1a-LLC-PK1 cells (A) and hMDR1-MDCKII cells (B). The uptake of oseltamivir (2.5 μM) by mMdr1a-LLC-PK1 (A) and hMDR1-MDCKII (B) cells was examined in the presence or absence of PSC833 (5 μM) at 37°C. Each point represents the mean ± S.E. (n = 4). Statistical significance was calculated by one-way analysis of variance followed by Tukey's multiple comparison test.

the small intestine (Chowbay et al., 2003). As far as the BBB is concerned, there was no significant relationship between the haplotype and brain concentrations of [^{11}C]verapamil (Brunner et al., 2005; Takano et al., 2006). However, Kimchi-Sarfaty et al. (2007) recently reported that the effect of double or triple haplotypes containing C3435T on P-gp activity is "substrate dependent." The possibility that SNPs of P-gp are associated with an interindividual difference in the BBB permeability of oseltamivir cannot be excluded. In addition to P-gp, as observed in newborn rats, the activity of hCES1 is the determinant factor for the systemic elimination. C70F and R128H of hCES1 were reported to be associated with reduced hydrolysis of oseltamivir (Shi et al., 2006). Subjects with these SNPs of hCES1 will result in a greater exposure of oseltamivir to the brain.

Ro 64-0802 is a potent and selective inhibitor of influenza virus neuraminidase (sialidase). Several sialidases are expressed in the human brain and are suggested to be involved in the mitochondrial apoptotic pathway in neuronal cell death (Yamaguchi et al., 2005; Hasegawa et al., 2007). Inhibition of sialidases in the brain may be associated with the abnormal behavior following oseltamivir medication. Based on this speculation, production of Ro 64-0802 in the human brain will be the key event that triggers the central nervous system side effects. Unlike the ester-type prodrug, Ro 64-0802 barely penetrates into the brain from the circulating blood because of its hydrophilic property. As hCES1 is also expressed in the brain (Satoh et al., 2002), it is possible that Ro 64-0802 is formed in the brain from the oseltamivir. Because of low membrane permeability, Ro 64-0802, once produced in the brain from oseltamivir, may accumulate in the brain. It is also possible that Ro 64-0802 undergoes active efflux from the brain at the BBB because Ro 64-0802 is a substrate of renal OAT1 (*SLC22A6*) (Hill et al., 2002), and OAT3, the homolog of OAT1, is expressed at the BBB and actively eliminates organic anions from the brain (Kikuchi et al., 2003, 2004). This should be examined in the future.

In conclusion, the present study showed that oseltamivir crosses the BBB, but the active form Ro 64-0802 barely crosses the BBB. P-gp limits the brain penetration of oseltamivir at the BBB of adult mice. Ontogenetic profile of P-gp and CES activities accounts for the greater accumulation of oseltamivir in the brain of neonates at least in rats.

Acknowledgments. We thank Dr. Glynis Nicholls (GlaxoSmithKline Research and Development) for the gift of GF120918 and Novartis Pharma AG for the gift of PSC833. We also thank Dr. Piet Borst (The Netherlands Cancer Institute) for providing the human MDR1-expressed MDCKII cells, Dr. Alfred H. Schinkel for providing the mouse Mdr1a-expressed LLC-PK1 cells, and Dr. Junko Iida and Futoshi Kurotobi (Shimadzu Corporation, Kyoto, Japan) for the technical support of LC/MS system.

References

Allen JD, Brinkhuis RF, Wijnholds J, and Schinkel AH (1999) The mouse Bcrp1/Mxr/Abcp gene: amplification and overexpression in cell lines selected for resistance to topotecan, mitoxantrone, or doxorubicin. *Cancer Res* 59:4237–4241.

Bardsley-Elliot A and Noble S (1999) Oseltamivir. *Drugs* 58:851–860; discussion 861–852.

Breedveld P, Pluim D, Cipriani G, Wielinga P, van Tellingen O, Schinkel AH, and Schellens JH (2005) The effect of Bcrp1 (Abcg2) on the in vivo pharmacokinetics and brain penetration of imatinib mesylate (Gleevec): implications for the use of breast cancer resistance protein and P-glycoprotein inhibitors to enable the brain penetration of imatinib in patients. *Cancer Res* 65:2577–2582.

Brunner M, Langer O, Sunder-Plassmann R, Dobrozemsky G, Muller U, Wadsak W, Krcal A, Kurch R, Mannhalter C, Dudczak R, et al. (2005) Influence of functional haplotypes in the drug transporter gene ABCB1 on central nervous system drug distribution in humans. *Clin Pharmacol Ther* 78:182–190.

Chowbay B, Cumaraswamy S, Cheung YB, Zhou Q, and Lee EJ (2003) Genetic polymorphisms in MDR1 and CYP3A4 genes in Asians and the influence of MDR1 haplotypes on cyclosporin disposition in heart transplant recipients. *Pharmacogenetics* 13:89–95.

Enokizono J, Kusuhara H, and Sugiyama Y (2007) Role of breast cancer resistance protein (Bcrp/Abcg2) in the disposition of phytoestrogens: the importance of Bcrp in the efflux transport in the blood-brain and -testis barriers. *Mol Pharmacol* 72:967–975.

Evers R, Kool M, Smith AJ, van Deemter L, de Haas M, and Borst P (2000) Inhibitory effect of the reversal agents V-104, GF120918 and Pluronic L61 on MDR1 Pgp-, MRP1- and MRP2-mediated transport. *Br J Cancer* 83:366–374.

Fromm MF (2002) The influence of MDR1 polymorphisms on P-glycoprotein expression and function in humans. *Adv Drug Deliv Rev* 54:1295–1310.

Fuyuno I (2007) Tamiflu side effects come under scrutiny. *Nature* 446:358–359.

Goralski KB, Acott PD, Fraser AD, Worth D, and Sinal CJ (2006) Brain cyclosporin A levels are determined by ontogenic regulation of mdr1a expression. *Drug Metab Dispos* 34:288–295.

Hasegawa T, Sugeno N, Takeda A, Matsuzaki-Kobayashi M, Kikuchi A, Furukawa K, Miyagi T, and Itoyama Y (2007) Role of Neu4L sialidase and its substrate ganglioside GD3 in neuronal apoptosis induced by catechol metabolites. *FEBS Lett* 581:406–412.

He G, Massarella J, and Ward P (1999) Clinical pharmacokinetics of the prodrug oseltamivir and its active metabolite Ro 64-0802. *Clin Pharmacokinet* 37:471–484.

Hill G, Cihlar T, Oo C, Ho ES, Prior K, Wiltshire H, Barrett J, Liu B, and Ward P (2002) The anti-influenza drug oseltamivir exhibits low potential to induce pharmacokinetic drug interactions via renal secretion-correlation of in vivo and in vitro studies. *Drug Metab Dispos* 30:13–19.

Izumi T, Hosiyama K, Enomoto S, Sasahara K, and Sugiyama Y (1997) Pharmacokinetics of troglitazone, an antidiabetic agent: prediction of in vivo stereoselective sulfation and glucuronidation from in vitro data. *J Pharmacol Exp Ther* 280:1392–1400.

Izumi Y, Tokuda K, O'Dell KA, Zorumski CF, and Narahashi T (2007) Neuroexcitatory actions of Tamiflu and its carboxylate metabolite. *Neurosci Lett* 426:54–58.

Kikuchi R, Kusuhara H, Abe T, Endou H, and Sugiyama Y (2004) Involvement of multiple

transporters in the efflux of 3-hydroxy-3-methylglutaryl-CoA reductase inhibitors across the blood-brain barrier. *J Pharmacol Exp Ther* 311:1147–1153.
Kikuchi R, Kusuhara H, Sugiyama D, and Sugiyama Y (2003) Contribution of organic anion transporter 3 (Slc22a8) to the elimination of p-aminohippuric acid and benzylpenicillin across the blood-brain barrier. *J Pharmacol Exp Ther* 306:51–58.
Kim CU, Lew W, Williams MA, Liu H, Zhang L, Swaminathan S, Bischofberger N, Chen MS, Mendel DB, Tai CY, et al. (1997) Influenza neuraminidase inhibitors possessing a novel hydrophobic interaction in the enzyme active site: design, synthesis, and structural analysis of carbocyclic sialic acid analogues with potent anti-influenza activity. *J Am Chem Soc* 119: 681–690.
Kim RB (2002) MDR1 single nucleotide polymorphisms: multiplicity of haplotypes and functional consequences. *Pharmacogenetics* 12:425–427.
Kimchi-Sarfaty C, Oh JM, Kim IW, Sauna ZE, Calcagno AM, Ambudkar SV, and Gottesman MM (2007) A "silent" polymorphism in the MDR1 gene changes substrate specificity. *Science* 315:525–528.
Kusuhara H and Sugiyama Y (2001) Efflux transport systems for drugs at the blood-brain barrier and blood-cerebrospinal fluid barrier (part 1). *Drug Discov Today* 6:150–156.
Lindegardh N, Davies GR, Tran TH, Farrar J, Singhasivanon P, Day NP, and White NJ (2006) Rapid degradation of oseltamivir phosphate in clinical samples by plasma esterases. *Antimicrob Agents Chemother* 50:3197–3199.
Maines LW, Antonetti DA, Wolpert EB, and Smith CD (2005) Evaluation of the role of P-glycoprotein in the uptake of paroxetine, clozapine, phenytoin and carbamazapine by bovine retinal endothelial cells. *Neuropharmacology* 49:610–617.
Matsuoka Y, Okazaki M, Kitamura Y, and Taniguchi T (1999) Developmental expression of P-glycoprotein (multidrug resistance gene product) in the rat brain. *J Neurobiol* 39:383–392.
Rousselle CH, Lefauconnier JM, and Allen DD (1998) Evaluation of anesthetic effects on parameters for the in situ rat brain perfusion technique. *Neurosci Lett* 257:139–142.
Sadeque AJ, Wandel C, He H, Shah S, and Wood AJ (2000) Increased drug delivery to the brain by P-glycoprotein inhibition. *Clin Pharmacol Ther* 68:231–237.
Sasongko L, Link JM, Muzi M, Mankoff DA, Yang X, Collier AC, Shoner SC, and Unadkat JD (2005) Imaging P-glycoprotein transport activity at the human blood-brain barrier with positron emission tomography. *Clin Pharmacol Ther* 77:503–514.
Satoh T, Taylor P, Bosron WF, Sanghani SP, Hosokawa M, and La Du BN (2002) Current progress on esterases: from molecular structure to function. *Drug Metab Dispos* 30:488–493.
Schinkel AH, Smit JJ, van Tellingen O, Beijnen JH, Wagenaar E, van Deemter L, Mol CA, van der Valk MA, Robanus-Maandag EC, te Riele HP, et al. (1994) Disruption of the mouse mdr1a P-glycoprotein gene leads to a deficiency in the blood-brain barrier and to increased sensitivity to drugs. *Cell* 77:491–502.
Schinkel AH, Wagenaar E, van Deemter L, Mol CA, and Borst P (1995) Absence of the mdr1a P-glycoprotein in mice affects tissue distribution and pharmacokinetics of dexamethasone, digoxin, and cyclosporin A. *J Clin Invest* 96:1698–1705.
Shi D, Yang J, Yang D, LeCluyse EL, Black C, You L, Akhlaghi F, and Yan B (2006) Anti-influenza prodrug oseltamivir is activated by carboxylesterase human carboxylesterase 1, and the activation is inhibited by antiplatelet agent clopidogrel. *J Pharmacol Exp Ther* 319:1477–1484.
Takano A, Kusuhara H, Suhara T, Ieiri I, Morimoto T, Lee YJ, Maeda J, Ikoma Y, Ito H, Suzuki K, et al. (2006) Evaluation of in vivo P-glycoprotein function at the blood-brain barrier among MDR1 gene polymorphisms by using 11C-verapamil. *J Nucl Med* 47:1427–1433.
Takasuto Y, Rapoport SI, and Smith QR (1984) An in situ brain perfusion technique to study cerebrovascular transport in the rat. *Am J Physiol* 247:H484–H493.
Tamai I and Tsuji A (2000) Transporter-mediated permeation of drugs across the blood-brain barrier. *J Pharm Sci* 89:1371–1388.
Wiltshire H, Wiltshire B, Citron A, Clarke T, Serpe C, Gray D, and Herron W (2000) Development of a high-performance liquid chromatographic-mass spectrometric assay for the specific and sensitive quantification of Ro 64-0802, an anti-influenza drug, and its pro-drug, oseltamivir, in human and animal plasma and urine. *J Chromatogr B Biomed Sci Appl* 745:373–388.
Yamaguchi K, Hata K, Koseki K, Shiozaki K, Akita H, Wada T, Moriya S, and Miyagi T (2005) Evidence for mitochondrial localization of a novel human sialidase (NEU4). *Biochem J* 390:85–93.
Yamatsugu K, Kamijo S, Suto Y, Kanai M, and Shibasaki M (2007) A concise synthesis of Tamiflu: third generation route via the Diels-Alder reaction and the Curtius rearrangement. *Tetrahedron Lett* 48:1403–1406.

Address correspondence to: Yuichi Sugiyama, Department of Molecular Pharmacokinetics, Graduate School of Pharmaceutical Sciences, The University of Tokyo, 7-3-1 Hongo, Bunkyo-ku, Tokyo 113-0033, Japan. E-mail: sugiyama@mol.f.u-tokyo.ac.jp

FLASH

今月のFLASH

- タミフルが脳へ移行する可能性
- CO_2を吸収する地球の能力が低下
- クリック化学で細胞現象を追う
- ニンニクで高血圧に対抗できる理由
- タンパク質のリン酸化を光制御

タミフルが脳へ移行する可能性

オセルタミビル（商品名タミフル）は，インフルエンザの特効薬として知られているが，実際に体内で働いているのは活性体（Ro 64-0802）である（図1）．生体内でCES1という酵素により，加水分解され，活性体へと変換される．活性体はインフルエンザウイルスが感染細胞表面から遊離することを阻害して，ほかの細胞への感染・増殖を抑制する．タミフルは服用後の異常行動が注目され，社会問題化している．

タミフル服用と異常行動との因果関係については，これまで多くの議論がなされているが，最終的な結論には至っていない（本誌2006年12月号，p.8参照）．もし，異常行動がタミフル服用と関連があるとすると，タミフル（およびその活性体）が脳内へ入り，神経細胞に作用することを確認する必要がある．最近，血液から脳内へのタミフルの移行に関して，実験動物（マウス・ラット）を用いた解析結果が，高崎健康福祉大学の荻原琢男らのグループと，東京大学の杉山雄一らのグループからそれぞれ発表された（K. Morimotoほか，*Drug. Metab. Dispos.*, 36, 6(2008)；A. Oseほか，*Drug. Metab. Dispos.*, in press）．これらの内容を紹介したい．

タミフルの話に入る前に，血液と神経細胞の間にある“関門”のことを説明しよう（図2）．脳には，神経細胞に酸素や糖を供給するため，網目のように毛細血管が張り巡らされている．この毛細血管は血液脳関門ともよばれ，栄養素の供給だけではなく，神経細胞へ作用する医薬品を含めた多様な化学物質の脳への進入を制限するための関門としても働いている．

この関門は図2に示したように，単層の内皮細胞で構成されており，細胞間は発達した密着結合で塞がれている．必然的に，血液中から神経細胞側へと到達するためには，内皮細胞の細胞膜を通り抜ける必要がある．

神経細胞の機能維持に必要なアミノ酸や糖など，極性の高い栄養素に対しては，細胞膜透過を促進するような輸送メカニズム（トランスポーター）が備わっている（図2の①）．そうしたものを除けば，極性の高い分子は，血液脳関門を通り抜けることができない．脂溶性の高い化合物は内皮細胞を十分通り抜けることができる（図2の②）．

こうした化合物の透過を制限するために，P糖タンパク質が細胞膜上（血液側の細胞膜）で医薬品を内皮細胞内から血液側方向へと積極的に汲み出すことで，医薬品が脳に入ることを制限している（図2の③）．つまり，血液脳関門の関門機構は，密着結合に代表される静的な障

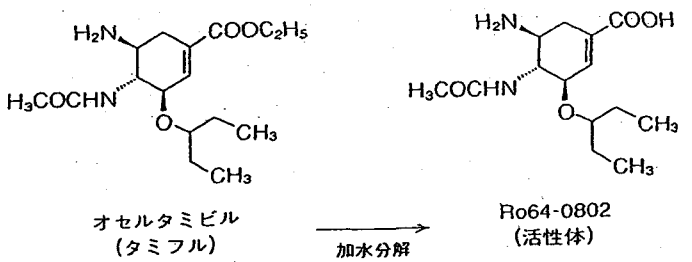

図1　タミフルの構造

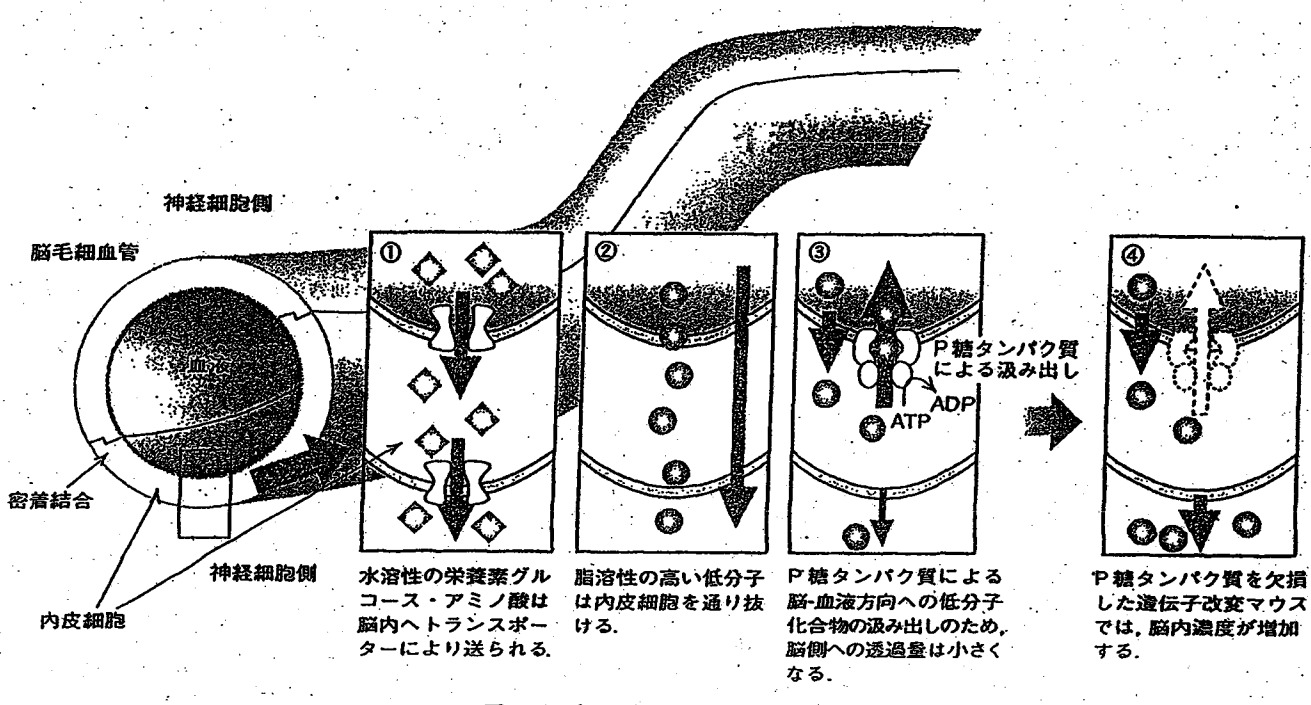

図2　脳毛細血管における物質透過

壁と，P糖タンパク質に代表される異物排除システムによる動的な障壁により構成されている．

タミフルに話を戻そう．上述の血液脳関門のメカニズムを考えると，水溶性の高い化合物を除いて，まったく脳内に入らないということはありえない．実際，マウスにタミフルを投与すると，脳内のタミフル量は毛細血管に残存している量をはるかに超えており，神経細胞周辺に移行していることがわかる．一方で，活性体自体の薬物量は毛細血管に残存している量と同程度であり，ほとんど血液脳関門を透過していないといえる．活性体はタミフルよりも極性が高いことから，合理的な結果といえる．

P糖タンパク質を過剰発現した細胞を用いた*in vitro*（生体外の）輸送試験の結果からは，タミフルがP糖タンパク質の基質となることが明らかにされた．P糖タンパク質が発現しないように遺伝子を改変したマウスにタミフルを投与すると，非改変マウス（野生型マウス）に比べて脳内のタミフル濃度が7倍近く高くなった．一方で，遺伝子改変マウスと非改変マウスとでは，活性体の脳内濃度は変わらなかった．つまり，タミフルは脳毛細血管でP糖タンパク質により汲み出され，脳内への移行は，ある程度制限されているといえる．さらに，生後2週間までの新生児ラットでは，脳毛細血管内皮細胞でのP糖タンパク質の発現量が低い上に，血液中からの消失が遅いこともあり，脳内のタミフル濃度は成熟ラットの6倍にもなる．

ヒト脳毛細血管も実験動物同様に関門として機能しており，P糖タンパク質が医薬品を血液中へと汲み出しに働いていることも報告されている（L. Sasongkoほか，*Clin. Pharmacol. Ther.*, 77, 503 (2005)）．タミフル服用後の血液中には，活性体に加えてタミフルも検出されていることから，タミフルはP糖タンパク質での汲み出しを受けるものの，少なくとも投与されたタミフルの一部は脳に移行していると考えられる．活性体については，血液脳関門透過性が低いことから，脳内でタミフルから生成されないかぎり，脳内濃度はかなり低いことが予想される．

タミフルの全合成を開発した東京大学の柴崎正勝教授が，タミフルのPET（陽電子放射断層撮影法）プローブ化を報告している（M. Moritaほか，*Bioorg. Med. Chem. Lett.*, in press）．放射線医学総合研究所でも，タミフルのPETプローブ化に成功しており，PETによりラット脳内におけるタミフルおよびその活性体の時間変化を測定することに成功している（平成19年12月11日のプレス発表）．可視化技術を用いてタミフルおよびその活性体が脳内にどの程度入るのか，ヒトで実証研究を行うことが可能になった．今後の臨床試験が期待される．

タミフルが脳内に入るという事実は，必ずしも異常行動とタミフル服用の因果関係を説明するものではない．有害作用も含めて，医薬品の効果は濃度に依存しており，仮に脳内に医薬品が入ったとしても，その濃度が十分に小さければ，作用の発現には至らない．タミフル（あるいはその活性体）が脳内で作用するタンパク質を解明し，臨床投与量で脳内に到達するタミフル濃度が，そうしたタンパク質に十分作用する濃度であるのか，あるいは異常行動がみられた患者では，脳内のタミフル濃度を増加させる（神経細胞への曝露を増やす）要因となる血液脳関門の機能破綻や，関連酵素（CES1）の活性低下などが見られるのかなど，まだまだ多くの裏づけ試験が必要である．

ANTIMICROBIAL AGENTS AND CHEMOTHERAPY, Oct. 2008, p. 3687–3693
0066-4804/08/$08.00+0 doi:10.1128/AAC.00327-08

Vol. 52, No. 10

D22279

Low Penetration of Oseltamivir and Its Carboxylate into Cerebrospinal Fluid in Healthy Japanese and Caucasian Volunteers▽†

S. S. Jhee,[1] M. Yen,[1] L. Ereshefsky,[1] M. Leibowitz,[1] M. Schulte,[2] B. Kaeser,[2] L. Boak,[2] A. Patel,[2] G. Hoffmann,[2] E. P. Prinssen,[2] and C. R. Rayner[2]*

California Clinical Trials, Glendale, California,[1] and F. Hoffmann-La Roche Ltd., Basel, Switzerland[2]

Received 10 March 2008/Returned for modification 26 May 2008/Accepted 18 July 2008

Oseltamivir is a potent, well-tolerated antiviral for the treatment and prophylaxis of influenza. Although no relationship with treatment could be demonstrated, recent reports of abnormal behavior in young individuals with influenza who were receiving oseltamivir have generated renewed interest in the central nervous system (CNS) tolerability of oseltamivir. This single-center, open-label study explored the pharmacokinetics of oseltamivir and oseltamivir carboxylate (OC) in the plasma and cerebrospinal fluid (CSF) of healthy adult volunteers over a 24-hour interval to determine the CNS penetration of both these compounds. Four Japanese and four Caucasian males were enrolled in the study. Oseltamivir and OC concentrations in CSF were low (mean of observed maximum concentrations [C_{max}], 2.4 ng/ml [oseltamivir] and 19.0 ng/ml [OC]) versus those in plasma (mean C_{max}, 115 ng/ml [oseltamivir] and 544 ng/ml [OC]), with corresponding C_{max} CSF/plasma ratios of 2.1% (oseltamivir) and 3.5% (OC). Overall exposure to oseltamivir and OC in CSF was also comparatively low versus that in plasma (mean area under the concentration-time curve CSF/plasma ratio, 2.4% [oseltamivir] and 2.9% [OC]). No gross differences in the pharmacokinetics of oseltamivir or OC were observed between the Japanese and Caucasian subjects. Oseltamivir was well tolerated. This demonstrates that the CNS penetration of oseltamivir and OC is low in Japanese and Caucasian adults. Emerging data support the idea that oseltamivir and OC have limited potential to induce or exacerbate CNS adverse events in individuals with influenza. A disease- rather than drug-related effect appears likely.

Oseltamivir is an orally administered anti-influenza agent of the neuraminidase inhibitor class. The ethyl ester prodrug oseltamivir is delivered orally as a phosphate salt and converted by hepatic esterases to the active metabolite oseltamivir carboxylate (OC) (10). OC specifically binds and inhibits the influenza virus neuraminidase enzyme that is essential for viral replication (21). In this way, oseltamivir limits the spread of influenza virus subtypes A and B within the infected host. When used as treatment, oseltamivir reduces the severity and duration of symptoms (22, 33), while prophylactic administration prevents their onset (9, 26).

In recent years, abnormal or delirious behaviors have been reported with a low incidence in young individuals with influenza who were also receiving oseltamivir (32). Cases arose most commonly in Japan but were also observed in Taiwan, Hong Kong, North America, Europe, and Australia. No causative association could be demonstrated, and similar events were also reported in the absence of oseltamivir (6, 12, 17, 24). Nevertheless, health and regulatory authorities in Japan and elsewhere have amended the product label to include precautions on the use of oseltamivir in young persons. These actions, and the associated media coverage, have fostered renewed interest in the central nervous system (CNS) tolerability of oseltamivir.

The currently available preclinical and clinical evidence suggests a low potential for oseltamivir to adversely affect CNS function, and no plausible mechanism for oseltamivir to cause CNS toxicity has been identified (32). However, only very limited data exist to describe the CNS penetration of oseltamivir and OC in humans. Equally little is known about the impact of ethnicity on the CNS profile of these entities. In this study, we investigated the pharmacokinetics of oseltamivir and OC in plasma and cerebrospinal fluid (CSF)—the latter being a recognized surrogate for CNS penetration (29)—in healthy adult volunteers after a single oral administration of oseltamivir phosphate. Although not powered to formally examine the impact of ethnicity on CNS penetration, we also considered whether any gross differences might exist by including both Caucasian and Japanese subjects in our study.

MATERIALS AND METHODS

Study design and subjects. This exploratory trial was a single-center, open-label, single-dose, pharmacokinetic study that was conducted in the United States between 16 July 2007 and 17 August 2007. The trial complied with the principles of the Declaration of Helsinki (as amended in Tokyo, Venice, Hong Kong, and South Africa). The study protocol and materials were approved by an independent ethics committee, and written informed consent was provided by all participants. The study fully adhered to good clinical practice guidelines (ICH Tripartite Guideline, January 1997).

The study aimed to recruit eight healthy adult male and female volunteers: four of Japanese origin (born in Japan of Japanese parents and grandparents and living for <5 years outside Japan) and four of Caucasian origin (white Hispanic or non-Hispanic). The numbers of males and females were intended to be the same in both ethnic groups. Inclusion criteria were age of 20 to 45 years, body mass index of 18 to 30 kg/m^2, and ability to give written informed consent and comply with the study restrictions. Female subjects were required to be surgically sterile or postmenopausal for ≥1 year or to use two methods of contraception (including one barrier method) from study commencement until 7 days postdosing. Exclusion criteria included clinically significant disease; allergy or immuno-

* Corresponding author. Mailing address: F. Hoffmann-La Roche Ltd., Pharmaceuticals Division, Bldg. 015/1.006, CH-4070 Basel, Switzerland. Phone: 41(0) 61 688 3133. Fax: 41(0) 61 688 6007. E-mail: craig.rayner@roche.com.

† Roche clinical trial number BP21288.

▽ Published ahead of print on 1 August 2008.

deficiency; history of raised intracerebral pressure or clinically significant vertebral joint pathology; major illness in the 30 days before *screening* or febrile illness in the 14 days prior to CSF sampling; pregnancy or lactation; relevant history of, or positive test for, drugs of abuse or alcohol; infection with hepatitis B or C virus or human immunodeficiency virus; or any other condition or disease rendering the subject unsuitable for the study. Prescription medication was not permitted to be taken within 7 days or six times its elimination half-life ($t_{1/2}$) (whichever was longer) before study drug administration (excluding hormone replacement therapy and oral contraception). Occasional use of acetaminophen/paracetamol (up to 3 g/day) was allowed up to 24 h before dosing and as needed for treatment of side effects related to the CSF sampling procedure. Intravenous caffeine was also permitted for headache prophylaxis or treatment of side effects caused by the CSF sampling procedure.

All subjects underwent a screening period from day −28 to day −2, during which eligibility was assessed and written informed consent was provided. Screening involved a full medical history, a physical examination, an electrocardiogram (ECG), and a lumbar spine X-ray (unless the subject had such an X-ray taken within 1 year of screening). Samples for laboratory safety assessments (including serum biochemistry, hematology, urinalysis, and serology) and drug and alcohol abuse tests were taken after a 4-h fasting period. Female subjects were to undertake pregnancy tests.

Following successful screening, volunteers were admitted to the study unit on day −1 for a baseline safety assessment (recording of *vital signs*, ECG and laboratory safety assessments, and drug/alcohol abuse and pregnancy tests). On day 1, following an overnight fast, all subjects were catheterized in the lumbar region (for example, L3 to L4) for CSF sampling. This was performed using the dynabridging technique (California Clinical Trials Inc., California), in which the catheter is connected to a peristaltic pump for automatic timed withdrawal of CSF samples (approximately 6 ml per withdrawal). Subjects then received a single oral dose of 150 mg oseltamivir phosphate (F. Hoffmann-La Roche Ltd.), which corresponds to the recommended daily adult treatment dose of 75 mg twice daily. Venous blood samples (2 ml per withdrawal) were taken at the same time as CSF sampling was performed. Blood and CSF samples were taken immediately before dosing and at 0.5, 1, 2, 3, 4, 5, 6, 7, 8, 9, 12, 20, and 24 h after dosing in the manner described above (14 sampling points in total). Subjects were discharged from the unit on day 4 and returned for a follow-up examination on days 10 to 12. Adverse events were recorded from screening until the end of follow-up.

Oseltamivir and OC assay. Blood samples were drawn into EDTA blood collection tubes, and plasma was separated by centrifugation for 10 min at 1,500 × *g* and 4°C. CSF and plasma samples were stored at −70°C until analysis. Concentrations of oseltamivir and OC in plasma and CSF were measured using a specific and validated high-performance liquid chromatography method coupled with tandem mass spectrometry (Bioanalytical Systems Inc., Kenilworth, United Kingdom; SAP.055) based on a previously published method (35). The CSF samples were analyzed along with human EDTA plasma and human CSF control samples against calibration standards prepared in human EDTA plasma.

Pharmacokinetic analysis. Concentration-versus-time profiles were generated, and the observed maximum concentration (C_{max}) and time to observed maximum concentration (T_{max}) were then determined for oseltamivir and OC in CSF and plasma. Standard noncompartmental methods were employed to characterize pharmacokinetic parameters using WinNonlin software (version 5.2; Pharsight Inc.). The following parameters were calculated where possible: area under the concentration-time curve from time zero to the last measurable concentration (AUC_{0-last}) and infinity ($AUC_{0-\infty}$), apparent $t_{1/2}$, and apparent oral clearance (CL/F). AUC values were computed using the linear-trapezoidal rule. $AUC_{0-\infty}$ was estimated using $AUC_{0-last} + C_{last}/\lambda_z$, where C_{last} is the last measurable concentration and λ_z is the apparent elimination rate constant determined by log-linear regression of the last four terminal concentration data points fitting with an adjusted residual squared value of ≥0.90. The ratios of CSF/plasma exposure for C_{max} and AUC_{0-last} were also determined for each of the two analytes. In addition, oseltamivir/OC ratios (adjusted for the molecular weight differences) were calculated for C_{max} and AUC_{0-last}, once for the matrix plasma and separately for the matrix CSF.

RESULTS

A total of eight healthy male volunteers (four Caucasian and four Japanese) entered the study. No females were available for enrollment within the study timeframe (approximately 1 month). Demographic baseline characteristics were well balanced between the Caucasian and Japanese groups (Table 1).

TABLE 1. Demographic baseline characteristics by ethnic group and total population

Parameter	Mean (range)		
	Caucasian (n = 4)	Japanese (n = 4)	Total (n = 8)
No. of subjects by gender			
Male	4	4	8
Female	0	0	0
Age (yrs)	29.0 (24–33)	26.8 (24–35)	27.9 (24–35)
Wt (kg)	66.9 (61.2–73.5)	65.6 (57.8–82.6)	66.3 (57.8–82.6)
Ht (cm)	173.3 (169–177)	172.8 (169–176)	173.0 (169–177)
Body mass index (kg/m^2)	22.2 (20.7–23.5)	22.1 (18.8–28.9)	22.2 (18.8–28.9)

Assay validation. In both matrices, the calibration curve ranged from lower limits of quantification of 1 ng/ml and 10 ng/ml for oseltamivir and OC, respectively, up to 250 ng/ml for oseltamivir and 10,000 ng/ml for OC. For the analysis in plasma, the interassay precision (coefficient of variation) ranged from 3.8% to 5.4% for oseltamivir and from 2.2% to 9.1% for OC, and the accuracy ranged from 100.0% to 105.7% for oseltamivir and from 97.5% to 99.3% for OC. For the analysis in CSF, the interassay precision ranged from 0.9% to 3.3% for oseltamivir and from 1.6% to 9.1% for OC, and the accuracy ranged from 104.0% to 114.5% for oseltamivir and from 98.2% to 105.8% for OC. No marked inaccuracies were found in the concentration ranges of the plasma and CSF study samples.

Pharmacokinetic analysis. Figure 1 and Fig. 2 show the mean (± standard deviation [SD]) plasma and CSF concentration-time profiles for oseltamivir and OC in plasma and CSF for Japanese and Caucasian subjects and the overall population after a single oral dose of 150 mg oseltamivir phosphate. For both analytes, mean concentrations in CSF were considerably lower than those in plasma. Table 2 and Table 3 summarize the measured and computed pharmacokinetic parameters for oseltamivir and OC in plasma and CSF. Mean (± SD) C_{max} plasma values were 115 (±40.0) ng/ml for oseltamivir and 544 (±92.6) ng/ml for OC. The corresponding median (range) T_{max} values were 1.0 (0.5 to 4.0) h and 5.0 (4.0 to 6.0) h for oseltamivir and OC postdosing, respectively. In CSF, mean (± SD) C_{max} values for oseltamivir and OC were 2.4 (±0.9) ng/ml and 19.0 (±14.9) ng/ml, respectively; these were measured at median (range) T_{max} values of 3.5 (1.0 to 5.0) h and 8.0 (6.0 to 12.0) h postdosing.

Oseltamivir concentrations were quantifiable for up to 12 h postdosing in plasma and 9 h in CSF. OC concentrations were detected for up to 24 h in plasma and for up to 12 h in CSF in all but one Caucasian subject. This subject displayed the highest CSF concentrations for OC with a C_{max} value of 45.9 ng/ml at 7 h postdosing, but the oseltamivir concentrations in CSF were not remarkably high compared to those for the remaining subjects. This subject was also shown to have blood contamination of the CSF up to 5 h postdosing, and OC persisted in the subject's CSF samples until 24 h after drug administration. In a different Caucasian subject, OC concentrations were not detected in CSF at any time point, while oseltamivir concen-

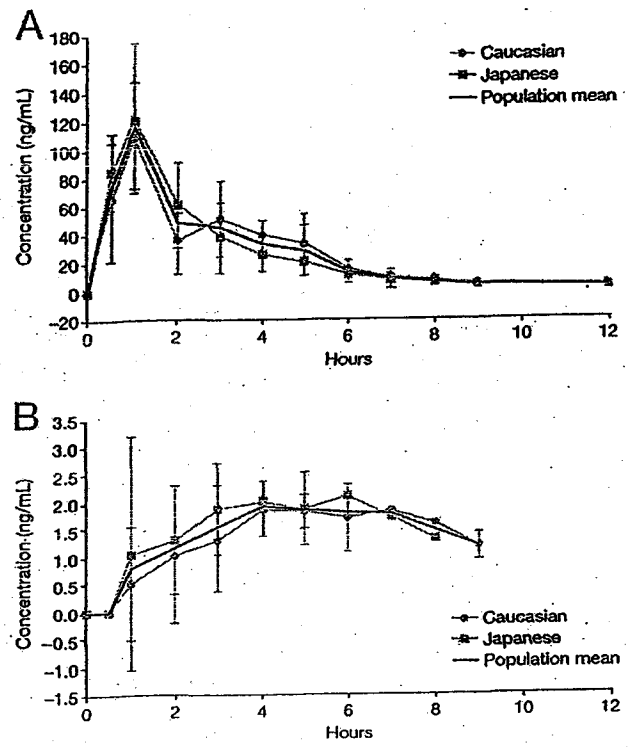

FIG. 1. (A) Mean (± SD) concentration-time profile for oseltamivir in plasma after a single oral dose of 150 mg oseltamivir phosphate in Caucasian (n = 4) and Japanese (n = 4) subjects and the overall population (n = 8). (B) Mean (± SD) concentration-time profile for oseltamivir in CSF after a single oral dose of 150 mg oseltamivir phosphate in Caucasian (n = 4) and Japanese (n = 4) subjects and the overall population (n = 8).

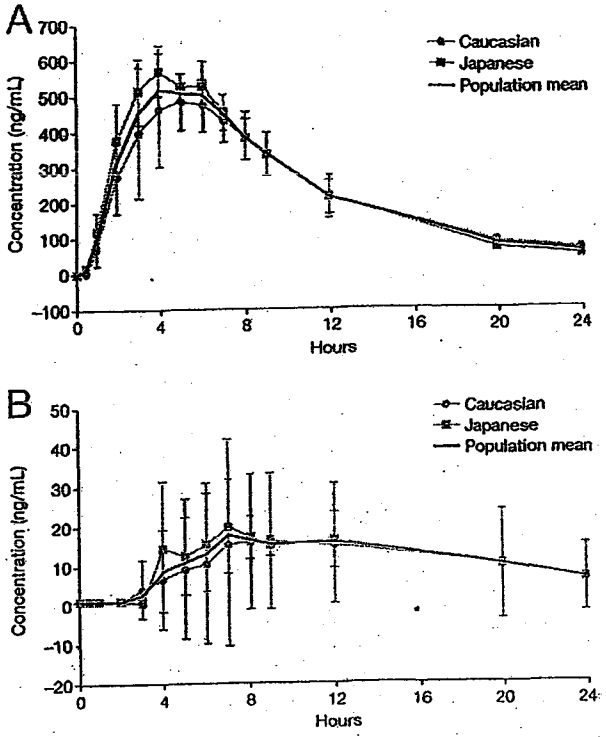

FIG. 2. (A) Mean (± SD) concentration-time profile for OC in plasma after a single oral dose of 150 mg oseltamivir phosphate in Caucasian (n = 4) and Japanese (n = 4) subjects and the overall population (n = 8). (B) Mean (± SD) concentration-time profile for OC in CSF after a single oral dose of 150 mg oseltamivir phosphate in Caucasian (n = 4) and Japanese (n = 4) subjects and the overall population (n = 8).

trations were measurable until 6 h postdosing. In this subject, values for OC in CSF of zero were assigned for C_{max}, AUC_{0-last}, and the respective CSF/plasma ratios, and these values were included in the respective summary statistics. The intersubject pharmacokinetic variabilities (SDs) for the parameters C_{max} and AUC_{0-last} in plasma in relation to the sample mean (percent coefficient of variation) were approximately 34% and 17% for oseltamivir and OC, respectively. This is consistent with previous experience with the drug (Roche data on file). The corresponding intersubject variabilities for C_{max} and AUC_{0-last} in CSF were higher for oseltamivir (36% for C_{max} and 48% for AUC_{0-last}) and OC (78% for C_{max} and 129% for AUC_{0-last}), the latter two percentages reflecting the most extreme C_{max} values measured for OC (0 ng/ml and 45.9 ng/ml).

In the overall population, the mean (± SD) C_{max} CSF/plasma ratios (in %) for oseltamivir and OC were 2.1% (±0.5%) and 3.5% (±2.9%), respectively (Tables 2 and 3). For both oseltamivir and OC, the concentration-versus-time profiles in plasma were sufficient to estimate $AUC_{0-\infty}$ and $t_{1/2}$ and to derive the apparent oral plasma clearance for oseltamivir. For both analytes, plasma AUC_{0-last} covered more than 90% of plasma $AUC_{0-\infty}$. The mean plasma $t_{1/2}$ of OC was triple that of oseltamivir (5.4 h versus 1.8 h), and the mean plasma CL/F for oseltamivir was 502 liters/h. In contrast to the pharmacokinetic plasma data, the CSF concentration-versus-time profiles did not allow a reliable assessment of $AUC_{0-\infty}$ for either analyte; hence, only AUC_{0-last} values are reported for CSF. The mean (± SD) AUC_{0-last} CSF/plasma ratios for the total population for oseltamivir and OC were 2.4% (±1.1%) and 2.9% (±4.1%), respectively. The individual AUC_{0-last} values in CSF covered a time period between 2 and 9 h for oseltamivir and 12 or 24 h for OC and the individual AUC_{0-last} values in plasma covered between 9 and 12 h for oseltamivir and 12 and 24 h for OC. If approximate free plasma concentrations (58% for oseltamivir and 95% for OC [Roche data on file]) were used to calculate the respective CSF/plasma ratios, these figures would double for oseltamivir (that is, to approximately 5%) but would remain similar for OC. In the subject with blood-contaminated CSF, in whom higher OC CSF concentrations were observed, the resulting CSF/plasma ratios based on total concentrations for OC were 9.5% (C_{max}) and 11.7% (AUC) (these values would be only slightly higher if free concentrations were considered). In the overall population, the mean (± SD) C_{max} oseltamivir (prodrug)/OC (active metabolite) ratios (adjusted for the molecular weight differences) were 18.8% (±4.1%) and 12.4% (±5.1%) in plasma and CSF, respectively. The AUC_{0-last} oseltamivir/OC molar ratios were 5.1% (±0.9%) and 9.4% (±8.8%) in plasma and CSF, respectively.

This study was not empowered to identify differences be-

TABLE 2. Summary of the pharmacokinetic parameters of oseltamivir in plasma and CSF by ethnic group and total population[a]

Group (n)	C_{max} (ng/ml)		T_{max} (h)		C_{last} (ng/ml)		T_{last} (h)		AUC_{0-last} (h · ng/ml)		$t_{1/2}$ (h)		$AUC_{0-\infty}$ (h · ng/ml)		CL/F (liters/h)		CSF/plasma ratio (%)	
	Plasma	CSF	Plasma	CSF	Plasma	CSF	Plasma	CSF	Plasma	CSF	Plasma	CSF	Plasma	CSF	Plasma	CSF	C_{max}	AUC_{0-last}
Caucasian (4)	100 ± 39.6	2.1 ± 0.5	2.0 (0.5–4.0)	4.0 (2.0–5.0)	1.9 ± 0.5	1.3 ± 0.3	12.0 (9.0–12.0)	7.5 (5.0–9.0)	299 ± 62.8	9.4 ± 4.6	1.8 ± 0.2	NC[b]	304 ± 64.0	NC	512 ± 118	NC	2.3 ± 0.5	3.0 ± 1.0
Japanese (4)	130 ± 39.8	2.6 ± 1.3	1.0 (0.5–1.0)	3.0 (1.0–5.0)	2.3 ± 0.9	1.4 ± 0.3	9.0 (9.0–12.0)	4.0 (2.0–8.0)	317 ± 92.3	5.9 ± 4.0	1.7 ± 0.4	NC	323 ± 93.6	NC	492 ± 126	NC	1.9 ± 0.5	1.7 ± 0.8
Total (8)	115 ± 40.0	2.4 ± 0.9	1.0 (0.5–4.0)	3.5 (1.0–4.0)	2.1 ± 0.7	1.4 ± 0.3	10.5 (9.0–12.0)	5.5 (2.0–9.0)	308 ± 73.7	7.6 ± 4.4	1.8 ± 0.3	NC	313 ± 74.9	NC	502 ± 113	NC	2.1 ± 0.5	2.4 ± 1.1

[a] Values are arithmetic means (± SDs) apart from T_{max} and T_{last}, which are medians (range). Values are reported with three significant figures and/or a maximum of one decimal place.
[b] NC, not calculated.

tween ethnic groups. Nevertheless, no gross differences for any pharmacokinetic parameters were observed for either oseltamivir or OC between the Caucasian and Japanese subjects (*Fig. 1 and 2*).

Safety. A total of 20 adverse events were reported during the study, all of which were mild to moderate in intensity and resolved without sequelae (Table 4). All but two events were unrelated to the study medication: one chest pain with a remote relationship to oseltamivir and one headache with a possible relationship to oseltamivir. In general, headache, back pain, and post-lumbar-puncture syndrome occurred due to the lumbar puncture procedure. Caffeine and paracetamol were administered to treat these conditions. No deaths, serious adverse events, or withdrawals after drug administration occurred during the study, and there were no clinically relevant changes in vital signs, ECG, or laboratory parameters at follow-up.

DISCUSSION

In the current exploratory study, we evaluated the pharmacokinetics of oseltamivir and OC in the CSF and plasma of healthy Japanese and Caucasian adult volunteers to further our understanding of the CNS penetration of these entities. Concentrations of oseltamivir and OC in CSF were low (mean C_{max}, 2.4 ng/ml for oseltamivir and 19.0 ng/ml for OC in CSF), and maximum concentrations were 2.1% and 3.5% of those attained in plasma, respectively (mean C_{max}, 115 ng/ml for oseltamivir and 544 ng/ml for OC in plasma). Overall exposure was also low in CSF compared with plasma (mean AUC CSF/plasma ratios of 2.4% for oseltamivir and 2.9% for OC). Collectively, these findings demonstrate that the CNS penetration of oseltamivir and OC is low in healthy individuals. The relative C_{max} and AUC_{0-last} oseltamivir/OC ratios in plasma reported in this study are consistent with data from previous studies with healthy volunteers (Roche data on file).

These findings are consistent with two case reports describing CNS penetration in influenza virus-infected individuals (5, 31). These cases comprise examination of the CSF of a 10-year-old male with influenza B virus-associated encephalitis (31) and a postmortem examination of several brain regions from a 13-year-old Japanese male with influenza who had taken a single dose of oseltamivir and subsequently fell to his death from a building (5). In both of these cases, no or low concentrations of oseltamivir or OC were detected in CSF or human brain homogenates (5, 31). Preclinical studies involving rats and ferrets also show uniformly low brain penetration following administration of oseltamivir phosphate (Roche data on file). For oseltamivir, brain exposure in rats after intravenous administration was approximately 20% of plasma values, whereas for OC it was approximately 3%. It should also be noted that these studies employed whole-brain homogenates and that concentrations in tissue may have been overestimated due to confounding by blood vessel content, especially in cases with high plasma-to-brain ratios (Roche data on file). Recent studies in mice showed that access to the CNS by oseltamivir was also restricted by P-glycoprotein (P-gp); it should be noted that in the absence of P-gp in knockout mice, the brain/plasma ratio was still low (around 0.35) (20, 25). The limited access of

OC to brain is thought to be due to its low lipophilicity leading to low passive diffusion across the blood-brain barrier (BBB).

It is recognized that, due to the short time period in which quantifiable concentrations in CSF could be measured, there was a potential for underestimation of CSF AUC_{0-last} values. This could also have led to underestimation of the calculated AUC_{0-last} CSF/plasma ratios. However, it is reassuring that even when a "worst-case scenario" was applied, with the last measurable CSF concentration for each subject extrapolated to the plasma time to last measurable concentration (T_{last}), the AUC_{0-last} values in CSF for the total population for oseltamivir and OC were 14.0 (±3.6) h · ng/ml and 291 (±204) h · ng/ml, respectively. The values remained of the same magnitude as those of the AUC_{0-last} values estimated using the actual CSF T_{last} values, which were 7.6 (±4.4) h · ng/ml for oseltamivir and 151 (±202) h · ng/ml for OC. The corresponding mean (± SD) AUC_{0-last} (CSF)/AUC_{0-last} (plasma) ratios for the total population were still very low when this conservative approach was employed: 4.6% (±1.0%) for oseltamivir and 5.2% (±3.9%) for OC.

No females were available for enrollment within the restraints imposed by the study timelines. This was not expected to affect the outcome of the study, as previous investigations within the wider oseltamivir clinical program have indicated no significant gender differences in the pharmacokinetics of either oseltamivir or OC (Roche data on file).

In the overall study population, oseltamivir was detectable in the CSF for a median duration of 5.5 h and in OC for a median duration of 12.0 h. In one subject, whose first six CSF samples were contaminated with blood, OC persisted in the CSF for 24.0 h. While oseltamivir is a P-gp substrate and is eliminated from the CNS by this transporter, it has been speculated that active efflux of OC from the brain at the BBB may occur via organic anion transporter 3 (OAT3) (25), which is a homologue of OAT1, the mediator of renal tubular secretion of OC (11). OAT3 is expressed at the BBB and actively eliminates organic anions from the brain (15, 16).

Within the limitations of the study design (i.e., exploratory nature and limited sample size), no gross differences in the CSF or plasma pharmacokinetics of oseltamivir or OC were observed between the Caucasian and Japanese subjects. This is consistent with published findings showing no discernible differences in the overall pharmacokinetic profiles of oseltamivir in plasma between Japanese and Caucasian adults (28) and children (7). It has been suggested that genetic variations may contribute to the higher incidence of CNS events reported in certain ethnic groups. For example, Shi et al. postulated that variations in the human carboxylesterases hCES1 and hCES2 could lead to decreased conversion and therefore higher-than-expected systemic concentrations of oseltamivir (30). Utilizing a population pharmacokinetic model, simulations of oseltamivir 75-mg twice-daily dosing without oseltamivir conversion to OC gave steady-state C_{max} values that were around 14-fold higher than those achieved when the metabolic pathway was intact (Roche data on file). Nevertheless, these estimated values were approximately 1.4-fold lower than those observed in a clinical trial of six subjects who received 1,000-mg doses, in which no neuropsychiatric adverse events of note were seen (Roche data on file). Genetic variants of OAT1 (which mediates renal secretion of OC) (1, 4, 19) and P-gp (which controls

TABLE 3. Summary of the pharmacokinetic parameters of OC in plasma and CSF by ethnic group and total population[a]

Group (*n*)	C_{max} (ng/ml)		T_{max} (h)		C_{last} (ng/ml)		T_{last} (h)		AUC_{0-last} (h · ng/ml)		$t_{1/2}$ (h)		$AUC_{0-\infty}$ (h · ng/ml)		CSF/plasma ratio (%)	
	Plasma	CSF	Plasma	CSF	Plasma	CSF	Plasma	CSF	Plasma	CSF	Plasma	CSF	Plasma	CSF	C_{max}	AUC_{0-last}
Caucasian[b] (4)	507 ± 117	17.7 ± 19.7	5.5 (4.0–6.0)	8.0 (7.0–12.0)	56.4 ± 9.8	12.0 ± 1.3	24.0 (24.0–24.0)	12.0 (12.0–24.0)	5,380 ± 1,180	185 ± 297	5.9 ± 0.4	NC[c]	5,860 ± 1,210	NC	3.5 ± 4.2	3.6 ± 6.0
Japanese (4)	581 ± 50.5	20.4 ± 11.3	4.5 (4.0–6.0)	7.5 (6.0–12.0)	44.0 ± 19.4	16.3 ± 7.3	24.0 (24.0–24.0)	12.0 (12.0–12.0)	5,700 ± 826	129 ± 67.6	5.0 ± 0.9	NC	6,030 ± 1,000	NC	3.5 ± 1.7	2.3 ± 1.1
Total (8)	544 ± 92.6	19.0 ± 14.9	5.0 (4.0–6.0)	8.0 (6.0–12.0)	50.2 ± 15.7	14.5 ± 5.7	24.0 (24.0–24.0)	12.0 (12.0–24.0)	5,540 ± 957	157 ± 202	5.4 ± 0.8	NC	5,950 ± 1,030	NC	3.5 ± 2.9	2.9 ± 4.1

[a] Values are arithmetic means (± SDs) apart from T_{max} and T_{last}, which are medians (ranges). Values are reported with three significant figures and/or a maximum of one decimal place.
[b] For one Caucasian subject, all CSF metabolite concentrations were below quantifiable limits and were interpreted as 0 ng/ml; pharmacokinetic parameters for OC in CSF were not calculated, but C_{max} and AUC_{0-last} values of 0 were included in the respective summary statistics for these parameters and were used to calculate the respective CSF/plasma ratios of 0.
[c] NC, not calculated.

TABLE 4. Subjects reporting adverse events by ethnic group and total population

Ethnic group (*n*)	All body system disorders		No. of subjects with:							
	No. of subjects with ≥1 AE[a]	Total no. of AEs	Nervous system disorders	Gastrointestinal disorders		Musculoskeletal and connective tissue disorders		Injury, poisoning, and procedural complications		Eye disorders
			Headache	Nausea	Vomiting	Back pain	Musculoskeletal stiffness	Post-lumbar-puncture syndrome		Photophobia
Caucasian (4)	2	6	2	1	0	1	1	1		0
Japanese (4)	4	14	4	3	1	2	0	2		1
Total (8)	6	20	6	4	1	3	1	3		1

[a] AE, adverse event.

BBB penetration of oseltamivir) (13, 27) do occur, but alterations to their function as a result have not been demonstrated.

Given the low CSF concentrations observed in subjects in the current study, the potential for oseltamivir and OC to induce or exacerbate CNS dysfunction appears low. Ose et al. have suggested that OC could act on human neuraminidase enzymes (sialidases) in the brain and disrupt the mitochondrial apoptotic pathway in neuronal cell death (25). However, in vitro data suggest that neither oseltamivir nor OC inhibits any of the four human neuraminidases at concentrations of up to 1 mM (32). Furthermore, investigation of 155 different molecular drug targets, covering a broad range of receptors, enzymes, and ion channels, many of which are relevant to the CNS, did not produce any relevant findings, indicating a lack of mechanism for neuropsychiatric adverse events with oseltamivir or OC (18). Clinical data also support the lack of an association between oseltamivir and CNS adverse events in young individuals with influenza. In two Japanese case series, the onset of abnormal or delirious behavior was found to occur both before and after the initiation of oseltamivir therapy (8, 23), suggesting no temporal association between the two events. Epidemiological studies also demonstrate that the incidence of neuropsychiatric adverse events is similar between patients with influenza who receive oseltamivir and those who receive no antiviral (2, 34).

Oseltamivir was well tolerated in this study, with the majority of adverse events related to the continuous indwelling lumbar catheterization lumbar puncture technique used to obtain CSF samples. Methods involving continuous collection of CSF for 12 to 36 h, with up to two sampling periods separated by a 7- to 14-day recovery period, are used in experimental medicine and proof-of-principle studies. They can establish pharmacokinetic-pharmacodynamic models (hence "dynabridging") and downstream (proteomic) effects of drug administration. Continuous indwelling lumbar catheterization has been performed in over 450 healthy volunteers and patients at California Clinical Trials, from 1997 to the present (3). There have been no serious adverse events from these procedures, and the rate of adverse events has been no different from that for single lumbar punctures (14).

This study supports the idea that the CNS penetration of oseltamivir and OC is low in healthy Japanese and Caucasian individuals. Preclinical and clinical data support the idea that oseltamivir and OC have a limited potential to induce or exacerbate CNS adverse events in individuals with influenza. A disease- rather than drug-related effect appears likely.

ACKNOWLEDGMENTS

The manuscript was prepared with the assistance of Stephen Purver and colleagues at Gardiner Caldwell Communications Ltd., Macclesfield, United Kingdom. Special thanks go to all study team members at F. Hoffmann-La Roche, especially the bioanalytical monitor, Caroline Kreuzer, for their assistance with this study.

Financial support for the preparation of the paper was provided by F. Hoffmann-La Roche Ltd., the manufacturer of oseltamivir. M.S., B.K., L.B., A.P., G.H., E.P.P., and C.R.R. are current employees of F. Hoffmann-La Roche Ltd.

REFERENCES

1. Bleasby, K., L. A. Hall, J. L. Perry, H. W. Mohrenweiser, and J. B. Pritchard. 2005. Functional consequences of single nucleotide polymorphisms in the human organic anion transporter hOAT1 (SLC22A6). J. Pharmacol. Exp. Ther. 314:923–931.

2. Blumentals, W. A., and X. Song. 2007. The safety of oseltamivir in patients with influenza: analysis of healthcare claims data from six influenza seasons. Med. Gen. Med. 9:23.
3. Ereshefsky, L., S. S. Jhee, M. T. Leibowitz, S. Moran, M. Yen, and L. Gertsik. 2006. Demonstrating proof of principle and finding the right dose: the role of CSF 'Dynabridging' studies. Abstr. 25th Bienn. Congr. Coll. Int. Neuro-Psychopharmacol. (CINP), Chicago, IL.
4. Fujita, T., C. Brown, E. J. Carlson, T. Taylor, M. de la Cruz, S. J. Johns, D. Stryke, M. Kawamoto, K. Fujita, R. Castro, C. W. Chen, E. T. Lin, C. M. Brett, E. G. Burchard, T. E. Ferrin, C. C. Huang, M. K. Leabman, and K. M. Giacomini. 2005. Functional analysis of polymorphisms in the organic anion transporter, SLC22A6 (OAT1). Pharmacogenet. Genomics 15:201–209.
5. Fuke, C., Y. Ihama, and T. Miyazaki. 2008. Analysis of oseltamivir active metabolite, oseltamivir carboxylate, in biological materials by HPLC-UV in a case of death following ingestion of Tamiflu. J. Leg. Med. (Tokyo) 10:83–87.
6. Fukumoto, Y., A. Okumura, F. Hayakawa, M. Suzuki, T. Kato, K. Watanabe, and T. Morishima. 2007. Serum levels of cytokines and EEG findings in children with influenza associated with mild neurological complications. Brain Dev. 29:425–430.
7. Gieschke, R., R. Dutkowski, J. Smith, and C. R. Rayner. 2007. Similarity in the pharmacokinetics of oseltamivir and oseltamivir carboxylate in Japanese and Caucasian children. Abstr. Options Control Influenza VI, Toronto, Ontario, Canada, abstr. P921.
8. Goshima, N., T. Nakano, M. Nagao, and T. Ihara. 2006. Clinical study of abnormal behavior during influenza. Infect. Immun. Childhood 18:376.
9. Hayden, F. G., R. Belshe, C. Villanueva, R. Lanno, C. Hughes, I. Small, R. Dutkowski, P. Ward, and J. Carr. 2004. Management of influenza in households: a prospective, randomized comparison of oseltamivir treatment with or without postexposure prophylaxis. J. Infect. Dis. 189:440–449.
10. He, G., J. Massarella, and P. Ward. 1999. Clinical pharmacokinetics of the prodrug oseltamivir and its active metabolite Ro 64-0802. Clin. Pharmacokinet. 37:471–484.
11. Hill, G., T. Ciblar, C. Oo, E. S. Ho, K. Prior, H. Wiltshire, J. Barrett, B. Liu, and P. Ward. 2002. The anti-influenza drug oseltamivir exhibits low potential to induce pharmacokinetic drug interactions via renal secretion-correlation of in vivo and in vitro studies. Drug Metab. Dispos. 30:13–19.
12. Huang, Y. C., T. Y. Lin, S. L. Wu, and K. C. Tsao. 2003. Influenza A-associated central nervous system dysfunction in children presenting as transient visual hallucination. Pediatr. Infect. Dis. J. 22:366–368.
13. Ishikawa, T., H. Hirano, Y. Onishi, A. Sakurai, and S. Tarui. 2004. Functional evaluation of ABCB1 (P-glycoprotein) polymorphisms: high-speed screening and structure-activity relationship analyses. Drug Metab. Pharmacokinet. 19:1–14.
14. Jhee, S. S., and V. Zarotsky. 2003. Safety and tolerability of serial cerebrospinal fluid (CSF) collections during pharmacokinetic/pharmacodynamic studies: 5 years' experience. Clin. Res. Regul. Aff. 20:357–363.
15. Kikuchi, R., H. Kusuhara, T. Abe, H. Endou, and Y. Sugiyama. 2004. Involvement of multiple transporters in the efflux of 3-hydroxy-3-methylglutaryl-CoA reductase inhibitors across the blood-brain barrier. J. Pharmacol. Exp. Ther. 311:1147–1153.
16. Kikuchi, R., H. Kusuhara, D. Sugiyama, and Y. Sugiyama. 2003. Contribution of organic anion transporter 3 (Slc22a8) to the elimination of p-aminohippuric acid and benzylpenicillin across the blood-brain barrier. J. Pharmacol. Exp. Ther. 306:51–58.
17. Lin, C. H., Y. C. Huang, C. H. Chiu, C. G. Huang, K. C. Tsao, and T. Y. Lin. 2006. Neurologic manifestations in children with influenza B virus infection. Pediatr. Infect. Dis. J. 25:1081–1083.
18. Lindemann, L., H. Jacobsen, C. Schweitzer, C. Schuhbauer, D. Reinhardt, C. Fischer, C. Diener, S. Gatti, J. Beck, J. G. Wettstein, H. Luetscher, E. Prinssen, and M. Brockhaus. 2008. Comprehensive in vitro pharmacological selectivity profile of oseltamivir prodrug (Tamiflu) and oseltamivir active metabolite. Abstr. Exp. Biol., San Diego, CA, abstr. LB671.
19. Marzolini, C., R. G. Tirona, and R. B. Kim. 2004. Pharmacogenomics of the OATP and OAT families. Pharmacogenomics J. 5:273–282.
20. Morimoto, K., M. Nakakariya, Y. Shirasaka, C. Kakinuma, T. Fujita, I. Tamai, and T. Ogihara. 2008. Oseltamivir (Tamiflu) efflux transport at the blood-brain barrier via P-glycoprotein. Drug Metab. Dispos. 36:6–9.
21. Moscona, A. 2005. Neuraminidase inhibitors for influenza. N. Engl. J. Med. 353:1363–1373.
22. Nicholson, K. G., F. Y. Aoki, A. D. Osterhaus, S. Trottier, O. Carewicz, C. H. Mercier, A. Rode, N. Kinnersley, P. Ward, et al. 2000. Efficacy and safety of oseltamivir in treatment of acute influenza: a randomised controlled trial. Lancet 355:1845–1850.
23. Okumura, A., T. Kubota, T. Kato, and T. Morishima. 2006. Oseltamivir and delirious behavior in children with influenza. Pediatr. Infect. Dis. J. 25:572.
24. Okumura, A., T. Nakano, Y. Fukumoto, K. Higuchi, H. Kamiya, K. Watanabe, and T. Morishima. 2005. Delirious behavior in children with influenza: its clinical features and EEG findings. Brain Dev. 27:271–274.
25. Ose, A., H. Kusuhara, K. Yamatsugu, M. Kanai, M. Shibasaki, T. Fujita, A. Yamamoto, and Y. Sugiyama. 2008. P-glycoprotein restricts the penetration of oseltamivir across the blood-brain barrier. Drug Metab. Dispos. 36:427–434.
26. Peters, P. H., Jr., S. Gravenstein, P. Norwood, V. De Bock, A. Van Couter, M. Gibbens, T. A. von Planta, and P. Ward. 2001. Long-term use of oseltamivir for the prophylaxis of influenza in a vaccinated frail older population. J. Am. Geriatr. Soc. 49:1025–1031.
27. Sakurai, A., A. Tamura, Y. Onishi, and T. Ishikawa. 2005. Genetic polymorphisms of ATP-binding cassette transporters ABCB1 and ABCG2: therapeutic implications. Expert Opin. Pharmacother. 6:2455–2473.
28. Schentag, J., G. Hill, T. Chu, and C. Rayner. 24 April 2007. Similarity in pharmacokinetics of oseltamivir and oseltamivir carboxylate in Japanese and Caucasian subjects. J. Clin. Pharmacol. 47:689–696. [Epub ahead of print.]
29. Shen, D. D., A. A. Artru, and K. K. Adkison. 2004. Principles and applicability of CSF sampling for the assessment of CNS drug delivery and pharmacodynamics. Adv. Drug Deliv. Rev. 56:1825–1857.
30. Shi, D., J. Yang, D. Yang, E. L. Lecluyse, C. Black, L. You, F. Akhlaghi, and B. Yan. 2006. Anti-influenza prodrug oseltamivir is activated by carboxylesterase HCE1, and the activation is inhibited by antiplatelet agent clopidogrel. J. Pharmacol. Exp. Ther. 319:1477–1484.
31. Straumanis, J. P., M. D. Tapia, and J. C. King. 2002. Influenza B infection associated with encephalitis: treatment with oseltamivir. Pediatr. Infect. Dis. J. 21:173–175.
32. Toovey, S., C. R. Rayner, E. Prinssen, T. Chu, B. Donner, R. Dutkowski, S. Sacks, J. Solsky, I. Small, and D. Reddy. 2008. Post-marketing safety assessment of neuropsychiatric adverse event risk in patients with influenza treated with oseltamivir. Abstr. X Int. Symp. Respir. Viral Infect., Singapore City, Singapore.
33. Whitley, R. J., F. G. Hayden, K. S. Reisinger, N. Young, R. Dutkowski, D. Ipe, R. G. Mills, and P. Ward. 2001. Oral oseltamivir treatment of influenza in children. Pediatr. Infect. Dis. J. 20:127–133.
34. Wilcox, M., and S. Zhu. 2007. Oseltamivir therapy appears not to affect the incidence of neuropsychiatric adverse events in influenza patients. Abstr. 47th Intersci. Conf. Antimicrob. Agents Chemother., Chicago, IL, abstr. V-1223a.
35. Wiltshire, H., B. Wiltshire, A. Citron, T. Clarke, C. Serpe, D. Gray, and W. Herron. 2000. Development of a high-performance liquid chromatographic-mass spectrometric assay for the specific and sensitive quantification of Ro 64-0802, an anti-influenza drug, and its pro-drug, oseltamivir, in human and animal plasma and urine. J. Chromatogr. B 745:373–388.

ANTIMICROBIAL AGENTS AND CHEMOTHERAPY, Oct. 2008, p. 3484–3491 Vol. 52, No. 10
0066-4804/08/$08.00+0 doi:10.1128/AAC.00344-08

Limited Inhibitory Effects of Oseltamivir and Zanamivir on Human Sialidases[▽]

Keiko Hata,[1,2] Koichi Koseki,[1,2] Kazunori Yamaguchi,[1,2] Setsuko Moriya,[1,2] Yasuo Suzuki,[2,3,4] Sangchai Yingsakmongkon,[3] Go Hirai,[5] Mikiko Sodeoka,[5] Mark von Itzstein,[6] and Taeko Miyagi[1,2]*

Division of Biochemistry, Miyagi Cancer Center Research Institute, Natori, Miyagi 981-1293,[1] CREST, Japan Science and Technology Agency, Kawaguchi-shi, Saitama,[2] Department of Biomedical Sciences, College of Life and Health Sciences, Chubu University, Kasugai, Aichi 487-8501,[3] Global COE Program for Innovation in Human Health Sciences, Yada, Shizuoka 422-8526,[4] and Synthetic Organic Chemistry Laboratory, RIKEN, Hirosawa, Wako 351-0198,[5] Japan, and Institute for Glycomics, Griffith University (Gold Coast Campus), PMB 50 Gold Coast Mail Centre, Queensland 9726, Australia[6]

Received 11 March 2008/Returned for modification 30 May 2008/Accepted 31 July 2008

Oseltamivir (Tamiflu) and zanamivir (Relenza), two extensively used clinically effective anti-influenza drugs, are viral sialidase (also known as neuraminidase) inhibitors that prevent the release of progeny virions and thereby limit the spread of infection. Recently mortalities and neuropsychiatric events have been reported with the use of oseltamivir, especially in pediatric cases in Japan, suggesting that these drugs might also inhibit endogenous enzymes involved in sialic acid metabolism, including sialidase, sialyltransferase, and CMP-synthase, in addition to their inhibitory effects on the viral sialidase. The possible inhibition could account for some of the rare side effects of oseltamivir. However, there has been little direct evidence in regard to the sensitivities of animal sialidases to these drugs. Here, we examined whether these inhibitors might indeed affect the activities of human sialidases, which differ in primary structures and enzyme properties but possess tertiary structures similar to those of the viral enzymes. Using recombinant enzymes corresponding to the four human sialidases identified so far, we found that oseltamivir carboxylate scarcely affected the activities of any of the sialidases, even at 1 mM, while zanamivir significantly inhibited the human sialidases NEU3 and NEU2 in the micromolar range (K_i, 3.7 ± 0.48 and 12.9 ± 0.07 μM, respectively), providing a contrast to the low nanomolar concentrations at which these drugs block the activity of the viral sialidases.

The continuing threat of an influenza pandemic is a serious worldwide concern. For the prevention of influenza, potent and selective anti-influenza drugs have been developed. The currently approved agents include inhibitors of the virus sialidase (8, 25). Viral sialidases are membrane components that destroy the sialic acid-containing receptors on the surfaces of infected cells and are thus involved in the release of newly budded virions from the host cell surface to begin a new round of infection. They may thus play key roles in the spread of the viral infection together with another viral surface glycoprotein, hemagglutinin, involved in the binding of the virus particles to receptors on the host cells. Studies of the crystal structures of some of the viral sialidases have facilitated the rational designing of sialidase inhibitors; the two potent inhibitors, oseltamivir (Tamiflu) and zanamivir (Relenza), are sialic acid analogues that interact with the active sites on the enzymes. Oseltamivir is a prodrug that is metabolized to its active form, oseltamivir carboxylate, after oral administration, while zanamivir is designed for delivery by inhalation. Recently mortalities and neuropsychiatric events have been reported with the use of oseltamivir, especially in pediatric cases in Japan (1, 2, 6, 9, 12). With the drug prescribed frequently for the treatment of influenza in Japan and its consumption accounting for more than 70% of that around the world, Tamiflu has been suspected to cause abnormal behavior and deaths in Japan, particularly in teenagers, although no statistically significant relationship has been established up to the present. Since both of the drugs are targeted against the viral sialidase, the question has arisen as to whether they may also affect the activities of the endogenous sialidases in humans. In fact, there have been a number of observations (5, 10, 18, 29) pointing to the inhibitory effects of oseltamivir on the endogenous sialidases in rats and mice; however, the question remains open, because direct validation of these findings remains limited to one recent report (11) of the effect of the drug against a recombinant sialidase. Under these circumstances, we were prompted to investigate the effects of these drugs on the activities of endogenous human sialidases.

Up to now, four types of human sialidases have been identified and characterized, designated NEU1, NEU2, NEU3, and NEU4 (15). They differ in their subcellular localization and enzymatic properties and in the chromosomal localization of the genes encoding them; the enzymes are expressed in a tissue-specific manner. The major subcellular localizations of NEU1, NEU2, and NEU3 are the lysosomes, cytosol, and plasma membranes, respectively, while NEU4 is localized in the lysosomal lumina or mitochondria and intracellular membranes. We previously discovered (14) that the primary structure of rat cytosolic sialidase, the first example of mammalian sialidase, contain several Asp boxes (-Ser-X-Asp-X-Gly-X-Thr-Trp-) and the Arg-Ile-Pro sequence, the conserved sequences found in sialidases from microorganisms (22), despite having no particular similarity to those sialidases. The sequence alignment of other mammalian sialidases successively

* Corresponding author. Mailing address: Division of Biochemistry, Miyagi Cancer Center Research Institute, Natori 981-1293, Japan. Phone: 81-22-384-3151. Fax: 81-22-381-1195. E-mail: miyagi-ta173@pref.miyagi.jp.

▽ Published ahead of print on 11 August 2008.

cloned revealed that they all contain the conserved sequences. A recent study of the crystal structure of human recombinant NEU2 (3) has provided further evidence of a canonical six-blade beta-propeller structure, as observed for viral sialidases, with the active site in a shallow crevice, but there are some differences from viral and bacterial sialidases in amino acid residues recognizing the *N*-acetyl and glycerol moieties of 2-deoxy-2,3-dehydro-*N*-acetylneuraminic acid (NeuAc2en). The lysosomal sialidase NEU1 acts effectively on oligosaccharides, glycopeptides, and a synthetic substrate, 4-methylumbelliferyl *N*-acetylneuraminic acid (4MU-NeuAc), and NEU3 is a plasma membrane-associated sialidase that almost specifically hydrolyzes gangliosides, while the other two enzymes possess broad substrate specificity, acting on oligosaccharides, glycopeptides, glycoproteins, and gangliosides, as well as on 4MU-NeuAc. Maximal activities are obtained at a pH of about 4.6 for NEU1, NEU3, and NEU4 and at pH 5.5 to 6.5 for NEU2. Sialidases of mammalian origin not only have been implicated in lysosomal catabolism, playing a role as general glycosidases, but are also believed to play roles in the modulation of functional molecules involved in many biological processes, whereas the roles of the sialidases from microorganisms appear to be limited to nutrition and pathogenicity (4). Although many functional aspects of the mammalian sialidases are not fully understood, partly due to the enzyme instability and low activity, recent developments in sialidase research have clarified their important biological roles, including their roles in events involved in cell differentiation, cell growth and apoptosis, and malignant transformation (16).

As described above, human sialidases, while differing from the viral enzymes in their primary structures and enzyme properties, show tertiary structures and active-site amino acids similar to those of the viral sialidases. Therefore, in this study, we examined whether the antiviral drugs might have effects on any of the four types of human recombinant sialidases.

MATERIALS AND METHODS

Cell culture and sialidase transfection. Human kidney 293T cells (Riken BRC Cell Bank, Tsukuba, Japan) were maintained in minimal essential medium supplemented with nonessential amino acids and 10% heat-inactivated fetal bovine serum. Eukaryote expression vectors for NEU1, NEU3, and NEU4 were prepared by inserting the respective human sialidase cDNAs covering the open reading frames (11, 28, 30) with the FLAG epitope at the C termini into the EcoRI site of the pCAGGS vector (a generous gift from Jun-ichi Miyazaki, Osaka University School of Medicine) under the control of the chicken β-actin promoter.

To obtain the NEU2 cDNA, the first-strand cDNAs were synthesized from poly(A)$^+$ RNA from human brain (Clontech) using oligo(dT)$_{12-18}$ primers and murine leukemia virus reverse transcriptase (SuperscriptII reverse transcriptase; Invitrogen) and applied as templates for the PCR described previously (30). To cover the entire coding sequence, the cDNA was amplified with the two primer pairs with EcoRI sites (5′-ATGGCGTCCCTTCCTGTCCTG-3′, forward, and 5′-TCACTGAGGCAGGTACTCAGC-3′) using LA *Taq* polymerase (Takara), subcloned into pBluescript, sequenced, and cloned into the expression vector.

Transient DNA transfection into the HK-293T cells was accomplished using the Effectene reagent (Qiagen) in accordance with the manufacturer's instructions. After 48 h of transfection, the cells were collected and homogenized, and the homogenates were used as the enzyme sources or for further purification. For the NEU1 enzyme, a cDNA for a protective protein (carboxypeptidase A), which is known to be associated with the NEU1 protein (13) and β-galactosidase as a complex in the lysosomes to maintain the sialidase activity (7), was cotransfected.

Quantitative analysis of transcripts of human sialidases by real-time PCR. Quantitative analysis of the transcripts for human sialidases was performed by real-time PCR using the LightCycler rapid thermal cycler system (Roche). The first-strand cDNAs were synthesized from poly(A)$^+$ RNAs from human lung and brain (Clontech) using random primers and murine leukemia virus reverse transcriptase (SuperscriptII) and applied as templates for the PCR. The PCRs were carried out in glass capillary reaction vessels (Roche) in 20-μl volume reaction mixtures containing 0.5 μM primers, cDNA, and QuantiTect SYBR green PCR master mix (Qiagen) using porphobilinogen deaminase as an internal control. A standard curve for each cDNA was generated by seal dilution of the pBluescript vector containing the gene encoding the entire open reading frame, as described previously (30).

Preparation and purification of the recombinant sialidases. The cells (2×10^7 to 5×10^7) transfected with FLAG-tagged sialidase cDNA as described above were collected, washed with phosphate-buffered saline, and sonicated on ice in 9 volumes of ice-cold lysis buffer. The lysates were centrifuged at 1,000 × *g* for 10 min at 4°C, and the resultant supernatants (homogenates) were then used for measurement of the sialidase activity or for further purification. The lysis buffer A for NEU1 and NEU2 contained 20 mM potassium phosphate (pH 6.8), 0.15 M NaCl, 1 mM phenymethylsulfonyl fluoride, and protease inhibitor cocktail (Roche), and the lysis buffer B for NEU3 and NEU4 was buffer A containing 1 mM EDTA and 1% Triton X-100. Purification of the recombinant sialidase proteins was performed using FLAG tag affinity chromatography as follows: NEU2 was purified from the cytosolic fraction after centrifugation of the homogenates at 100,000 × *g* for 1 h, followed by affinity chromatography. The cytosolic fraction of the cells was applied to an anti-FLAG M2 agarose column (1 ml) (Sigma), washed with 20 ml of lysis buffer A and successively with 10 ml of the buffer containing 1 M NaCl, and eluted with buffer A containing the FLAG peptides (100 μg/ml) and 10% glycerol. For NEU3 purification, the solubilized fraction after centrifugation at 20,000 × *g* for 15 min was applied to the column and then washed with buffer B containing 0.1% Triton X-100 (buffer C), followed by buffer containing 1 M NaCl, and then eluted with buffer C plus FLAG peptides and 10% glycerol.

Sialidase activity assays. The homogenates or purified fractions obtained above were used for measurement of sialidase activity using the synthetic substrate 4MU-NeuAc or ganglioside GM3 (NeuAcα2-3Galβ1-4Glcβ1-1Cer) (Alexis Biochemicals). The activities for NEU1, NEU2, and NEU4 were measured routinely in 0.1 ml of a reaction mixture containing 10 μmol sodium acetate buffer (pH 4.6 for NEU1 and NEU4; pH 5.5 for NEU2), 40 nmol 4MU-NeuAc, 0.1 mg bovine serum albumin, and enzyme. After incubation for 15 to 30 min at 37°C, the 4-methylumbelliferone released was determined fluorometrically (14). The reaction mixture for NEU3 activity contained 5 μmol sodium acetate buffer (pH 4.5), 10 nmol gangliosides GM3, 50 μg Triton X-100, 50 μg bovine serum albumin, and enzyme in 50 μl and was incubated for 20 to 30 min at 37°C. The sialic acids released from GM3 were measured by fluorometric high-performance liquid chromatography with malononitrile (27). Occasionally, NEU4 activity was also assayed with GM3 as the substrate in the same manner. Protein concentrations were determined by dye-binding assay (Bio-Rad Laboratories). One unit was defined as the amount of enzyme cleaving 1 nmol of sialic acid/h.

TLC. After 48 h of transfection, the cells were cultured in serum-depleted medium for 5 h, followed by treatment of each drug for a further 5 h, and the cells were collected and subjected to thin-layer chromatography (TLC). Glycolipids were extracted from the cells (1×10^7) in sequence with 2 ml of isopropanol-hexane-water (55:25:20 [vol/vol/vol]) and hydrolyzed with 0.1 M NaOH-methanol. After desalting was done using a Sep-Pak C_{18} cartridge, total lipid extracts were fractionated by TLC on high-performance TLC plates (Baker, Phillipsburg, NJ) in C–M–0.5% $CaCl_2$ (60:40:9 [vol/vol/vol]) and visualized with orcinol-H_2SO_4. Densitometric analyses were performed using the Scion Image (Scion Corp., Frederick, MD) and Quantity One (Bio-Rad Laboratories) software programs.

Lectin blotting. To observe the changes in the amounts of the endogenous glycoproteins, lectin blot analysis was conducted with peanut agglutinin (PNA) and *Ricinus communis* agglutinin (RCA) (Honen, Tokyo, Japan). After 48 h of transfection, the cells were cultured in serum-depleted medium for 5 h, followed by treatment of each drug for a further 5 h, and the cells collected were subjected to lectin blotting. Cell homogenates were resolved by sodium dodecyl sulfate-polyacrylamide gel electrophoresis (SDS-PAGE) and transferred to polyvinylidene difluoride membranes. The blots were washed in a solution containing 10 mM Tris-HCl, pH 7.5, 100 mM NaCl, and 0.1% Tween 20 and incubated with the solution containing biotinylated lectins. After washing, the lectin-bound glycoproteins were visualized with horseradish peroxidase-streptavidin (Vector, Burlingame, CA).

Inhibition assay of influenza virus sialidase activity. Inhibitory activity against the influenza sialidase activity was assessed using a fluorometric method with slight modification (21). Influenza viruses from human and animal isolates were propagated in allantoic cavities of 11-day-old chicken eggs for 48 h at 35°C and

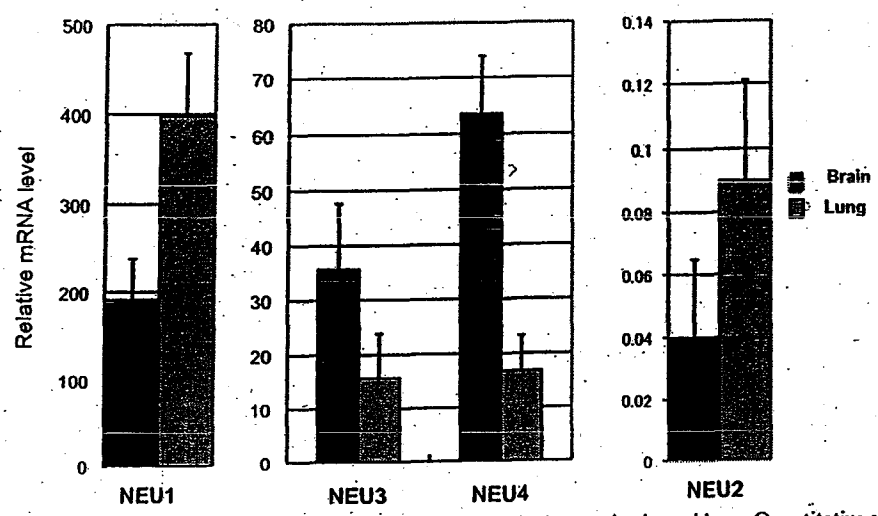

FIG. 1. Comparison of the endogenous expression levels of four sialidases in the human brain and lung. Quantitative analyses of the transcripts were performed with real-time PCR using porphobilinogen deaminase as an internal standard as described in Materials and Methods. Bars indicate the standard deviations of the means for experiments performed in triplicate.

purified by sucrose density gradient centrifugation as described previously (24). To obtain an appropriate virus concentration for use in the assay, the sialidase activity of each virus was first determined in a total volume of 10 μl containing 10 mM acetate buffer (pH 6.0), 80 μM 4MU-NeuAc substrate, and various concentrations of influenza virus solution. After incubation for 30 min at 37°C, the reaction was stopped and 100 μl of the solution was transferred to a 96-well black plastic plate, and the fluorescence was monitored. For the inhibition assay, 4 μl of each dilution of each inhibitor was preincubated with 4 μl of influenza virus solution for 1 h at 4°C before the addition of 2 μl of 400 μM 4MU-NeuAc substrate in 10 mM acetate buffer (pH 6.0) to begin the reaction.

RESULTS

Inhibition assays of human sialidase activities for oseltamivir and zanamivir. Our previous results from quantitative real-time PCR indicated that the expressions of NEU1, NEU3, and NEU4 are readily detectable but expression of NEU2 is hardly detectable in human tissues (30). To determine whether NEU2 is actually expressed in humans, we attempted to clone the cDNA, because NEU2 has been characterized only using a genomic clone constructed by ligation of two genomic fragment sequences (17). A NEU2 cDNA clone was obtained from a cDNA synthesized from poly(A)$^+$ RNA from the human brain as the template by PCR and was employed for preparation of the NEU2 enzyme protein. Consistent with our previous data, the expression levels of four sialidases were found to be markedly different. The endogenous levels of four sialidases were compared with one another as they were measured quantitatively using standard curves of respective cDNAs; those from the brain and lung are shown in Fig. 1. NEU1, known as a target gene for sialidosis, was expressed at the highest level, followed by NEU3 and NEU4, which were generally expressed at 1/10 or 1/20 of the level of NEU1. Expression of NEU2 was observed at extremely low levels, being at most only 1/4,000 to 1/10,000 that of NEU1 in several tissues.

To obtain preparations of all four enzymes, we transiently transfected the respective expression plasmids into 293T cells. The cell homogenates and the enzymes, highly purified by FLAG peptide elution through FLAG affinity chromatography (Fig. 2A), were assayed for sialidase activity in the presence of oseltamivir phosphate, oseltamivir carboxylate (Toronto Research Chemicals Inc., ON, Canada), or zanamivir (26). Considering the substrate specificity, the substrates exogenously added routinely were 4MU-NeuAc for NEU1, NEU2, and NEU4 and the ganglioside GM3 for NEU3, because the former three can preferentially hydrolyze 4MU-NeuAc and NEU3 acts almost specifically on gangliosides (15). Due to the broad specificity of NEU4, the activity was also assayed here with GM3 and 4MU-NeuAc to exclude the effects of differences in the substrate. After 15 to 30 min of incubation, the released 4MU and sialic acids were determined using a fluorometer and using fluorometric high-performance liquid chromatography, respectively. The 50% inhibitory concentration (IC_{50}) of each compound was calculated by plotting the decrease in activity against the log of the agent concentration. Oseltamivir phosphate did not affect any of the human sialidases (data not shown), since the prodrug osetamivir is expected to be ineffective in vitro, and oseltamivir carboxylate also showed no appreciable inhibition of the sialidases even at the concentration of 1 mM (Table 1). Only the activity of NEU2 appeared to be inhibited, but with a very high IC_{50}. In contrast, oseltamivir carboxylate was fully active against the influenza virus sialidases, with IC_{50}s in the nanomolar range under the conditions described in Materials and Methods. In addition, a nonselective sialidase inhibitor, NeuAc2en, showed clear inhibition in the micromolar range. While zanamivir did cause substantial inhibition of the human sialidases, the effects were much less marked than those in testing against the viral enzymes. NEU2 and NEU3 seemed to be more susceptible than the other two sialidases to zanamivir. Interestingly, the IC_{50} was the lowest for NEU3, which is expressed abundantly in the brain and is colocalized in the plasma membrane with its substrate gangliosides. The K_m and K_i values of the compounds for human sialidases were then compared using the homogenates (Table 2). Zanamivir was less inhibitory against NEU1 and NEU4, with K_i values approximately 300- and 20-fold higher, respectively, than

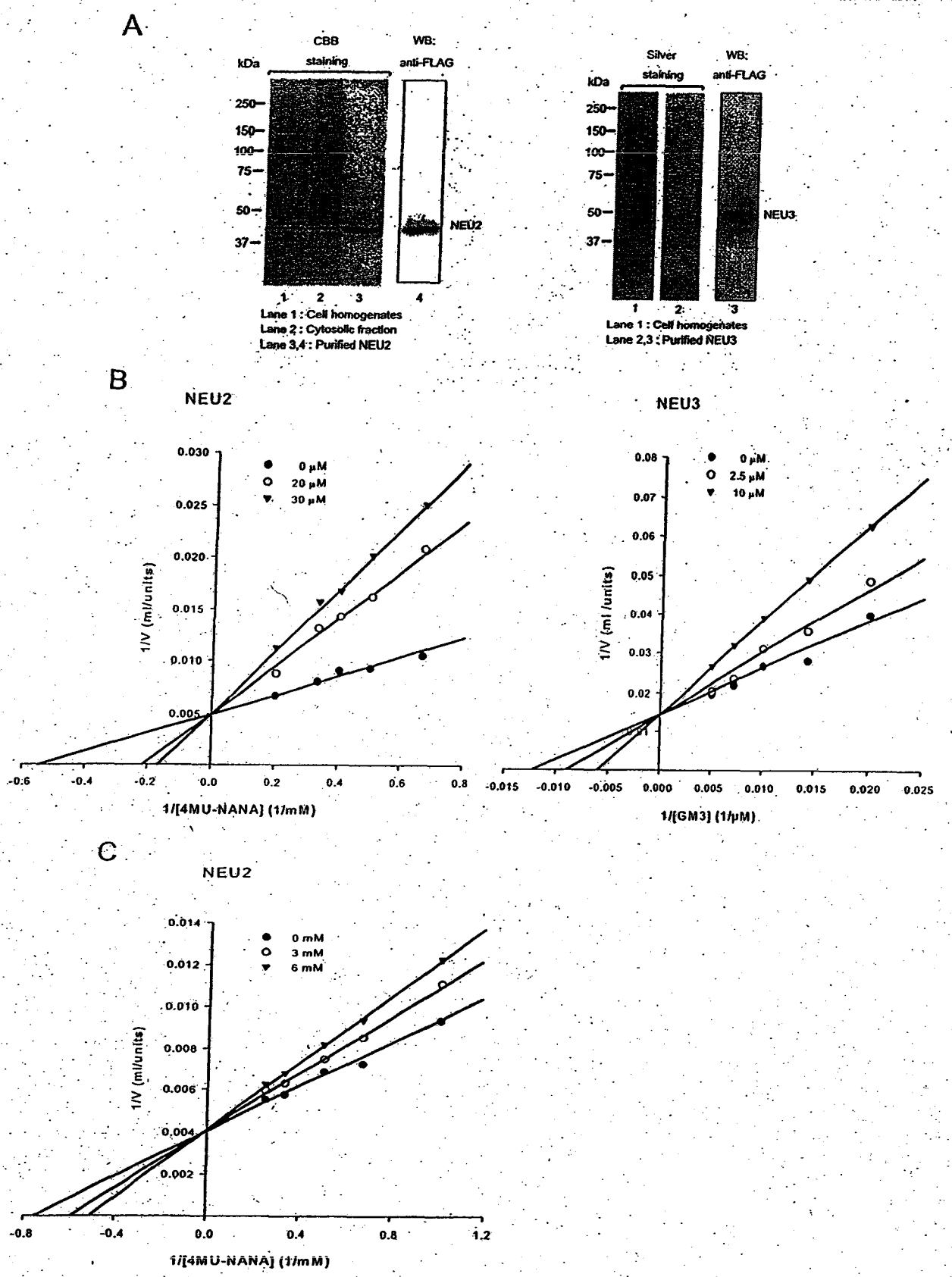

FIG. 2. The effects of oseltamivir carboxylate and zanamivir on sialidase activities. (A) After SDS-PAGE of NEU2 (left) and NEU3 (right) enzymes purified by FLAG affinity chromatography, protein staining, Coomassie brilliant blue (CBB) for NEU2 and silver staining for NEU3, and Western blotting (WB) were performed to evaluate the degree of purification. The enzymes were assayed with increasing concentrations of 4MU-NeuAc or GM3 as a substrate with or without zanamivir (B) or oseltamivir carboxylate (C). The K_m and K_i values were calculated from these results.

TABLE 1. IC_{50}s of oseltamivir carboxylate, zanamivir, and NeuAc2en for activities of human and influenza virus sialidases[a]

Sialidase	IC_{50}[a] of inhibitor with substrate				
	Oseltamivir carboxylate with 4MU-NeuAc	Zanamivir with:		NeuAc2en with:	
		4MU-NeuAc	GM3	4MU-NeuAc	GM3
Human sialidases					
NEU1	>10,000 μM	2,713 ± 239 μM	ND	168 ± 23.2 μM	ND
NEU2	>6,000 μM	16.4 ± 2.0 μM	ND	45.5 ± 2.2 μM	ND
NEU3	>10,000 μM	ND	6.8 ± 3.1 μM	ND	70.3 ± 15.3 μM
NEU4	>10,000 μM	487 ± 29.2 μM	690 ± 127 μM	73.1 ± 8.7 μM	ND
Sialidases from:					
A/PR/8/34 virus (H1N1)	7.09 nM	1.56 nM	ND		
A/Aichi2/68 virus (H3N2)	1.55 nM	2.66 nM	ND		
A/DK/HK/313/4/78 virus (H5N3)	4.95 nM	3.97 nM	ND		

[a] NEU3 was evaluated using the ganglioside GM3 as a substrate because of its strict preference, and in addition to GM3, 4MU-NeuAc was used as another substrate for NEU4. In the experiments with human sialidases, each value for zanamivir or NeuAc2en represents the mean ± SD of three or four experiments. For virus sialidase, each value was obtained by performing two experiments. ND, not determined.

against NEU3. On the other hand, the K_i value of oseltamivir carboxylate for NEU2 was much higher than that of zanamivir. To confirm these results, NEU2 and NEU3, which were found in this experiment to be a little more sensitive to the drugs than the other enzymes, were then purified by FLAG tag affinity chromatography. The final enzyme fractions were determined to be apparently homogeneous by SDS-PAGE (Fig. 2A). The specific activities of the purified fractions were 1,906 ± 659 U/μg protein for NEU2 and 934 ± 183 U/μg protein for NEU3. The K_{cat} values calculated were 22.92 ± 8.0/s for NEU2 and 13.0 ± 2.4/s for NEU3. The K_i values of oseltamivir carboxylate and zanamivir for purified NEU2 were 8,373 ± 1,491 and 11.2 ± 0.89 μM, respectively, and the K_m toward 4MU-NeuAc was 1,865 ± 285 μM. For NEU3, the K_i of zanamivir was 5.12 ± 1.12 μM and the K_m 99.4 ± 15.2 mM with the GM3 substrate. These values are similar to those obtained with the homogenates as the enzyme sources, as shown in Table 2. The enzymes were assayed with increasing concentrations of substrates in the presence or absence of the drugs, and the kinetic data indicated the drug to be a competitive inhibitor, as expected. It should be noted that the K_i value of oseltamivir carboxylate for NEU2 was much greater in this study (8,373 ± 1,491 μM) than that (432 μM) reported by Li et al. (11).

TABLE 2. K_m and K_i values for human sialidases[a]

Sialidase	K_m (μM) of substrate		K_i (μM) of inhibitor with substrate		
	4MU-NeuAc	GM3	Oseltamivir carboxylate with 4MU-NeuAc	Zanamivir with:	
				4MU-NeuAc	GM3
NEU1	1,816 ± 490	ND	ND	1,121 ± 250	ND
NEU2	1,795 ± 272	ND	6,032 ± 2,183	12.9 ± 0.07	
NEU3	ND	45.6 ± 10.5	ND	ND	3.72 ± 0.48
NEU4	20.3 ± 2.91	ND	ND	74.5 ± 1.48	ND

[a] Each value represents the mean ± standard deviation of three or four experiments. The ganglioside GM3 was used as a substrate for NEU3 because of its strict preference. ND, not determined. The K_m and K_i values measured with purified enzymes are described in the text.

Effects of oseltamivir and zanamivir on desialylation of endogenous substrates in cells. In addition to the inhibition test with an exogenously added substrate in the assay tube described above, we examined whether desialylation of endogenous substrates by NEU2 or NEU3 was blocked in the presence of these drugs in the cell culture. The homogenates of sialidase transfected and mock-transfected cells were subjected to lectin blotting or TLC to analyze the changes in the amounts of glycoproteins or gangliosides, respectively. As shown in Fig. 3, the significant changes were observed in the transfected cells compared with those in the control cells. A marked increase in several bands of RCA and PNA lectins, recognizing Gal-GlcNAc and Gal-GalNAc, respectively, was observed in the NEU2-transfected cells. Considering that the increase in the intensities of the glycoprotein bands occurred as a result of hydrolysis by the transfected sialidase, it is in agreement with substrate preference of NEU2. However, no significant changes were observed in the intensities of the corresponding protein bands (Fig. 3A), either after the addition of oseltamivir phosphate or after the addition of oseltamivir carboxylate at a concentration of 500 μM, as expected from the results of the activity assays. Although zanamivir at this concentration was effective in the activity assays, as shown in Tables 1 and 2, the drug did not seem to inhibit NEU2-mediated hydrolysis of endogenous glycoproteins. This may not be contradictory, because the activity of the drug is known to be extracellular and the drug does not undergo metabolism. In line with the substrate preference of NEU3 for gangliosides, the glycolipid patterns were altered by NEU3 transfection, especially in a marked decrease in GM3 amounts compared with that in the mock-transfected cells (Fig. 3B). The reduction in the GM3 hydrolyzing activity was scarcely detected in treatment with oseltamivir phosphate nor in that with oseltamivir carboxylate, while zanamivir significantly abrogated GM3 reduction by the NEU3 enzyme. The zanamivir effects may be reasonable, because NEU3 is localized in cell surface membranes. The cells did not show any morphological changes after the addition of these drugs to the culture. These results suggest that oseltamivir at this concentration inhibits neither the hydrolytic reac-

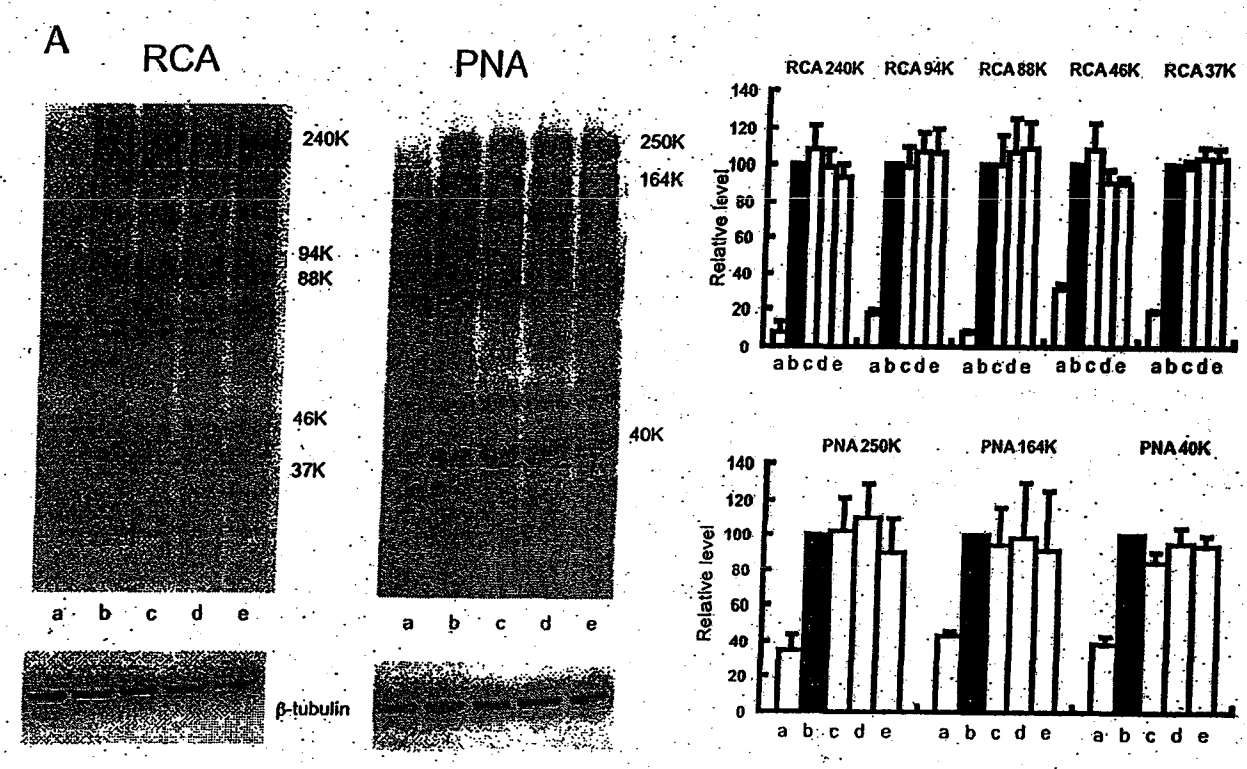

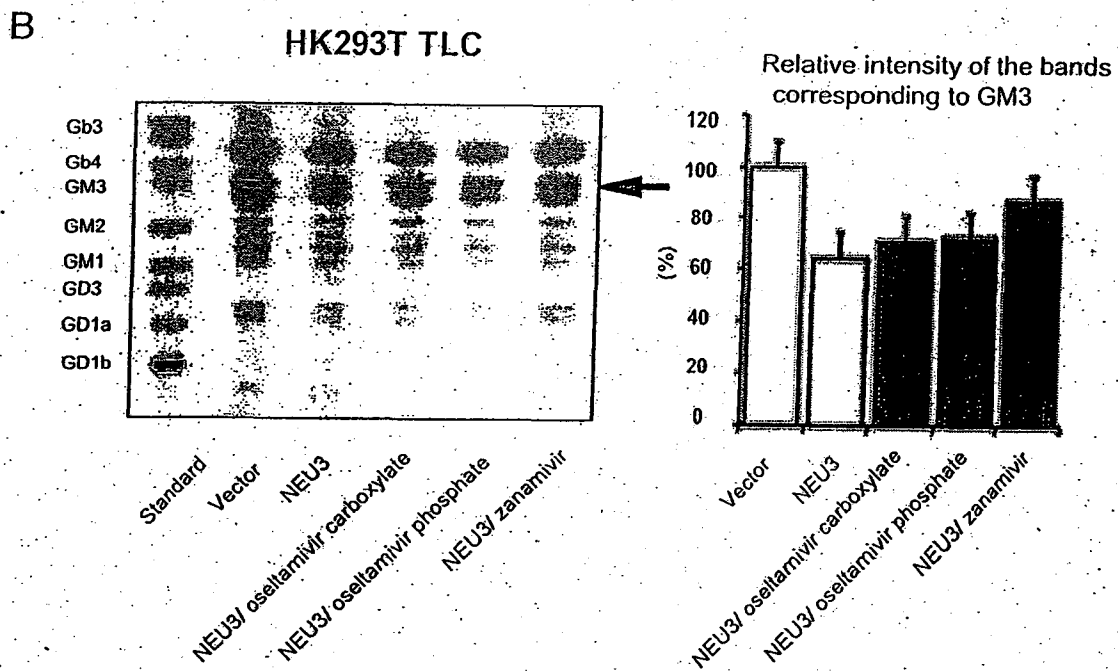

FIG. 3. Effects of oseltamivir and zanamivir on desialylation of endogenous substrates of 293T cells. (A) Alterations of glycoproteins by transfection of NEU2 into 293T cells were observed by PNA and RCA lectin blotting. Intensities of several protein bands (right panel) indicated were markedly increased in the NEU2-transfected cells compared to the mock-transfected cells, but no significant changes were observed in the NEU2-transfected cells after treatment with any of the drugs at the concentration of 500 μM. (B) The glycolipids were examined by TLC in the NEU3-transfected cells. The transfected cells showed a marked decrease in GM3 amounts compared to mock-transfected cells. Neither addition of oseltamivir phosphate nor that of oseltamivir carboxylate changed the patterns, while zanamivir inhibited GM3 hydrolysis by NEU3. The relative intensities of the bands corresponding to GM3 in TLC are shown in the right panel.

tions of the sialidases inside the cells nor the sialidase activity following exogenous addition of substrates.

DISCUSSION

In the present study, we explored the inhibitory effects of oseltamivir and zanamivir on four human sialidases using their recombinant proteins. The effects were examined by two methods, namely, measurement of the inhibitory activity in sialidase activity assays and estimation of the reduced desialylation of endogenous glycoprotein and glycolipid substrates inside the cells. Recent observations have suggested a possible inhibitory potential of oseltamivir against endogenous sialidases. In mice, the drug decreased the GM1 of activated $CD8^+$ T cells infected with a respiratory syncytial virus (18) and also blocked GM1-mediated opioid hyperalgesia induced by low doses of morphine (5). In rats, it exhibited neuroexcitatory effects, especially under conditions of simultaneous administration of ethanol (10). With these animal models, however, no direct inhibitory effects of the drugs on endogenous sialidases could be shown. We do not yet know the molecular mechanisms underlying these phenomena at present, but our data suggest that they may not be the direct consequences of sialidase inhibition. Decreased GM1 may not always be due to sialidase inhibition and may also involve other processes, such as disturbance of the ganglioside synthetic pathway. In a report on the effects of the drugs on the sialidases of PC12 cells, Tamiflu was found to inhibit the sialidase activity induced by nerve growth factor-dependent Trk receptor activation (29). Although we tried to examine the inhibitory effects under the same experimental conditions and confirmed induction of sialidase activity toward 4MU-NeuAc in a nerve growth factor-dependent manner, we were not able to detect any inhibition of the activity in the cells at a Tamiflu dose of 1 mM. This ineffectiveness of Tamiflu is probably due to the absence or low expression of carboxyesterase 1 (23) and P-glycoprotein (19) in the cells, which are involved in activation and transport of the prodrug osetamivir, respectively. Studies using recombinant NEU2 sialidase (11) have shown that a variant with a nonsynonymous single nucleotide polymorphism frequently observed in some Asian populations is associated with lower sialidase activity and higher sensitivity to oseltamivir than the wild-type enzyme. This is of particular interest in the context of the frequent occurrence of abnormal behavior and deaths associated with Tamiflu use in Japan. However, in addition to the extremely low expression of NEU2 in human tissues, including the brain, as shown in Fig. 1, our present data demonstrate that very high concentrations of oseltamivir carboxylate are needed to inhibit the sialidase activity, which is 14- to 20-fold higher than the concentration reported by Li et al. (11). The other sialidases were not susceptible to the drug, even in the millimolar range, despite the drug inhibiting viral sialidases in the nanomolar range. In contrast, zanamivir inhibited NEU3 at micromolar levels. In consistency with this, Nan et al. (20) reported that less than 1 mM zanamivir inhibited the endogenous sialidase activity of human T lymphocytes, although no information is available with regard to the type of sialidase involved in this phenomenon.

Taken together, the data indicate that oseltamivir carboxylate does not significantly inhibit constitutively expressed NEU1, NEU3, or NEU4 human sialidases while zanamivir exhibits inhibitory effects in the micromolar range against NEU3 as the most sensitive form. We cannot arrive at any firm conclusions at present regarding the potential association between Tamiflu and the abnormal behavior and deaths reported among Japanese teenagers with influenza virus infection treated with the drug, but our results do indicate that the drug might not exert any direct effects on the ganglioside-specific plasma membrane-associated sialidase NEU3, expressed abundantly in the brain. The present results were obtained with only recombinant enzymes, and we also need to stress that the observed effects might not directly reflect the effects that might be observed under physiological conditions inside the cells. Since the plasma concentration of oseltamivir carboxylate is reported to be 1.2 μM following oral administration of the 75-mg capsule twice daily to patients (http://www.rocheusa.com/products/tamiflu/), endogenous sialidase is unlikely to be a direct target molecule. In the case of zanamivir, the plasma concentration is observed to be 0.05 to 0.43 μM within 1 to 2 h following administration of a 10-mg dose (http://us.gsk.com/products/assets/us_relenza.pdf). Our results also suggest negligible effects, although it should be borne in mind that the concentration in the respiratory tract after inhalation may be much higher than that achieved in the blood. In conclusion, it may be desirable to examine newly discovered drugs targeting viral sialidases for their effects on endogenous human sialidases, in order to minimize potential side effects in patients.

REFERENCES

1. Anonymous. 2007. New concerns about oseltamivir. Lancet 369:1056.
2. Anonymous. 2007. Japan's health ministry calls for tests on Tamiflu. Nature 447:626–627.
3. Chavas, L. M., C. Tringali, P. Fusi, B. Venerando, G. Tettamanti, R. Kato, E. Monti, and S. Wakatsuki. 2005. Crystal structure of the human cytosolic sialidase Neu2. Evidence for the dynamic nature of substrate recognition. J. Biol. Chem. 280:469–475.
4. Corfield, T. 1992. Bacterial sialidases—roles in pathogenicity and nutrition. Glycobiology 2:509–521.
5. Crain, S. M., and K. F. Shen. 2004. Neuraminidase inhibitor, oseltamivir blocks GM1 ganglioside-regulated excitatory opioid receptor-mediated hyperalgesia, enhances opioid analgesia and attenuates tolerance in mice. Brain Res. 995:260–266.
6. Fuyuno, I. 2007. Tamiflu side effects come under scrutiny. Nature 446:358–359.
7. Galjart, N. J., N. Gillemans, A. Harris, G. T. van der Horst, F. W. Verheijen, and A. d'Azzo. 1988. Expression of cDNA encoding the human "protective protein" associated with lysosomal beta-galactosidase and neuraminidase: homology to yeast proteases. Cell 54:755–764.
8. Gubareva, L. V., L. Kaiser, and F. G. Hayden. 2000. Influenza virus neuraminidase inhibitors. Lancet 355:827–835.
9. Hama, R. 2007. Fifty sudden deaths may be related to central suppression. BMJ 335:59.
10. Izumi, Y., K. Tokuda, K. A. O'Dell, C. F. Zorumski, and T. Narahashi. 2007. Neuroexcitatory actions of Tamiflu and its carboxylate metabolite. Neurosci. Lett. 426:54–58.
11. Li, C. Y., Q. Yu, Z. Q. Ye, Y. Sun, Q. He, X. M. Li, W. Zhang, J. Luo, X. Gu, X. Zheng, and L. Wei. 2007. A nonsynonymous SNP in human cytosolic sialidase in a small Asian population results in reduced enzyme activity: potential link with severe adverse reactions to oseltamivir. Cell Res. 17:357–362.
12. Maxwell, S. R. 2007. Tamiflu and neuropsychiatric disturbance in adolescents. BMJ 334:1232–1233.
13. Milner, C. M., S. V. Smith, M. V. Carrillo, G. L. Taylor, M. Hollinshead, and R. D. Campbel. 1997. Identification of a sialidase encoded in the human major histocompatibility complex. J. Biol. Chem. 272:4549–4558.
14. Miyagi, T., K. Konno, Y. Emori, H. Kawasaki, K. Suzuku, A. Yasui, and S. Tsuiki. 1993. Molecular cloning and expression of cDNA encoding rat skeletal muscle cytosolic sialidase. J. Biol. Chem. 268:26435–26440.
15. Miyagi, T., and K. Yamaguchi. 2007. Biochemistry of glycans: sialic acids, p. 297–322. *In* J. P. Kamerling, G. Boons, Y. C. Lee, A. Suzuki, N. Taniguchi, and A. G. J. Voragen (ed.), Comprehensive glycoscience. Elsevier BV, Amsterdam, The Netherlands.

16. Miyagi, T., T. Wada, K. Yamaguchi, and K. Hata. 2004. Sialidase and malignancy: a minireview. Glycoconj. J. 20:189–198.
17. Monti, E., A. Preti, E. Rossi, A. Ballabio, and G. Borsani. 1999. Cloning and characterization of Neu2, a human gene homologous to rodent soluble sialidases. Genomics 57:137–143.
18. Moore, M. L., M. H. Chi, W. Zhou, K. Goleniewska, J. F. O'Neal, J. N. Higginbotham, and R. S. Peebles, Jr. 2007. Oseltamivir decreases T cell GM1 expression and inhibits clearance of respiratory syncytial virus: potential role of endogenous sialidase in antiviral immunity. J. Immunol. 178:2651–2654.
19. Morimoto, K., M. Nakakariya, Y. Shirasaka, C. Kakinuma, T. Fujita, I. Tamai, and T. Ogihara. 2008. Oseltamivir (Tamiflu) efflux transport at the blood-brain barrier via P-glycoprotein. Drug Metab. Dispos. 36:6–9.
20. Nan, X., I. Carubelli, and N. M. Stamatos. 2007. Sialidase expression in activated human T lymphocytes influences production of IFN-gamma. J. Leukoc. Biol. 81:284–296.
21. Potier, M., L. Mameli, M. Belisle, L. Dallaire, and S. B. Melancon. 1979. Fluorometric assay of neuraminidase with a sodium (4-methylumbelliferyl-alpha-D-N-acetylneuraminate) substrate. Anal. Biochem. 94:287–296.
22. Roggentin, P., B. Rothe, J. B. Kaper, J. Galen, L. Lawrisuk, E. R. Vimr, and R. Schauer. 1989. Conserved sequences in bacterial and viral sialidases. Glycoconj. J. 6:349–353.
23. Shi D., J. Yang, D. Yang, E. L. LeCluyse, C. Black, L. You, F. Akhlaghi, and B. Yan. 2006. Anti-influenza prodrug oseltamivir is activated by carboxylesterase human carboxylesterase 1, and the activation is inhibited by antiplatelet agent clopidogrel. J. Pharmacol. Exp. Ther. 319:1477–1484.
24. Suzuki, Y., Y. Nagano, H. Kato, M. Matsumoto, K. Nerome, K. Nakajima, and E. Nobusawa. 1986. Human influenza A virus hemagglutinin distinguishes sialyloligosaccharides in membrane-associated gangliosides as its receptor which mediates the adsorption and fusion processes of virus infection. Specificity for oligosaccharides and sialic acids and the sequence to which sialic acid is attached. J. Biol. Chem. 261:17057–17061.
25. von Itzstein, M. 2007. The war against influenza: discovery and development of sialidase inhibitors. Nat. Rev. Drug Discov. 6:967–974.
26. von Itzstein, M., W. Y. Wu, G. B. Kok, M. S. Pegg, J. C. Dyason, B. Jin, T. van Phan, M. L. Smythe, H. F. White, and S. W. Oliver. 1993. Rational design of potent sialidase-based inhibitors of influenza virus replication. Nature 363:418–423.
27. Wada, T., K. Hata, K. Yamaguchi, K. Shiozaki, K. Koseki, S. Moriya, and T. Miyagi. 2007. A crucial role of plasma membrane-associated sialidase (NEU3) in the survival of human cancer cells. Oncogene 26:2483–2490.
28. Wada, T., Y. Yoshikawa, S. Tokuyama, M. Kuwahara, H. Akita, and T. Miyagi. 1999. Cloning, expression and chromosomal mapping of a human ganglioside sialidase. Biochem. Biophys. Res. Commun. 261:21–27.
29. Woronowicz, A., S. R. Amith, K. De Vusser, W. Laroy, R. Contreras, S. Basta, and M. R. Szewczuk. 2007. Dependence of neurotrophic factor activation of Trk tyrosine kinase receptors on cellular sialidase. Glycobiology 17:10–24.
30. Yamaguchi, T., K. Hata, K. Koseki, K. Shiozaki, H. Akita, T. Wada, S. Moriya, and T. Miyagi. 2005. Evidence for mitochondrial localization of a novel human sialidase (NEU4). Biochem. J. 390:85–93.

Available online at www.sciencedirect.com
ScienceDirect
Nuclear Medicine and Biology 36 (2009) 47–55
NUCLEAR MEDICINE — AND — BIOLOGY
www.elsevier.com/locate/nucmedbio

Biodistribution and metabolism of the anti-influenza drug [^{11}C]oseltamivir and its active metabolite [^{11}C]Ro 64-0802 in mice

Akiko Hatori, Takuya Arai, Kazuhiko Yanamoto, Tomoteru Yamasaki, Kazunori Kawamura, Joji Yui, Fujiko Konno, Ryuji Nakao, Kazutoshi Suzuki, Ming-Rong Zhang*

Department of Molecular Probes, Molecular Imaging Center, National Institute of Radiological Sciences (NIRS), Inage-ku, Chiba 263-8555, Japan

Received 22 July 2008; received in revised form 10 October 2008; accepted 15 October 2008

Abstract

Introduction: Oseltamivir phosphate (Tamiflu) is an orally active anti-influenza drug, which is hydrolyzed by esterase to its carboxylate metabolite Ro 64-0802 with potent activity to inhibit the influenza virus. The abnormal behavior and death associated with the use of oseltamivir have developed into a major problem in Japan where Tamiflu is often prescribed for seasonal influenza. It is critical to determine the amount of oseltamivir and Ro 64-0802 in the human brain and to elucidate the relationship between their amounts and neuropsychiatric side effects. The aim of this study was to evaluate [^{11}C]oseltamivir and [^{11}C]Ro 64-0802 in mice as promising positron emission tomography (PET) ligands for measuring their amounts in living brains.

Methods: Whole-body biodistribution of [^{11}C]oseltamivir and [^{11}C]Ro 64-0802 was determined in mice using the dissection method and micro-PET. In vitro and in vivo metabolite assay was performed in the plasma and brain of mice.

Results: Between 1 and 60 min after injection of [^{11}C]oseltamivir and [^{11}C]Ro 64-0802, 0.20–0.06% and 0.39–0.03% ID/g were detected in the mouse brains, respectively (dissection method). Radioactivity concentrations in the living brains between 0 and 90 min after injection were measured at standardized uptake values of 0.25–0.05 for [^{11}C]oseltamivir and 0.38–0.02 for [^{11}C]Ro 64-0802 (micro-PET). In vivo metabolite assay demonstrated the presence of [^{11}C]oseltamivir and [^{11}C]Ro 64-0802 in the brains after [^{11}C]oseltamivir injection.

Conclusion: This study determined the distribution and metabolism of [^{11}C]oseltamivir and [^{11}C]Ro 64-0802 in mice. PET could be used to measure their amounts in the living brain and to elucidate the relationship between the amounts in the brain and the side effects of Tamiflu in the central nervous system.

Keywords: Anti-influenza drug; [^{11}C]Oseltamivir; [^{11}C]Ro 64-0802; Micro-PET; Brain uptake

1. Introduction

Oseltamivir phosphate (Tamiflu, Fig. 1) is an orally active anti-influenza drug for the treatment of influenza types A and B [1–3]. It is a prodrug that is hydrolyzed by esterase to its carboxylate metabolite Ro 64-0802 (Fig. 1), a potent inhibitor of the influenza virus [4–6]. This drug is regularly prescribed as a treatment for seasonal influenza in Japan, and Japanese consumption accounts for up to 75% of all Tamiflu use worldwide. However, the safety of oseltamivir has been questioned because suicidal or abnormal behavior, especially in young patients, has been reported after Tamiflu ingestion [7].

At present, the Japan label of the drug specifies that the drug should not be administrated to young patients as there is a possible risk of neurological adverse effects [8], but the mechanisms of this abnormal behavior are uncertain. Oseltamivir may affect the central nervous system (CNS) because neuraminidase, a key enzyme relative to the proliferation of influenza virus inhibited by Ro 64-0802, plays a role in CNS development and impulse conduction [9–11]. In vitro study on brain slices demonstrated that Ro 64-0802 had clear effects on neuronal excitability and oseltamivir enhanced hippocampal network synchronization [12,13]. A high dose of oseltamivir damaged the brain of experimental animals and was likely caused by uptake of

* Corresponding author. Tel.: +81 43 206 4041; fax: +81 43 206 3261.
E-mail address: zhang@nirs.go.jp (M.-R. Zhang).

0969-8051/$ – see front matter © 2009 Elsevier Inc. All rights reserved.
doi:10.1016/j.nucmedbio.2008.10.008

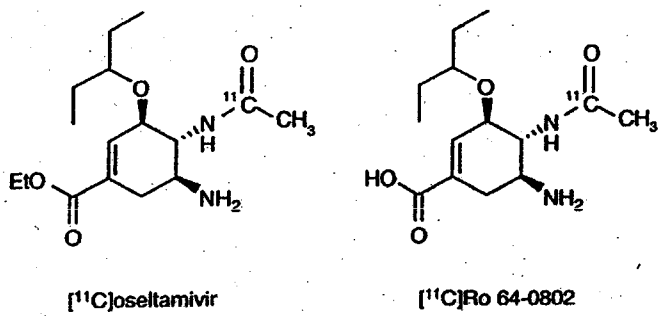

Fig. 1. Chemical structures of [^{11}C]oseltamivir and [^{11}C]Ro 64-0802.

oseltamivir and/or Ro 64-0802 into the CNS. Thus, although it is believed that the two compounds do not easily pass the blood–brain barrier (BBB), they may enter the brain if the BBB is immature or damaged [14]. However, the presence and amounts of oseltamivir and Ro 64-0802 in the human brain, and the relationship between their presence and the side effects of Tamiflu, have not been elucidated clearly [15–18].

Positron emission tomography (PET) is a useful imaging modality employing radioactive ligands labeled with positron-emitting radioactive isotopes, such as carbon-11 (^{11}C; half life: 20.3 min), fluorine-18, nitrogen-13 and oxygen-15 [19]. PET can be used to provide pharmacokinetic and pharmacodynamic information about a drug to determine drug efficacy and potential biochemical mechanisms of drug action, including the adverse and toxic effects. Since influenza is a serious seasonal illness, especially in the winter, and Tamiflu is the first-choice drug [20,21], it is critical to determine the presence and amount of oseltamivir and Ro 64-0802 in the human brain and to explore the relationship between their uptake and side effects on the brain. The effectiveness of PET on the living body prompted us to label oseltamivir and Ro 64-0802 with a positron emitter isotope and to measure their amounts in brains using radiolabeled ligands.

We have recently synthesized [^{11}C]oseltamivir and [^{11}C] Ro 64-0802 and determined their presence in mouse brains using the dissection method [22]. Here, to aim their clinical usefulness, we performed a detailed preclinical evaluation of [^{11}C]oseltamivir and [^{11}C]Ro 64-0802, respectively. Using a dissection method and a small-animal PET (micro-PET), we determined the biodistribution of [^{11}C]oseltamivir and [^{11}C] Ro 64-0802 in various organs of the mouse, including the brain. To elucidate the putative influence of radioactive metabolites on PET imaging and data analysis, we then examined the metabolism of [^{11}C]oseltamivir and [^{11}C]Ro 64-0802 in the brain and the plasma of mice.

2. Materials and methods

2.1. General

Oseltamivir phosphate was purchased from Sequoia Research Products (Pangbourne, UK). Ro 64-0802 was synthesized by hydrolyzing oseltamivir with 1% NaOH solution in our laboratory. All chemicals and solvents were of analytic or high-performance liquid chromatography (HPLC) grade from Aldrich (Milwaukee, WI) and Wako Pure Industries (Osaka, Japan). Carbon-11 was produced by ^{14}N(p, α)^{11}C nuclear reaction using CYPRIS HM18 cyclotron (Sumitomo Heavy Industry, Tokyo, Japan). A dose calibrator (IGC-3R Curiemeter; Aloka, Tokyo, Japan) was used for all radioactivity measurements if not otherwise stated. Reverse-phase HPLC was performed using a JASCO (JASCO, Tokyo, Japan) system: effluent radioactivity was determined using a NaI (Tl) scintillation detector system.

2.2. Production of [^{11}C]oseltamivir and [^{11}C]Ro 64-0802

Radiosynthesis of [^{11}C]oseltamivir and [^{11}C]Ro 64-0802 has been previously published by us elsewhere [22]. Briefly, [^{11}C]AcCl [23], a labeling agent for radiosynthesis, was prepared by reacting methylmagnesium bromide with [^{11}C]CO_2, followed by chlorination with oxalyl chloride [24]. Purified [^{11}C]AcCl was reacted with the precursor [22] in the presence of Et_3N for 3 min at 80°C, followed by treatment with 6 N HCl. After the two-step reactions, the radioactive mixture was purified by HPLC [Waters XBridge Prep C18 5 μm column, 10 mm ID×250 mm, $CH_3CN/H_2O/Et_3N$ (30/70/1), 5 ml/min, 254 nm] to give [^{11}C]oseltamivir. [^{11}C]Oseltamivir was then hydrolyzed with 1% NaOH for 5 min at 100°C to yield [^{11}C]Ro 64-0802. From the end of bombardment, the synthesis times of [^{11}C]oseltamivir and [^{11}C]Ro 64-0802 were about 30 and 35 min, respectively. Starting from cyclotron-produced [^{11}C]CO_2 of 30–37 GBq, [^{11}C]oseltamivir (n=5) or [^{11}C] Ro 64-0802 (n=3) was produced with 450–1130 MBq as an injectable solution.

Radiochemical purity, identity and specific activity were assayed by analytical HPLC (CAPCELL PAK C_{18} column: 4.6 mm ID×250 mm). The retention time (t_R) was 6.5 min for [^{11}C]oseltamivir [$CH_3CN/H_2O/Et_3N$ (30/70/0.1), 1.0 ml/min, 254 nm] and 5.2 min for [^{11}C]Ro 64-0802 [CH_3OH/pH 6.8 phosphate buffer (4/6), 1.0 ml/min, 210 nm], respectively. The identity was confirmed by coinjecting with the corresponding nonradioactive sample. Radiochemical purity was >98% for [^{11}C]oseltamivir (n=5) and >97% for [^{11}C]Ro 64-0802 (n=3), and the specific activity was averaged to be 8.9 GBq/μmol as determined from the mass measured from HPLC UV analysis.

2.3. Animals

Male mice weighing 30–40 g (ddY, 7–8 weeks, SLC, Shizuoka, Japan) were used. The animals were maintained and handled in accordance with recommendations by the U. S. National Institutes of Health and our guidelines (National Institute of Radiological Sciences, NIRS, Chiba, Japan). The studies were approved by the Animal Ethics Committee of NIRS.

2.4. Biodistribution study

2.4.1. Dissection method

A saline solution of [^{11}C]oseltamivir or [^{11}C]Ro 64-0802 (average, 15 MBq/200 μl) was injected into mice through the tail vein. Four mice were sacrificed by cervical dislocation at 1, 5, 15, 30 or 60 min after injection. The whole-brain, liver, lung, heart, kidney, stomach, small intestine, spleen, large intestine, muscle and blood samples were quickly removed. The radioactivity present in these tissues was measured using a 1480 Wizard gamma counter (PerkinElmer Japan, Yokohama, Japan) and expressed as a percentage of the injected dose per gram of wet tissue (% ID/g; mean±S.D., n=4). All radioactivity measurements were corrected for decay.

2.4.2. Micro-PET

PET scans were performed using a small-animal PET Inveon scanner (Siemens Medical Solutions USA, Knoxville, TN). These experiments were performed three times for each ligand using different mice (n=3). Prior to the scans, the mice were anesthetized with 1.5% (v/v) isoflurane. After transmission scans for attenuation correction for 2 cycles (803 s) using a ^{57}Co point source, dynamic emission scans were acquired over 90 min in a 3D list mode with an energy window of 350–650 keV. [^{11}C]Oseltamivir or [^{11}C]Ro 64-0802 (average, 15 MBq/100–300 μl) was injected via the tail vein, while the animals were positioned on the scanner bed before a dynamic PET study was acquired for 90 min. All list-mode data were sorted into 3D sinograms, which were then Fourier rebinned into 2D sinograms (frames, 4×1, 8×2 and 20×5 min). Dynamic images were reconstructed with filtered back-projection using a Ramp filter. Regions of interest (ROIs) were placed on the brain, lung, heart, liver, kidney and so forth using ASIPro VM (Analysis Tools and System Setup/Diagnostics Tool; Siemens Medical Solutions USA).

Time–activity curves (corrected for decay) in the organs were obtained for each scan. For image analysis, CAPP software, version 7.1 (CTI/Siemens), was used. Images were calibrated to standardized uptake values (SUVs) or to units of becquerel per milliliter. The SUV was calculated according to the following formula: measured activity concentration (Bq/ml)×body weight (g)/injected activity (Bq).

2.5. Metabolite assay in plasma and brain homogenate

2.5.1. In vitro

After mice (n=3 for each ligand) were sacrificed by cervical dislocation, blood and whole-brain samples were removed quickly from mice. A blood sample was centrifuged at 15,000 rpm for 2 min at 4°C to separate plasma, 300 μl of which was collected and stored at 0°C until used. The brain was homogenized in threefold volume of 50 mM phosphate buffer (pH 7.4) and also stored at 0°C until used. The plasma and brain homogenate should be used for incubation within 30 min, respectively.

After preincubation of plasma (130 μl) and brain homogenate (200 μl) at 37°C for 5 min, [^{11}C]oseltamivir or [^{11}C]Ro 64-0802 (0.4 MBq/0.24 nmol/10 μl) was added to the tissues, respectively. At 1, 5, 15 and 30 min after incubation, 15 μl of the incubation mixture was withdrawn and immediately added to 45 μl of CH_3CN. The mixture was vortexed for deproteination within 15 s and centrifuged at 15,000 rpm for 2 min at 4°C. The supernatant was collected for analysis.

An aliquot of the supernatant (10 μl) prepared from the plasma or brain homogenate was developed in the following thin-layer chromatography (TLC) mobile phase: $CHCl_3$/CH_3OH/AcOH (5/2/0.1). The TLC plate was air-dried and placed in contact with a imaging plate (BAS-MS2025, FUJIFILM Co., Tokyo) for 60 min, and the radioactivity distribution on the plate was analyzed using a "Bio-Imaging Analyzer (BAS-5000, FUJIFILM Co.). The percentage of [^{11}C]oseltamivir (R_f: 0.75) or [^{11}C]Ro 64-0802 (R_f: 0.38) to total radioactivity on the TLC chromatogram was calculated as %=(peak area for [^{11}C]ligand/total peak area)×100.

After radioactivity decay, the protein concentration in each incubation mixture was measured by the Lowry method. From [^{11}C]oseltamivir experiment, the formation rate of [^{11}C]Ro 64-0802 in plasma protein and brain protein was calculated as:

$$F = (A \times R)/(100 \times P \times T)$$

where F is the [^{11}C]Ro 64-0802 formation rate (pmol/min/mg protein), A is the amount of [^{11}C]oseltamivir added to the incubation mixture (pmol), R is the percentage of [^{11}C]Ro 64-0802 at an observation time point (%), P is the protein concentration in plasma or brain incubation mixture (mg protein/tube) and T is the observation time (min).

2.5.2. In vivo

After intravenous injection of [^{11}C]oseltamivir (30–44 MBq/200–300 μl) into mice (n=3), these mice were sacrificed by cervical dislocation at 1, 5, 15 and 30 min. Blood (0.5–1.0 ml) and whole-brain samples were removed quickly. The blood sample was centrifuged at 15,000 rpm for 2 min at 4°C to separate plasma, which (300 μl) was collected in a test tube containing CH_3CN (300 μl). After the tube was vortexed for 15 s and centrifuged at 15,000 rpm for 2 min for deproteinization, the supernatant was collected and diluted with the same amount of distilled water for analysis. At the same time, the mouse brains were homogenized in twofold volume of ice-cooled phosphate buffer (pH 7.4) solution. The homogenate was centrifuged at 15,000 rpm for 2 min at 4°C, and the supernatant was collected and deproteinized for analysis.

An aliquot of the sample (100–500 μl) prepared from the plasma or brain homogenate was injected into the analytic HPLC system and analyzed for [^{11}C]oseltamivir under the same conditions described above except for a flow rate of 1.5 ml/min. The percentage of [^{11}C]oseltamivir (t_R=5.6 min) or [^{11}C]Ro 64-0802 (t_R=2.4 min) to total radioactivity (corrected for decay) on the HPLC chromatogram was

calculated as %=(peak area for [^{11}C]ligand/total peak area)×100. The recovery ratio of radioactivity eluted from the HPLC column was >95% for the plasma and brain homogenate samples.

3. Results

3.1. Biodistribution

The biodistribution of [^{11}C]oseltamivir and [^{11}C]Ro 64-0802 in mice was measured as the decay-corrected percentage injected activity per gram of tissue (% ID/g).

Fig. 2A shows the data of [^{11}C]oseltamivir in 11 specific regions of mice. After the tracer injection, high initial uptake of radioactivity was found in the blood, lung and heart, followed by a rapid decrease of radioactivity in these organs. Radioactivity accumulated in the liver, small intestine and kidney from the early time point, peaked at about 15 min and declined until the end of this experiment. The maximum level of radioactivity was detected in the kidney among all the organs examined. Compared to other peripheral organs, relatively low uptake was measured in the spleen, stomach and muscle. Radioactivity accumulated in the large intestine over time. The lowest radioactivity was found in the brain (0.20±0.01% at 1 min, 0.16±0.01% at 5 min, 0.14±0.01% at 15 min, 0.09±0.02% at 30 min and 0.06±0.02% ID/g at 60 min after injection). Despite the low level, the decrease rate of radioactivity in the brain was much slower than that in the blood. Calculated from the averaged weight (0.45 g) of the mouse brains used here, 0.09–0.027% of injected [^{11}C] oseltamivir was present in the whole brains between 1 and 60 min after injection.

Fig. 2B shows the data of [^{11}C]Ro 64-0802 in the same regions as in the [^{11}C]oseltamivir experiment. [^{11}C]Ro 64-0802 displayed higher initial radioactivity in the blood and then faster washout from the blood than [^{11}C]oseltamivir described above. A high level of radioactivity was detected in the kidney, which decreased rapidly from 5 min after the tracer injection. Except in the kidney, radioactivity concentration in the other organs was extremely low. In the brain, radioactivity was 0.39±0.08% at 1 min, 0.19±0.06% at 5 min, 0.08±0.01% at 15 min, 0.06±0.02% at 30 min and 0.03±0.01% ID/g at 60 min after injection. Calculated from the averaged weight (0.45 g) of the mouse brains used here,

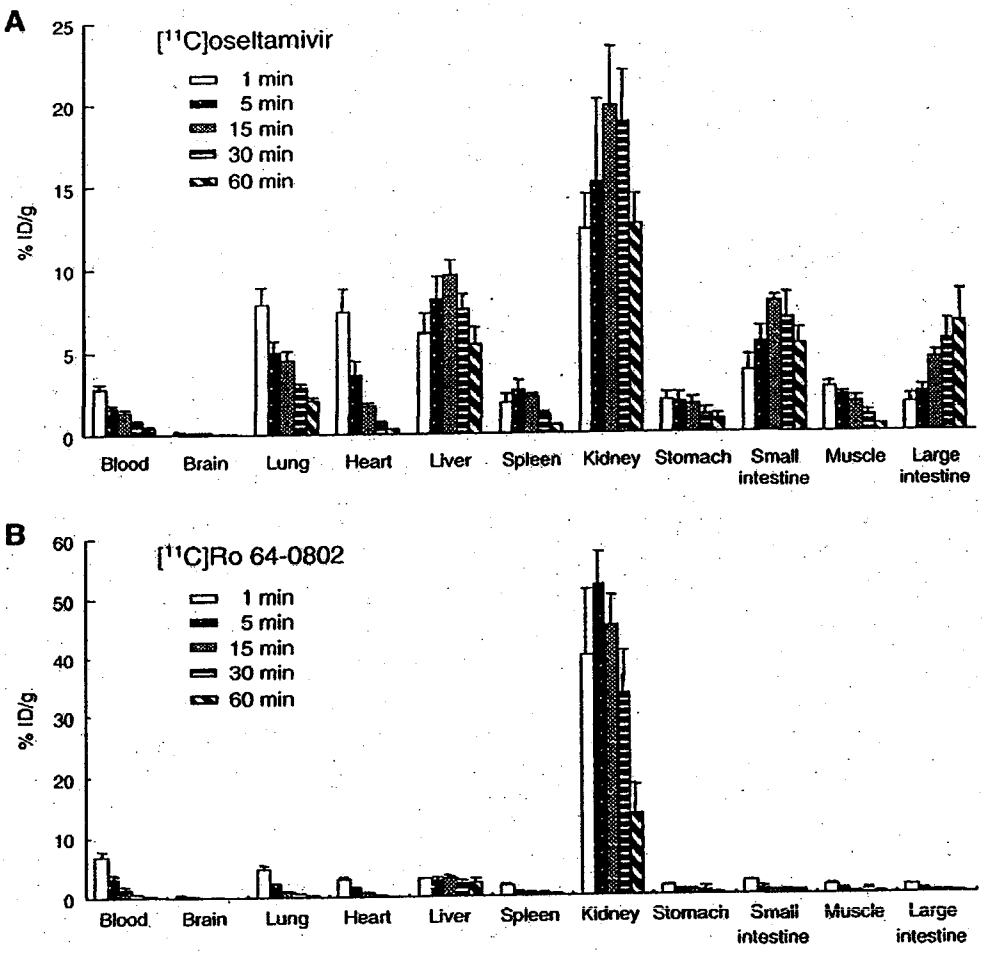

Fig. 2. Biodistribution in mice (n=4 for each ligand) by the dissection method. Radioactivity was expressed as the percentage of the injected dose per gram of tissue or organ (% ID/g; mean±S.D., n=4). (A) [^{11}C]oseltamivir. (B) [^{11}C]Ro 64-0802.

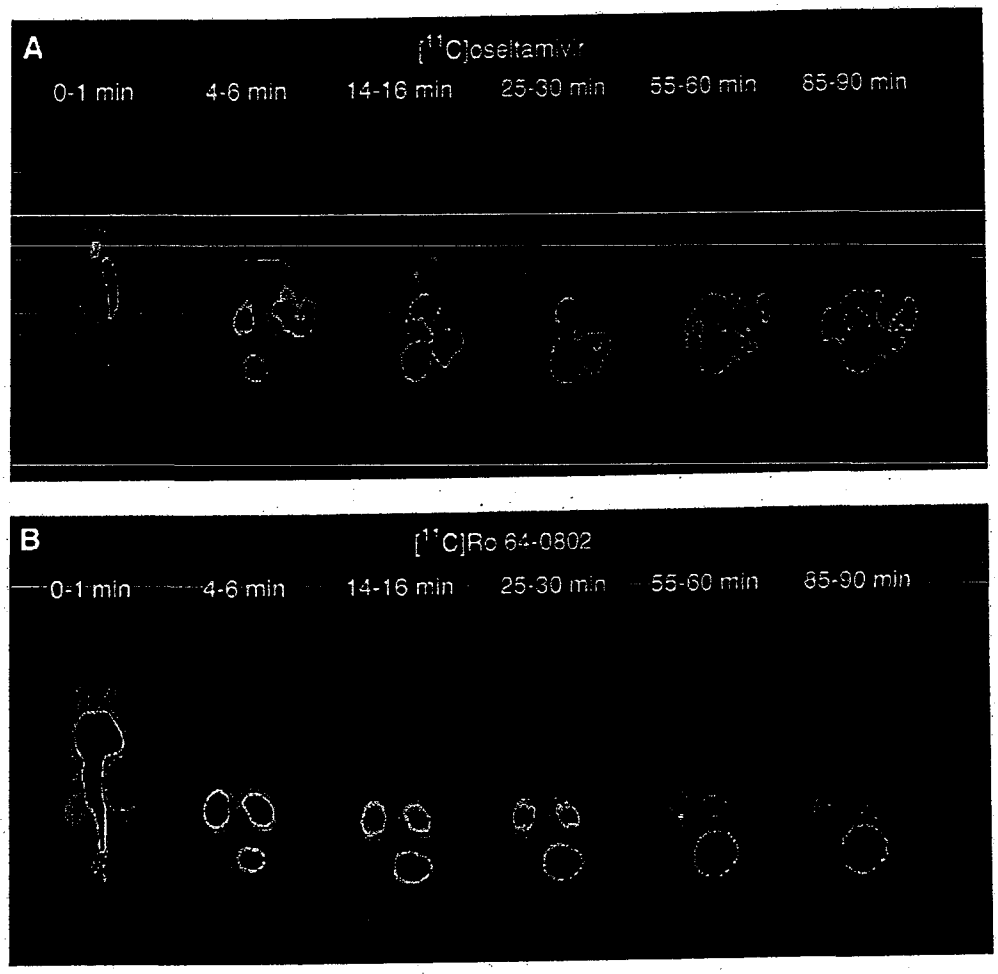

Fig. 3. Typical static micro-PET images at different time points after tracer injection. (A) [^{11}C]oseltamivir. (B) [^{11}C]Ro 64-0802. PET scans were performed for three mice for each ligand.

0.176–0.014% of injected [^{11}C]Ro 64-0802 was present in the whole brains within this experiment.

3.2. Micro-PET

The biodistribution of [^{11}C]oseltamivir and [^{11}C]Ro 64-0802 in mice was determined by micro-PET scans. All micro-PET images were corrected for decay. Fig. 3 shows two typical PET images of mice at different time points after injection of [^{11}C]oseltamivir (Fig. 3A) and [^{11}C]Ro 64-0802 (Fig. 3B). The injected dosing solution was carried through the vena cava to the heart, and then [^{11}C] oseltamivir or [^{11}C]Ro 64-0802 was distributed to the whole body. At 1 min after the [^{11}C]oseltamivir injection (Fig. 3A), radioactivity immediately appeared in the lung, heart and kidneys. Uptake in these organs peaked rapidly and was then eliminated. Radioactivity accumulation in urinary bladder represented rapid and significant excretion in urine. High radioactivity in the liver, gall bladder and small intestine from the early time period also suggested biliary excretion of radioactivity. Radioactive concentrations in liver and other tissues and organs, except digestive organs and urinary bladder, decreased gradually around 16 min after injection. On the other hand, after the injection of [^{11}C]Ro 64-0802, the renal elimination pathways dominated the whole-body distribution. Most radioactivity

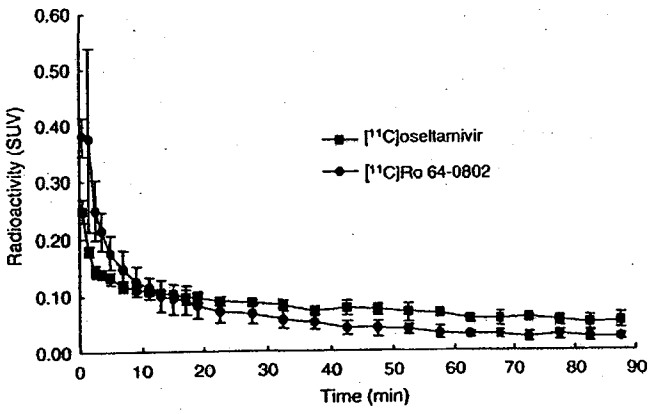

Fig. 4. Time–activity curves of [^{11}C]oseltamivir and [^{11}C]Ro 64-0802 in mouse brains (n=3 for each ligand). Radioactivity was detected and expressed as SUV. The SUV (mean±S.D., n=3) was calculated according to the following formula: measured activity concentration (Bq/ml)×body weight (g)/injected activity (Bq).

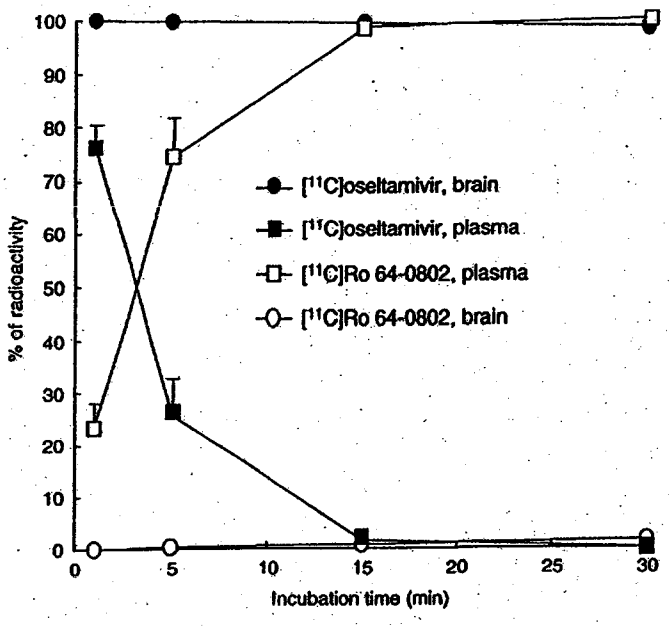

Fig. 5. Percentage (mean±S.D., n=3) of [^{11}C]oseltamivir and [^{11}C]Ro 64-0802 in the plasma and brain homogenate of mice (n=3) at four time points after incubation of [^{11}C]oseltamivir.

was rapidly cleared from the kidneys and directly excreted by the bladder.

Quantitative results of the radioactivity concentrations of [^{11}C]oseltamivir and [^{11}C]Ro 64-0802 in the brains over time are shown in Fig. 4. Despite the relatively high initial uptake, about 50% of highest radioactivity in the brain had rapidly decreased by 5 min after the injection of both ligands. After this phase of initial rapid decline, from 10 min to the end (90 min) of the PET experiments, the radioactivity level in the brains decreased slowly, from SUV 0.11 to 0.05 for [^{11}C] oseltamivir and from SUV 0.12 to 0.02 for [^{11}C]Ro 64-0802.

3.3. Metabolite assay

Fig. 5 shows the in vitro metabolic results of [^{11}C] oseltamivir and [^{11}C]Ro 64-0802 in the plasma and brain homogenate of mice. After incubation of [^{11}C]oseltamivir with plasma, [^{11}C]oseltamivir was rapidly metabolized to [^{11}C]Ro 64-0802. The fraction corresponding to unmetabolized [^{11}C]oseltamivir in the plasma decreased to 25% at 5 min and had almost disappeared at 15 min. In the brain homogenate, [^{11}C]oseltamivir displayed a slight decrease over time. [^{11}C]Ro 64-0802 was identified with radio-TLC as the main radioactive metabolite. Fig. 6 shows the amounts of [^{11}C]Ro 64-0802 produced by the enzymatic hydrolysis of [^{11}C]oseltamivir in the plasma (Fig. 6A) and brain homogenate (Fig. 6B). The formation rate of [^{11}C]Ro 64-0802 in the plasma by 5 min was calculated as 5.1 pmol/min/mg protein. In the brain homogenate, its formation rate by 15 min was calculated as 0.02 pmol/min/mg protein. The in vitro enzymatic activity hydrolyzing [^{11}C]oseltamivir to [^{11}C]Ro 64-0802 in the brain was about 250 times lower than that in the plasma.

On the other hand, [^{11}C]Ro 64-0802 was stable when exposing this ligand to the plasma and brain homogenate for 30 min.

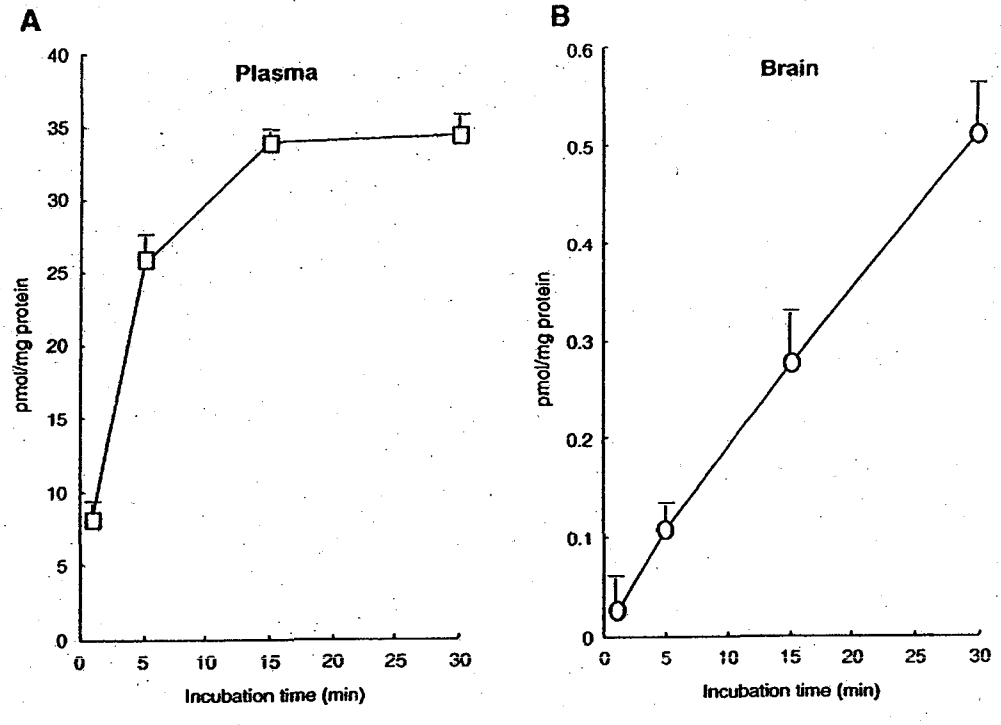

Fig. 6. Amounts (mean±S.D., n=3) of [^{11}C]Ro 64-0802 produced by enzymatic hydrolysis of [^{11}C]oseltamivir in the plasma (A) and brain homogenate (B) of mice (n=3) at four time points after incubation of [^{11}C]oseltamivir.

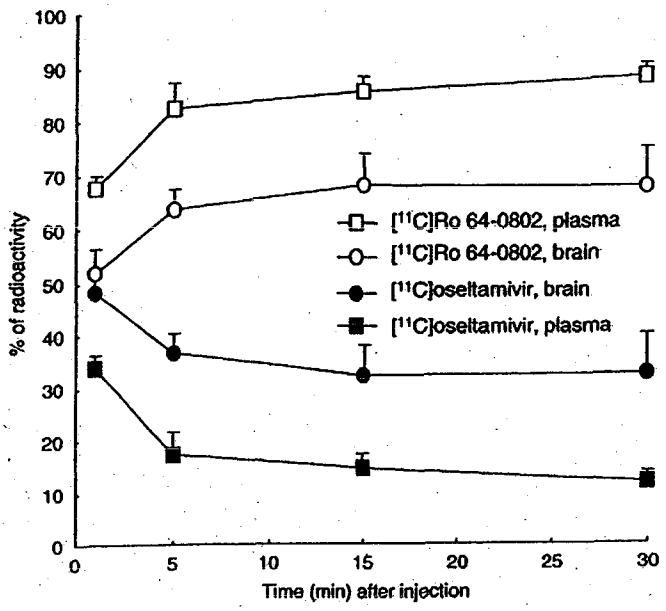

Fig. 7. Percentage (mean±S.D., n=3) of [^{11}C]oseltamivir and [^{11}C]Ro 64-0802 in the plasma and brain of mice at four time points after injection of [^{11}C]oseltamivir (30–44 MBq) into mice (n=3).

Fig. 7 shows the in vivo metabolic results of [^{11}C] oseltamivir in the plasma and brain. After injection into the mouse, [^{11}C]oseltamivir in the plasma decreased to 34% at 1 min and to 17% at 5 min and maintained this level until 30 min. In the brain, [^{11}C]oseltamivir decreased to 48% at 1 min and to 37% at 5 min. [^{11}C]Ro 64-0802 was observed as another main radioactive component on HPLC charts. Within this experiment, 66–88% and 52–68% of total radioactivity in the plasma and brain were assigned to [^{11}C] Ro 64-0802, respectively.

4. Discussion

This study describes the biodistribution and metabolism of the anti-influenza drug [^{11}C]oseltamivir and its active metabolite [^{11}C]Ro 64-0802 in mice. In these experiments, we determined the presence and amounts of the two PET ligands in the living brains of mice. These findings are useful in elucidating the cause of the side effect of Tamiflu in the CNS.

As can be seen from the distribution data (Fig. 2), at 1 min after tracer injection, [^{11}C]Ro 64-0802 displayed higher initial uptakes in the brain (0.39% ID/g) and blood (6.69% ID/g) than [^{11}C]oseltamivir in the brain (0.20% ID/g) and blood (2.79% ID/g). At 15 min, the radioactivity of [^{11}C]oseltamivir (0.14% ID/g) in the brain became higher than that of [^{11}C]Ro 64-0802 (0.08% ID/g). From that point, the two ligands displayed a slow decline of radioactivity in the brain. At 60 min, the level of [^{11}C] oseltamivir (0.06% ID/g) was twofold higher than that of [^{11}C]Ro 64-0802 (0.03% ID/g) in the brain. The ratio of brain/blood radioactivity was calculated to examine the characteristics of the ligands passing through the BBB and accumulating in the brain. The ratios increased from 0.07 to 0.14 for [^{11}C]oseltamivir and from 0.06 to 0.13 for [^{11}C]Ro 64-0802 during this experiment. By analyzing the micro-PET data and time–activity curves (Figs. 3 and 4), SUVs of the two ligands in the living brains could be obtained with statistical significance. The radioactivity concentration of [^{11}C]oseltamivir in the brain was quantified at SUV 0.25–0.05 (0.72–0.15% ID/g) between 0 and 90 min after injection, while that of [^{11}C]Ro 64-0802 was at SUV 0.38–0.02 (1.15–0.07% ID/g). The uptake difference between the two ligands persisted until the end of PET experiments. These results obtained by the dissection method and micro-PET demonstrated that a small amount of the two PET ligands passed the BBB and entered the brain.

Despite their presence, the radioactivity levels of [^{11}C] oseltamivir and [^{11}C]Ro 64-0802 in the mouse brains were much lower than some useful PET probes [25–27] developed by us for clinical brain imaging. Ro 64-0802 is a potent inhibitor of the influenza virus. However, this acidic compound has low lipophilicity, with a clog$P$ (P: octanol/water partition coefficient) value of −0.97 calculated with a Pallas 3.4 software. The low lipophilicity of [^{11}C]Ro 64-0802 may restrict its passage through the BBB at a high concentration. On the other hand, oseltamivir, an ester prodrug of Ro 64-0802, becomes more lipophilic (clog$P$: 1.29) than Ro 64-0802. This improved lipophilicity increased the uptake of [^{11}C]oseltamivir through various peripheral organs, as reflected in Fig. 3A. By contrast, [^{11}C]Ro 64-0802 was not distributed into various organs efficiently (Fig. 3B). The present PET study supported that oseltamivir is a successful prodrug of Ro 64-0802. However, although the uptake of [^{11}C]oseltamivir into the peripheral organs was significantly improved, the radioactivity level of [^{11}C] oseltamivir in the brain was limited to only twofold higher than that of [^{11}C]Ro 64-0802 (Fig. 4). This result could be explained as oseltamivir being a substrate of P-glycoprotein (P-gp) [28,29]. The high density of P-gp at the BBB may restrict the entrance of [^{11}C]oseltamivir into the brain.

In the PET study, radioactive metabolites of a radioligand in the ROI can confound the imaging and measurement, regardless of whether the metabolite binds to the target sites. To elucidate the putative influence of radioactive metabolites on PET experiments, we first performed an in vitro metabolite assay of the two ligands in the brain homogenate and plasma of mice. As shown in Fig. 5, [^{11}C]oseltamivir was metabolized to [^{11}C]Ro 64-0802 in the plasma. In the brain homogenate, [^{11}C]Ro 64-0802 was also identified, although its formation rate (0.02 pmol/min/mg protein) was much slower than that (5.1 pmol/min/mg protein) in the plasma. In vivo metabolite analysis of [^{11}C]oseltamivir demonstrated the presence of [^{11}C]oseltamivir and [^{11}C]Ro 64-0802 in the plasma as well as the brain, respectively (Fig. 7). The presence of [^{11}C]Ro 64-0802 in the brain may be because (a) [^{11}C]Ro 64-0802 itself entered the brain from the plasma or (b) [^{11}C]Ro 64-0802 was yielded by the

hydrolysis of [^{11}C]oseltamivir with esterase in the brain. This result could be supported by the following: (a) 0.39% ID/g was measured in the brain at 1 min after [^{11}C]Ro 64-0802 injection; (b) [^{11}C]Ro 64-0802 of 0.5 pmol/mg brain protein was measured after exposing [^{11}C]oseltamivir to the brain homogenate for 30 min (Fig. 6). Thus, while determining [^{11}C]oseltamivir in the brain with PET, the influence of [^{11}C]Ro 64-0802 on the result may be considered. On the other hand, we tried to perform an in vivo metabolite assay of [^{11}C]Ro 64-0802 in the brain. Unfortunately, due to the low radioactivity in the brain, we failed to obtain statistically significant results. We assumed that the in vitro stability of [^{11}C]Ro 64-0802 in the plasma and brain homogenate may guarantee that the PET experiment with [^{11}C]Ro 64-0802 is not influenced by its putative radioactive metabolites.

Our in vivo result differs from the previous report in the metabolism of oseltamivir. It was reported that this agent was not metabolized in the rodent brain [4,30]. The difference could be explained by the characteristic of a PET ligand with high specific activity. Since the carrier mass contained in the injected [^{11}C]oseltamivir was only 0.01-0.1 mg/kg, the carrier might be easily hydrolyzed by esterase present in the brain. However, the amount of nonradioactive oseltamivir used for the previous analysis was 1000 mg/kg by oral administration [29]. In that case, even trace oseltamivir was hydrolyzed, and the resulting Ro 64-0802, compared to the high concentration of unmetabolized oseltamivir, might be easily ignored. On the other hand, it was reported that oseltamivir was not metabolized in human plasma but was metabolized in the liver fraction in humans [31]. In contrast to humans, this drug was metabolized in the plasma but was stable in the liver fraction of rats [31]. This result may be due to the species difference of esterase between primates and rodents. Thus, for clinical PET investigation of [^{11}C]oseltamivir and [^{11}C]Ro 64-0802, a radioactive metabolite assay should be performed using human plasma.

The present evaluation of adult mice showed that micro-PET could be used to measure the amount of [^{11}C]oseltamivir and [^{11}C]Ro 64-0802 in the living brain with a mature BBB. Although radioactivity levels in the brain were not so high, their uptake may be increased if the BBB is immature or impaired. In fact, the amount of nonradioactive oseltamivir in the brain was reported to be significantly high in newborn rats [29]. On the other hand, organic solvents such as alcohol sometimes enhance BBB permeability [32]. Interaction with other CNS-active drugs may also raise the possibility of the two ligands entering brains. Therefore, PET could be used to elucidate the difference between mature and immature (adult and young) or normal and abnormal states of living brains. Although PET scan on young patients is not easy, a PET study on human adults may be helpful to estimate the amounts of [^{11}C]oseltamivir and [^{11}C]Ro 64-0802 in the brains of young patients. Now, we are comparing the uptake of the two ligands into the brain using rodents of different ages and are searching for their binding sites in animal brains. The present results provide evidence that the two PET ligands are worth investigating in human brains.

5. Conclusions

This study determined the distribution and metabolism of [^{11}C]oseltamivir and [^{11}C]Ro 64-0802 in mice. The two promising PET ligands could be used to measure their amounts in living brains and to elucidate the relationship between their presence and amounts in the brain and the side effects of Tamiflu on the CNS.

Acknowledgments

We are grateful to Makoto Takei and Takeshi Mori (Tokyo Nuclear Service Co., Ltd., Tokyo, Japan) and Hisashi Suzuki (NIRS) for their excellent radiochemistry assistance. We also thank other NIRS staff for support with the cyclotron operation, radioisotope production and animal experiments. This study was partially supported by a consignment grant for the Molecular Imaging Program on Research Base for PET Diagnosis from the Ministry of Education, Culture, Sports, Science and Technology (MEXT), Japanese Government.

References

[1] Kim CU, Lew W, Williams MA, Liu H, Zhang L, Swaminathan S, et al. Influenza neuraminidase inhibitor possessing a novel hydrophobic interaction in the enzyme active site: design, synthesis, and structural analysis of carbocyclic sialic acid analogues with potent anti-influenza activity. J Am Chem Soc 1997;119:681–90.

[2] Calfee DP, Hayden FG. New approaches to influenza chemotherapy. Neuraminidase inhibitors. Drugs 1998;56:537–53.

[3] Kim CU, Chen X, Mendel DB. Neuraminidase inhibitors as anti-influenza virus agents. Antivir Chem Chemother 1999;10:141–54.

[4] Eisenberg EJ, Bidgood A, Cundy KC. Penetration of GS4071, a novel influenza neuraminidase inhibitor, into rat bronchoalveolar lining fluid following oral administration of the prodrug GS4104. Antimicrob Agents Chemother 1997;41:1949–52.

[5] Li W, Escarpe PA, Eisenberg EJ, Cundy KC, Sweet C, Kakeman KJ, et al. Identification of GS 4104 as an orally bioavailable prodrug of the influenza virus neuraminidase inhibitor GS 4071. Antimicrob Agents Chemother 1998;42:647–53.

[6] He J, Massarella P, Ward P. Clinical pharmacokinetics of the prodrug oseltamivir and its active metabolite Ro 64-0802. Clin Pharmacokinet 1999;37:471–84.

[7] (a) http://www.nature.com/news/2007/070319/full/446358a.html. (b) http://www.forbes.com/feeds/ap/2007/04/04/ap3582952.html.

[8] http://www.mhlw.go.jp/shingi/2007/12/2/1225-7.html.

[9] Rodriguez JA, Piddini E, Hasegawa T, Miyagi T, Dotti CG. Plasma membrane ganglioside sialidase regulates axonal growth and regeneration in hippocampal neurons in culture. J Neurosci 2001; 21:8387–95.

[10] Crain SM, Shen KF. Neuraminidase inhibitor, oseltamivir blocks GM1 ganglioside-regulated excitatory opioid receptor-mediated hyperalgesia, enhances opioid analgesia and attenuates tolerance in mice. Brain Res 2004;995:260–6.

[11] Ono H, Nagano Y, Matsunami N, Sugiyama S, Yamamoto S, Tanabe M. Oseltamivir, an anti-influenza virus drug, produces hypothermia in mice. Biol Pharm Bull 2008;31:638–42.

[12] Izumi Y, Tokuda K, O'dell KA, Zorumski CF, Narahashi T. Neuroexcitatory actions of Tamiflu and its carboxylate metabolite. Neurosci Lett 2007;426:54–8.
[13] Usami A, Sasaki T, Satoh N, Akiba T, Yokoshima S, Fukuyama T, et al. Oseltamivir enhances hippocampal network synchronization. J Pharmacol Sci 2008;106:659–62.
[14] http://www.fda.gov/cder/foi/label/2006/021087s0331b1.pdf.
[15] Dutkowski R, Thakrar B, Froehlich E, Suter P, Oo C, Ward P. Safety and pharmacology of oseltamivir in clinical use. Drug Saf 2003;26: 787–801.
[16] Blumentals WA, Song X. The safety of oseltamivir in patients with influenza: analysis of healthcare claims data from six influenza seasons. Med GenMed 2007;9:23.
[17] Okamoto S, Kamiya M, Kishida K, Shimakawa T, Fukui T, Morimoro T. Experience with oseltamivir for infants younger than 1 year old in Japan. Pediatr Infect Dis J 2005;24:575–6.
[18] Hama R. Oseltamivir's adverse reactions: fifty sudden deaths may be related to central suppression. BMJ 2007;335:59.
[19] Fowler JS, Volkow ND, Wang GJ, Ding YS, Dewey SL. PET and drug research and development. J Nucl Med 1999;4:1154–63.
[20] Whitley RJ. The role of oseltamivir in the treatment and prevention of influenza in children. Expert Opin Drug Metab Toxicol 2007;3: 755–67.
[21] Crusat M, de Jong MD. Neuraminidase inhibitors and their role in avian and pandemic influenza. Antivir Ther 2007;12:593–602.
[22] Konno F, Arai T, Zhang MR, Hatori A, Yanamoto K, Ogawa M, et al. Radiosynthesis of two positron emission tomography probes: [^{11}C] oseltamivir and its active metabolite [^{11}C]Ro 64-0802. Bioorg Med Chem Lett 2008;18:1260–3.
[23] Le Bars D, Luthra SK, Pike VW, Luu Duc C. The preparation of a carbon-11 labelled neurohormone—[^{11}C]melatonin. Appl Radiat Isot 1987;38:1073–7.
[24] Arai T, Zhang MR, Ogawa M, Fukumura T, Kato K, Suzuki K. Efficient and reproducible synthesis of [1-^{11}C]acetyl chloride using the loop method. Appl Rad Isot 2008 [doi:10.1016/j.apradiso.2008.09.013].
[25] Zhang MR, Kida T, Noguchi J, Furutsuka K, Maeda M, Suhara T, et al. [^{11}C]DAA1106: radiosynthesis and in vivo binding to peripheral benzodiazepine receptors in mouse brain. Nucl Med Biol 2003;30: 513–9.
[26] Zhang MR, Maeda J, Ogawa M, Noguchi J, Ito T, Yoshida Y, et al. Development of a new radioligand, *N*-(5-fluoro-2-phenoxyphenyl)-*N*-(2-[^{18}F]fluoroethyl-5-methoxybenzyl)acetamide, for PET imaging of peripheral benzodiazepine receptor in primate brain. J Med Chem 2004;47:2228–35.
[27] Zhang MR, Kumata K, Maeda J, Yanamoto K, Hatori A, Okada M, et al. [^{11}C]AC-5216: a novel positron emission tomography ligand for peripheral-type benzodiazepine receptors in primate brain. J Nucl Med 2007;48:1853–61.
[28] Morimoto K, Nakakariya M, Shirasaka Y, Kakinuma C, Fujita T, Tamai I, et al. Oseltamivir (Tamiflu) efflux transport at the blood–brain barrier via P-glycoprotein. Drug Metab Dispos 2008;36:6–9.
[29] Ose A, Kusuhara H, Yamatsugu K, Kanai M, Shibasaki M, Fujita T, et al. P-glycoprotein restricts the penetration of oseltamivir across the blood–brain barrier. Drug Metab Dispos 2008;36:427–34.
[30] Sweeny DJ, Lynch G, Bidgood AM, Lew W, Wang KY, Cundy KC. Metabolism of the influenza neuraminidase inhibitor prodrug oseltamivir in the rat. Drug Metab Dispos 2000;28:737–41.
[31] Shi D, Yang J, Yang D, LeCluyse EL, Black C, You L, et al. Anti-influenza prodrug oseltamivir is activated by carboxylesterase human carboxylesterase 1, and the activation is inhibited by antiplatelet agent clopidogrel. J Pharmacol Exp Ther 2006;319:1477–84.
[32] Stewart PA, Hayagawa EM, Carlen PL. Ethanol and pentobarbital in combination increase blood–brain barrier permeability to horseradish peroxidase. Brain Res 1998;443:12–20.

基礎WGにおいて調査検討した後に
公表されたため追加するもの

Human & Experimental Toxicology (2008) 27: 911–917
www.het.sagepub.com

Synaptic and behavioral interactions of oseltamivir (Tamiflu) with neurostimulants

Y Izumi[1], K Tokuda[1], KA O'Dell[1], CF Zorumski[1] and T Narahashi[2]

[1]*Washington University, School of Medicine, Department of Psychiatry, St. Louis, Missouri; and*
[2]*Northwestern University, Feinberg School of Medicine, Department of Molecular Pharmacology and Biological Chemistry, Chicago, Illinois*

Oseltamivir (Tamiflu), a neuraminidase inhibitor, is widely used for treatment of influenza. Because abnormal behaviors have been observed in some Japanese teenagers following oseltamivir use, its safety has been questioned. Oseltamivir is known to alter neuronal function and behavior in animals, particularly when administered in combination with ethanol. Based on this, it has been hypothesized that interactions of oseltamivir with other drugs may result in altered CNS excitability in this study. It has been found that injection of ephedrine and caffeine overcame inactivity induced by oseltamivir and ethanol but did not alter changes in novelty seeking behavior in a Y-maze test. In ex-vivo hippocampal slices, oseltamivir carboxylate (OTC), an active form of oseltamivir, alters excitability in the absence of ethanol. In slices pretreated with OTC, long-term depression (LTD), a form of synaptic plasticity that is correlated with Y-maze performance was not altered if caffeine or ephedrine was administered individually. However, LTD could not be induced in slices pretreated with OTC if caffeine and ephedrine were administered simultaneously. These observations suggest that combination of oseltamivir with other neurostimulants may alter synaptic plasticity and this may contribute to behavioral changes associated with the drug.

Key words: avian influenza; caffeine; ephedrine; long-term depression; oseltamivir; Tamiflu

Introduction

The outbreak of bird flu (highly pathogenic avian influenza A caused by H5N1 and H9N2 strains) may kill millions of people worldwide if the infection spreads by human-to-human contact.[1,2] Because oseltamivir (Tamiflu®), an antiviral agent that acts as a neuraminidase inhibitor, may be effective in treating avian influenza,[3,4] governments of multiple countries are storing the drug to minimize the risk of outbreak. However, the safety of oseltamivir has been questioned based on accidental deaths and behavioral changes following its use by young people including teenagers in Japan.[5,6] Sudden death of infants has also been reported after use of oseltamivir. These deaths may have resulted from influenza-associated encephalopathy but questions about the safety of oseltamivir have arisen in Japan where oseltamivir was commonly prescribed until last year. Although there are a few reports to conclude that a causal relationship between oseltamivir use and the abnormal behaviors or accidental deaths are less likely,[7,8] the United States Food and Drug Administration (FDA) issued a stronger psychiatric warning about oseltamivir in 2008.[9]

Oseltamivir is metabolized to oseltamivir carboxylate (OTC)[10] and other metabolites in the body.[11] Sialic acid, which may inhibit cellular adhesion, is cleaved by neuraminidase. Thus, it is speculated that neuraminidase, which is blocked by OTC, may play important roles in the central nervous system (CNS) function, including neuronal development and impulse conduction.[12–14] While treatment of hippocampal neurons with neuraminidase increases seizure threshold, its blockade decreases seizure threshold, suggesting that endogenous neuraminidase participates in the regulation of neuronal activity.[15] Furthermore, it has been shown that neuraminidase activity in the hippocampus is increased during seizures.[16] Taken together, these results suggest that OTC could have effects on the CNS and thus play a role in behavioral changes.

We previously examined behavioral and neurophysiological effects of oseltamivir and OTC in rat hippocampal slices and found that propagation of excitatory synaptic inputs from dendrites to cell bodies is enhanced by oseltamivir and OTC.[17] In hippocampal slices, it has also been shown that oseltamivir and OTC induced spike bursts through neuronal synchronization.[18] Although it has been

Correspondence to: Yukitoshi Izumi, MD, PhD, Department of Psychiatry, Washington University School of Medicine, Box 8134 660 S Euclid Avenue, St. Louis, Missouri.
Email: Izumiy@wustl.edu

10.1177/0960327109102367

claimed that oseltamivir does not enter the brain, high doses cause brain damage in animals,[19] and a recent study has shown that oseltamivir does cross the blood brain barrier (BBB).[20] It has been shown that systemic administration of oseltamivir causes hypothermia in mice[21] and increases dopamine release from the prefrontal cortex in rats,[22] indicating that systemically administered oseltamivir reaches the CNS to alter neuronal function. We previously observed that loss of righting reflex in rats following injection of ethanol was diminished by pretreatment with oseltamivir, suggesting that oseltamivir has neurological actions when administered with other agents.[17]

In light of this, it is important to note that patients typically take antiviral agents with other CNS-active drugs, including stimulants like caffeine and ephedrine, as well as alcohol. In Japan, where most problems with oseltamivir have been reported, alcohol use among teenagers is relatively common, though use of other abused drugs is less frequent.[23] Furthermore, BBB permeability to OTC could be enhanced by the presence of alcohol, a solvent that is known to increase BBB permeability to other agents.[24] Caffeine is also routinely ingested, and ephedra (ma huang) is often prescribed to treat flu-like symptoms in Japan. Thus, it is possible that the putative neuropsychiatric effects of oseltamivir occur as a result of interactions with other CNS-active agents.

The primary aim of the present study is to determine whether oseltamivir has adverse CNS interactions when administered with other agents used to treat flu-like symptoms. Such findings could help to establish a safety profile for using oseltamivir and other neuraminidase inhibitors to manage viral infections. In this study, we examined interactions of oseltamivir and ethanol in *combination with* caffeine and ephedrine in a rat-behavioral test using a Y-maze. Because prior studies have indicated that Y-maze performance is correlated with synaptic long-term depression (LTD),[25–27] we also examined drug interactions on LTD in rat hippocampal slices, a preparation that allows direct examination of how drugs influence neuronal function. In this ex-vivo study where we can apply drugs directly at known concentrations, we used OTC instead of oseltamivir, because we previously observed that in hippocampal slices OTC is more potent than its prodrug oseltamivir.[17] Because OTC has effects on slices in the absence of ethanol, we specifically focused on the interactions of OTC with ephedrine and caffeine.

Materials and methods

Animals

All experiments were performed in accordance with the guidelines of the Washington University Animal Study Committee. Every effort was made to minimize the number of animals used and their suffering in all experimental procedures. Male Spague Dawley rats obtained from Harlan (Indianapolis, Indiana, USA) at postnatal date (PND) 23 were reared with a cycle of 12 h white light and 12 h dim light until experiments.

Behavioral studies and drug injections

The first trial experiment was done to determine the effects of treating rats (postnatal day 28–33) with a combination of oseltamivir, ephedrine, and caffeine. In this experiment, oseltamivir (2% volume of body weight, 50 mg/kg, i.p.) or the same volume of saline was followed in 2 h by simultaneous intraperitoneal injection (0.3% volume of body weight) of caffeine (30 mg/kg) and ephedrine (30 mg/kg) in saline at an interval of 2 h.

In subsequent studies, spontaneous alternation behavior was examined using a Y-maze as previously described.[26,27] In this test, a rat was placed in the center of a maze with three arms that were 95 mm wide, 636 mm long, and 240 mm deep at angles of 120° with respect to each other. Rats were allowed to explore the apparatus for up to 10 min and entry into an arm was counted only when the hind limbs completely entered the arm. An alternation was defined as any three consecutive choices of three different arms without re-exploration of a previously visited arm. The percentage of alternations was determined by dividing the total number of alternations by the total number of choices minus 2.[27] The number of completed alternations was determined by counting the number of times that the rats successively entered each of the three arms of the maze without reentering a previously visited arm in first 12 entries or in 10 min, whichever came first. Thus, the highest score possible on this measure is 10. Y-maze tests were videotaped.

The initial Y-maze test was performed 1–2 h after transfer of rats from the animal care facility. After the initial Y-maze test, ethanol (1.0 g/kg, i.p. as 26% v/v in saline) or ethanol and oseltamivir in saline (2% volume of body weight, 45 min apart) was administered (i.p.) to albino rats (postnatal day 30 ± 2) at an interval of 2 h. After these injections, the Y-maze test was repeated. The third Y-maze test was done 20 min after simultaneous intraperitoneal injection (0.3% volume of body weight) of caffeine (30 mg/kg) and ephedrine (30 mg/kg).

Hippocampal slice electrophysiology

Naïve rats (postnatal date 28–35) were anesthetized with isoflurane and decapitated. Hippocampi were rapidly dissected, placed in artificial cerebrospinal fluid (ACSF) containing (in mM) 124 NaCl, 5 KCl, 2 $MgSO_4$, 2 $CaCl_2$, 1.25 NaH_2PO_4, 22 $NaHCO_3$, 10 glucose, gassed with 95% O_2-5% CO_2 at 4-6 °C, and cut transversely into 400 μm slices using a vibratome. Slices were prepared from the septal half of the hippocampus and were placed in an incubation chamber containing gassed ACSF for 1 h at 30 °C. Artificial cerebrospinal fluid was perfused at 2 mL/min. At the time of experiment, slices were transferred individually to a submersion recording chamber. Experiments were done at 30 °C.

Extracellular recordings were obtained from the apical dendritic region for analysis of population excitatory postsynaptic potentials (EPSPs) using 2 M NaCl glass electrodes with resistances of 5-10 MΩ. Evoked synaptic responses were elicited with 0.2 ms constant current pulses through a bipolar electrode placed in the Schaffer collateral-commissural pathway. Synaptic responses in CA1 were monitored by applying single stimuli to the Schaffer collateral pathway every 60 s at an intensity sufficient to elicit 50% maximal EPSPs. After establishing a stable baseline for at least 10 min and a control input-output (IO) curve, LTD or long-term potentiation (LTP) was induced by applying low-frequency stimulation (LFS) consisting of 900 individual pulses at 1 Hz (LTD) or high-frequency stimulation (HFS) consisting of a single 100 Hz × 1 s stimulus train (LTP) using pulses of the same amplitude. Following LFS and HFS, responses were monitored every 60 s for 60 min.

Chemicals

The test solution of oseltamivir was prepared by dissolving a Tamiflu tablet (75 mg) in saline. Oseltamivir carboxylate was obtained from Toronto Research Chemicals Inc. (North York, Ontario, Canada). Other chemicals were obtained from Sigma-Aldrich (St. Louis, Missouri, USA).

Statistics

Statistical analyses were done in SigmaStat (Jandel Scientific Software, San Rafael, California, USA). ANOVA test was used for analysis of results from the Y-maze test. Results from LTD studies were analyzed with Student's *t*-test or Mann–Whitney *U*-test where appropriate. Chi-square test was used for analysis of occurrence of odd behaviors.

Results

As previously reported, injection of oseltamivir alone in rats did not induce abnormal patterns of behavior.[17] Because CNS stimulants such as ephedra and caffeine are often taken by patients with flu in Japan, ephedrine (30 mg/kg) and caffeine (30 mg/kg) were injected simultaneously into 12 rats housed in four separate cages. Administration of both agents caused hyperactivity, including hopping, darting, and sweating lasting over 30 min. While sweating may be unusual in rodents, we observed that drug-treated animals developed a wet appearance of their fur beginning in the neck region and eventually covering their entire body. No abnormal behaviors were noticed subsequently. Another group of 12 rats was pretreated with oseltamivir (50 mg/kg) and showed similar hyperactivity immediately after injection of ephedrine and caffeine. Interestingly, two of these 12 rats attempted to mount other cage mates 2–3 hours after injection. This behavior was observed even though other hyperactive behaviors had diminished. However, no significant difference in the number of affected animals was detected with a Chi-square test compared to 12 control rats. Mounting was not observed in rats treated with ephedrine alone ($N = 11$) or caffeine alone ($N = 11$) after oseltamivir injection.

In subsequent studies, we examined spontaneous alternation behavior in a Y-maze. For these studies, rats were studied individually. The Y-maze test provides a measure of novelty seeking and exploratory behavior.[27] When placed at the center of the Y-maze, control rats typically checked the arms of the maze in an alternating fashion without re-exploring previously visited arms and routinely entered the arms of the maze 12 times within a 10 min observation period. Y-maze performance was not altered when the test was repeated 2 to 3 hours after injection of oseltamivir (50 mg/kg) alone. Similarly, the number of arm entries and the alternation score were not altered after simultaneous injection of ephedrine and caffeine (30 mg/kg each) after oseltamivir treatment.

Because we previously observed additive effects of ethanol and oseltamivir in an animal behavioral study,[17] we treated rats with oseltamivir and ethanol. When oseltamivir was administered 40 min after injection of ethanol (1.0 g/kg), rats exhibited diminished overall activity, resulting in a decreased number of arm entries in the Y-maze (Figure 1A, 6.8 ± 1.8 vs 12 times, only two of six rats achieved 12 arm entries within 10 min). Although the four rats that failed to achieve 12 arm entries initially groomed themselves when they were put in the Y-maze, they

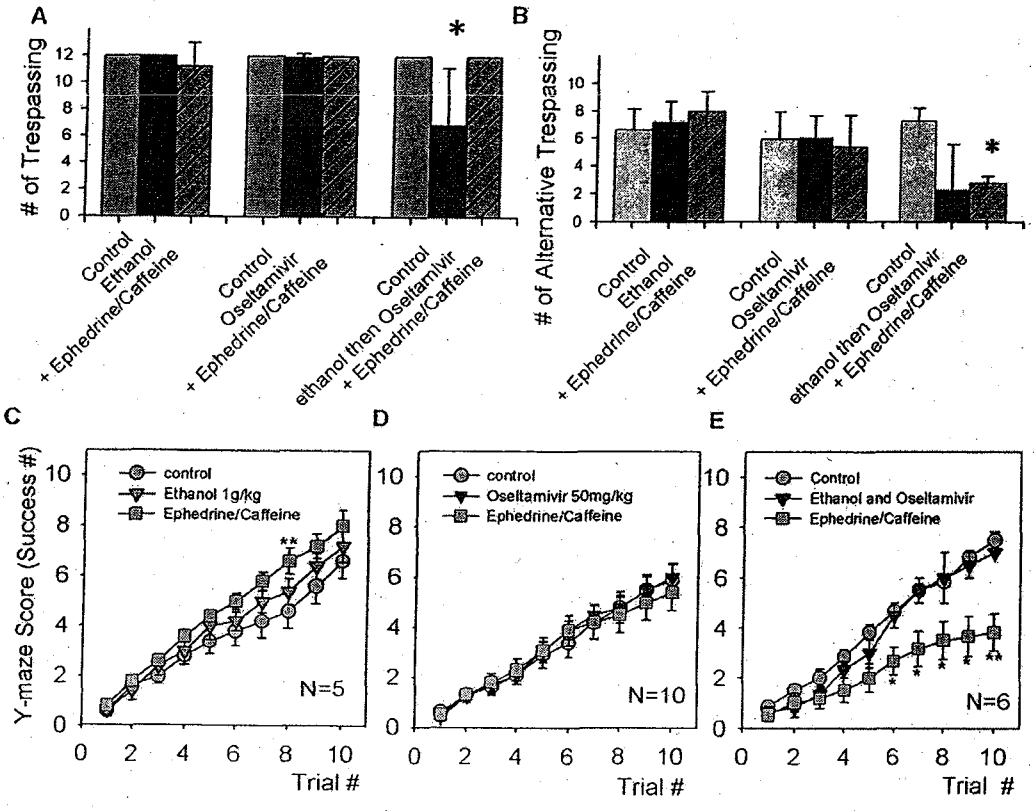

Figure 1 The graphs show effects of systemic treatment of male rats (postnatal date 29–32) with a non-sedating dose of ethanol (1.0 g/kg, i.p.) (left cluster of bars), oseltamivir (50 mg/kg, i.p.) (center) or both (right) on spontaneous alternation in a Y-maze for up to 10 min. Two hours after treatment with oseltamivir and/or ethanol, ephedrine (30 mg/kg) and caffeine (30 mg/kg) were simultaneously injected (right bars in each bar cluster). Rats were exposed to the Y-maze three times: before treatment with oseltamivir and/or ethanol, and 40 min after injection of ethanol alone or 2 h after injection of oseltamivir, and 40 min after injection of ephedrine and caffeine. Panel A depicts the total numbers of entries into arms of the Y-maze (up to 12) in 10 min and is a measure of activity in the task. Rats treated with ethanol 40 min prior to the treatment with oseltamivir show decreased activity in the maze (right purple column in A) $^{*}P < 0.05$ against control before treatment. Panel B depicts the number of completed alternations in the Y-maze, defined as successive entry into each of the three arms of the maze without reentry into a previously visited arm. Rats treated with ethanol 40 min prior to the treatment with oseltamivir also showed impaired performance compared with ethanol alone treated rats after injection of ephedrine and caffeine (right green column in B). $^{**}P < 0.01$ against control Y-maze score obtained before treatment. Panel C–E show again the effects of systemic treatment of male rats with ethanol (1.0 g/kg, i.p.) alone (C), or oseltamivir (50 mg/kg, i.p.) alone (D) or both (E) on spontaneous alternation in the Y-maze for up to 10 min. Rats were placed in the Y-maze three times: before treatment (open circles), 40 min after injection of ethanol alone or 2 h after injection of oseltamivir (triangles), and 40 min after injection of ephedrine and caffeine (squares). In rats pretreated with ethanol and oseltamivir, injection of ephedrine and caffeine results in poor performance in the Y-maze (squares in E). $^{*}P < 0.05$ by one way ANOVA test.

subsequently became immobile with widely opened ears and ceased self-grooming. Because of this limited activity, the number of alternating arm entries was also reduced (Figure 1B). However, the Y-maze score, the ratio of alternative arm entries compared to the total number of entries of active rats, was not reduced (triangles in Figure 1E, only two of six rats entered the arms 12 times within 10 min, so the last Y-maze score of 7 comes from these two rats). In rats pretreated with ethanol and oseltamivir, subsequent injection of ephedrine and caffeine resulted in no decrease in activity and restored the number of arm entries (12 times in 10 min for all six rats) (right bar in the right cluster of Figure 1A). Interestingly, these rats entered the arms of the maze randomly and the Y-maze score remained low (Figure 1B and squares in Figure 1E; Y-maze score: 7.5 ± 0.3 before and 3.8 ± 0.7 after treatment). In rats treated with ethanol alone, the number of arm entries and the Y-maze score were not altered (left cluster of histograms in Figure 1A and B, triangles in Figure 1C). In these rats, the Y-maze parameters were not altered following injection of ephedrine and caffeine (Squares in Figure 1C).

Because Y-maze scores are correlated with LTD in the hippocampus,[25–27] we examined the effects of

OTC, an active metabolite of oseltamivir, on LTD induction in the CA1 region. Oseltamivir is metabolized to OTC in the brain after passing the BBB,[20] and we previously found that OTC is more potent than oseltamivir in causing paired pulse facilitation of population spikes. This enhanced excitability results from altered dendritic propagation in hippocampal slices and does not require the presence of ethanol.[17] Therefore, in the following study, slices were pretreated with 3 μM OTC for 2 h prior to delivery of LFS consisting of 900 pulses at 1 Hz. In the pretreated slices, LTD was successfully induced without any significant difference from LTD in naïve slices (Figure 2A, EPSP slope 60 min after LFS: 71.0 ± 4.7% of control in pretreated slices, $N = 5$, and 67.1 ± 1.5% in naïve slice, $N = 5$). In pretreated slices, LTD was also induced when LFS was delivered in the presence of 100 μM caffeine (squares in Figure 2C, EPSP slope 60 min after LFS: 80.7 ± 3.9% in caffeine, $N = 5$) or 100 μM ephedrine (circles in Figure 2C, EPSPS slope: 60.4 ± 9.3% in ephedrine, $N = 5$). However, LTD was not induced in OTC-pretreated slices when LFS was delivered in the presence of both caffeine and ephedrine (Figure 2B, EPSP slope 60 min after LFS: 100.9 ± 3.6%, $N = 5$, $P < 0.01$ vs control LTD in both naïve and pretreated slices). In contrast, LTD was induced in the presence of both agents in naïve slices (Figure 2B, EPSP slope 60 min after LFS: 76.9 ± 5.4%, $N = 5$). Neither OTC alone nor the combination of OTC, caffeine, and ephedrine had an effect on induction of LTP induced by a single 100 Hz × 1 s HFS (EPSP slope 60 min after HFS: 140.1 ± 4.5% in slices treated with OTC alone, $N = 5$; 138.8 ± 1.0%, $N = 3$, in the presence of OTC, caffeine and ephedrine, data not shown).

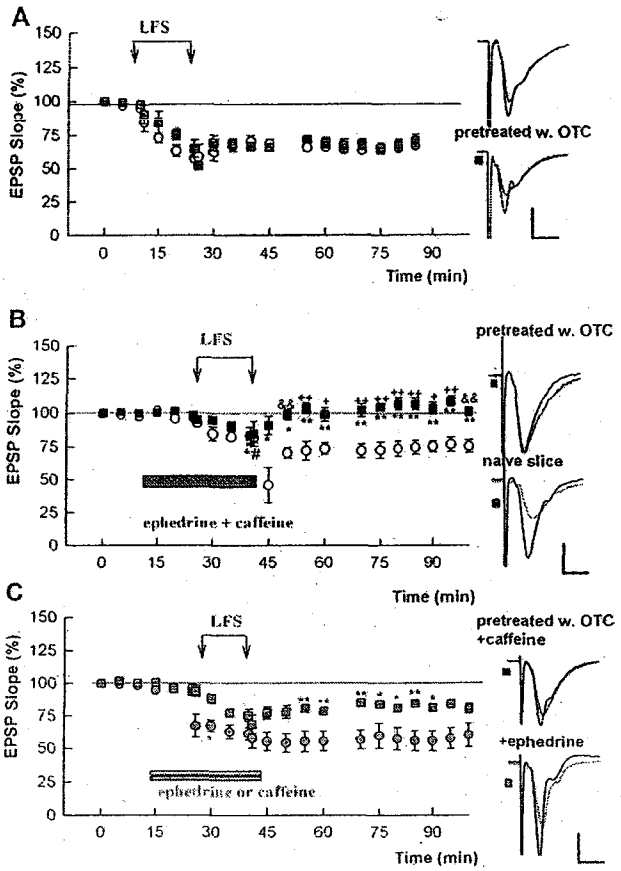

Figure 2 Impaired induction of hippocampal long-term depression (LTD) with ephedrine and caffeine in slices pretreated with 3 μM oseltamivir carboxylate (OTC). (A) Time courses of change in EPSPs in the CA1 region following LFS (arrows) in naïve slices (open circles) and slices treated with OTC (filled squares) ($N = 5$, each) are similar, suggesting that oseltamivir alone does not alter LTD. (B) Simultaneous administration of 100 μM ephedrine and 100 μM caffeine inhibits LTD in slices pretreated with OTC (filled squares) but not in naïve slices (open circles) ($N = 5$ in each). (C) In slices pretreated with OTC, caffeine alone (squares) or ephedrine alone (circles) failed to inhibit LTD induction. However, the inhibition was only partial with caffeine. Note that filled symbols in each graph denote pretreatment with OTC. $^{*}P < 0.05$, $^{**}P < 0.01$ by Student's *t*-test and $^{\#}P < 0.05$ by Mann–Whitney *U*-test against oseltamivir alone. In panel B, $^{+}P < 0.05$, $^{++}P < 0.01$ by Student *t*-test and $^{\&\&}P < 0.01$ by Mann–Whitney *U*-test against ephedrine plus caffeine without oseltamivir. Traces to the right depict EPSPs obtained before (solid line) and 60 min after (dotted line) LFS. Scales: 1 mV, 5 ms.

Discussion

This study shows that administration of a non-sedating dose of ethanol in combination with oseltamivir resulted in diminished behavioral activity and poor locomotion in rats. Evaluation of the changes in behaviors is difficult, but the pattern of response in the alternation task may represent a form of anxious or fearful behavior as manifest by altered exploration.[28] This behavioral restraint may result from risk assessment, the first line of defense against a threat, and appears as a decrease in environmental exploration and locomotion. Some rats were simply immobile without self-grooming, also suggesting an augmented risk-assessing behavior.[29] Immobility (freezing) is also believed to be a second level of defense and may involve assessment of a perceived threat from an undetermined source. If this is the case, random movement after injection of caffeine and ephedrine, which results in the impaired Y-maze performance, may represent a form of flight from an unknown threat as a third level of defense rather than environmental exploration. This may also reflect a form of a behavioral agitation.

It is also possible that oseltamivir alters cognitive processes maintained through synaptic plasticity. Of

importance is that oseltamivir, when combined with CNS stimulants, clearly impairs Y-maze performance. Thus, the random movements observed may have features similar to abnormal and agitated behaviors reported in humans following oseltamivir ingestion. Previous studies have indicated that Y-maze scores are correlated with induction of LTD, a form of hippocampal synaptic plasticity that may contribute to novelty-seeking behaviors.[27] We previously showed that administration of ethanol inhibits both LTD and Y-maze performance.[26] Impairment of LTD induction by the combination of OTC and CNS stimulants, which was observed in the present study, suggests that the combination of drugs affects the synaptic plasticity that may underlie this form of cognitive processes. It is also possible that the combination of drugs changes synaptic function and plasticity in other than regions of the CNS resulting in more profound changes in behavior.

Intentionally or unintentionally, patients with flu may consume CNS stimulants and other drugs. Alcohol, for example, is commonly used socially and may be ingested to relieve some flu-like symptoms by young teenagers.[23] Caffeine and related compounds are often included in soft drinks, nutritional supplements, and common cold regimens.[30] In Japan, ephedra is often taken by flu patients as part of a prescription of Chinese herbal medications that are believed to have antiviral effects.[31] Importantly, herbs such as ma huang (ephedra) are not free from adverse effects.[32] Just as with oseltamivir, suicides have been reported with abuse of ephedra.[33] Thus, it is possible that oseltamivir results in enhanced stimulant actions in the CNS and agitated behavior when combined with other stimulants. It is also possible that the interactions are more complicated during viral infections when there may be changes in the integrity of the BBB.[34,35] It has been reported that P-glycoprotein at the BBB plays an important role in accumulation of oseltamivir in the CNS.[20] In P-glycoprotein knock-out mice, oseltamivir concentration in the cerebrospinal fluid (CSF) is 5.5-fold higher.[36] Moreover, it was previously described that brain levels of oseltamivir were 1500 times those of adult animals exposed to the same dose.[19] The accumulated oseltamivir is likely converted to OTC in the CNS. Although it has been reported that OTC concentrations in the CSF in adult healthy volunteers administered 150 mg oseltamivir reach only approximately 0.1 μM,[37] much higher levels are expected if the BBB is immature or impaired.

The relation between use of oseltamivir and abnormal behaviors remain uncertain. It also remains unclear why these abnormal behaviors occurred primarily in Japan. This may simply reflect the frequency with which oseltamivir is used to treat influenza in Japan while oseltamivir use in the United States is relatively less common. We hypothesize that the combination of oseltamivir with CNS stimulants and/or alcohol could play a role in producing abnormal behaviors and accidental deaths. However, it is also possible that genetic variation resulting in reduced sialidase activities, which is detected in only some Asians, may account for the adverse effect of oseltamivir.[38] Taken together, these observations suggest that multiple factors are likely to contribute to the adverse effects of oseltamivir.[39] The present study suggests that oseltamivir, if combined with common neurostimulants, may alter a specific form of synaptic plasticity in the CNS; in turn, this could contribute to some of behaviors changes reported after use of oseltamivir. Further investigations, especially neurochemical analyses, will be required to elucidate the interactions of oseltamivir with other agents. This information will be important for determining the conditions under which antiviral agents can be used safely in humans given the potential need for widespread use of these drugs in event of an avian flu pandemic.

Acknowledgments

This work was supported in part by NIH grants MH77791, Neuroscience Blueprint Grant NS057105, and the Bantly Foundation.

References

1 Abdel-Ghafar, AN, Chotpitayasunondh, T, Gao, Z, Hayden, FG, Nguyen, DH, de Jong, MD, *et al.* Update on avian influenza A (H5N1) virus infection in humans. *N Engl J Med* 2008; **358**: 261–273.
2 Cinatl Jr, J, Michaelis, M, Doerr, HW. The threat of avian influenza A (H5N1). Part I: Epidemiologic concerns and virulence determinants. *Med Microbiol Immunol* 2007; **196**: 181–190.
3 Crusat, M, de Jong, MD. Neuraminidase inhibitors and their role in avian and pandemic influenza. *Antivir Ther* 2007; **12**(4 Pt B): 593–602.
4 Lowen, AC, Palese, P. Influenza virus transmission: basic science and implications for the use of antiviral drugs during a pandemic. *Infect Disord Drug Targets* 2007; **7**: 318–328.
5 Fuyuno, I. Tamiflu side effects come under scrutiny. *Nature* 2007; **446**: 358–359.
6 Maxwell, SR. Tamiflu and neuropsychiatric disturbance in adolescents. *BMJ* 2007; **334**: 1232–1233.
7 Blumentals, WA, Song, X. The safety of oseltamivir in patients with influenza: analysis of healthcare claims

data from six influenza seasons. *Med Gen Med* 2007; **9**: 23.
8 Terada, K, Kawai, Y, Monju, A, Wakabayashi, T, Ouchi, K. Adolescent jump case in Japan associated with influenza but not oseltamivir. *Pediatr Infect Dis J* 2008; **27**: 88–89.
9 FDA. 2008 Safety Alerts for Human Medical Products (Drugs, Biologics, Medical Devices, Special Nutritionals, and Cosmetics). http://www.fda.gov/medwatch/safety/2008/safety08.htm#Tamiflu. Posted on March 4, 2008 [accessed 06.11.08].
10 He, G, Massarella, J, Ward, P. Clinical pharmacokinetics of the prodrug oseltamivir and its active metabolite Ro 64-0802. *Clin Pharmacokinet* 1999; **37**: 471–484.
11 Sweeny, DJ, Lynch, G, Bidgood, AM, Lew, W, Wang, KY, Cundy, KC. Metabolism of the influenza neuraminidase inhibitor prodrug oseltamivir in the rat. *Drug Metab Dispos* 2000; **28**: 737–741.
12 Crain, SM, Shen, KF. Neuraminidase inhibitor, oseltamivir blocks GM1 ganglioside-regulated excitatory opioid receptor-mediated hyperalgesia, enhances opioid analgesia and attenuates tolerance in mice. *Brain Res* 2004; **995**: 260–266.
13 Da Silva, JS, Hasegawa, T, Miyagi, T, Dotti, CG, Abad-Rodriguez, J. Asymmetric membrane ganglioside sialidase activity specifies axonal fate. *Nat Neurosci* 2005; **8**: 606–615.
14 Rodriguez, JA, Piddini, E, Hasegawa, T, Miyagi, T, Dotti, CG. Plasma membrane ganglioside sialidase regulates axonal growth and regeneration in hippocampal neurons in culture. *J Neurosci* 2001; **21**: 8387–8395.
15 Isaev, D, Isaeva, E, Shatskih, T, Zhao, Q, Smits, NC, Shworak, NW, *et al.* Role of extracellular sialic acid in regulation of neuronal and network excitability in the rat hippocampus. *J Neurosci* 2007; **27**: 11587–11594.
16 Boyzo, A, Ayala, J, Gutiérrez, R. Hernández-RJ. Neuraminidase activity in different regions of the seizing epileptic and non-epileptic brain. *Brain Res.* 2003; **964**: 211–217.
17 Izumi, Y, Tokuda, K. O'dell, KA, Zorumski, CF, Narahashi, T. Neuroexcitatory actions of Tamiflu and its carboxylate metabolite. *Neurosci Lett* 2007; **426**: 54–58.
18 Usami, A, Sasaki, T, Satoh, N, Akiba, T, Yokoshima, S, Fukuyama, T, *et al.* Oseltamivir enhances hippocampal network synchronization. *J Pharmacol Sci* 2008; **106**: 659–662.
19 Wooltorton, E. Oseltamivir (Tamiflu) unsafe in infants under 1 year old. *CMAJ* 2004; **170**: 336.
20 Morimoto, K, Nakakariya, M, Shirasaka, Y, Kakinuma, C, Fujita, T, Tamai, I, *et al.* Oseltamivir (Tamiflu) Efflux Transport at the Blood-Brain Barrier via P-Glycoprotein. *Drug Metab Dispos* 2008; **36**: 6–9.
21 Ono, H, Nagano, Y, Matsunami, N, Sugiyama, S, Yamamoto, S, Tanabe, M. Oseltamivir, an anti-influenza virus drug, produces hypothermia in mice. *Biol Pharm Bull* 2008; **31**: 638–642.
22 Yoshino, T, Nisijima, K, Shioda, K, Yui, K, Kato, S. Oseltamivir (Tamiflu) increases dopamine levels in the rat medial prefrontal cortex. *Neurosci Lett* 2008; **438**: 67–69.
23 Wada, K, Price, RK, Fukui, S. Reflecting adult drinking culture: prevalence of alcohol use and drinking situations among Japanese junior high school students in Japan. *J Stud Alcohol* 1998; **59**: 381–386.
24 Stewart, PA, Hayakawa, EM, Carlen, PL. Ethanol and pentobarbital in combination increase blood-brain barrier permeability to horseradish peroxidase. *Brain Res* 1988; **443**: 12–20.
25 Gallitano-Mendel, A, Izumi, Y, Tokuda, K, Zorumski, CF, Howell, MP, Muglia, LJ, *et al.* The immediate early gene early growth response gene 3 mediates adaptation to stress and novelty. *Neuroscience* 2007; **148**: 633–643.
26 Izumi, Y, Kitabayashi, R, Funatsu, M, Izumi, M, Yuede, C, Hartman, RE, *et al.* A single day of ethanol exposure during development has persistent effects on bi-directional plasticity, N-methyl-D-aspartate receptor function and ethanol sensitivity. *Neuroscience* 2005; **136**: 269–279.
27 Nakao, K, Ikegaya, Y, Yamada, MK, Nishiyama, N, Matsuki, N. Spatial performance correlates with long-term potentiation of the dentate gyrus but not of the CA1 region in rats with fimbria-fornix lesions. *Neurosci Lett* 2001; **307**: 159–162.
28 Shuhama, R, Del-Ben, CM, Loureiro, SR, Graeff, FG. Animal defense strategies and anxiety disorders. *An Acad Bras Cienc* 2007; **79**: 97–109.
29 Blanchard, RJ, Hebert, MA, Ferrari, PF, Palanza, P, Figueira, R, Blanchard, DC, *et al.* Defensive behaviors in wild and laboratory (Swiss) mice: the mouse defense test battery. *Physiol Behav* 1998; **65**: 201–209.
30 Gregory, PJ. Evaluation of the stimulant content of dietary supplements marketed as "ephedra-free". *J Herb Pharmacother* 2007; **7**: 65–72.
31 Abourashed, EA, El-Alfy, AT, Khan, IA, Walker, L. Ephedra in perspective–a current review. *Phytother Res* 2003; **17**: 703–712.
32 Jacobs, KM, Hirsch, KA. Psychiatric complications of Ma-huang. *Psychosomatics* 2000; **41**: 58–62.
33 Doyle, H, Kargin, M. Herbal stimulant containing ephedrine has also caused psychosis. *BMJ* 1996; **313**: 756.
34 Haverkos, HW, Amsel, Z, Drotman, DP. Adverse virus-drug interactions. *Rev Infect Dis* 1991; **13**: 697–704.
35 Levy, M. Role of viral infections in the induction of adverse drug reactions. *Drug Saf* 1997; **16**: 1–8.
36 Ose, A, Kusuhara, H, Yamatsugu, K, Kanai, M, Shibasaki, M, Fujita, T, *et al.* P-glycoprotein restricts the penetration of oseltamivir across the blood-brain barrier. *Drug Metab Dispos* 2008; **36**: 427–434.
37 Jhee, SS, Yen, M, Ereshefsky, L, Leibowitz, M, Schulte, M, Kaeser, B, *et al.* Low penetration of oseltamivir and its carboxylate into cerebrospinal fluid in healthy Japanese and Caucasian volunteers. *Antimicrob Agents Chemother* 2008; **52**: 3687–3693.
38 Li, CY, Yu, Q, Ye, ZQ, Sun, Y, He, Q, Li, XM, *et al.* A nonsynonymous SNP in human cytosolic sialidase in a small Asian population results in reduced enzyme activity: potential link with severe adverse reactions to oseltamivir. *Cell Res* 2007; **17**: 357–362.
39 Long, M. Side effects of Tamiflu: clues from an Asian single nucleotide polymorphism. *Cell Res* 2007; **17**: 309–310.